ALSTOM	Client	J-Power (Electric Power Development Co. Ltd.,)
	Project	Turbine and System Assessment for NTPC-Korba Unit #4
	Order No.	CGP10028C
	Contractor	ALSTOM K.K. NASL Ltd. (Nominated subcontractor in India)
NTPC ALSTOM Power Services Pvt. Ltd.	**Document**	**FINAL REPORT VOL. I B(RLA OF TURBINE)**

Name of Component: IP CV-4
Location: IP CV-4_CONE
Hardness: 160-164HB

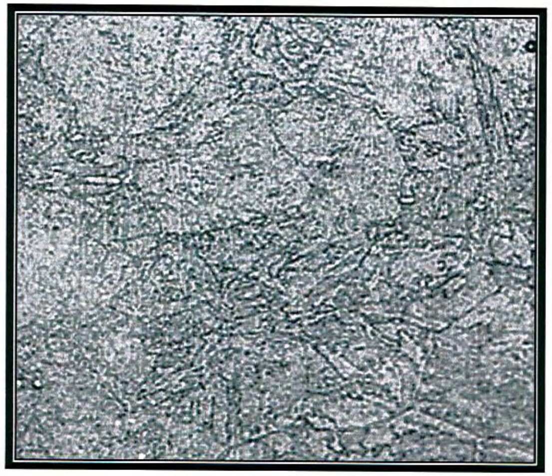	
200X	400X
Observation: Microstructure shows tempered Bainite with precipitation of carbides.	Degradation Level- IIL

Fig: 130

Name of Component: IP CV-4
Location: IP CV-4_BUSH
Hardness: 130-135HB

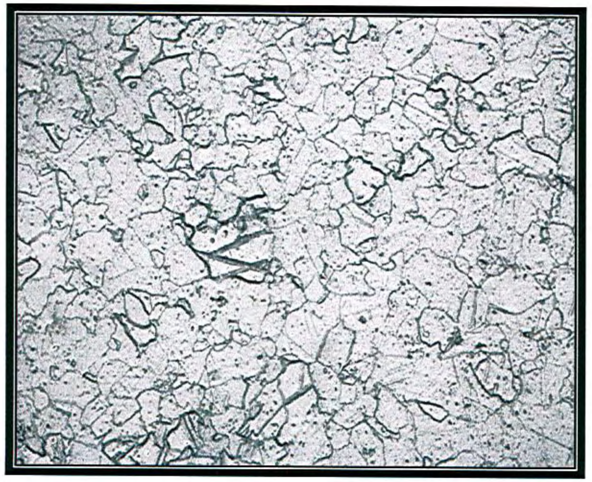

200X

400X

Observation: Microstructure shows tempered Bainite precipitation of carbides at grain boundary.

Degradation Level- IVL

Fig: 131

263

Name of Component: HP SV-1
Location: HP SV-1_CONE
Hardness: 155-156HB

	
200X	400X
Observation: Microstructure shows tempered Bainite precipitation of carbides at grain boundary.	Degradation Level- IVL

Fig: 132

Name of Component: HP SV-1
Location: HP SV-1_BUSH
Hardness: 136-139HB

200X

400X

Observation: Microstructure shows tempered Bainite precipitation of carbides at grain boundary.

Degradation Level- IVL

Fig: 133

Name of Component: HP SV-2
Location: HP SV-2_CONE
Hardness: 136-138HB

	
200X	400X
Observation: Microstructure shows tempered Bainite precipitation of carbides at grain boundary.	Degradation Level- IVL

Fig: 134

Name of Component: HP SV-2
Location: HP SV-2_BUSH
Hardness: 130-136HB

	
200X	400X
Observation: Microstructure shows tempered Bainite precipitation of carbides at grain boundary.	Degradation Level- IVL

Fig: 135

495

Name of Component: HP SV-2
Location: HP SV-2_BUSH
Hardness: 131-135HB

	
200X	400X
Observation: Microstructure shows tempered Bainite precipitation of carbides at grain boundary.	Degradation Level- IVL

Fig: 136

Name of Component: HP SV-3
Location: HP SV-3_BUSH
Hardness: 132-133HB

	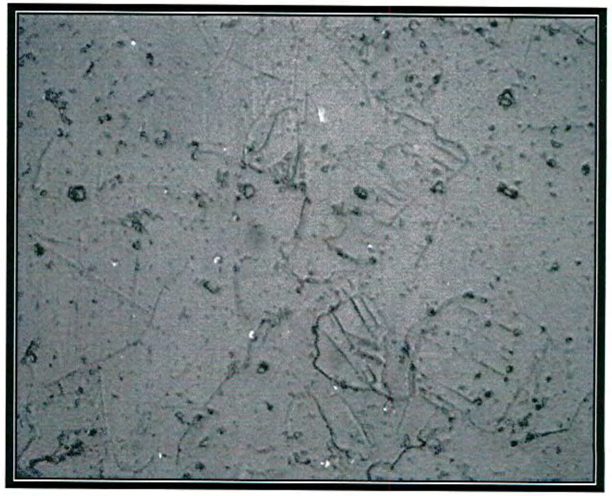
200X	400X
Observation: Microstructure shows tempered Bainite precipitation of carbides at grain boundary.	Degradation Level- IVL

Fig: 137

270

	Client	J-Power (Electric Power Development Co. Ltd.,)
ALSTOM	Project	Turbine and System Assessment for NTPC-Korba Unit #4
	Order No.	CGP10028C
	Contractor	ALSTOM K.K. NASL Ltd. (Nominated subcontractor in India)
NTPC ALSTOM Power Services Pvt. Ltd.	**Document**	**FINAL REPORT VOL. I B(RLA OF TURBINE)**

Name of Component: HP SV-3
Location: HP SV-3_BUSH
Hardness: 130-135HB

	
200X	400X
Observation: Microstructure shows tempered Bainite with precipitation of carbides..	Degradation Level- IIL

Fig: 138

Name of Component: HP SV-3
Location: HP SV-3_BUSH
Hardness: 130-131HB

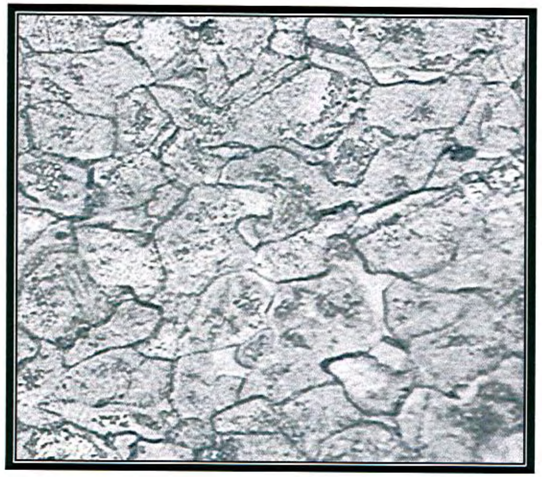	
200X	400X
Observation: Microstructure shows tempered Bainite with spherodisation carbides.	Degradation Level- IIL

Fig: 139

Name of Component: HP SV-4
Location: HP SV-4_CONE
Hardness: 140-143HB

200X

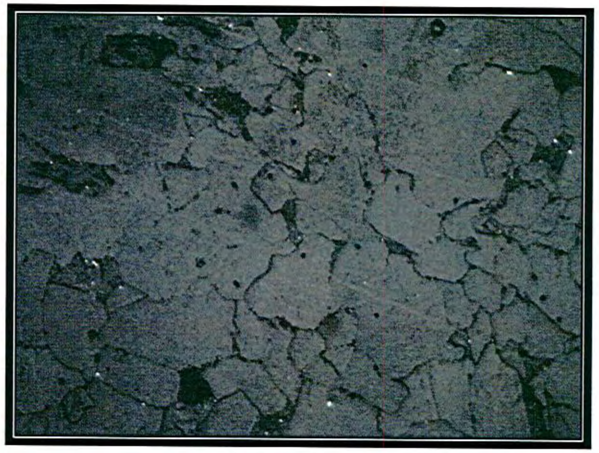

400X

Observation: Microstructure shows tempered Bainite with spherodisation carbides.

Degradation Level- IIL

Fig: 141

Name of Component: HP SV-4
Location: HP SV-4_BUSH
Hardness: 140-145HB

	
200X	400X
Observation: Microstructure shows ferrite and Bainite with precipitation of carbides at grain boundary.	Degradation Level- IVL

Fig: 142

273

Name of Component: HP SV-4
Location: HP SV-4 BUSH
Hardness: 130-135HB

200X

400X

Observation: Microstructure shows ferrite and Bainite with precipitation of carbides at grain boundary.	Degradation Level- IVL

Fig: 143

7.5 EDDY CURRENT TEST REPORT

15

CONTENT

SR. No.	DESCRIPTION	PAGE No.
1.0	Introduction	1
2.0	Equipment used	2
3.0	Observations	2
4.0	Observation Tables & Graphs	3
5.0	Conclusions and Recommendations	9

7.5.1 INTRODUCTION:

Eddy current inspection is one of the significant NDE methods that use the principal of "electromagnetism" as the basis for conducting examinations. Eddy currents are created through a process called electromagnetic induction. When alternating current is applied to the conductor, such as copper wire, a magnetic field develops in and around the conductor. This magnetic field expands as the alternating current rises to maximum and collapses as the current is reduced to zero. If another electrical conductor is brought into the close proximity to this changing magnetic field, current will be induced in this second conductor. Eddy currents are induced electrical currents that flow in a circular path. They get their name from "eddies" that are formed when a liquid or gas flows in a circular path around obstacles when conditions are right. Without any conductive material in the neighborhood, the probe coil behaves like the primary of transformer without any secondary circuit.The basic philosophy of this simplified theory is that the probe coil can be considered as the primary of an electrical transformer, whereas the Eddy currents flowing in the material being tested form the closed secondary circuit of the transformer. Assume that there is a deep crack in the surface immediately underneath the coil. These will interrupt or reduce the eddy current flow as a resistance against the current in the circuit, thus decreasing the loading on the coil and increasing its effective impedance. Note that cracks must interrupt the surface eddy current flow to be detected. Cracks lying parallel to the current path will not cause any significant interruption and may not be detected.

LP Rotor blades were subjected to eddy current inspection. The technical details of the equipment used as well as the details of the singular observations made during this examination are summarized in the following sections:

227

7.5.2 EQUIPMENT USED:

For this inspection, the eddy current test set up with advanced software and specially designed search units supported by laptop computer were used.

1) Eddy current source machine : EddyMax, TMT Germany
2) Software supported by pc : Asus
3) Search units : Differential, Absolute & Edge probe

7.5.3 OBSERVATIONS:

The eddy current inspection was carried out on LP turbine rotor blades to examine surface abnormalities viz erosion damage, crack, material variation. The detailed observations for individual rotors are described below.

7.5.4 LP Turbine Rotor Blades (Moving blades):

The eddy current inspection was carried out on LP turbine rotor blades to examine root area, blade surface, leading edge and trailing edge of the blades. No rubbing marks were observed on rotor blade surface. No any recordable indication observed on root area and trailing edge in any of the blades, while Erosion observed on the leading edge of some of the last stages blades i.e. TS-6 and GS-6.

Individual observations are given in Table below.

OBSERVATION TABLES & GRAPHS:

Table-1

Place of testing: 500 MW Turbine Unit # 4,NTPC-Korba			**Period ;** 23/05/2010 to 24/05/2010
Party Name & Address: KK ALSTOM			**Material Specification:** --
Sample Description/Identification: **LP Turbine Stage No. 6GS – Rotor Blades**			**Stage:** RLA Study
Test Details:			
Particular of test	Eddy Current Testing		
Surface condition	Free from loose scale, dust, paint, oil & grease. Surface was clean & dry.		
Reference Sample	Turbine Blades with natural crack and "V" notch of 0.2, 0.5 and 1mm depth		
Equipment used	EddyMax, Make: TMT,Germany		
Probe used	SD 3E S/N 2332		
Frequency (Hz)	200 kHz		
Source (dB)	0		
Pre Gain (dB)	18.0		
Gain (Db)	10.0		
Phase (°)	192.0		
LP (Hz)	30.0		
HP (Hz)	Off		
Locations	Leading edge, Trailing edge, Root area, Blade surface		
Test Result:			
Sr. No.	**Blade No.**	**Finding/ Observation**	**Remark**
1	1L	No significant defect indication observed	Acceptable
2	2L	No significant defect indication observed	Acceptable
3	3L	No significant defect indication observed	Acceptable
4	4L	No significant defect indication observed	Acceptable
5	5L	No significant defect indication observed	Acceptable
6	6L	No significant defect indication observed	Acceptable
7	7L	No significant defect indication observed	Acceptable
8	8L	No significant defect indication observed	Acceptable
9	9L	No significant defect indication observed	Acceptable
10	10L	No significant defect indication observed	Acceptable
11	11L	No significant defect indication observed	Acceptable
12	12L	No significant defect indication observed	Acceptable
13	13L	No significant defect indication observed	Acceptable
14	14L	No significant defect indication observed	Acceptable
15	15L	No significant defect indication observed	Acceptable
16	16L	No significant defect indication observed	Acceptable

647

Table-1 cont.....

Place of testing: 500 MW Turbine Unit # 4,NTPC-Korba	**Period** 23/05/2010 to 24/05/2010
Party Name & Address: K.K.Alstom	**Material Specification:** --
Sample Description/Identification: **LP Turbine Stage No. 6GS – Rotor Blades**	**Stage:** RLA Study

Test Details:

Particular of test	Eddy Current Testing
Surface condition	Free from loose scale, dust, paint, oil & grease. Surface was clean & dry.
Reference Sample	Turbine Blades with natural crack and "V" notch of 0.2, 0.5 and 1mm depth
Equipment used	Eddy Max, Make: TMT,Germany
Probe used	SD 3E S/N 2332
Frequency (Hz)	200 kHz
Source (dB)	0
Pre Gain (dB)	18.0
Gain (Db)	10.0
Phase (°)	192.0
LP (Hz)	30.0
HP (Hz)	Off
Locations	Leading edge, Trailing edge, Root area, Blade surface

Test Result:

Sr. No.	Blade No.	Finding/ Observation	Remark
17	17L	No significant defect indication observed	Acceptable
18	18L	No significant defect indication observed	Acceptable
19	19L	No significant defect indication observed	Acceptable
20	20L	No significant defect indication observed	Acceptable
21	21L	No significant defect indication observed	Acceptable
22	22L	No significant defect indication observed	Acceptable
23	23L	No significant defect indication observed	Acceptable
24	24L	No significant defect indication observed	Acceptable
25	25L	No significant defect indication observed	Acceptable
26	26L	No significant defect indication observed	Acceptable
27	27L	No significant defect indication observed	Acceptable
28	28L	No significant defect indication observed	Acceptable
29	29L	No significant defect indication observed	Acceptable
30	30L	No significant defect indication observed	Acceptable
31	31L	No significant defect indication observed	Acceptable
32	32L	No significant defect indication observed	Acceptable

Table-1 **cont.....**

Place of testing: 500 MW Turbine Unit # 4,NTPC-Korba			**Period** 23/05/2010 to 24/05/2010
Party Name & Address: K.K.Alstom			**Material Specification:** --
Sample Description/Identification: **LP Turbine Stage No. 6GS – Rotor Blades**			**Stage:** RLA Study
Test Details:			
Particular of test	Eddy Current Testing		
Surface condition	Free from loose scale, dust, paint, oil & grease. Surface was clean & dry.		
Reference Sample	Turbine Blades with natural crack and "V" notch of 0.2, 0.5 and 1mm depth		
Equipment used	EddyMax, Make: TMT,Germany		
Probe used	SD 3E S/N 2332		
Frequency (Hz)	200 kHz		
Source (dB)	0		
Pre Gain (dB)	18.0		
Gain (Db)	10.0		
Phase (°)	192.0		
LP (Hz)	30.0		
HP (Hz)	Off		
Locations	Leading edge, Trailing edge, Root area, Blade surface		
Test Result:			

Sr. No.	Blade No.	Finding/ Observation	Remark
33	33L	No significant defect indication observed	Acceptable
34	34L	No significant defect indication observed	Acceptable
35	35L	No significant defect indication observed	Acceptable
36	36L	No significant defect indication observed	Acceptable
37	37L	No significant defect indication observed	Acceptable
38	38L	No significant defect indication observed	Acceptable
39	39L	No significant defect indication observed	Acceptable
40	40L	No significant defect indication observed	Acceptable
41	41L	No significant defect indication observed	Acceptable
42	42L	No significant defect indication observed	Acceptable
43	43L	No significant defect indication observed	Acceptable
44	44L	No significant defect indication observed	Acceptable
45	45L	No significant defect indication observed	Acceptable
46	46L	No significant defect indication observed	Acceptable
47	47L	No significant defect indication observed	Acceptable
48	48L	No significant defect indication observed	Acceptable

281

Table-2

Place of testing: 500 MW Turbine Unit # 4,NTPC-Korba	**Period** 23/05/2010 to 24/05/2010
Party Name & Address: K.K.Alstom	**Material Specification:** --
Sample Description/Identification: **LP Turbine Stage No. 6TS – Rotor Blades**	**Stage:** RLA Study

Test Details:

Particular of test	Eddy Current Testing
Surface condition	Free from loose scale, dust, paint, oil & grease. Surface was clean & dry.
Reference Sample	Turbine Blades with natural crack and "V" notch of 0.2, 0.5 and 1mm depth
Equipment used	EddyMax, Make: TMT,Germany
Probe used	SD 3E S/N 2332
Frequency (Hz)	200 kHz
Source (dB)	0
Pre Gain (dB)	18.0
Gain (Db)	10.0
Phase (°)	192.0
LP (Hz)	30.0
HP (Hz)	Off
Locations	Leading edge, Trailing edge, Root area, Blade surface

Test Result:

Sr. No.	Blade No.	Finding/ Observation	Remark
1	1T	No significant defect indication observed	Acceptable
2	2T	No significant defect indication observed	Acceptable
3	3T	No significant defect indication observed	Acceptable
4	4T	No significant defect indication observed	Acceptable
5	5T	No significant defect indication observed	Acceptable
6	6T	No significant defect indication observed	Acceptable
7	7T	No significant defect indication observed	Acceptable
8	8T	No significant defect indication observed	Acceptable
9	9T	No significant defect indication observed	Acceptable
10	10T	No significant defect indication observed	Acceptable
11	11T	No significant defect indication observed	Acceptable
12	12T	No significant defect indication observed	Acceptable
13	13T	No significant defect indication observed	Acceptable
14	14T	No significant defect indication observed	Acceptable
15	15T	No significant defect indication observed	Acceptable
16	16T	No significant defect indication observed	Acceptable

Table-2 cont.....

Place of testing: 500 MW Turbine Unit # 4,NTPC-Korba			**Period** 23/05/2010 to 24/05/2010
Party Name & Address: K.K.Alstom			**Material Specification:** --
Sample Description/Identification: **LP Turbine Stage No. 6TS – Rotor Blades**			**Stage:** RLA Study
Test Details:			
Particular of test	Eddy Current Testing		
Surface condition	Free from loose scale, dust, paint, oil & grease. Surface was clean & dry.		
Reference Sample	Turbine Blades with natural crack and "V" notch of 0.2, 0.5 and 1mm depth		
Equipment used	EddyMax, Make: TMT,Germany		
Probe used	SD 3E S/N 2332		
Frequency (Hz)	200 kHz		
Source (dB)	0		
Pre Gain (dB)	18.0		
Gain (Db)	10.0		
Phase (°)	192.0		
LP (Hz)	30.0		
HP (Hz)	Off		
Locations	Leading edge, Trailing edge, Root area, Blade surface		
Test Result:			
Sr. No.	**Blade No.**	**Finding/ Observation**	**Remark**
17	17T	No significant defect indication observed	Acceptable
18	18T	No significant defect indication observed	Acceptable
19	19T	No significant defect indication observed	Acceptable
20	20T	No significant defect indication observed	Acceptable
21	21T	No significant defect indication observed	Acceptable
22	22T	No significant defect indication observed	Acceptable
23	23T	No significant defect indication observed	Acceptable
24	24T	No significant defect indication observed	Acceptable
25	25T	No significant defect indication observed	Acceptable
26	26T	No significant defect indication observed	Acceptable
27	27T	No significant defect indication observed	Acceptable
28	28T	No significant defect indication observed	Acceptable
29	29T	No significant defect indication observed	Acceptable
30	30T	No significant defect indication observed	Acceptable
31	31T	No significant defect indication observed	Acceptable
32	32T	No significant defect indication observed	Acceptable

Table-2 **cont.....**

Place of testing: 500 MW Turbine Unit # 4,NTPC-Korba	**Period** 23/05/2010 to 24/05/2010
Party Name & Address: K.K.Alstom	**Material Specification:** --
Sample Description/Identification: **LP Turbine Stage No. 6TS – Rotor Blades**	**Stage:** RLA Study

Test Details:

Particular of test	Eddy Current Testing
Surface condition	Free from loose scale, dust, paint, oil & grease. Surface was clean & dry.
Reference Sample	Turbine Blades with natural crack and "V" notch of 0.2, 0.5 and 1mm depth
Equipment used	Eddy Max, Make: TMT, Germany
Probe used	SD 3E S/N 2332
Frequency (Hz)	200 kHz
Source (dB)	0
Pre Gain (dB)	18.0
Gain (Db)	10.0
Phase (°)	192.0
LP (Hz)	30.0
HP (Hz)	Off
Locations	Leading edge, Trailing edge, Root area, Blade surface

Test Result:

Sr. No.	Blade No.	Finding/ Observation	Remark
33	33T	No significant defect indication observed	Acceptable
34	34T	No significant defect indication observed	Acceptable
35	35T	No significant defect indication observed	Acceptable
36	36T	No significant defect indication observed	Acceptable
37	37T	No significant defect indication observed	Acceptable
38	38T	No significant defect indication observed	Acceptable
39	39T	No significant defect indication observed	Acceptable
40	40T	No significant defect indication observed	Acceptable
41	41T	No significant defect indication observed	Acceptable
42	42T	No significant defect indication observed	Acceptable
43	43T	No significant defect indication observed	Acceptable
44	44T	No significant defect indication observed	Acceptable
45	45T	No significant defect indication observed	Acceptable
46	46T	No significant defect indication observed	Acceptable
47	47T	No significant defect indication observed	Acceptable
48	48T	No significant defect indication observed	Acceptable

7.5.5 CONCLUSIONS AND RECOMMENDATIONS:

In the light of the inspection and analysis made in different stages and critical locations of LP turbine rotor, the following conclusions are derived:

LP TURBINE:

Overall condition of the LP rotor moving blades is found to be satisfactory. Erosion observed on leading edge of some of the blades during eddy current inspection. Based on explicit observations in various locations i.e. blade root area , leading edge , trailing edge and blade surface of LP turbine rotor, no immediate action is required, however the blades needs replacement in next opportunity..

REPORT

ON

NATURAL FREQUENCY TEST

CONDUCTED ON

LP ROTOR OF STEAM TURBINE (500 MW)

986

CONTENT

Sr.No.	DESCRIPTION	Page No.
1.0	Introduction	01
2.0	Instrumentation System & Accelerometer	03
3.0	Experimental Methodology	04
4.0	Block Diagram Of Test Setup	05
5.0	LP Rotor	06
5.1	Test Report of LP Stage – 44	07
5.2	Test Report of LP Stage – 43	09
5.3	Test Report of LP Stage – 42	11
5.4	Graph Showing Time & Frequency Domain Response of blades	12

1.0 INTRODUCTION:

If a system, after an initial disturbance, is left to vibrate on its own, the frequency with which it oscillates without external forces is known as its natural frequency. In general, a vibratory system having "n" degrees of freedom will have "n" distinct natural frequencies of vibration.

The vibration energy associated with an engineering structure undergoing dynamical excitation under time varying externally applied forces is primarily concentrated at the characteristic frequencies (eigen values) of the structure. Since concentration of excessive vibration energy can lead to excessive vibration amplitudes with accompanying large time varying stresses, the vibrating structure becomes prone to failure by the process of fatigue. In a turbine, one of the components most prone to failure by this mechanism are the rotor blades. Among the various turbine stages, the blading associated with the low pressure stages - especially the last couple of stages – are the most prone to excessive vibrations excited by the various disturbing forces encountered in a turbine. It is thus important that the fundamental vibration frequency of the low-pressure blading be accurately determined using a suitable technique. The technique used to determine the natural frequency of blading involves exciting of blade packets by hammering (to simulate an impulse load) with an instrumented hammer and the resulting vibration, as picked up by an accelerometer, is recorded using a digital storage oscilloscope and subsequently converted into a frequency domain transfer function record of the original signal using a Fast Fourier Transform (FFT) algorithm. The natural frequency of the first three vibration modes is subsequently extracted from this transfer function record.

The natural frequency of a system can be changed either by varying the mass "m" or the stiffness "K". In many practical cases, however, the mass cannot be changed easily, since its value is determined by the functional requirements of the system. For example, the mass of a flywheel on a shaft is determined by the functional requirements of the system. For example, the mass of a flywheel on a shaft is determined by the amount of energy it must store in one cycle. Therefore, the stiffness of the system is the factor that is most often changed to alter its natural frequencies. For example, the stiffness of a rotating shaft can be alerted by varying one or more of its parameters, such as the material or number and location of support points (bearings).

2.0 INSTRUMENTATION SYSTEM & ACCELEROMETER:

The portable conditioning monitoring system consists of portable fast Fourier transform vibration analyzer. This vibration analyzer can be used for fault detection by recording and storing vibration spectra from each of the measurement points. Each newly recorded spectrum can be compared with a reference spectrum that was recorded at that particular measurement point, when the machine was known to be in good condition. Any significant increase in the amplitudes in the new spectrum indicates a fault that needs further investigation. The vibration analyzer also has certain diagnostic capability to identify the problems such as looseness of assembled rotor blades, faulty belt drives, gearboxes, and loose bearings. If a rotor requires balancing, the vibration analyzer can be used to compute the location and magnitudes of the correction masses necessary to rebalance the rotor.

An Accelerometer is an instrument that measures the acceleration of a vibrating body. Accelerometers are widely used for vibration measurement and also record earthquakes. They are preferred because of their smaller size and superior frequency response, dynamic range, reliability over long periods and robustness. When an accelerometer is used as vibration pick up, the velocity and displacement can be obtained from integrators built in the analyzer. Thus, the user can choose between acceleration, velocity and displacement as the monitoring parameter. Any of these three spectra can be used for the condition monitoring of a machine.

3.0 EXPERIMENTAL METHODOLOGY:

For determining the fundamental natural frequency of assembled blades of turbine rotor, an accelerometer is mounted (affixed) on a blade in case of free standing blades. For a blade packet, the accelerometer is usually affixed on the central blade of the packet. The blade/blade packet is excited by giving an impact on the blade with the help of a tuned hammer. The response of the blade/blade packet is picked up by the accelerometer and the charge amplifier amplifies the vibration signal to a level required for the oscilloscope and the captured time domain signal is displayed & stored. The time domain signal is also transformed into the frequency domain using the Discrete Fourier Transform (DFT) technique. This DFT spectra is displayed and also stored in the oscilloscope for subsequent analysis and processing.

The first major peak in the DFT spectra should be considered as a fundamental frequency of particular blade under test. For a well-tuned blade/blade packet the first fundamental frequency should not go close to 50 Hz & in general should not be a multiple of 50 Hz, which is the rotational velocity of the rotor.

4.0 BLOCK DIAGRAM

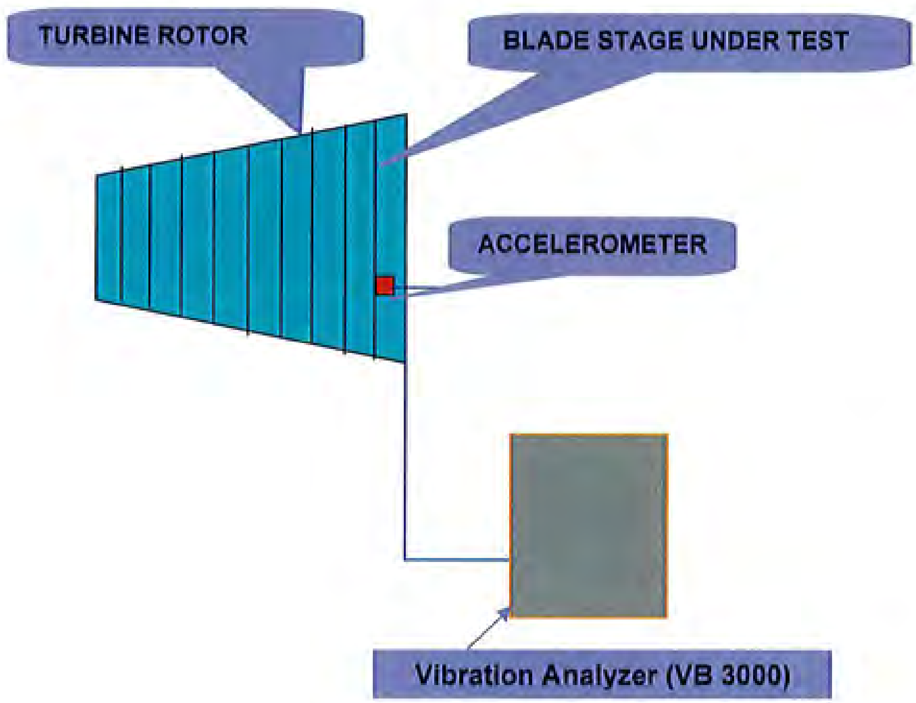

BLOCK DIAGRAM FOR NFT SETUP

5.0 LP ROTOR

5.1 Natural Frequency Test Report (4GS)

Party Name & Address: M/s. KK ALSTOM			**Site :** NTPC -Korba	
Component Description/Identification: LP Rotor Stage No. : 4 Generator Side			**Total No. Of blades:** 68	
Fréquency Range : F_1 : 242-263 Hz			**Drop Allowed : 8**	
Test Result:				
Sr.No.	**Blade no.**	**Previous Press (F_1)**	**Rotor (F_2)**	**Difference**
1	2229	258.0	257.5	0.5
2	2215	256.0	255.0	1
3	2226	256.0	257.5	1.5
4	2240	258.0	257.5	0.5
5	2231	253.0	250.0	3
6	2218	256.0	255.0	1
7	2238	257.0	252.5	4.5
8	2280	253.0	252.5	0.5
9	2275	257.0	255.0	2
10	2239	253.0	253.0	0
11	2206	258.0	258.0	0
12	2270	257.0	252.5	4.5
13	2241	257.0	252.5	4.5
14	2222	261.0	258.0	3
15	2221	260.0	257.5	2.5
16	2223	260.0	255.0	5
17	2220	256.0	250.0	6
18	2224	257.0	252.5	4.5
19	2225	256.0	257.5	1.5
20	2208	258.0.	257.5	0.5
21	2228	257.0	255.0	2
22	2217	257.0	257.5	0.5
23	2230	258.0	257.5	0.5
24	2210	257.0	255.0	2
25	2232	256.0	255.0	1
26	2233	256.0	255.0	1
27	2234	256.0	255.0	1
28	2235	260.0	258.0	2
29	2236	253.0	252.5	0.5
30	2237	256.0	252.5	3.5
31	2213	251.0	252.5	1.5
32	2216	256.0	252.5	3.5
33	2209	251.0	257.5	6.5
34	2219	253.0	250.0	3

Note:
1) "*" Number as punched on the blade.

292

Cont......

Party Name & Address: M/s. KK ALSTOM				**Site :** NTPC - Korba
Component Description/Identification: LP Rotor Stage No. : 4 Generator Side				**Total No. Of blades:** 68
Fréquency Range : **F_1 : 242-263 Hz**				**Drop Allowed : 8**
Test Result:				
Sr.No.	**Blade no.**	**Previous Press (F_1)**	**Rotor (F_2)**	**Difference**
35	2242	252.0	255.0	3
36	2243	256.0	260.0	4
37	2244	256.0	252.5	3.5
38	2245	256.0	252.5	3.5
39	2246	253.0	252.5	0.5
40	2247	256.0	255.0	1
41	2248	248.0	250.0	2
42	2255	255.0	252.5	2.5
43	2256	252.0	252.5	0.5
44	2257	256.0	252.5	3.5
45	2259	248.0	252.5	4.5
46	2262	248.0	252.5	4.5
47	2263	252.0	252.5	0.5
48	2264	252.0	255.0	3
49	2265	253.0	252.5	0.5
50	2266	256.0	255.0	1
51	2268	260.0	260.0	0
52	2267	257.0	257.0	0
53	2269	253.0	252.5	0.5
54	2211	257.0	257.5	0.5
55	2272	256.0	255.0	1
56	2273	253.0	252.5	0.5
57	2274	252.0	252.5	0.5
58	2207	253.0	252.5	0.5
59	2276	256.0	255.0	1
60	2277	257.0	256.0	1
61	2279	256.0	255.0	1
62	2214	256.0	257.5	1.5
63	2281	256.0	260.0	4
64	2282	253.0	252.5	0.5
65	2283	257.0	255.0	2
66	2284	253.0	252.5	0.5
67	2285	252.0	252.0	0
68	2286	253.0	250.0	3

Note:
1) '*' Number as punched on the blade.

393

5.1 Natural Frequency Test Report (4TS)

Party Name & Address: M/s. KK ALSTOM	Site : NTPC – Korba.
Component Description/Identification: LP Rotor Stage No. : 4 Turbine Side	Total No. Of blades: 68
Fréquency Range : F_1 : 242-263 Hz	Drop Allowed : 8

Test Result:

Sr.No.	Blade no.	Previous Press (F_1)	Rotor (F_2)	Difference
1	2352	260.0	255.0	5.0
2	2341	245.0	257.5	12.5
3	2349	258.0	260.0	2
4	2305	255.0	255.0	0
5	2384	248.0	252.5	4.5
6	2354	257.0	257.5	0.5
7	2381	255.0	255.0	0
8	2347	251.0	255.0	4
9	2416	255.0	252.5	2.5
10	2394	256.0	257.5	1.5
11	2387	255.0	255.0	0
12	2337	256.0	255.0	1
13	2334	256.0	260.0	4
14	2345	257.0	260.0	3
15	2263	253.0	255.0	2
16	2346	257.0	257.0	0
17	2275	253.0	252.5	0.5
18	2351	252.0	252.5	0.5
19	2270	247.0	252.5	5.5
20	2350	248.0	252.5	4.5
21	2348	248.0	252.5	4.5
22	2261	248.0	255.0	7
23	2353	256.0	257.5	1.5
24	2265	255.0	255.0	0
25	2356	256.0	257.5	1.5
26	2355	256.0	257.5	1.5
27	2357	257.0	257.5	0.5
28	2360	256.0	255.0	1
29	2359	257.0	257.5	0.5
30	2361	257.0	255.0	2
31	2358	255.0	257.5	2.5
32	2362	257.0	257.5	0.5
33	2363	257.0	260.0	3
34	2364	257.0	257.5	0.5

Note:
1) '*' Number as punched on the blade.

394

Cont......

Party Name & Address: M/s. KK ALSTOM	Site : NTPC - Korba
Component Description/Identification: LP Rotor Stage No. : 4 Turbine Side	**Total No. Of blades:** 68

Fréquency Range :

F_1 : 242-263 Hz **Drop Allowed : 8**

Test Result:

Sr.No.	Blade no.	Previous Press (F_1)	Rotor (F_2)	Difference
35	2365	256.0	257.5	1.5
36	2366	257.0	255.0	2
37	2367	255.0	255.0	0
38	2368	256.0	255.0	1
39	2370	253.0	255.0	2
40	2369	252.0	252.5	0.5
41	2372	257.0	257.5	0.5
42	2371	257.0	255.0	2
43	2373	256.0	255.0	1
44	2375	257.0	257.5	0.5
45	2376	257.0	255.0	2
46	2377	257.0	257.0	0
47	2378	256.0	256.0	0
48	2379	256.0	257.0	1
49	2272	257.0	257.0	0
50	2380	260.0	260.0	0
51	2382	257.0	255.0	2
52	2383	257.0	255.0	2
53	2269	256.0	255.0	1
54	2386	257.0	257.5	0.5
55	2332	247.0	257.5	10.5
56	2388	251.0	260.0	9
57	2390	252.0	255.0	3
58	2392	253.0	252.5	0.5
59	2393	248.0	255.0	7
60	2266	251.0	255.0	4
61	2395	248.0	255.0	7
62	2411	253.0	253.0	0
63	2396	245.0	253.0	8
64	2414	237.0	252.5	15.5
65	2276	263.0	260.0	3
66	2420	253.0	255.0	2
67	2421	251.0	250.0	1
68	2422	252.0	257.5	5.5

Note:
1) '*' Number as punched on the blade.

5.1 Natural Frequency Test Report (5TS)

Party Name & Address: M/s. KK ALSTOM	Site : NTPC -Korba
Component Description/Identification: LP Rotor Stage No. : 5 Generator Side	**Total No. Of blades:** 58
Fréquency Range : F_1 : 136-160 Hz **F_2 : 287-308 Hz**	**Drop Allowed : 4** **Drop Allowed : 9**

Test Result:

Sr. No.	Blade no.	Previous Press (F_1)	Rotor (F_1)	Difference	Previous Press (F_2)	Rotor (F_2)	Difference
1	1382	137.5	136.0	1.5	295.0	292.0	3
2	1340	137.5	138.0	0.5	290.0	290.0	0
3	1385	137.5	136.0	1.5	295.0	292.0	3
4	1323	135.0	136.0	1	290.0	291.0	1
5	1358	135.0	133.0	2	292.5	295.0	2.5
6	1333	135.0	136.0	1	290.0	293.0	3
7	1327	135.0	135.0	0	292.5	291.0	1.5
8	1325	135.0	135.0	0	290.0	287.0	3
9	1324	137.5	135.0	2.5	295.0	291.0	4
10	1328	135.0	135.0	0	295.0	290.0	5
11	1329	137.5	137.0	0.5	292.5	293.0	0.5
12	1321	135.0	141.0	6	287.5	288.0	0.5
13	1331	135.0	135.0	0	292.5	290.0	2.5
14	1332	135.0	135.0	0	287.5	287.0	0.5
15	1330	135.0	135.0	0	292.5	293.0	0.5
16	1334	137.5	135.0	2.5	295.0	295.0	0
17	1335	145.0	147.0	2	292.5	295.0	2.5
18	1336	135.0	133.0	2	292.5	290.0	2.5
19	1243	135.0	135.0	0	292.5	290.0	2.5
20	1338	152.5	151.0	1.5	292.5	292.0	0.5
21	1344	138.0	143.0	5	290.0	288.0	2
22	1337	137.5	135.0	2.5	295.0	288.0	7
23	1341	137.5	135.0	2.5	297.5	295.0	2.5
24	1342	135.5	135.0	0.5	295.0	293.0	2
25	1343	135.0	135.0	0	292.5	291.0	1.5
26	1339	137.5	136.0	1.5	295.0	295.0	0
27	1345	135.0	133.0	2	290.0	295.0	5
28	1346	137.5	137.0	0.5	295.0	288.0	7
29	1347	137.5	135.0	2.5	295.0	293.0	2

Note:

1) '*' Number as punched on the blade.

Cont......

Party Name & Address: M/s. KK ALSTOM	Site : NTPC - Korba
Component Description/Identification: LP Rotor Stage No. : 5 Generator Side	**Total No. Of blades:** 58
Fréquency Range : F_1 : 136-160 Hz **F_2 : 287-308 Hz**	**Drop Allowed : 4** **Drop Allowed : 9**

Test Result:

Sr. No.	Blade no.	Previous Press (F_1)	Rotor (F_2)	Difference	Previous Press (F2)	Rotor (F_2)	Difference
30	1349	137.5	135.0	2.5	292.5	288.0	4.5
31	1350	137.5	136.0	1.5	295.0	288.0	7
32	1353	135.0	135.0	0	295.0	290.0	5
33	1352	137.5	135.0	2.5	295.0	291.0	4
34	1351	135.0	135.0	0	290.0	286.0	4
35	1354	135.0	135.0	0	292.5	292.0	0.5
36	1355	135.0	135.0	0	292.5	292.0	0.5
37	1356	135.0	136.0	1	290.0	288.0	2
38	1357	135.0	135.0	0	295.0	290.0	5
39	1322	135.0	135.0	0	292.5	287.0	5.5
40	1389	135.0	133.0	2	290.0	283.0	7
41	1360	135.0	132.0	3	292.5	283.0	10.5
42	1361	135.0	135.0	0	287.5	296.0	8.5
43	1362	135.0	136.0	1	292.5	291.0	1.5
44	1363	135.0	135.0	0	292.5	288.0	4.5
45	1365	135.0	133.0	2	292.5	288.0	4.5
46	1366	135.0	133.0	2	290.0	288.0	2
47	1367	137.5	136.0	1.5	290.0	286.0	4
48	1368	135.0	135.0	0	290.0	292.0	2
49	1369	135.0	135.0	0	290.0	290.0	0
50	1370	135.0	135.0	0	292.5	293.0	0.5
51	1371	135.0	135.0	0	292.5	293.0	0.5
52	1372	135.0	135.0	0	292.5	293.0	0.5
53	1373	136.0	136.0	0	287.5	287.0	0.5
54	1232	135.0	135.0	0	290.0	288.0	2
55	1383	135.0	135.0	0	292.5	288.0	4.5
56	1251	137.0	135.0	2	290.0	288.0	2
57	1386	137.5	145.0	7.5	295.0	292.0	3
58	1288	135.0	135.0	0	295.0	295.0	0

Note:

1) '*' Number as punched on the blade.

5.1 Natural Frequency Test Report (5TS)

Party Name & Address: M/s. KK ALSTOM.	**Site :** NTPC , Korba
Component Description/Identification: LP Rotor Stage No. : 5 Turbine Side	**Total No. Of blades:** 58
Fréquency Range : F_1 : 136-160 Hz **F_2 : 287-308 Hz**	**Drop Allowed : 4** **Drop Allowed : 9**

Test Result:

Sr. No.	Blade no.	Previous Press (F_1)	Rotor (F_1)	Difference	Previous Press (F_2)	Rotor (F_2)	Difference
1	1214	135.0	135.0	0	292.5	295.0	2.5
2	1184	137.5	136.0	1.5	295.0	296.0	1
3	1237	135.0	137.0	2	297.5	298.0	0.5
4	1228	135.0	135.0	0	295.0	296.0	1
5	1176	137.5	137.0	0.5	295.0	293.0	2
6	1182	135.0	135.0	0	295.0	296.0	1
7	1180	135.0	135.0	0	292.5	292.0	0.5
8	1243	135.0	135.0	0	295.0	292.0	3
9	1240	135.0	135.0	0	295.0	295.0	0
10	1177	135.0	135.0	0	292.5	296.0	4.5
11	1187	137.5	136.0	1.5	297.5	297.0	0.5
12	1178	135.0	135.0	0	295.0	293.0	2
13	1179	135.0	135.0	0	292.5	290.0	2.5
14	1172	135.0	135.0	0	295.0	293.0	2
15	1180	135.0	133.0	2	295.0	293.0	2
16	1173	135.0	135.0	0	297.5	296.0	1.5
17	1183	135.0	132.0	3	295.0	288.0	7
18	1168	135.0	133.0	2	295.0	291.0	4
19	1185	135.0	135.0	0	292.5	291.0	1.2
20	1186	135.0	135.0	0	295.0	292.0	3
21	1171	135.0	136.0	1	297.5	296.0	1.5
22	1188	135.0	136.0	1	292.5	292.0	0
23	1190	137.5	135.0	2.5	297.5	296.0	1.5
24	1189	137.5	135.0	2.5	295.0	291.0	4
25	1191	135.0	133.0	2	295.0	288.0	7
26	1192	137.5	136.0	1.5	297.5	295.0	2.5
27	1193	135.0	135.0	0	295.0	292.0	3
28	1194	137.5	135.0	2.5	295.0	291.0	4
29	1205	135.0	133.0	2	297.5	292.0	5.5

Note:

1) '*' Number as punched on the blade.

298

Cont......

Party Name & Address: M/s. KK ALSTOM

Site : NTPC - Korba

Component Description/Identification: LP Rotor Stage No. : 5 Turbine Side

Total No. Of blades: 58

Fréquency Range : F_1 : 136-160 Hz **Drop Allowed : 4**

F_2 : 287-308 Hz **Drop Allowed : 9**

Test Result:

Sr. No.	Blade no.	Previous Press (F_1)	Rotor (F_2)	Difference	Previous Press (F2)	Rotor (F_2)	Difference
30	1206	135.0	133.0	2	295.0	288.0	7
31	1167	135.0	133.0	2	295.0	288.0	7
32	1215	135.0	135.0	0	295.0	288.0	7
33	1216	135.0	135.0	0	295.0	292.0	3
34	1217	137.5	136.0	1.5	297.5	296.0	1.5
35	1218	135.0	135.0	0	295.0	297.0	2
36	1220	135.0	133.0	2	297.5	288.0	10.5
37	1222	135.0	135.0	0	297.5	293.0	4.5
38	1224	135.5	135.0	0.5	295.0	292.0	3
39	1225	135.0	135.0	0	287.0	288.0	1
40	1226	135.0	135.0	0	295.0	295.0	0
41	1229	137.5	135.0	2.5	297.5	292.0	5.5
42	1170	137.0	135.0	2	297.0	295.0	2
43	1227	135.0	136.0	1	292.5	293.0	0.5
44	1230	135.0	132.0	3	292.5	285.0	7.5
45	1231	135.0	135.0	0	292.5	292.0	0.5
46	1234	137.5	135.0	2.5	297.5	296.0	1.5
47	1233	135.0	136.0	1	290.0	291.0	1
48	1235	135.0	133.0	2	295.0	292.0	3
49	1236	135.0	133.0	2	295.0	288.0	7
50	1169	137.5	133.0	4.5	297.5	288.0	10.5
51	1238	137.5	135.0	2.5	300.0	297.0	3
52	1239	137.5	136.0	1.5	297.5	295.0	2.5
53	1175	137.5	135.0	2.5	297.5	295.0	2.5
54	1242	137.5	135.0	2.5	295.0	293.0	2
55	1174	135.0	135.0	0	292.5	293.0	0.5
56	1244	135.0	136.0	1	295.0	296.0	1
57	1245	135.0	135.0	0	295.0	297.0	2
58	1246	137.5	136.0	1.5	297.5	298.0	0.5

Note:

1) '*' Number as punched on the blade.

5.1 Natural Frequency Test Report (5TS)

Party Name & Address:
M/s. KK ALSTOM

Site :
NTPC - Korba

Component Description/Identification:
LP Rotor Stage No. : 6 Generator Side

Total No. Of blades:
48

Fréquency Range : F_1 : 20- 45 Hz — **Drop Allowed : 1**
F_2 : 95- 123 Hz — **Drop Allowed : 4**

Test Result:

Sr. No.	Blade no.	Previous Press (F_1)	Rotor (F_1)	Difference	Previous Press (F_2)	Rotor (F_2)	Difference
1	655	45.0	45.0	0	102.5	103.0	1.5
2	720	45.0	45.0	0	102.5	102.0	0.5
3	684	45.0	45.0	0	105.0	103.0	2
4	507	45.0	45.0	0	102.5	98.0	4.5
5	749	45.0	45.0	0	102.5	103.0	1
6	752	45.0	45.0	0	105.0	103.0	2
7	542	45.0	44.0	1	100.0	100.0	0
8	698	45.0	45.0	0	102.5	102.0	0.5
9	522	45.0	45.0	0	102.5	102.0	0.5
10	675	45.0	45.0	0	102.5	103.0	0.5
11	534	45.0	45.0	0	100.0	99.0	1
12	540	42.5	44.0	1.5	100.0	101.0	1
13	508	42.5	44.0	1.5	100.0	100.0	0
14	C5362	45.0	44.0	1	102.5	101.0	1.5
15	556	45.0	44.0	1	100.0	102.0	2
16	563	44.0	44.0	0	100.0	101.0	1
17	566	43.0	43.0	0	100.0	114.0	14
18	572	42.5	44.0	1.5	115.0	123.0	8
19	574	42.5	41.0	1.5	102.5	128.0	25.5
20	579	44.0	43.0	1	100.0	100.0	0
21	583	45.0	44.0	1	100.0	99.0	1
22	651	45.0	45.0	0	100.0	100.0	0
23	484	42.5	43.0	0.5	100.0	100.0	0
24	661	45.0	44.0	1	102.5	103.0	0.5
25	663	45.0	45.0	0	102.5	99.0	3.5
26	664	45.0	45.0	0	102.5	123.0	21.5
27	669	45.0	45.0	0	102.5	102.0	0.5
28	533	45.0	45.0	0	102.5	102.0	0.5
29	493	45.0	44.0	1	102.5	100.0	2.5

Note:
1) "*" Number as punched on the blade.

Cont......

Party Name & Address: M/s. KK ALSTOM	**Site :** NTPC – Korba.
Component Description/Identification: LP Rotor Stage No. : 6 Generator Side	**Total No. Of blades:** 58
Fréquency Range : F_1 : 136-160 Hz **F_2 : 287-308 Hz**	**Drop Allowed : 4** **Drop Allowed : 9**

Test Result:

Sr. No.	Blade no.	Previous Press (F_1)	Rotor (F_2)	Difference	Previous Press (F2)	Rotor (F_2)	Difference
30	703	45.0	45.0	0	102.5	100.0	2.5
31	509	42.5	43.0	1.5	100.0	100.0	0
32	687	45.0	43.0	2	100.0	98.0	2
33	709	45.0	45.0	0	100.0	102.0	2
34	717	45.0	45.0	0	102.5	102.0	0.5
35	486	45.0	43.0	2	100.0	100.0	0
36	726	45.0	44.0	1	97.5	100.0	3.5
37	745	45.0	44.0	1	100.0	96.0	4
38	746	45.0	44.0	1	97.5	102.0	5.5
39	505	45.0	44.0	1	100.0	101.0	1
40	494	45.0	45.0	0	100.0	102.0	2
41	754	45.0	45.0	0	102.5	101.0	1.5
42	760	45.0	45.0	0	100.0	102.0	2
43	497	45.0	44.0	1	100.0	100.0	0
44	766	45.0	45.0	0	100.0	98.0	2
45	774	45.0	45.0	0	102.5	102.0	0.5
46	767	45.0	45.0	0	100.0	101.0	1
47	792	45.0	44.0	1	102.5	102.0	0.5
48	800	45.0	45.0	0	102.0	103.0	1

Note:

1) '*' Number as punched on the blade.

301

5.1 Natural Frequency Test Report (5TS)

Party Name & Address: M/s. KK ALSTOM.

Site : NTPC , Korba

Component Description/Identification: LP Rotor Stage No. : 6 Turbine Side

Total No. Of blades: 48

Fréquency Range : F_1 : 20- 45 Hz — **Drop Allowed : 1**

F_2 : 95- 123 Hz — **Drop Allowed : 4**

Test Result:

Sr. No.	Blade no.	Previous Press (F_1)	Rotor (F_1)	Difference	Previous Press (F_2)	Rotor (F_2)	Difference
1	534	42.5	41.0	1.5	102.5	103.0	0.5
2	561	42.5	43.0	0.5	100.0	95.0	5
3	539	45.0	37.0	7	100.0	101.0	1
4	578	42.5	42.0	0.5	100.0	101.0	1
5	574	42.5	40.0	2.5	100.0	103.0	3
6	714	42.5	41.0	1.5	97.5	98.0	0.5
7	731	42.5	43.0	0.5	100.0	101.0	1
8	758	45.0	43.0	2	100.0	99.0	1
9	579	42.5	45.0	2.5	100.0	100.0	0
10	733	42.5	43.0	0.5	100.0	98.0	2
11	766	45.0	45.0	0	100.0	101.0	1
12	710	45.0	44.0	1	100.0	95.0	5
13	757	45.0	42.0	3	100.0	99.0	1
14	527	45.0	43.0	2	97.5	101.0	3.5
15	770	45.0	43.0	2	102.5	102.0	0.5
16	562	42.5	41.0	1.5	100.0	98.0	2
17	526	45.0	43.0	2	100.0	101.0	1
18	538	45.0	44.0	1	100.0	101.0	1
19	619	45.0	44.0	1	100.0	99.0	1
20	604	45.0	44.0	1	100.0	101.0	1
21	592	45.0	44.0	1	100.0	100.0	0
22	607	45.0	44.0	1	97.5	99.0	1.5
23	605	42.5	43.0	0.5	97.5	100.0	2.5
24	621	42.5	43.0	0.5	100.0	99.0	1
25	629	45.0	44.0	1	100.0	100.0	0
26	635	42.5	43.0	0.5	100.0	99.0	1
27	640	45.0	45.0	0	102.5	103.0	0.5
28	655	45.0	43.0	2	100.0	101.0	1
29	662	45.0	44.0	1	100.0	101.0	1

Note:

1) '*' Number as punched on the blade.

302

Cont......

Party Name & Address: M/s. KK ALSTOM.	**Site :** NTPC , Korba
Component Description/Identification: LP Rotor Stage No. : 6 Turbine Side	**Total No. Of blades:** 48

Fréquency Range : F_1 : 20- 45 Hz **Drop Allowed : 1**
F_2 : 95- 123 Hz **Drop Allowed : 4**

Test Result:

Sr. No.	Blade no.	Previous Press (F_1)	Rotor (F_2)	Difference	Previous Press (F2)	Rotor (F_2)	Difference
30	673	45.0	43.0	2	100.0	102.0	2
31	670	45.0	44.0	1	97.5	100.0	2.5
32	675	45.0	44.0	1	100.0	102.0	2
33	694	45.0	44.0	1	102.0	110.0	8
34	558	45.0	45.0	0	102.0	102.0	0
35	533	42.5	44.0	1.5	97.5	97.0	0.5
36	721	45.0	44.0	1	100.0	102.0	2
37	498	42.5	43.0	0.5	97.5	98.0	0.5
38	518	45.0	44.0	1	100.0	102.0	2
39	737	45.0	44.0	1	102.5	101.0	1.5
40	748	45.0	45.0	0	100.0	101.0	1
41	751	45.0	45.0	0	100.0	102.0	2
42	754	45.0	43.0	2	100.0	94.0	6
43	517	45.0	45.0	0	102.5	95.0	7.5
44	535	45.0	44.0	1	100.0	97.0	2.5
45	759	45.0	44.0	1	102.5	99.0	3.5
46	763	45.0	44.0	1	102.5	103.0	0.5
47	543	45.0	45.0	0	102.5	115.0	12.5
48	572	45.0	44.0	1	100.0	99.0	1

Note:
1) '*' Number as punched on the blade.

303

ALSTOM	Client	J-Power (Electric Power Development Co. Ltd.,)
	Project	Turbine and System Assessment for NTPC-Korba Unit #4
	Order No.	CGP10028C
	Contractor	ALSTOM K.K. NASL Ltd. (Nominated subcontractor in India)
NTPC ALSTOM Power Services Pvt. Ltd.	**Document**	**FINAL REPORT VOL. I B (RLA of Turbine)**

5.4 Graphs showing Time & Frequency Domain Response

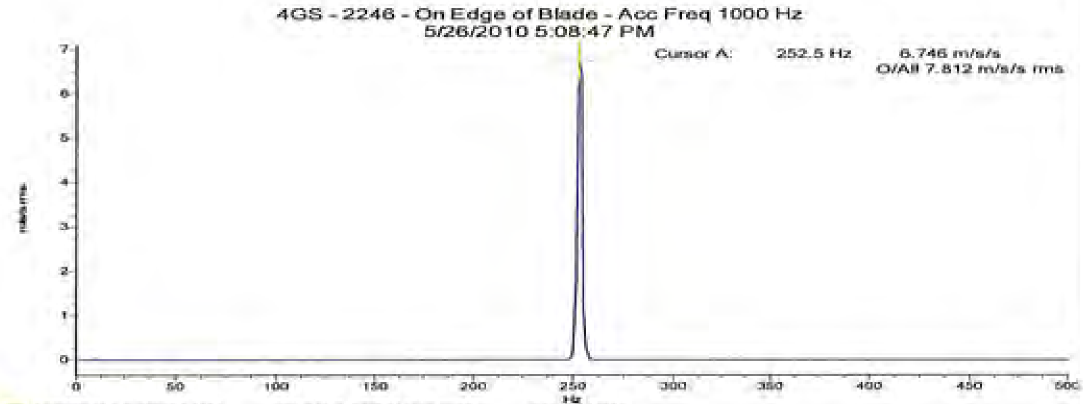

5/26/2010 5:08:47 PM O/All 7.812 m/s/s rms <set RPM>

Top 10 Peaks

252.188 Hz	6.746 m/s/s rms
588.016 Hz	0.321 m/s/s rms
583.022 Hz	0.308 m/s/s rms
576.78 Hz	0.141 m/s/s rms
937.578 Hz	0.059 m/s/s rms
955.019 Hz	0.055 m/s/s rms
982.522 Hz	0.037 m/s/s rms
558.053 Hz	0.037 m/s/s rms
9.988 Hz	0.026 m/s/s rms
991.261 Hz	0.013 m/s/s rms

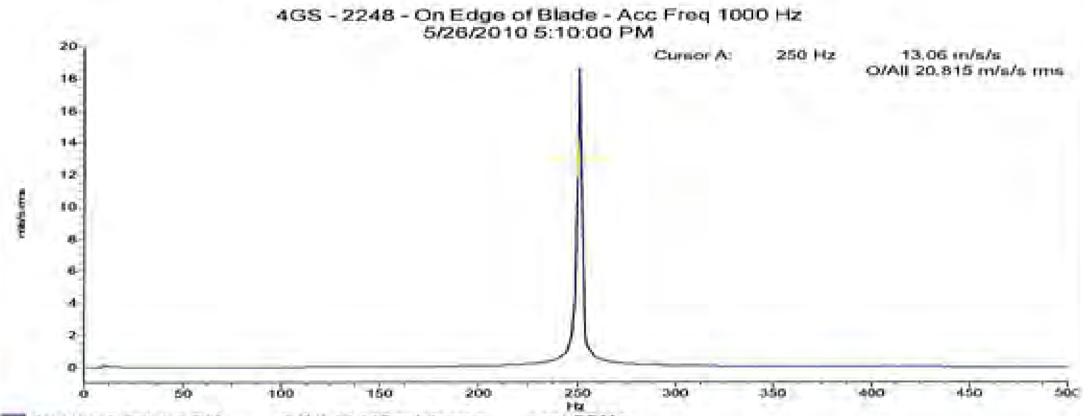

5/26/2010 5:10:00 PM O/All 20.815 m/s/s rms <set RPM>

Top 10 Peaks

250.938 Hz	18.581 m/s/s rms
568.041 Hz	0.511 m/s/s rms
583.022 Hz	0.335 m/s/s rms
933.833 Hz	0.264 m/s/s rms
985.267 Hz	0.255 m/s/s rms
588.016 Hz	0.176 m/s/s rms
218.727 Hz	0.176 m/s/s rms
9.988 Hz	0.159 m/s/s rms
213.494 Hz	0.141 m/s/s rms
208.491 Hz	0.123 m/s/s rms

304

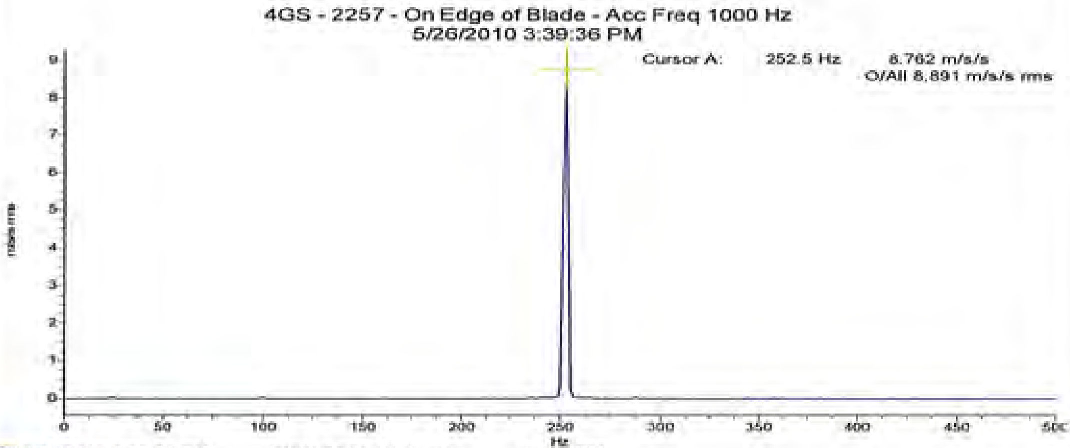

5/26/2010 3:39:36 PM O/All 8.891 m/s/s rms <set RPM>

Top 10 Peaks

252.186 Hz	8.762 m/s/s rms
927.591 Hz	0.037 m/s/s rms
936.33 Hz	0.032 m/s/s rms
931.336 Hz	0.019 m/s/s rms
907.616 Hz	0.017 m/s/s rms
921.348 Hz	0.015 m/s/s rms
580.525 Hz	0.013 m/s/s rms
992.509 Hz	0.012 m/s/s rms
585.519 Hz	0.004 m/s/s rms
986.267 Hz	0.004 m/s/s rms

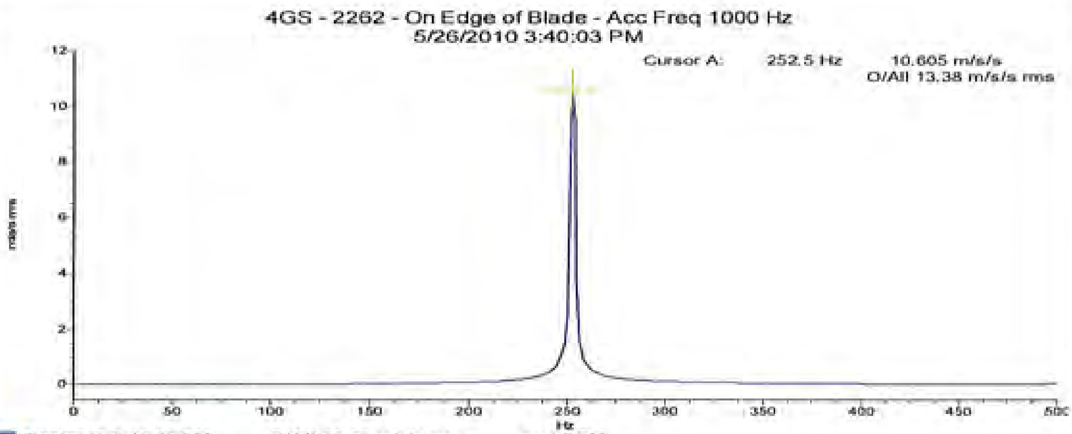

5/26/2010 3:40:03 PM O/All 13.38 m/s/s rms <set RPM>

Top 10 Peaks

252.186 Hz	10.605 m/s/s rms
505.619 Hz	0.601 m/s/s rms
935.081 Hz	0.489 m/s/s rms
584.27 Hz	0.401 m/s/s rms
757.603 Hz	0.268 m/s/s rms
573.034 Hz	0.249 m/s/s rms
584.295 Hz	0.167 m/s/s rms
993.758 Hz	0.165 m/s/s rms
931.336 Hz	0.141 m/s/s rms
940.075 Hz	0.136 m/s/s rms

5GS - 1322 - On Edge of Blade - Acc Freq 1000 Hz
5/26/2010 4:08:37 PM

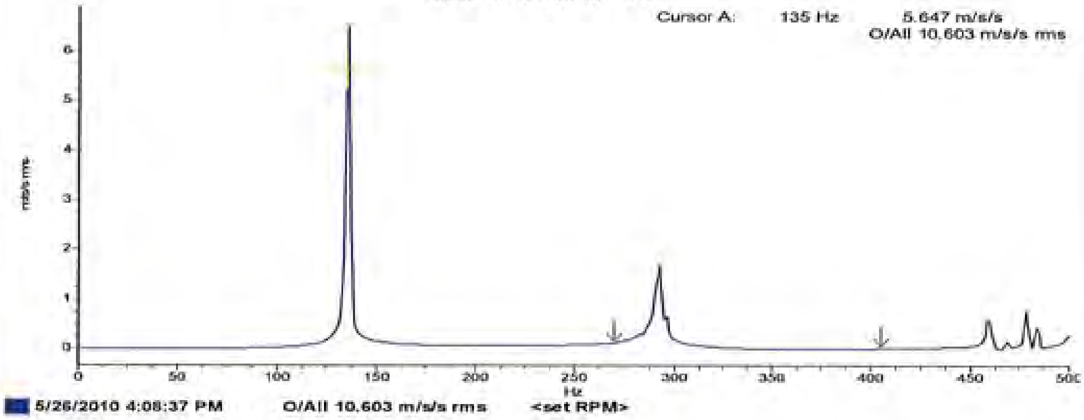

5/26/2010 4:08:37 PM O/All 10.603 m/s/s rms <set RPM>

Top 10 Peaks

135.081 Hz	6.498 m/s/s rms
509.364 Hz	5.328 m/s/s rms
515.606 Hz	2.727 m/s/s rms
513.109 Hz	2.62 m/s/s rms
292.136 Hz	1.715 m/s/s rms
501.873 Hz	1.158 m/s/s rms
478.153 Hz	0.768 m/s/s rms
295.881 Hz	0.653 m/s/s rms
459.427 Hz	0.583 m/s/s rms
483.147 Hz	0.43 m/s/s rms

5GS - 1356 - On Edge of Blade - Acc Freq 1000 Hz
5/26/2010 4:06:51 PM

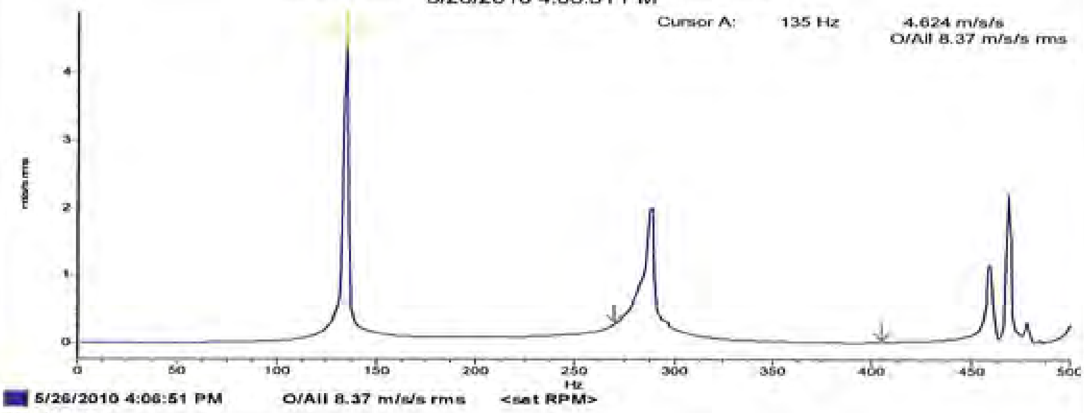

5/26/2010 4:06:51 PM O/All 8.37 m/s/s rms <set RPM>

Top 10 Peaks

134.833 Hz	4.624 m/s/s rms
509.364 Hz	3.05 m/s/s rms
468.166 Hz	2.208 m/s/s rms
288.391 Hz	1.997 m/s/s rms
513.109 Hz	1.348 m/s/s rms
505.618 Hz	1.276 m/s/s rms
459.427 Hz	1.151 m/s/s rms
503.122 Hz	1.021 m/s/s rms
685.304 Hz	0.98 m/s/s rms
682.807 Hz	0.806 m/s/s rms

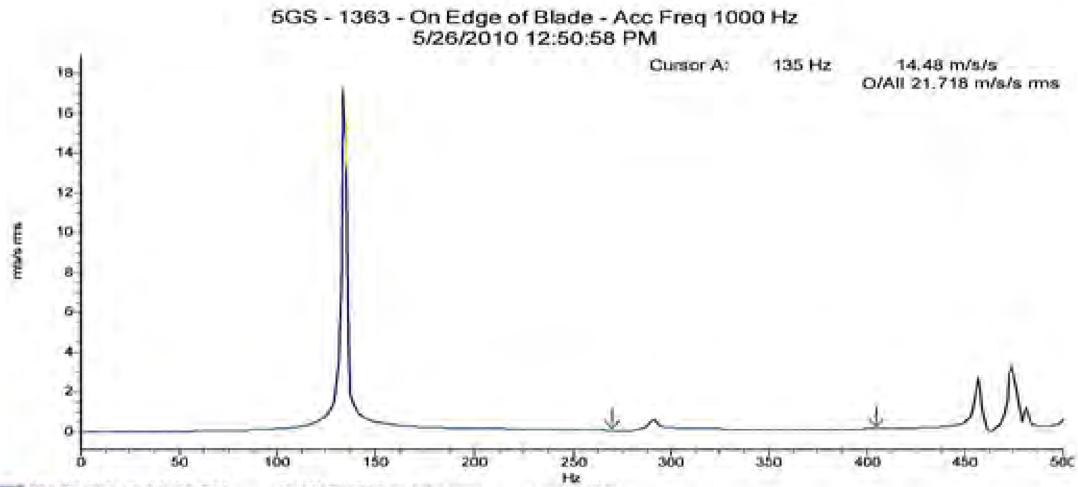

5/26/2010 12:50:58 PM O/All 21.718 m/s/s rms <set RPM>

Top 10 Peaks

133.584 Hz	17.221 m/s/s rms
473.159 Hz	3.311 m/s/s rms
455.681 Hz	2.743 m/s/s rms
480.65 Hz	1.204 m/s/s rms
501.873 Hz	1.18 m/s/s rms
505.619 Hz	1.074 m/s/s rms
511.861 Hz	0.92 m/s/s rms
290.887 Hz	0.608 m/s/s rms
664.17 Hz	0.542 m/s/s rms
515.606 Hz	0.368 m/s/s rms

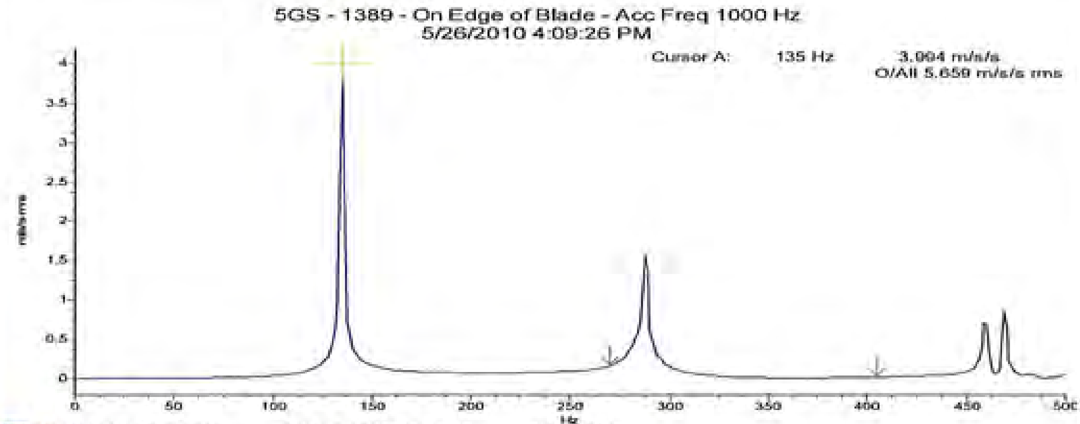

5/26/2010 4:09:26 PM O/All 5.659 m/s/s rms <set RPM>

Top 10 Peaks

134.833 Hz	3.994 m/s/s rms
287.142 Hz	1.58 m/s/s rms
511.861 Hz	0.968 m/s/s rms
514.358 Hz	0.893 m/s/s rms
468.160 Hz	0.862 m/s/s rms
459.178 Hz	0.712 m/s/s rms
505.619 Hz	0.254 m/s/s rms
958.303 Hz	0.125 m/s/s rms
681.848 Hz	0.11 m/s/s rms
995.253 Hz	0.107 m/s/s rms

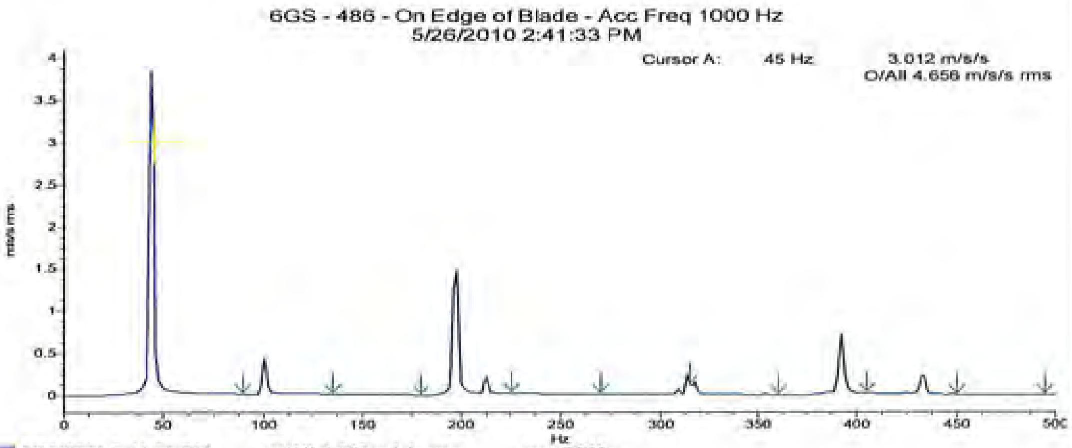

5/26/2010 2:41:33 PM O/All 4.656 m/s/s rms <set RPM>

Top 10 Peaks

43.897 Hz	3.847 m/s/s rms
197.255 Hz	1.479 m/s/s rms
392.011 Hz	0.712 m/s/s rms
99.877 Hz	0.433 m/s/s rms
313.359 Hz	0.251 m/s/s rms
433.209 Hz	0.226 m/s/s rms
212.236 Hz	0.211 m/s/s rms
317.105 Hz	0.161 m/s/s rms
308.366 Hz	0.073 m/s/s rms
746.587 Hz	0.042 m/s/s rms

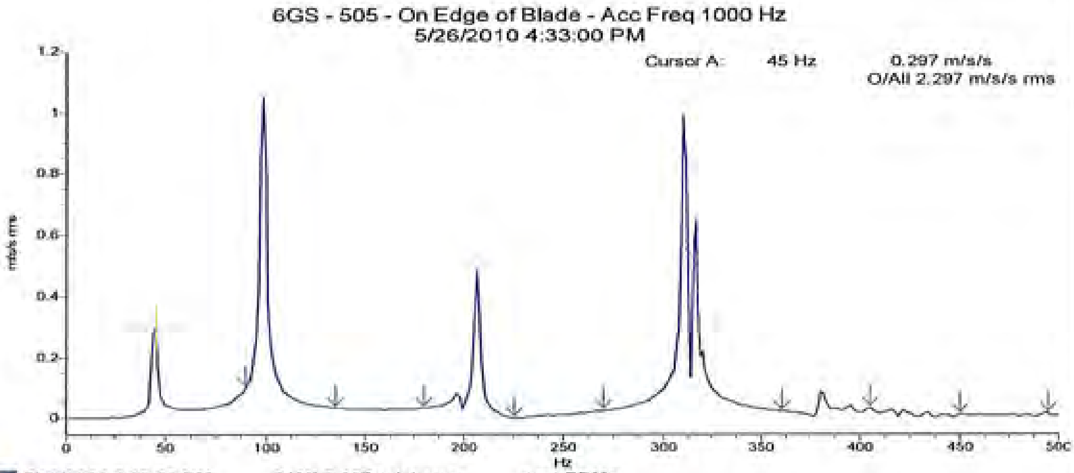

5/26/2010 4:33:00 PM O/All 2.297 m/s/s rms <set RPM>

Top 10 Peaks

98.628 Hz	1.051 m/s/s rms
309.614 Hz	0.99 m/s/s rms
315.856 Hz	0.649 m/s/s rms
205.994 Hz	0.479 m/s/s rms
44.945 Hz	0.297 m/s/s rms
319.602 Hz	0.22 m/s/s rms
548.066 Hz	0.188 m/s/s rms
645.444 Hz	0.1 m/s/s rms
379.327 Hz	0.088 m/s/s rms
196.006 Hz	0.084 m/s/s rms

308

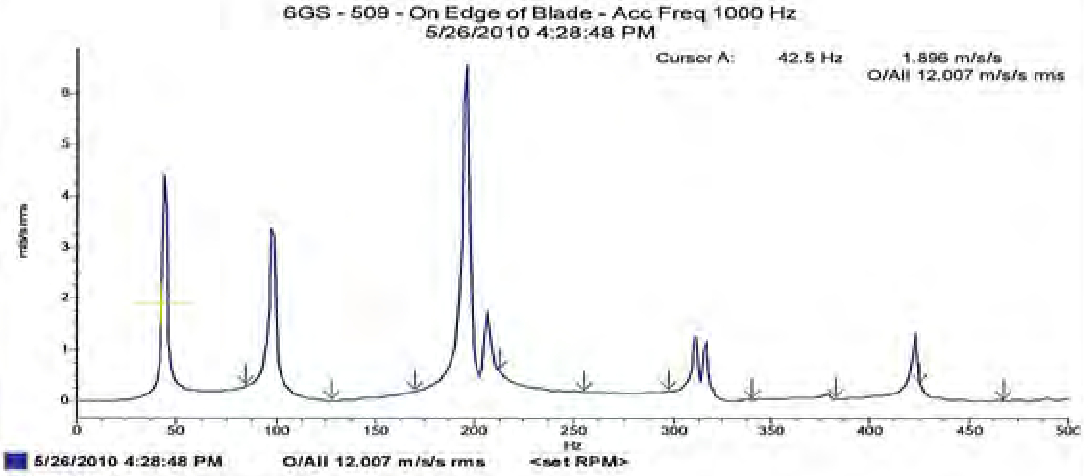

Top 10 Peaks

196.066 Hz	6.565 m/s/s rms
43.697 Hz	4.42 m/s/s rms
97.38 Hz	3.354 m/s/s rms
205.994 Hz	1.759 m/s/s rms
421.973 Hz	1.344 m/s/s rms
310.863 Hz	1.247 m/s/s rms
315.856 Hz	1.175 m/s/s rms
544.32 Hz	0.6 m/s/s rms
541.823 Hz	0.506 m/s/s rms
991.261 Hz	0.33 m/s/s rms

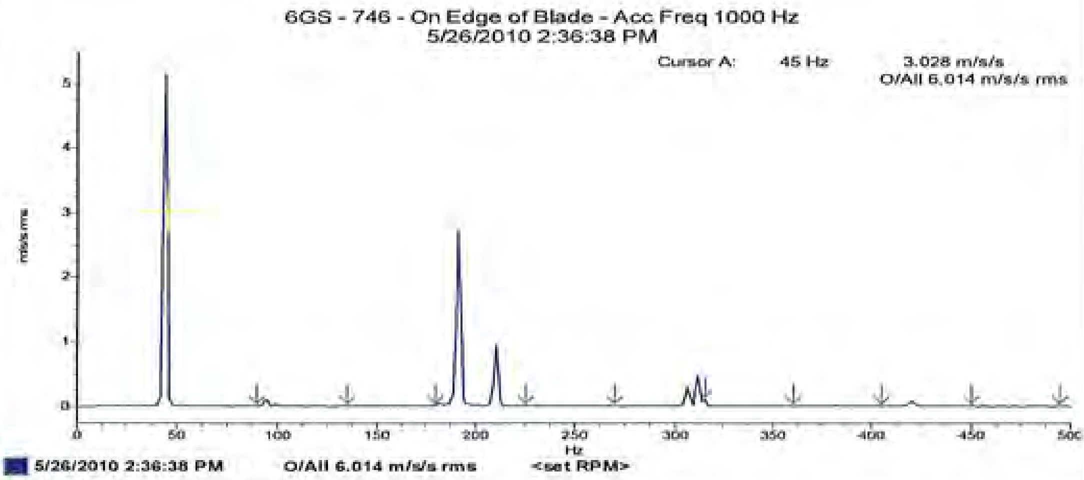

Top 10 Peaks

43.697 Hz	5.15 m/s/s rms
191.012 Hz	2.726 m/s/s rms
209.739 Hz	0.952 m/s/s rms
310.863 Hz	0.474 m/s/s rms
305.869 Hz	0.293 m/s/s rms
314.608 Hz	0.106 m/s/s rms
94.883 Hz	0.094 m/s/s rms
419.477 Hz	0.084 m/s/s rms
181.025 Hz	0.037 m/s/s rms
551.811 Hz	0.028 m/s/s rms

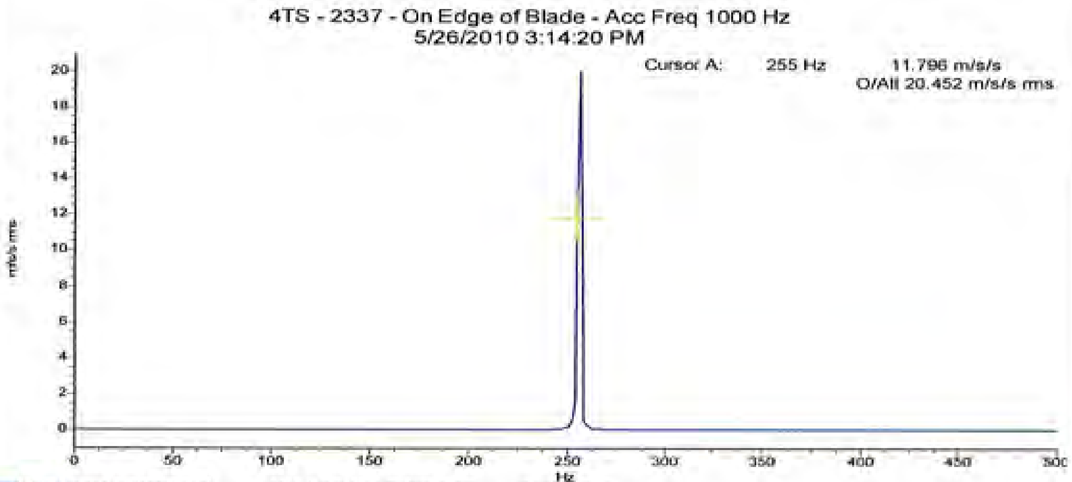

5/26/2010 3:14:20 PM **O/All 20.452 m/s/s rms** **<set RPM>**

Top 10 Peaks

255.931 Hz	19.973 m/s/s rms
583.022 Hz	1.317 m/s/s rms
928.839 Hz	1.013 m/s/s rms
590.512 Hz	0.898 m/s/s rms
569.289 Hz	0.881 m/s/s rms
916.355 Hz	0.652 m/s/s rms
576.78 Hz	0.612 m/s/s rms
511.861 Hz	0.524 m/s/s rms
925.094 Hz	0.445 m/s/s rms
583.047 Hz	0.198 m/s/s rms

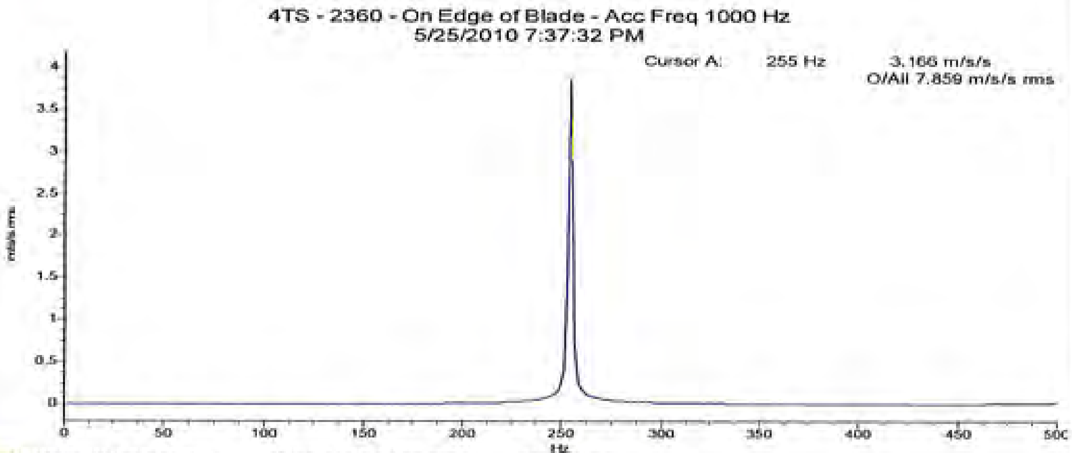

5/25/2010 7:37:32 PM **O/All 7.859 m/s/s rms** **<set RPM>**

Top 10 Peaks

580.525 Hz	3.907 m/s/s rms
253.434 Hz	3.849 m/s/s rms
584.27 Hz	2.842 m/s/s rms
574.283 Hz	1.428 m/s/s rms
505.544 Hz	1.133 m/s/s rms
916.355 Hz	0.854 m/s/s rms
910.113 Hz	0.845 m/s/s rms
900.125 Hz	0.806 m/s/s rms
932.584 Hz	0.522 m/s/s rms
926.342 Hz	0.38 m/s/s rms

4TS - 2362 - On Edge of Blade - Acc Freq 1000 Hz
5/25/2010 7:39:22 PM

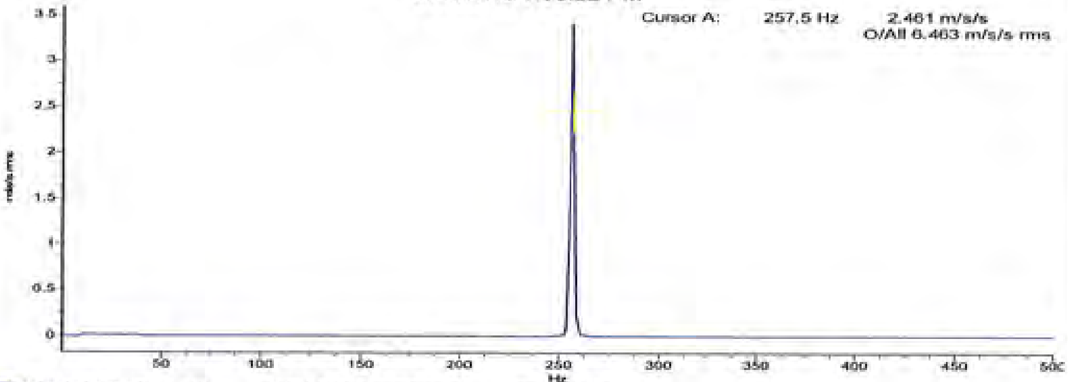

5/25/2010 7:39:22 PM O/All 6.463 m/s/s rms <set RPM>

Top 10 Peaks

255.931 Hz	3.42 m/s/s rms
595.506 Hz	3.02 m/s/s rms
589.264 Hz	2.918 m/s/s rms
598.003 Hz	1.532 m/s/s rms
574.283 Hz	1.126 m/s/s rms
585.519 Hz	0.994 m/s/s rms
942.572 Hz	0.442 m/s/s rms
925.094 Hz	0.41 m/s/s rms
932.564 Hz	0.368 m/s/s rms
551.773 Hz	0.363 m/s/s rms

4TS - 2381 - On Edge of Blade - Acc Freq 1000 Hz
5/26/2010 4:55:31 PM

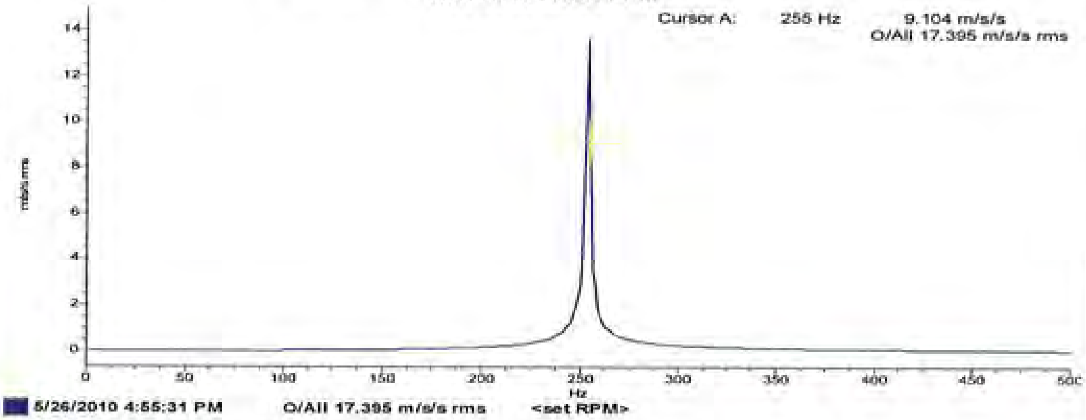

5/26/2010 4:55:31 PM O/All 17.395 m/s/s rms <set RPM>

Top 10 Peaks

253.434 Hz	13.615 m/s/s rms
573.034 Hz	1.772 m/s/s rms
584.27 Hz	1.587 m/s/s rms
913.858 Hz	1.173 m/s/s rms
564.295 Hz	1.147 m/s/s rms
925.094 Hz	0.735 m/s/s rms
591.761 Hz	0.654 m/s/s rms
902.622 Hz	0.478 m/s/s rms
930.088 Hz	0.346 m/s/s rms
955.006 Hz	0.313 m/s/s rms

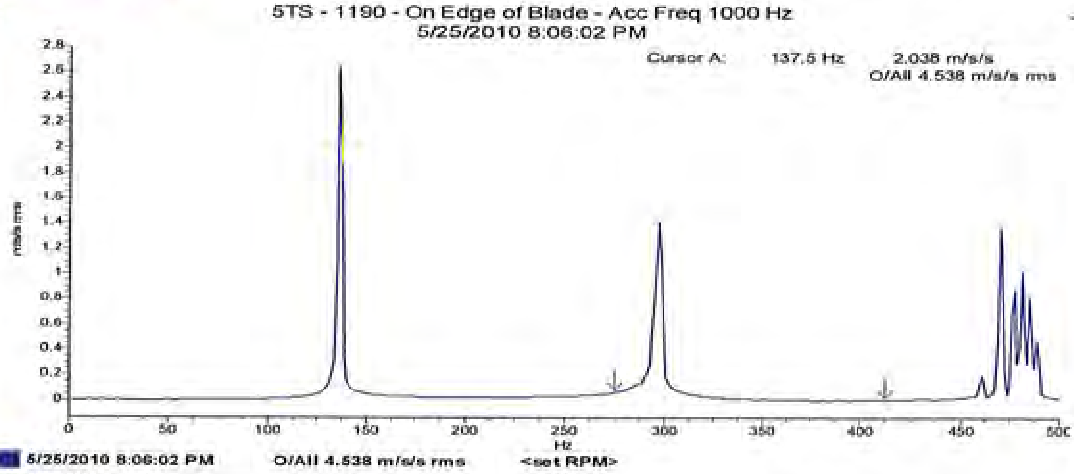

5/25/2010 8:06:02 PM O/All 4.538 m/s/s rms <set RPM>

Top 10 Peaks

136.081 Hz	2.639 m/s/s rms
297.13 Hz	1.413 m/s/s rms
469.414 Hz	1.37 m/s/s rms
480.65 Hz	1.016 m/s/s rms
476.905 Hz	0.877 m/s/s rms
484.395 Hz	0.819 m/s/s rms
687.891 Hz	0.799 m/s/s rms
518.103 Hz	0.684 m/s/s rms
514.358 Hz	0.604 m/s/s rms
488.141 Hz	0.467 m/s/s rms

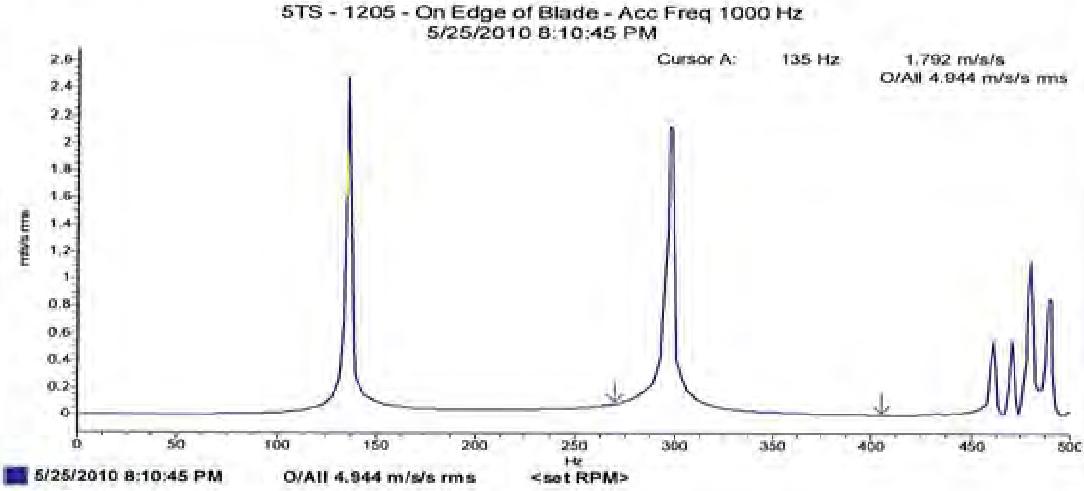

5/25/2010 8:10:45 PM O/All 4.944 m/s/s rms <set RPM>

Top 10 Peaks

136.081 Hz	2.484 m/s/s rms
297.13 Hz	2.132 m/s/s rms
479.402 Hz	1.137 m/s/s rms
489.388 Hz	0.858 m/s/s rms
515.606 Hz	0.762 m/s/s rms
691.636 Hz	0.574 m/s/s rms
469.414 Hz	0.552 m/s/s rms
460.675 Hz	0.55 m/s/s rms
503.122 Hz	0.34 m/s/s rms
510.613 Hz	0.285 m/s/s rms

312

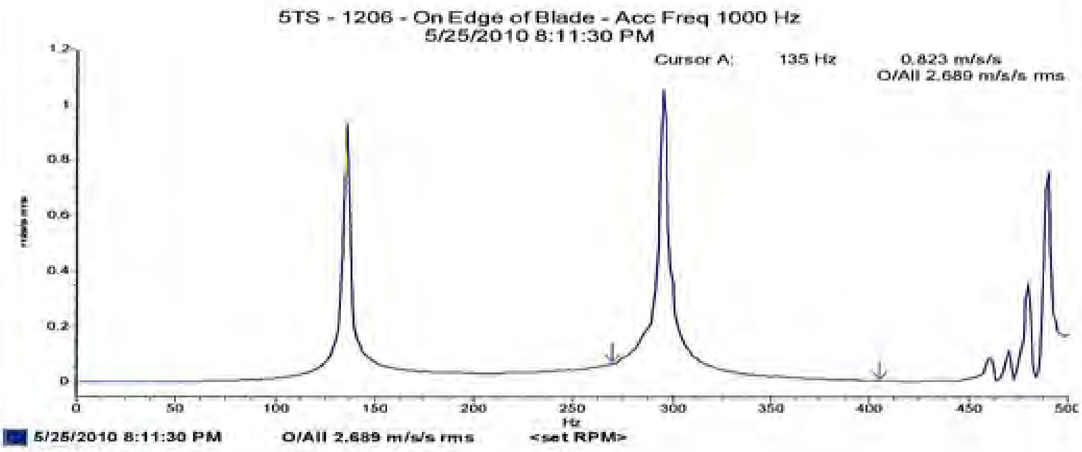

Top 10 Peaks

294.633 Hz	1.056 m/s/s rms
136.081 Hz	0.933 m/s/s rms
489.389 Hz	0.757 m/s/s rms
510.613 Hz	0.421 m/s/s rms
515.606 Hz	0.384 m/s/s rms
479.402 Hz	0.354 m/s/s rms
506.867 Hz	0.304 m/s/s rms
714.108 Hz	0.302 m/s/s rms
501.873 Hz	0.225 m/s/s rms
880.025 Hz	0.143 m/s/s rms

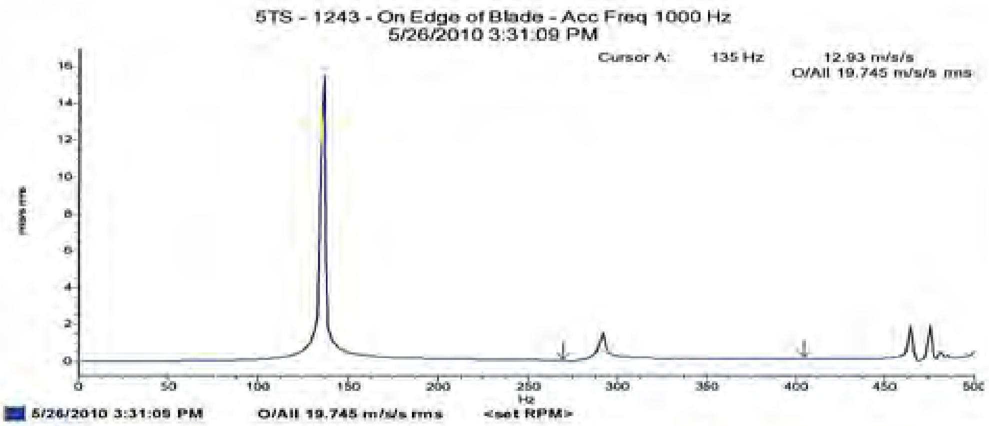

Top 10 Peaks

136.081 Hz	15.495 m/s/s rms
511.861 Hz	3.263 m/s/s rms
503.122 Hz	2.983 m/s/s rms
508.116 Hz	1.664 m/s/s rms
474.408 Hz	1.939 m/s/s rms
463.172 Hz	1.9 m/s/s rms
290.887 Hz	1.553 m/s/s rms
888.642 Hz	1.438 m/s/s rms
515.606 Hz	1.255 m/s/s rms
891.836 Hz	0.935 m/s/s rms

6TS - 527 - On Edge of Blade - Acc Freq 1000 Hz
5/26/2010 12:38:30 PM

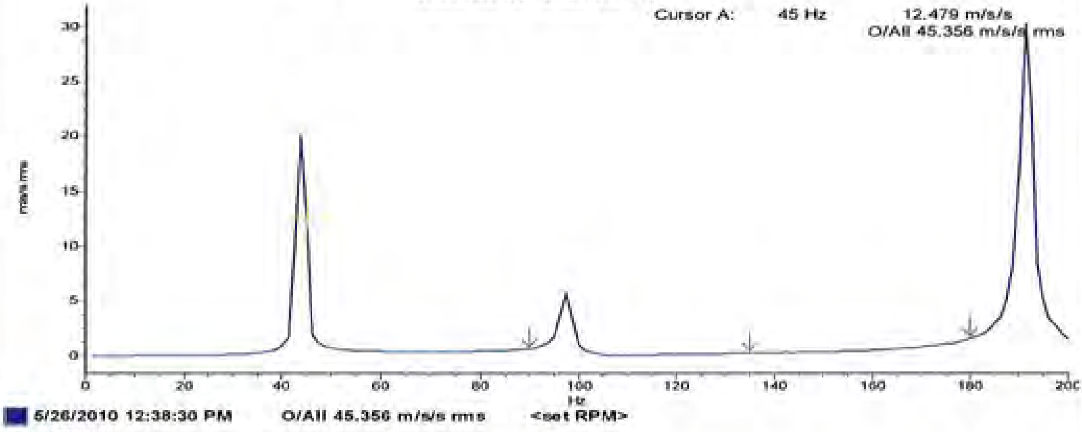

5/26/2010 12:38:30 PM O/All 45.356 m/s/s rms <set RPM>

Top 10 Peaks

191.012 Hz	30.373 m/s/s rms
43.697 Hz	20.123 m/s/s rms
97.38 Hz	5.724 m/s/s rms
340.575 Hz	5.636 m/s/s rms
205.994 Hz	4.262 m/s/s rms
383.272 Hz	2.228 m/s/s rms
721.598 Hz	2.193 m/s/s rms
380.775 Hz	1.855 m/s/s rms
533.064 Hz	1.629 m/s/s rms
419.477 Hz	1.259 m/s/s rms

6TS - 714 - On Edge of Blade - Acc Freq 1000 Hz
5/26/2010 5:34:00 PM

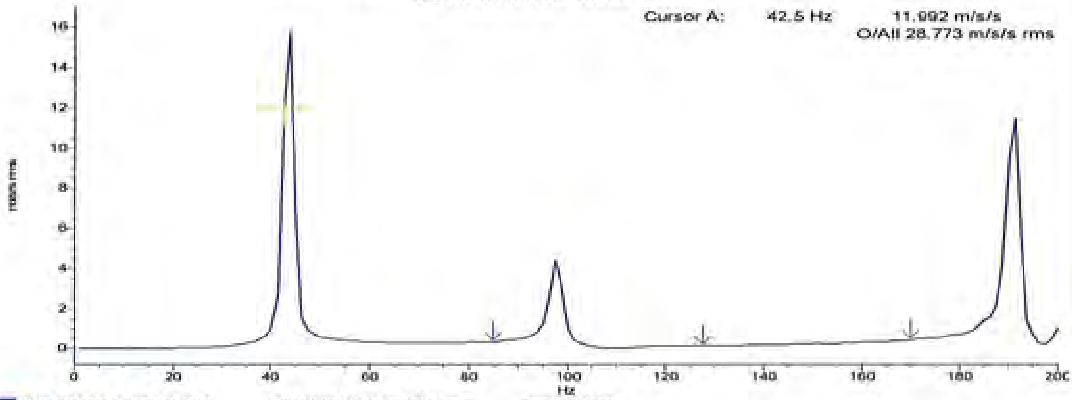

5/26/2010 5:34:00 PM O/All 28.773 m/s/s rms <set RPM>

Top 10 Peaks

43.697 Hz	15.607 m/s/s rms
204.745 Hz	13.863 m/s/s rms
191.012 Hz	11.532 m/s/s rms
97.38 Hz	4.415 m/s/s rms
309.614 Hz	2.14 m/s/s rms
531.836 Hz	2.028 m/s/s rms
313.359 Hz	1.964 m/s/s rms
416.98 Hz	1.772 m/s/s rms
710.362 Hz	0.647 m/s/s rms
714.108 Hz	0.502 m/s/s rms

314

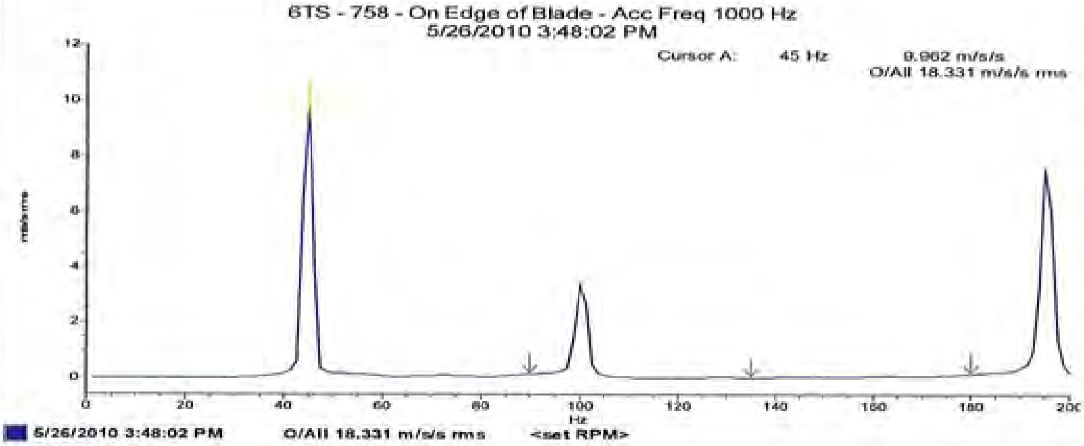

Top 10 Peaks

208.491 Hz	11.266 m/s/s rms
44.945 Hz	9.962 m/s/s rms
194.756 Hz	7.591 m/s/s rms
99.877 Hz	3.397 m/s/s rms
317.105 Hz	1.354 m/s/s rms
312.111 Hz	0.601 m/s/s rms
307.117 Hz	0.379 m/s/s rms
416.98 Hz	0.176 m/s/s rms
383.272 Hz	0.161 m/s/s rms
235.063 Hz	0.132 m/s/s rms

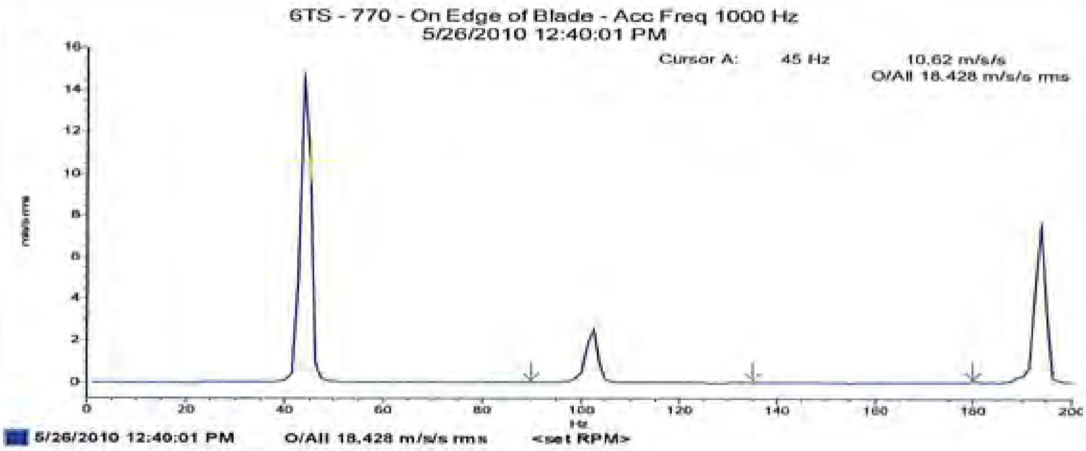

Top 10 Peaks

43.697 Hz	14.821 m/s/s rms
193.509 Hz	7.701 m/s/s rms
209.739 Hz	5.075 m/s/s rms
102.373 Hz	2.628 m/s/s rms
314.608 Hz	1.473 m/s/s rms
317.105 Hz	0.928 m/s/s rms
387.017 Hz	0.773 m/s/s rms
343.072 Hz	0.427 m/s/s rms
308.366 Hz	0.379 m/s/s rms
383.272 Hz	0.128 m/s/s rms

ALSTOM	Client	J-Power (Electric Power Development Co. Ltd.,)
	Project	Turbine and System Assessment for NTPC-Korba Unit #4
	Order No.	CGP10028C
	Contractor	ALSTOM K.K. NASL Ltd. (Nominated subcontractor in India)
NTPC ALSTOM Power Services Pvt. Ltd.	**Document**	**FINAL REPORT VOL. I B(RLA of Turbine)**

7.7 Deposit Analysis Report

Deposit was collected from 14th stage of turbine side moving blades and spectrography analysis was carried out.

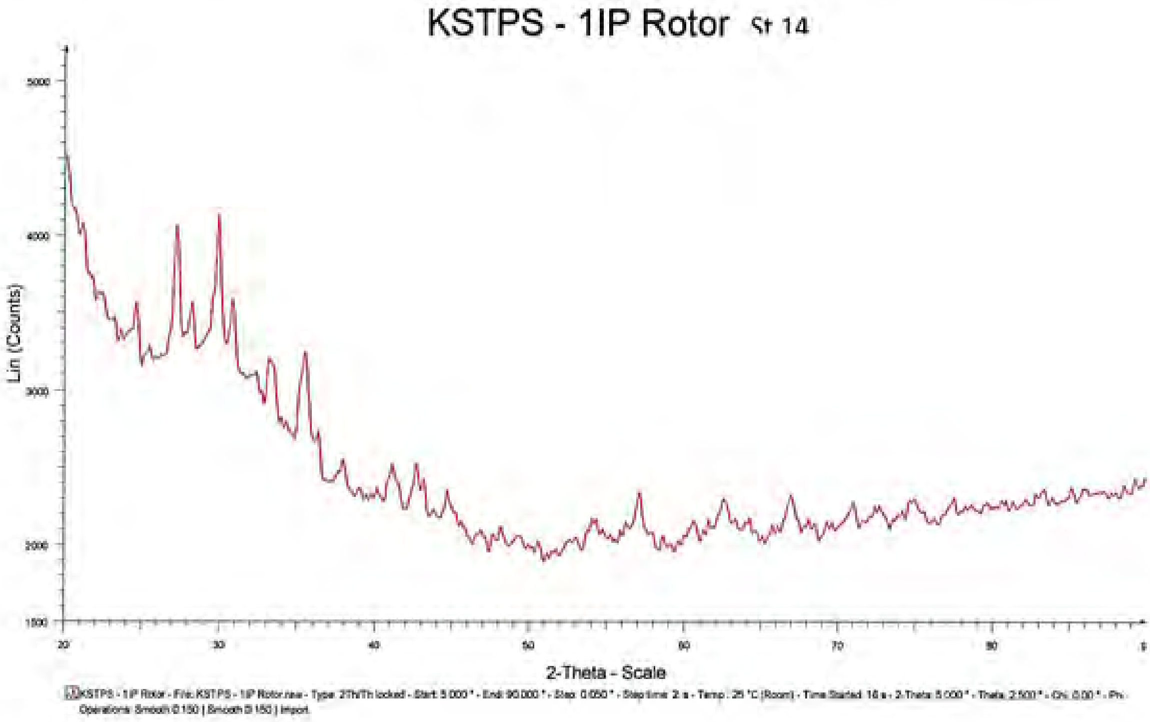

KSTPS - 1IP Rotor St 14

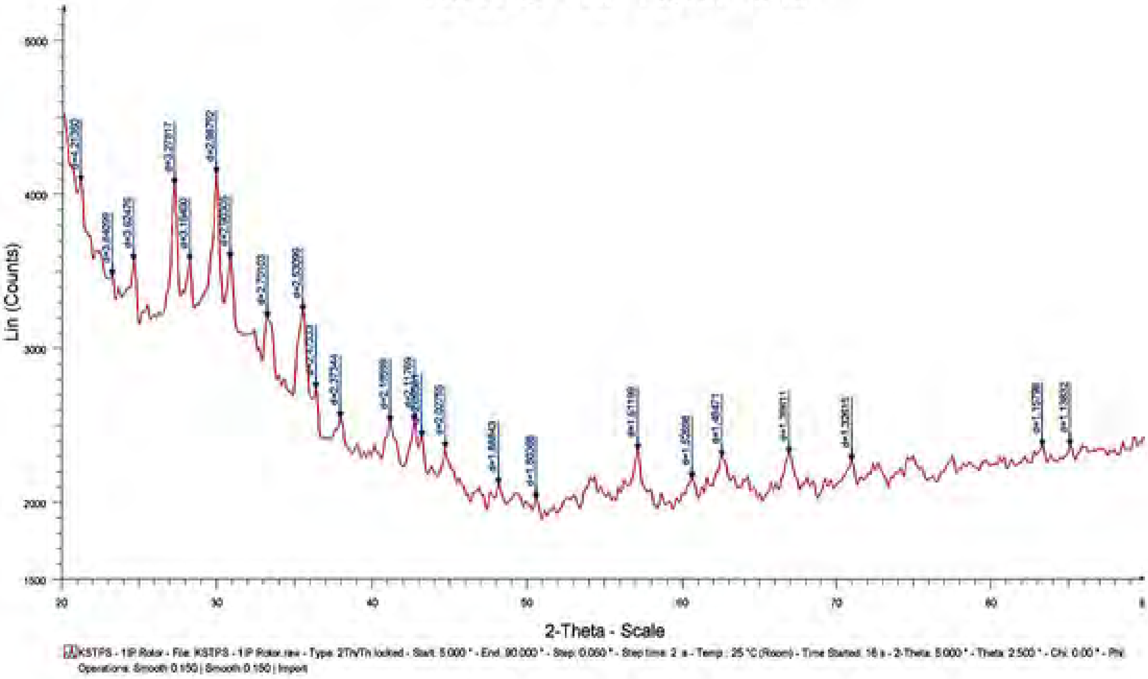

317

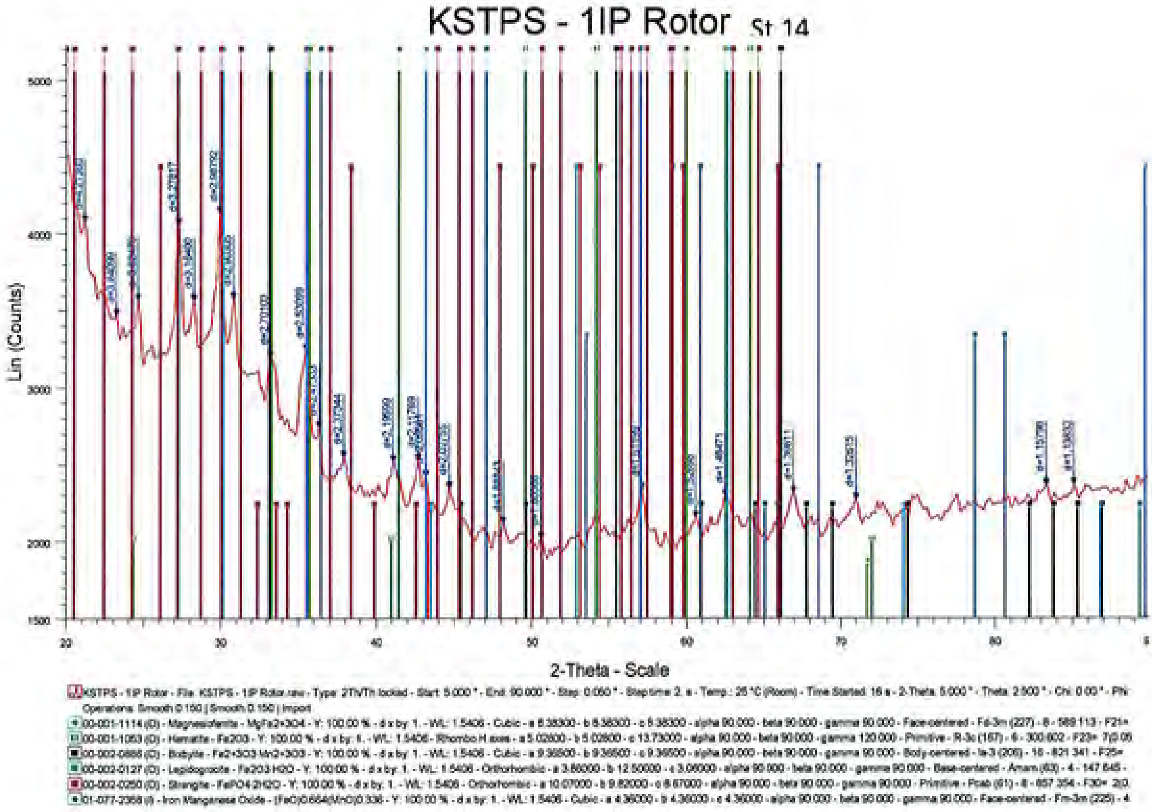

KSTPS - 1IP Rotor St 14
Lin (Counts)
2-Theta - Scale
KSTPS - 1IP Rotor
00-001-1114 (D) - Magnesioferrite - MgFe2+3O4
00-001-1053 (D) - Hematite - Fe2O3
00-002-0888 (D) - Bixbyite - Fe2+3O3 Mn2+3O3
00-002-0127 (D) - Lepidocrocite - Fe2O3·H2O
00-002-0250 (D) - Strengite - FePO4·2H2O
01-077-2368 (I) - Iron Manganese Oxide

318

Sample name: KSTPS - 1IP Rotor St. 14

File name: KSTPS - 1IP Rotor.raw

Date of fitting: 7/6/2010 5:54:07 PM

00-001-1114 33.8%MgFe2+3O4

Magnesioferrite

00-001-1053 1.5% Fe2O3

Hematite

00-002-0886 17.7%Fe2+3O3·Mn2+3O3

Bixbyite

00-002-0127 37.9%Fe2O3·H2O

Lepidogrocite

00-002-0250 5.2% FePO4·2H2O

Strengite

01-077-2358 3.9% (FeO)0.664(MnO)0.336

Iron Manganese Oxide

H	0.5%	H2O	4.8%
O	33.8%	Excess	+0.6%
Mg	4.1%	MgO	6.8%
P	0.9%	P2O5	2.0%
Mn	7.1%	MnO	9.2%
Fe	53.6%	Fe2O3	76.6%

KSTPS - 3 Fork LP St - 4

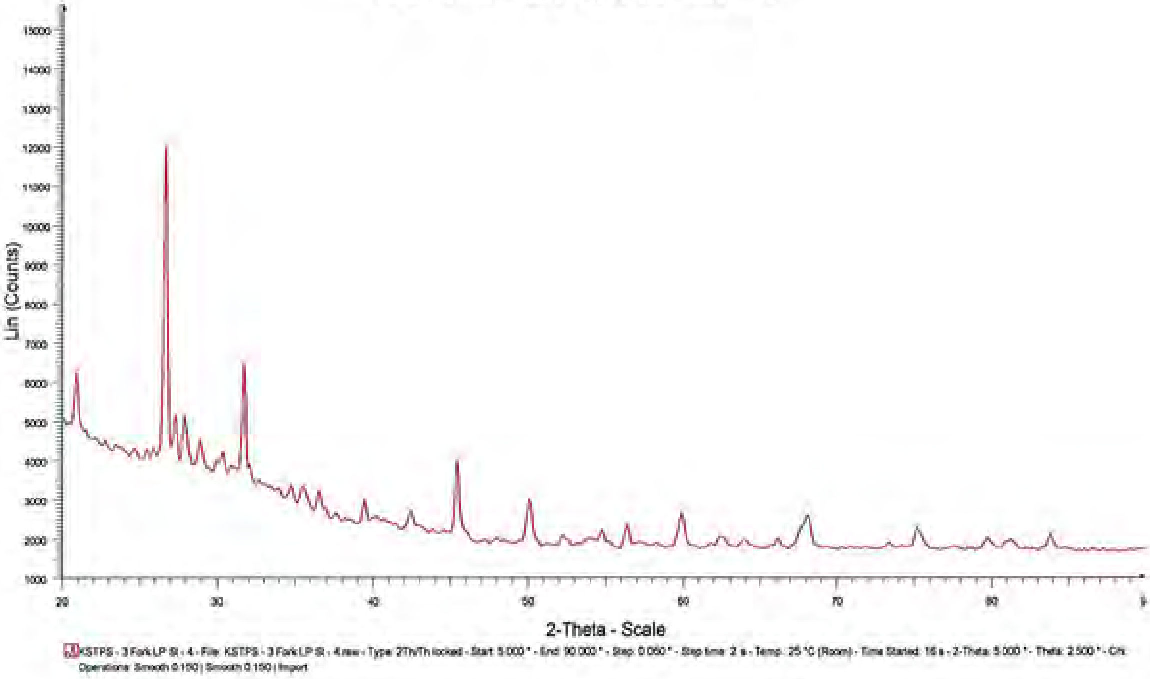

KSTPS - 3 Fork LP St - 4

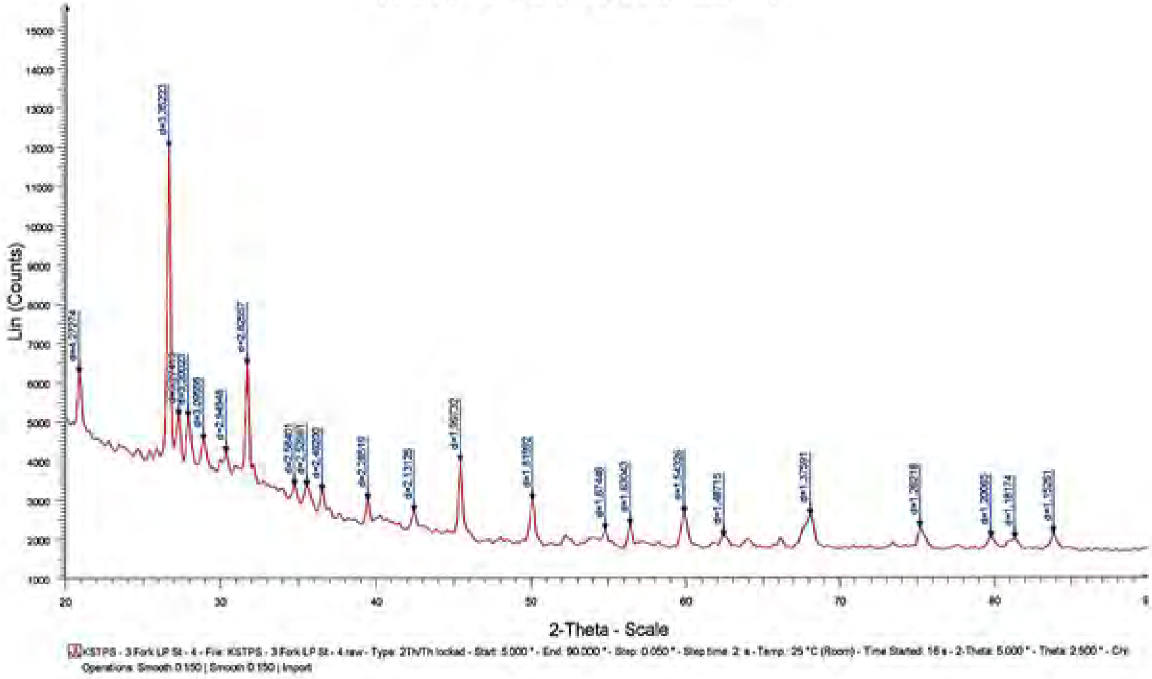

321

KSTPS - 3 Fork LP St - 4

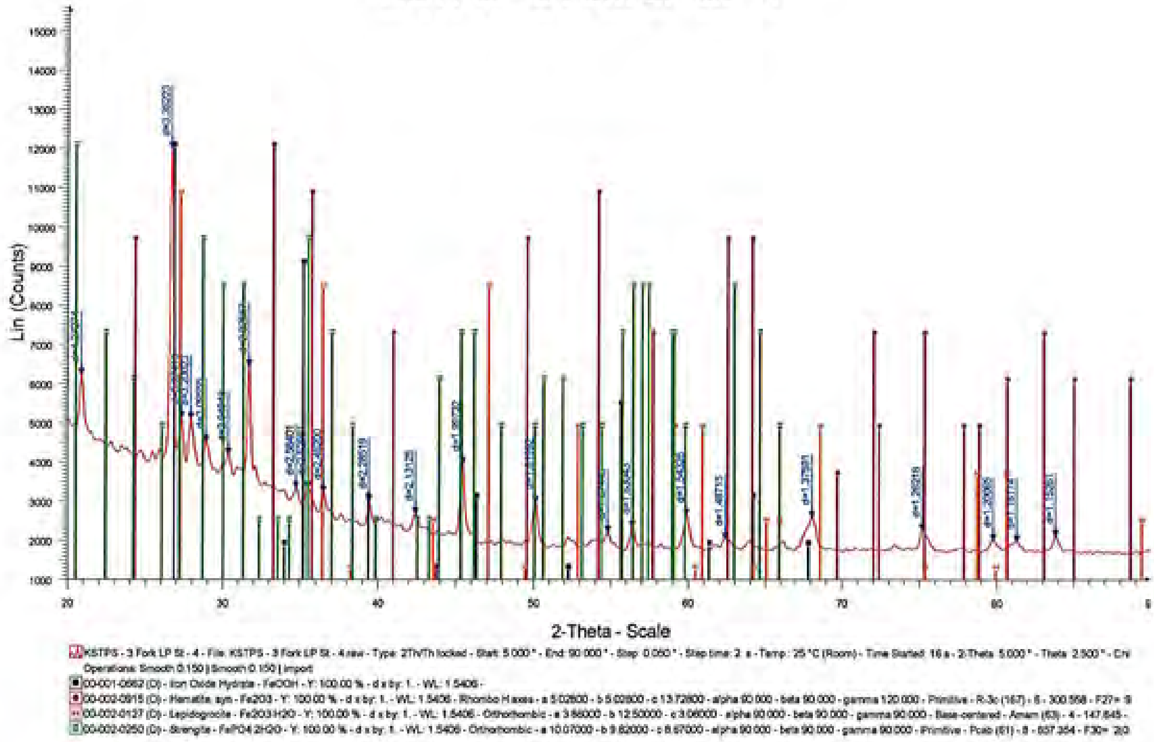

Sample name: KSTPS - 3 Fork LP St - 4

File name: KSTPS - 3 Fork LP St - 4.raw

Date of fitting: 7/6/2010 5:39:48 PM

00-001-0662 38.9%FeOOH

Iron Oxide Hydrate

00-002-0915 1.5% Fe2O3

Hematite, syn

00-002-0127 52.5%Fe2O3·H2O

Lepidogrocite

00-002-0250 7.2% FePO4·2H2O

Strengite

H	1.2%	H2O	10.6%
O	37.0%		
P	1.2%	P2O5	2.7%
Fe	60.6%	Fe2O3	86.6%

KSTPS - 4 LP - St 5

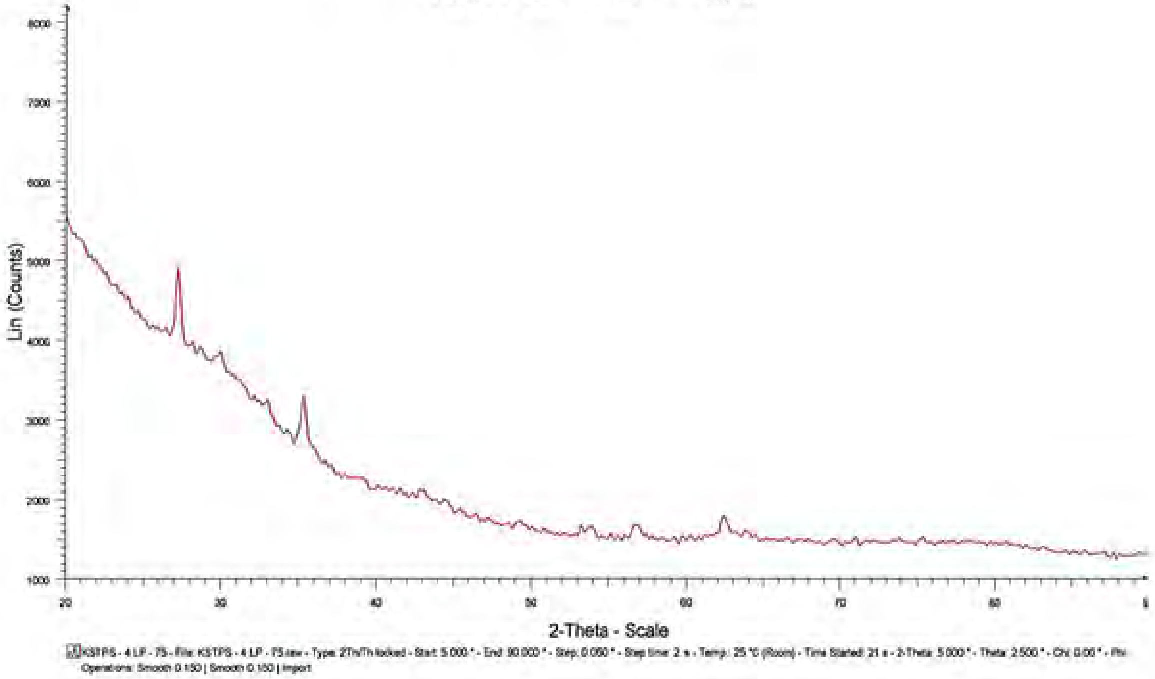

324

KSTPS - 4 LP St 5

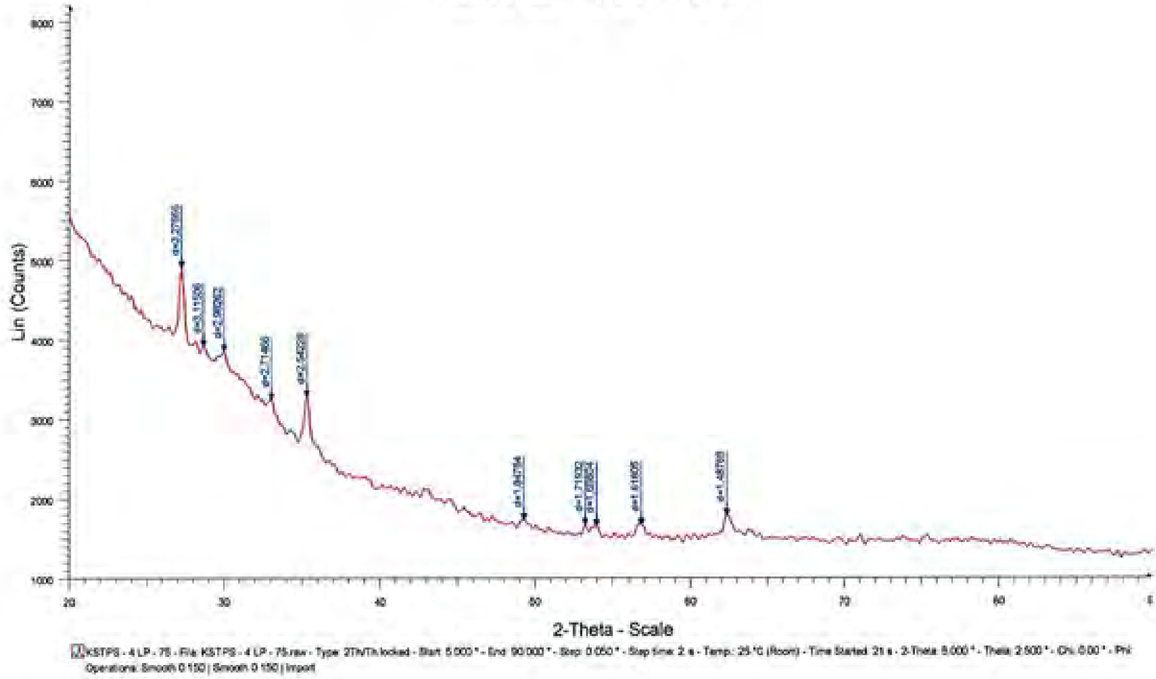

325

ALSTOM	Client	J-Power (Electric Power Development Co. Ltd.,)
	Project	Turbine and System Assessment for NTPC-Korba Unit #4
	Order No.	CGP10028C
	Contractor	ALSTOM K.K. NASL Ltd. (Nominated subcontractor in India)
NTPC ALSTOM Power Services Pvt. Ltd.	**Document**	**FINAL REPORT VOL. I B(RLA of Turbine)**

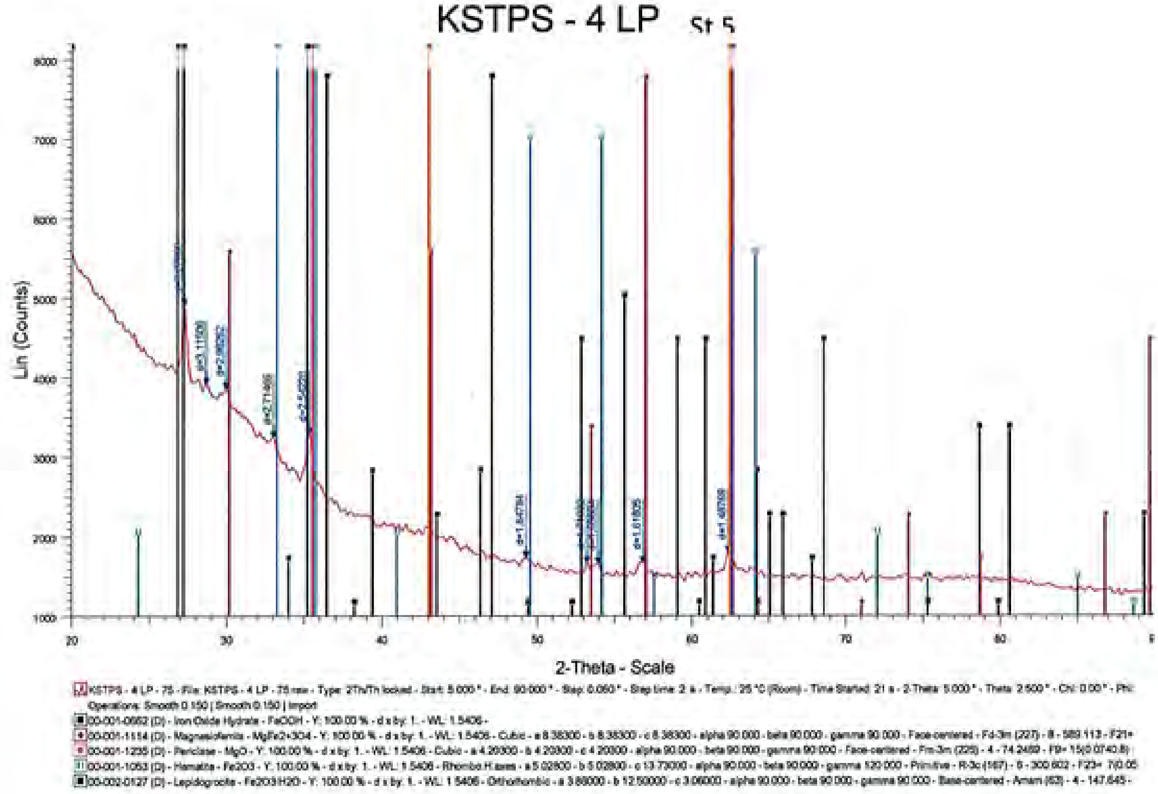

Sample name: KSTPS - 4 LP – St.5

File name: KSTPS - 4 LP – St. 5.raw

Date of fitting: 7/6/2010 5:46:57 PM

00-001-0662 5.7% FeOOH

Iron Oxide Hydrate

00-001-1114 26.2%MgFe2+3O4

Magnesioferrite

00-001-1235 8.5% MgO

Periclase

00-001-1053 9.9% Fe2O3

Hematite

00-002-0127 49.7%Fe2O3·H2O

Lepidogrocite

H	0.6%	H2O	5.6%
O	34.7%		
Mg	8.3%	MgO	13.8%
Fe	56.4%	Fe2O3	80.6%

Observation: The major oxide component is of Iron Oxide which as usual. No abnormal constituent like Cl, Cu etc. are not present. Water chemistry seems to be good.

KSTPS - 2 LP Inner - Outer Top Half St 5

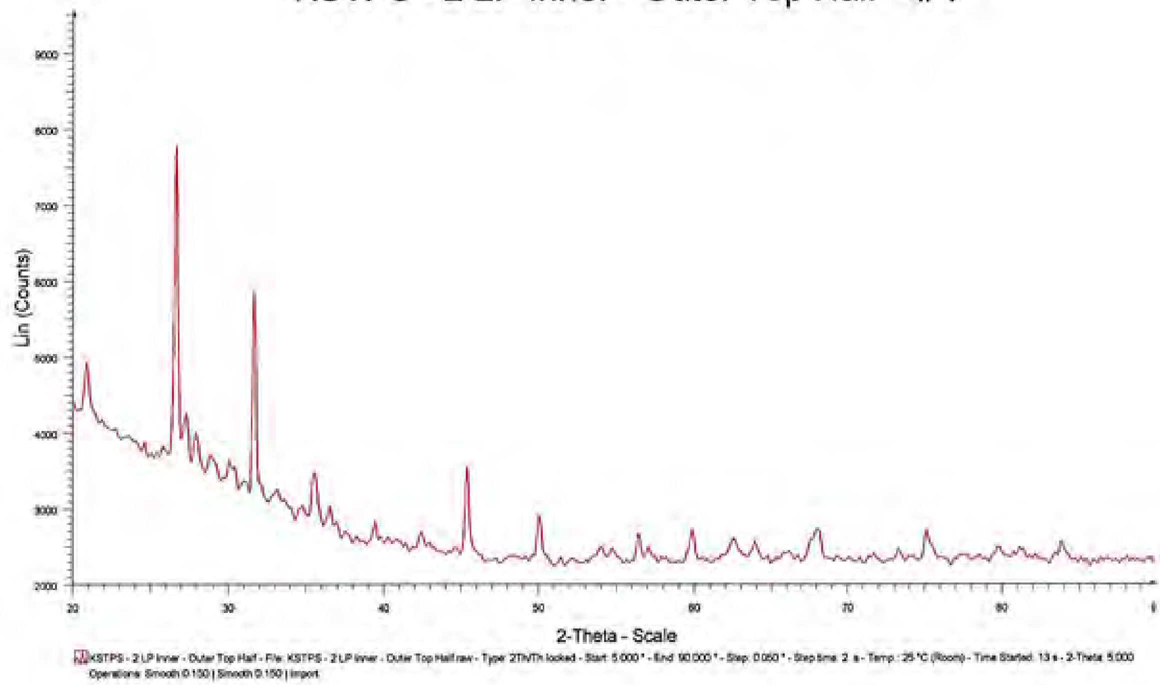

328

KSTPS - 2 LP Inner - Outer Top Half St 5

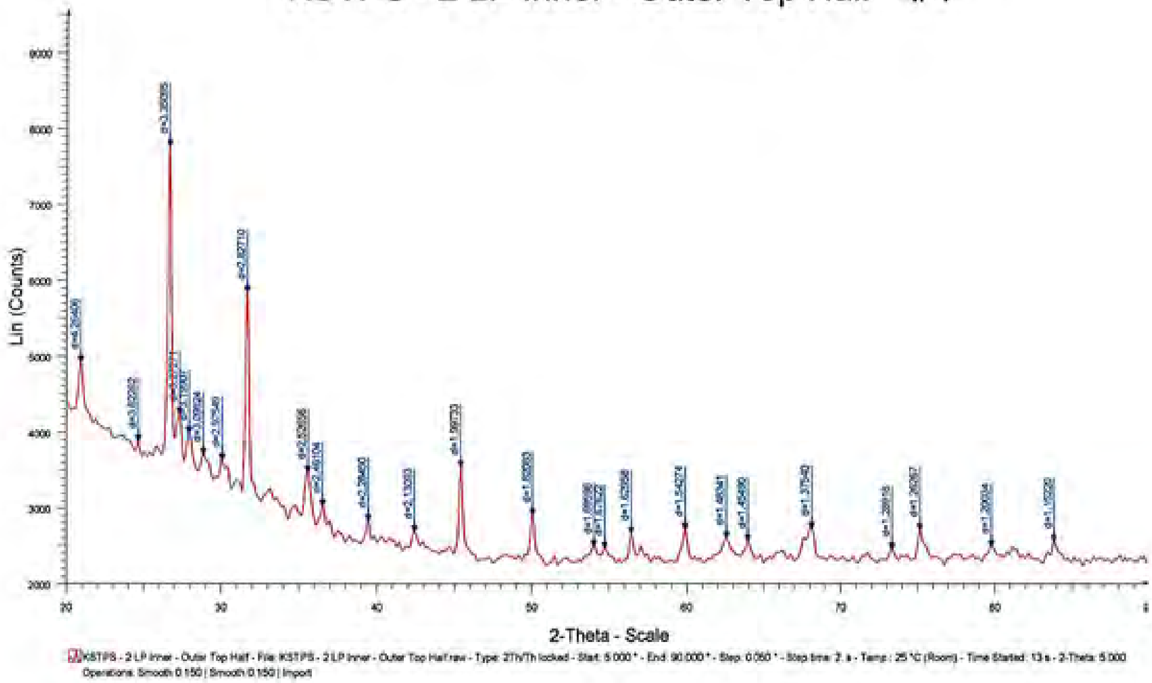

729

KSTPS - 2 LP Inner - Outer Top Half St 5

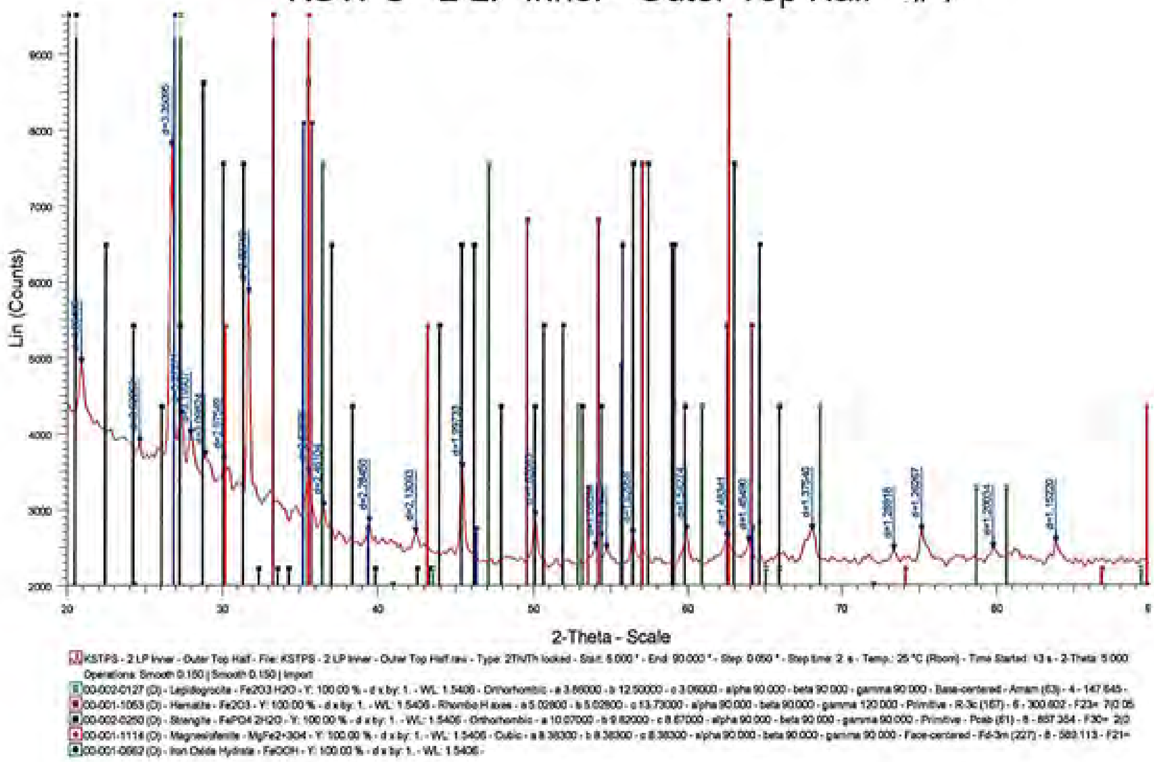

330

Sample name: KSTPS - 2 LP Inner - Outer Top Half St. 5

File name: KSTPS - 2 LP Inner - Outer Top Half .raw

Date of fitting: 7/6/2010 5:30:10 PM

00-002-0127	**49.0%**	**$Fe_2O_3 \cdot H_2O$**
Lepidogrocite		
00-001-1053	**9.0%**	**Fe_2O_3**
Hematite		
00-002-0250	**11.3%**	**$FePO_4 \cdot 2H_2O$**
Strengite		
00-001-1114	**1.1%**	**$MgFe2+3O_4$**
Magnesioferrite		
00-001-0662	**29.6%**	**FeOOH**
Iron Oxide Hydrate		

H	1.1%	H_2O	10.1%
O	37.2%		
Mg	0.1%	MgO	0.2%
P	1.9%	P_2O_5	4.3%
Fe	59.7%	Fe_2O_3	85.3%

Observation: The major oxide component is of Iron Oxide which as usual. No abnormal constituent like Cl, Cu etc. are not present. Water chemistry seems to be good.

7.8 DESTRUCTIVE TESTING

Chapter7.8: Destructive Test Report

Total Samples received from Customer: **01 nos of IP stud.**

Description & Result:

We have conducted the Charpy test to carry out the destructive analysis on the IP stud. Charpy Impact samples were taken from one IP Stud. These samples were tested at seven different temperatures. Predicated charpy values were extrapolated. Actual Test values & predicated values were plotted and found to be matching with each other.

Hence it can be concluded that the IP Studs are in healthy condition.

Equations used:

The below linear regression model is used to determine the phase shift and sensitivity coefficient using a two variable global error minimization algorithm. The data pair points are chosen to ensure a high coefficient of determination, R^2

$$J_i = \alpha + \beta T_i + \hat{\varepsilon}_i\left[0, \sigma^2\right]$$

$$J_i = \text{Impact Energy at } i^{th} \text{ Temperature, a NRV}$$

$$\alpha = \text{Phase Shift Constant}$$

$$\beta = \text{Sensitivity Coefficient}$$

$$T_i = i^{th} \text{ Temperature}$$

$$\hat{\varepsilon}_i\left[0, \sigma^2\right] = \text{Error Random Variable With Zero Expectation and Constant Variance}, \sigma^2$$

The unknown coefficients are determined as:

$$\alpha = \text{Phase Shift Constant} = 10.7$$

$$\beta = \text{Sensitivity Coefficient} = 0.38$$

$$R^2 = 0.97$$

The above derived coefficients enable us to write our regression equation as:

$$J_i = 10.7 + 0.38 T_i$$

The above derived equation is used to obtain the 20 J transition temperature as 24.5^0 C. The raw charpy impact data as well as the predicted values are compiled below:

Serial No.	Temperature, T_i, ^{0} C	Specific Charpy Impact Energy, J_i, J/cm^2	Predicted Specific Charpy Impact Energy, $(Jpre)_i$, J/cm^2
1	-100	2	Lower Shelf
2	-50	3.33	Lower Shelf
3	-20	5.33	3.04
4	0	10.67	10.68
5	+20	16	18.31
6	+50	28	29.77
7	+100	50.67	48.86

The above experimental as well predicted values are plotted in Fig.1, below:

Fig. 1: Graph showing the correlation between specific Charpy impact energy and temperature

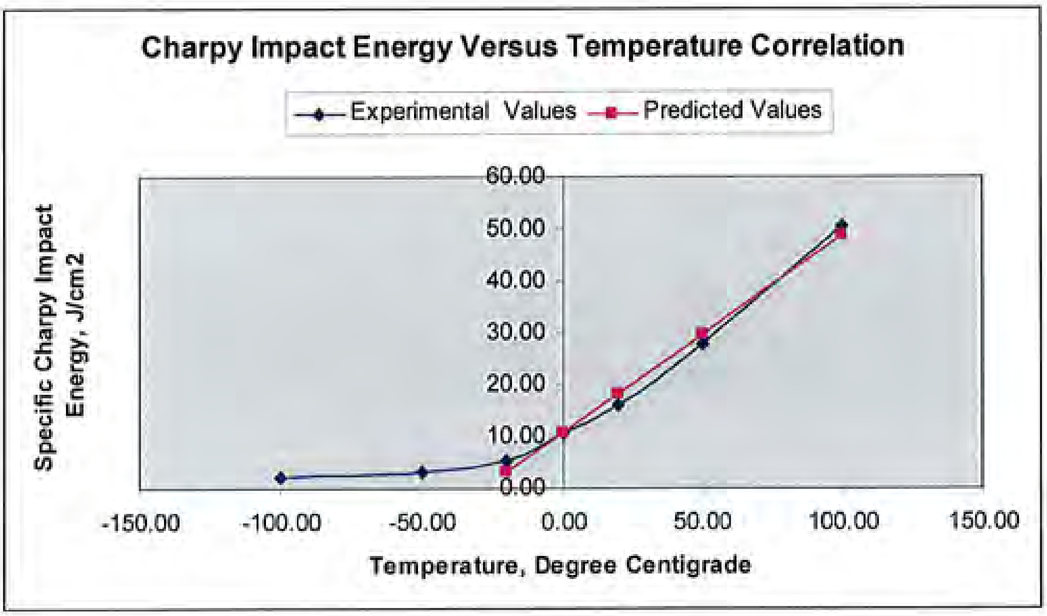

In the above graph series 1 (blue points) are the experimental values while series 2 (pink points) are the derived/predicted points.

Conclusion: IP stud is found to be in healthy condition, hence based on this sample analysis we can recommend to use the other studs in operation.

----------X---------

ALSTOM

Volume- I-B

Chapter – 08

Finite Element Analysis data on Turbine

NTPC ALSTOM
Power Services Pvt. Ltd.

337

	Client	J-Power (Electric Power Development Co. Ltd.,)
ALSTOM	Project	Turbine and System Assessment for NTPC-Korba Unit #4
	Order No.	CGP10028C
	Contractor	ALSTOM K.K. NASL Ltd. (Nominated subcontractor in India)
NTPC ALSTOM Power Services Pvt. Ltd.	**Document**	**FINAL REPORT VOL. I B (RLA OF TURBINE)**

September 2010

Life Assessment Studies (FEA) of Turbine IP/LP rotors and Casing

NO. OF PAGES: 119 NO. OF FIGURES: 117 NO. OF TABLES: 9

336

Executive Summary

Computer simulation using powerful numerical technique, Finite Element Method, is used to analyze IP and LP components of 500 MW Steam Turbine (Unit 4) located at Korba. Intermediate Pressure and Low Pressure turbine analyzed for thermal and mechanical loading. The stress variation during the transient events in the operation of steam turbine is captured.

Temperature and stress loading cycle is further post-processed to identify the critical failure locations and residual life of the turbine. FE analysis is performed for Cold start; Warm start and Hot start conditions by applying the pressure, temperature at different stages for IP, LP components w.r.t the operation data provided by NTPC for last 15 years. Fatigue analysis is performed by using the stress, temperature data from FE analysis.

Table 0-1: Transient Peak Stress in the IP and LP Steam Turbine components

Component	Peak Transient Stress(MPa)		
	Cold Start	Warm Start	Hot Start
IP Casing Assembly	530	490	275
IP Shaft	220	360	150
LP Casing Assembly	270	256	262
LP Shaft	360	280	230

Fatigue analysis is performed by using the stress, temperature data from FE analysis. It has been concluded, the residual life of the turbine is beyond 20 Years except IP Rotor, in which remaining life is observed to be 16 Years, provided there are no physical damages.

Table 0-2: Remaining life of the component in terms of cycles

Component	Remaining Hot Start-up Cycles	Remaining Warm Start-up cycles	Remaining Cold Start-up cycles
IP Casing Assembly	75	345	90
IP Shaft	60	276	72
LP Casing Assembly	113	520	136
LP Shaft	47	216	57

Abaqus, Nx-Nastran are used for FE analysis, fe-safe software is used to find life for crack initiation and Zencrack can be used for crack propagation simulation.

From the analysis the residual life of the different turbine components are found to be as follows:

- IP Casing Assembly = 22 Years
- IP rotor = 16 Years
- LP Casing Assembly = 113 Years
- LP Rotor = 47 Years

Table of Contents

Table of Contents iv

List of Figures vii

List of Tables xiii

Section 1 Objective 2-1

Section 2 Introduction 2-1

2.1. Introduction to ABAQUS 2-1

Section 3 Problem description 3-1

3.1. Load cases 3-1

Section 4 Material specification 4-1

Section 5 CAD Model Details 5-1

5.1. IP Outer Casing (Dwg # 0-10601-02000-C) 5-1

5.2. IP Inner Casing (Dwg # 0-10602-02000C) 5-4

5.3. IP Shaft (Dwg # 0-10201-02000C) 5-8

5.4. LP Outer Casing 5-9

5.5. LP Inner Casing (Dwg # 0-10743-02000C) 5-13

5.6. LP Inner Outer Casing 5-16

5.7. LP Shaft (Dwg # 0-10301-02000C) 5-18

5.8. Steam Turbine IP and LP Assembly 5-20

Section 6 Mesh Model Details 6-1

6.1. FE Model of IP Outer Casing 6-2

6.2. FE Model of IP Inner Casing 6-3

6.3. Axisymmetric Solid FE model – IP casing assembly 6-4

6.4. FE Model of IP Shaft 6-4

6.5. Axi symmetric FE model – IP shaft 6-5

6.6. FE Models of LP Outer Casing 6-6

6.7. FE Models of LP Inner Casing 6-7

6.8. FE Model of LP Inner outer casing 6-7

6.9. Axi symmetric Solid FE model – LP Casing assembly 6-8

6.10. FE Model of LP Shaft 6-9

6.11. Axi symmetric Solid FE model – LP shaft 6-9

Section 7 FE Analysis and Results 7-1

7.1. Thermo-Mechanical Analysis of IP Casing Assembly 7-1

7.2. IP Casing Assembly - Mechanical & Thermal Loading 7-1

7.3. IP Casing Assembly - Cold Start 7-5

7.4. IP Casing Assembly - Warm Start 7-9

7.5. IP Casing Assembly - Hot Start 7-12

7.6. IP Shaft - Mechanical & Thermal Loading 7-15

7.7. IP Shaft – Cold Start 7-16

7.8. IP Shaft – Warm Start 7-18

7.9. IP Shaft – Hot Start 7-20

7.10. IP Shaft – Cold start (Radial and Axial stress) 7-22

7.11. IP Shaft – Warm start (Radial and Axial stress) 7-23

7.12. IP Shaft – Hot start (Radial and Axial stress) 7-24

7.13. LP Casing Assembly - Mechanical & Thermal Loading 7-25

7.14. LP Casing Assembly – Cold start 7-27

7.15. LP Casing Assembly – Warm Start 7-31

7.16. LP Casing Assembly – Hot Start 7-35

7.17. LP Shaft – Mechanical & Thermal Loading 7-39

7.18. LP Shaft – Cold Start 7-40

7.19. LP Shaft – Warm Start 7-42

7.20. LP Shaft – Hot Start 7-44

7.21. LP Shaft – Cold start (Radial and Axial stress) 7-46

7.22. LP Shaft – Warm start (Radial and Axial stress) 7-47

7.23. LP Shaft – Hot start (Radial and Axial stress) 7-48

7.24. Observations 7-49

Section 8 Life Assessment 8-1

8.1. Introduction to fatigue 8-1

8.2. Three stages of fatigue failure 8-1

8.3. Thermo mechanical fatigue (TMF) 8-2

8.4. Creep fatigue 8-10

8.5. Introduction to FESAFE 8-12

8.6. Fe-safe analysis procedure 8-12

8.7. Loading Cycle 8-14

8.8. Critical Locations of failure 8-15

8.9. Observations 8-18

Section 9 Conclusion 9-1

List of Figures

Figure 3:1: Transient Temperature variation 3-4

Figure 5:1: CAD model of steam turbine IP Outer Casing 5-3

Figure 5:2: CAD model of steam turbine IP Outer Casing 5-7

Figure 5:3: CAD model of steam turbine IP Shaft 5-8

Figure 5:4: CAD model of steam turbine LP Outer Casing 5-13

Figure 5:5: CAD model of steam turbine LP Inner Casing 5-15

Figure 5:6: CAD model of steam turbine LP Inner Outer Casing 5-17

Figure 5:7: CAD model of steam turbine LP Shaft Outer Casing 5-19

Figure 5:8: CAD Model of IP & LP Assembly 5-20

Figure 6:1: FE Model of Steam Turbine IP Outer Casing 6-2

Figure 6:2: FE Model of Steam Turbine IP Inner Casing 6-3

Figure 6:3: Axi symmetric Solid FE model of Steam Turbine IP casing assembly 6-4

Figure 6:4: FE Model of Steam Turbine IP Shaft 6-4

Figure 6:5 Axisymmetric Solid FE model of Steam Turbine IP Shaft 6-5

Figure 6:6: FE Model of Steam Turbine LP Outer Casing 6-6

Figure 6:7: FE Model of Steam Turbine LP Inner Casing Assembly 6-7

Figure 6:8: FE Model of Steam Turbine LP outer Casing 6-8

Figure 6:9: Axisymmetric Solid FE model of steam Turbine LP Casing Assembly 6-8

Figure 6:10: FE Model of Steam Turbine LP Shaft 6-9

Figure 6:11: Axisymmetric Solid FE model of steam Turbine LP Shaft 6-9

Figure 7:1: Longitudinal Displacement (Y) along Edge of the IP casing Assembly (Cut Section) is constrained 7-1

Figure 7:2: Longitudinal Displacement (Y) along Edge of the IP casing Assembly (3D View) is constrained 7-2

Figure 7:3:Translational displacement (z) along Edge of the IP casing Assembly (3D View) is constrained 7-3

Figure 7:4: Pressure and thermal loading applied on 14 stages of IP Casing Assembly (Cut Section) 7-4

Figure 7:5: Pressure and thermal loading applied on 14 stages – IP Casing Assembly (3D View) 7-4

Figure 7:6: Steady State Temperature (Max. 526^{0}C) profile at the end of cold start – IP Casing Assembly (Cut Section) 7-5

Figure 7:7: Steady State Temperature (Max. 527^{0}C) profile at the end of cold start – IP Casing Assembly (3D View) 7-6

Figure 7:8: Transient Temperature plot at the end of cold start – IP Casing Assembly7-7

Figure 7:9: vonMises Stress Contour (Max. 262 MPa) at the end of cold start - IP Casing Assembly (Cut Section) 7-7

Figure 7:10: vonMises Stress Contour (Max. 280 MPa) at the end of cold start - IP Casing Assembly (3D View) 7-8

Figure 7:11: Transient Stress plot at the end of cold Start – IP Casing Assembly 7-8

Figure 7:12: Steady State Temperature (Max. 526^{0}C) profile at the end of warm start – IP Casing Assembly (Cut Section) 7-9

Figure 7:13: Transient Temperature plot at the end of warm start – IP Casing Assembly 7-9

Figure 7:14: vonMises Stress Contour (Max. 284 MPa) at the end of warm start - IP Casing Assembly (Cut Section) 7-10

Figure 7:15: vonMises Stress Contour (Max. 278 MPa) at the end of warm start - IP Casing Assembly (3D View) 7-11

Figure 7:16: Transient Stress plot at the end of warm Start – IP Casing Assembly 7-11

Figure 7:17: Steady State Temperature (Max. 526^{0}C) profile at the end of hot start – IP Casing Assembly (Cut Section) 7-12

Figure 7:18: Transient Temperature plot at the end of hot start – IP Casing Assembly7-12

Figure 7:19: vonMises Stress Contour (Max. 274 MPa) at the end of hot start - IP Casing Assembly (Cut Section) 7-13

Figure 7:20: vonMises Stress Contour (Max. 234 MPa) at the end of hot start - IP Casing Assembly (3D View) 7-14

Figure 7:21: Transient Stress plot at the end of hot start – IP Casing Assembly 7-15

Figure 7:22: Longitudinal Displacement (Y) along Edges of the LP Shaft (Cut Section) is constrained 7-15

Figure 7:23: Pressure and thermal loading applied on 14 stages of IP Shaft (Cut Section) 7-15

Figure 7:24: Steady State Temperature (Max. 526^{0}C) profile at the end of cold start – IP Shaft (Cut Section) 7-16

Figure 7:25: Transient Temperature plot at the end of cold start – IP Shaft 7-16

Figure 7:26: vonMises Stress Contour (Max. 91 MPa) at the end of cold start - IP Shaft (Cut Section) 7-17

Figure 7:27: Transient Stress plot at end of cold Start – IP Shaft 7-17

Figure 7:28: Steady State Temperature (Max. 516^{0}C) profile at the end of warm start – IP Shaft (Cut Section) 7-18

Figure 7:29: Transient Temperature plot at the end of warm start – IP Shaft 7-18

Figure 7:30: vonMises Stress Contour (Max. 113 MPa) at the end of warm start - IP Shaft (Cut Section) 7-19

Figure 7:31: Transient Stress plot at end of warm Start – IP Shaft 7-19

Figure 7:32: Steady State Temperature (Max. 525^{0}C) profile at the end of hot start – IP Shaft (Cut Section) 7-20

Figure 7:33: Transient Temperature plot at the end of hot start – IP Shaft 7-20

Figure 7:34: vonMises Stress Contour (Max. 77 MPa) at the end of hot start - IP Shaft (Cut Section) 7-21

Figure 7:35: Transient Stress plot at end of hot Start – IP Shaft 7-21

Figure 7:36: Radial stress at the end of cold start is 29MPa – IP Shaft (Cut Section).7-22

Figure 7:37: Axial stress at the end of cold start is 36MPa – IP Shaft 7-22

Figure 7:38: Radial stress at the end of warm start is 47MPa – IP Shaft (Cut Section)7-23

Figure 7:39: Axial stress at the end of warm start is 76MPa – IP Shaft 7-23

Figure 7:40: Radial stress at the end of Hot start is 25MPa – IP Shaft (Cut Section)..7-24

Figure 7:41: Axial stress at the end of Hot start is 37MPa – IP Shaft 7-24

Figure 7:42: Longitudinal Displacement (Y) along Edges of the casing is constrained – LP Casing Assembly (Cut Section and 3D View) 7-25

Figure 7:43: Pressure and thermal boundary conditions applied for 6 stages – LP Casing Assembly (Cut Section and 3D View) 7-26

Figure 7:44: Steady State Temperature (Max. 297^{0}C) profile at the end of cold start – LP Casing Assembly (Cut Section) 7-27

Figure 7:45: Steady State Temperature (Max. 299^{0}C) profile at the end of cold start – LP Casing Assembly (3D view) 7-28

Figure 7:46: Transient Temperature plot at the end of cold start – LP Casing Assembly 7-28

Figure 7:47: vonMises Stress Contour (Max. 270 MPa) at the end of cold start LP Casing Assembly (Cut Section) 7-29

Figure 7:48: vonMises Stress Contour (Max. 213 MPa) at the end of cold start LP Casing Assembly (3D view) 7-30

Figure 7:49: Transient Stress plot at end of cold Start – LP Casing Assembly 7-30

Figure 7:50: Steady State Temperature (Max. 292^{0}C) profile at the end of warm start – LP Casing Assembly (Cut Section) 7-31

Figure 7:51: Steady State Temperature (Max. 299^{0}C) profile at the end of warm start – LP Casing Assembly (3D view) 7-32

Figure 7:52: Transient Temperature plot at the end of warm start – LP Casing Assembly 7-32

Figure 7:53: vonMises Stress Contour (Max. 256 MPa) at the end of warm start LP Casing Assembly (Cut Section) 7-33

Figure 7:54: vonMises Stress Contour (Max. 216 MPa) at the end of warm start LP Casing Assembly (3D View) 7-34

Figure 7:55: Transient Stress plot at end of warm Start – LP Casing Assembly 7-34

Figure 7:56: Steady State Temperature (Max. 294^{0}C) profile at the end of hot start – LP Casing Assembly (Cut Section) 7-35

Figure 7:57: Steady State Temperature (Max. 299^{0}C) profile at the end of hot start – LP Casing Assembly (3D View) 7-36

Figure 7:58: Transient Temperature plot at the end of hot start – LP Casing Assembly 7-36

Figure 7:59: vonMises Stress Contour (Max. 262 MPa) at the end of hot start - LP Casing Assembly (Cut Section) 7-37

Figure 7:60: vonMises Stress Contour (Max. 225 MPa) at the end of hot start - LP Casing Assembly (3D view) 7-38

Figure 7:61: Transient Stress plot at end of hot Start – LP Casing Assembly 7-38

Figure 7:62: Longitudinal Displacement (Y) along Edges of the LP shaft is constrained 7-39

Figure 7:63: Pressure and thermal boundary conditions applied for 6 stages – LP Shaft 7-39

344

Figure 7:64: Steady State Temperature (Max. 276^{0}C) profile at the end of cold start – LP Shaft (Cut Section) 7-40

Figure 7:65: Transient Temperature plot at the end of cold start - LP Shaft 7-40

Figure 7:66: vonMises Stress Contour (Max. 210 MPa) at the end of cold start - LP Shaft (Cut Section) 7-41

Figure 7:67: Transient Stress plot at end of cold Start – LP Shaft 7-41

Figure 7:68: Steady State Temperature (Max. 273^{0}C) profile at the end of warm start – LP Shaft (Cut Section) 7-42

Figure 7:69: Transient Temperature plot at the end of warm start - LP Shaft 7-42

Figure 7:70: vonMises Stress Contour (Max. 228MPa) at the end of warm start– LP Shaft (Cut Section) 7-43

Figure 7:71: Transient Stress plot at the end of Warm Start – LP Shaft 7-43

Figure 7:72: Steady State Temperature (Max. 278^{0}C) profile at the end of Hot Start – LP Shaft (Cut Section) 7-44

Figure 7:73: Transient Temperature plot at the end of Hot start – LP Shaft 7-44

Figure 7:74: vonMises Stress Contour (Max. 193 MPa) at the end of hot start – LP Shaft (Cut Section) 7-45

Figure 7:75: Transient Stress plot at the end of Hot Start – LP Shaft 7-45

Figure 7:76: Radial stress at the end of cold start is 56MPa – LP Shaft (Cut Section)7-46

Figure 7:77: Axial stress at the end of cold start is 65MPa – LP Shaft 7-46

Figure 7:78: Radial stress at the end of warm start is 65MPa – LP Shaft (Cut Section) 7-47

Figure 7:79: Axial stress at the end of warm start is 70MPa – LP Shaft 7-47

Figure 7:80: Radial stress at the end of Hot start is 45MPa – LP Shaft (Cut Section).7-48

Figure 7:81: Axial stress at the end of Hot start is 37MPa – LP Shaft 7-48

Figure 8:1: Three stages of fatigue failure 8-1

Figure 8:2: strain time history 8-3

Figure 8:3: Fatigue stress- strain cycle constructed considering the effect of strain rate and temperature 8-4

Figure 8:4: strain time history (In phase and out of phase) 8-6

Figure 8:5: Effect of phase relationship on fatigue strength 8-6

Figure 8:6: Bulk stress relaxation 8-8
Figure 8:7: Reduction in strength as a result of pre-soak 8-9
Figure 8:8: Stages of creep(Strain vs. time) 8-11
Figure 8:9: Combined creep fatigue failure 8-11
Figure 8:10: Scaling stress tensor by loading history 8-13
Figure 8:11: Cyclic plasticity model 8-14
Figure 8:12: Loading Cycle 8-15
Figure 8:13: Critical Locations of failure – IP Casing Assembly 8-16
Figure 8:14: Critical Locations of failure – IP Shaft 8-16
Figure 8:15: Critical Locations of failure – LP Casing Assembly 8-17
Figure 8:16: Critical Locations of failure – LP Shaft 8-17

346

List of Tables

Table 3-1: Load case specifications 3-2
Table 3-2: Pressure and Temperature at 14 stages of IP Casings 3-3
Table 3-3: Pressure and Temperature at 6 stages of LP Casings 3-3
Table 4-1: Material properties for IP and LP Casings 4-1
Table 4-2: Material properties for IP and LP Rotor 4-2
Table 6-1: quality criteria for meshing 6-1
Table 7-1: Transient Peak Stress in the IP and LP Steam Turbine 7-49
Table 7-2: Steady State Peak Stress in the IP and LP Steam Turbine 7-49
Table 7-3: Steady State Peak Stress in the LP shaft for temperature and pressure variation 7-49

347

Section 1 Objective

The objective is to perform the Finite Element analysis of 500 MW Steam Turbine components. Intermediate Pressure (IP) and Low Pressure (LP) turbine needs to be analyzed for thermal and mechanical loading. Temperature and stress results are further post-processed to evaluate the life of the turbine and identify the critical failure locations and further to determine the remaining life.

Components considered:

- IP rotor
- IP Casing Assembly.
- LP Rotor
- LP Casing Assembly.

Section 2 Introduction

The 500MW Steam Turbine located at Korba is of Axial Flow type. The turbine cylinder is essentially a pressure vessel with its weight supported at each end on the horizontal centerline. It is designed to withstand hoop stress in the transverse plane, and to be very stiff in the longitudinal direction in order to maintain accurate clearances between the stationary and rotating parts of the turbine. Casings are split along their horizontal centerline to allow the rotor to be inserted as a complete assembly.

The present scope involves performing Finite element analysis of IP and LP subjected to pressure and temperature loading and estimate the remaining life of the turbine.

2.1. Introduction to ABAQUS

In this work Abaqus is used as the Solver for Finite Element Analysis.

The ABAQUS suite of software for finite element analysis (FEA) has the ability to solve a wide variety of numerical simulations. The ABAQUS suite consists of three core products - ABAQUS/Standard, ABAQUS/Explicit and ABAQUS/CAE.

We have used ABAQUS/Standard (a general-purpose finite element program) which is designed to solve traditional implicit finite element analyses, such as static, dynamics, and thermal. It is equipped with a wide range of contact and nonlinear material options. ABAQUS/Standard also has optional add-on and interface products, as well as integration with third party software.

2.2 Assumptions and other Remarks

FE analysis is carried out by following assumptions:

- Linear elastic FE analysis is performed. Plasticity correction as per Neubeur's principle is used.
- Corrosion and Erosion effects were not Significant (during inspections). However if there is a quantification of such damage, the same can be incorporated in the FEA analysis.
- Temperature based material properties were taken from the reference literatures.

The boundary conditions, thermo-mechanical loading and results for each case is discussed in each sub section.

Section 3 FE Analysis Description

- The Steam Turbine and the shaft are numerically simulated using Finite Element Method. The IP casing is made of "GS22 MO4" and the IP shaft is made of "30Cr Mo Ni V 511" material. The LP casing is made of st. 37-2N & LP shaft is made of "26 Ni Cr Mo V 145" material. The FE analysis is carried out for different start-up (cold, warm and hot) and shut-down (warm drop and hot drop) conditions and operating loading conditions, which are given in the Table 3-1. During the transient events in the operation of a steam turbine, thermal stresses occurs causing high fatigue loading. At the same time, turbines experience gradual creep loading as result of general operation at high temperatures. Combining creep and fatigue loading over time puts stresses on the turbine, eventually leading to crack initiation and growth that can limit turbine life. The temperature changes cause cyclic loading, leading to fatigue failure. The present study involves numerical study of the steam turbine subjected to thermo-mechanical forces and life estimation due to thermo-mechanical, creep and fatigue loads.

3.1. Load cases

Following **Table 3-1** shows the different load cases to be analyzed. Temperature changes during startup (cold, warm, and hot) conditions are shown in Figure 3:1

1. Cold start (Shut down more than 48 hours and turbine metal temperatures < 200 Degree C) – Cold start and reaching the steady state.
2. Warm start (Shut down between 8 to 48 hours and turbine metal temperatures > 200 Degree C) – Warm drop then warm start and reaching to steady state.
3. Hot start (Short shut down less than 8 hours and turbine metal temperatures > 350 Degree C) – Hot drop then Hot start and reaching to steady state.
4. Operating conditions like rpm, Steam pressure.

Table 3-1: Load case specifications

1	**IP Casing**
	Thermo-mechanical Loading
	Creep and Fatigue Loading
2	**IP shaft**
	Thermo-mechanical Loading
	Body Force (including Gravity, Inertial Forces & Centrifugal Forces)
	Creep and Fatigue Loading
3	**LP Casing**
	Thermo-mechanical Loading
	Fatigue Loading
4	**LP shaft**
	Thermo-mechanical Loading
	Body Force (including Gravity, Inertial Forces & Centrifugal Forces)
	Fatigue Loading

Temperature and pressure is applied at 14 different stages of IP Inner and outer casings as given in **Table 3-2**. Temperature and pressure is applied at 6 different stages of LP Inner and outer casings are given in **Table 3-3**. Units followed are SI. The pressure given in these tables is converted to N/mm^2.

For LP casing and shaft creep is not significant. So creep is not considered for LP casing and shaft analysis.

For IP casing and shaft Creep & fatigue are both considered. However, the dominant damage mechanism will be fatigue.

351

Table 3-2: Pressure and Temperature at 14 stages of IP Casings

IP Casing		
Stages	**Pressure (Bar)**	**Temperature(°C)**
INLET	47.802	537
l	45.887	530
2	41.808	520
3	40.78	500
4	34.67	470
5	30.591	460
6	28.522	445
7	20.605	428.3
8	20.394	405
9	18.354	385
10	16.825	375
11	15.295	355
12	13.256	345
13	12.236	325
14	7.9373	299.6

Table 3-3: Pressure and Temperature at 6 stages of LP Casings

LP TURBINE		
Stages	**Pressure (Bar)**	**Temperature(° C)**
INLET	7.9373	299.6
1	5.047	245
2	2.8534	194.2
3	1.4501	135

4	0.866	70
5	0.293	65.4
6	0.0884	46.4

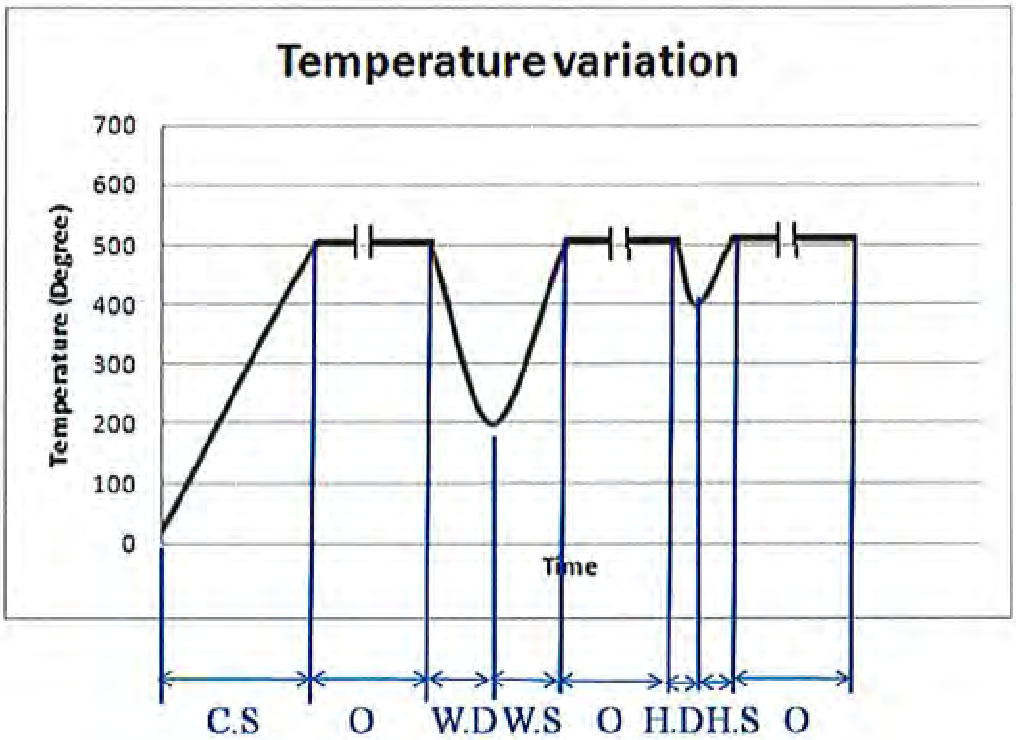

C.S – Cold start, O – Operating, W.D -Warm drop, W.S- Warm start, H.D - Hot drop, H.S- Hot start.

Figure 3:1: Transient Temperature variation

Section 4 Material specification

Table 4-1 gives the list of temperature dependent material properties IP Casing (GS22 MO4) and LP casing is (st.37-2N). Table 4-2 gives the list of temperature dependent material properties IP (30Cr Mo Ni V 511) & LP Rotor (26 Ni Cr Mo V 145) used in the analysis. All the above material properties were taken from the relevant standards / references. The material properties are extrapolated beyond specified temperatures.

Table 4-1: Material properties considered for IP and LP Casings

Temperature T (°C)	Thermal conductivity, K (W/m K)	Specific heat (J/Kg K)	Co efficient of thermal expansion , α (/°C)	Young's Modulus , E (MPa)
0	54	425	1.20E-05	210000
50	52.33	459.7	1.23E-05	210000
100	50.67	487.62	1.25E-05	210000
150	49	510.41	1.27E-05	199500
200	47.34	529.76	1.29E-05	189000
250	45.67	547.31	1.31E-05	178500
300	44.01	564.74	1.33E-05	168000
350	42.34	583.7	1.35E-05	157500

Table 4-2: Material properties consiedred for IP and LP Rotor

Temperature, T (°C)	Thermal conductivity, K (W/m K)	Specific heat (J/Kg K)	Co efficient of thermal expansion , α (/°C)	Young's Modulus , E (MPa)
0	43.27	485.67	1.17E-05	2.06795E+11
20	43.27	485.67	1.17E-05	2.06795E+11
25	43.18	485.67	1.17E-05	2.06643E+11
50	43.05	489.86	1.19E-05	2.04971E+11
100	42.75	498.23	1.22E-05	2.02234E+11
150	42.32	510.79	1.24E-05	1.99192E+11
200	41.8	527.54	1.27E-05	1.95847E+11
250	41.19	546.38	1.30E-05	1.92198E+11
300	40.41	569.4	1.33E-05	1.88549E+11
350	39.55	596.62	1.35E-05	1.94595E+11
400	38.6	628.02	1.37E-05	1.80338E+11
450	37.47	665.7	1.39E-05	1.75776E+11
500	36.35	695.01	1.41E-05	1.7091E+11
550	34.87	736.88	1.43E-05	1.65436E+11

355

Section 5 CAD Model Details

The CAD modeling of Steam Turbine is carried out in CATIA V5 R17 Software. The snap shot of assembly & individual components are shown in Figure 5:1 to Figure 5:8. The inner parts are not modeled. Dimensions in green color are missing in the drawing sheet. They have been measured on the sheet, scaled appropriately and modeled.

5.1. IP Outer Casing (Dwg # 0-10601-02000-C)

Fig 1

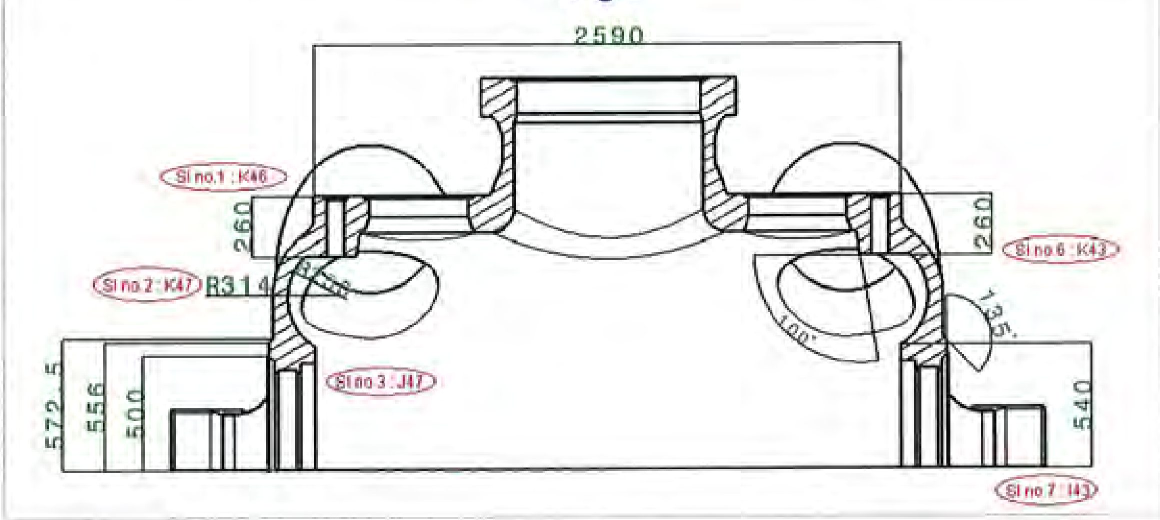

356

Fig 2

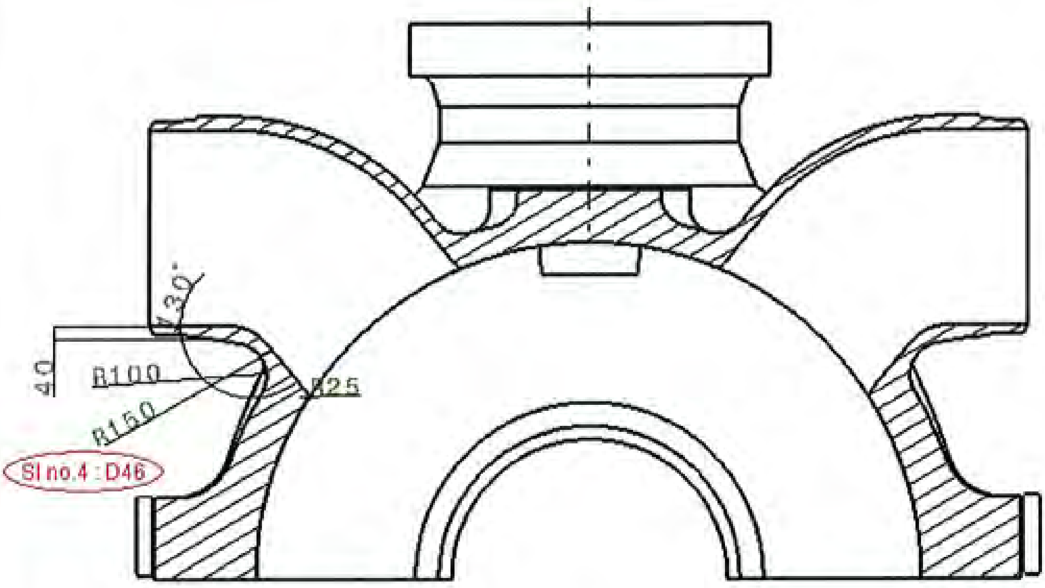

30°
40
R100
R25
R150
Sl no.4 : D46

Fig 3

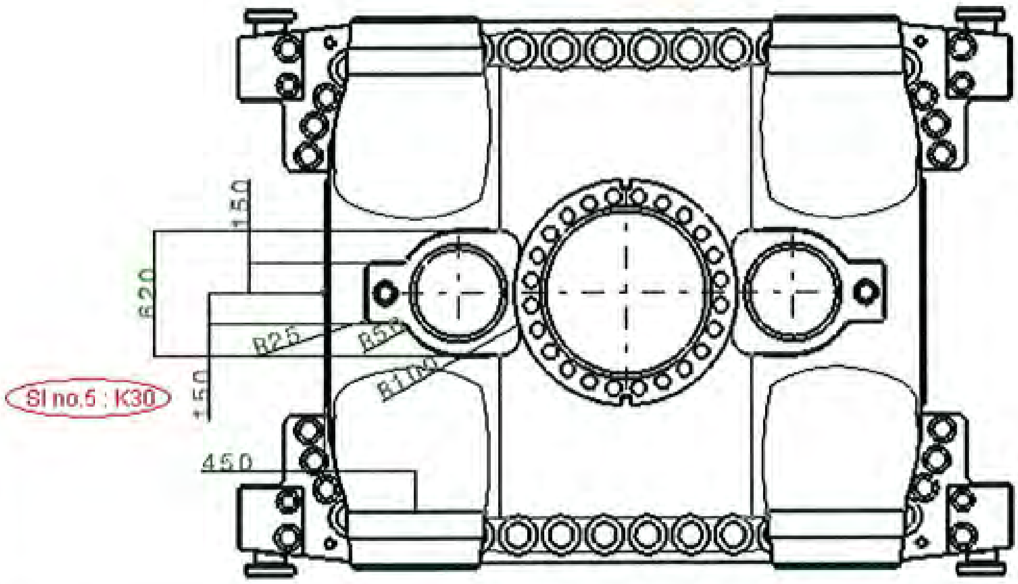

150
620
R25
R50
R100
Sl no.5 : K30
150
450

Figure 5:1: CAD model of steam turbine IP Outer Casing

5.2. IP Inner Casing (Dwg # 0-10602-02000C)

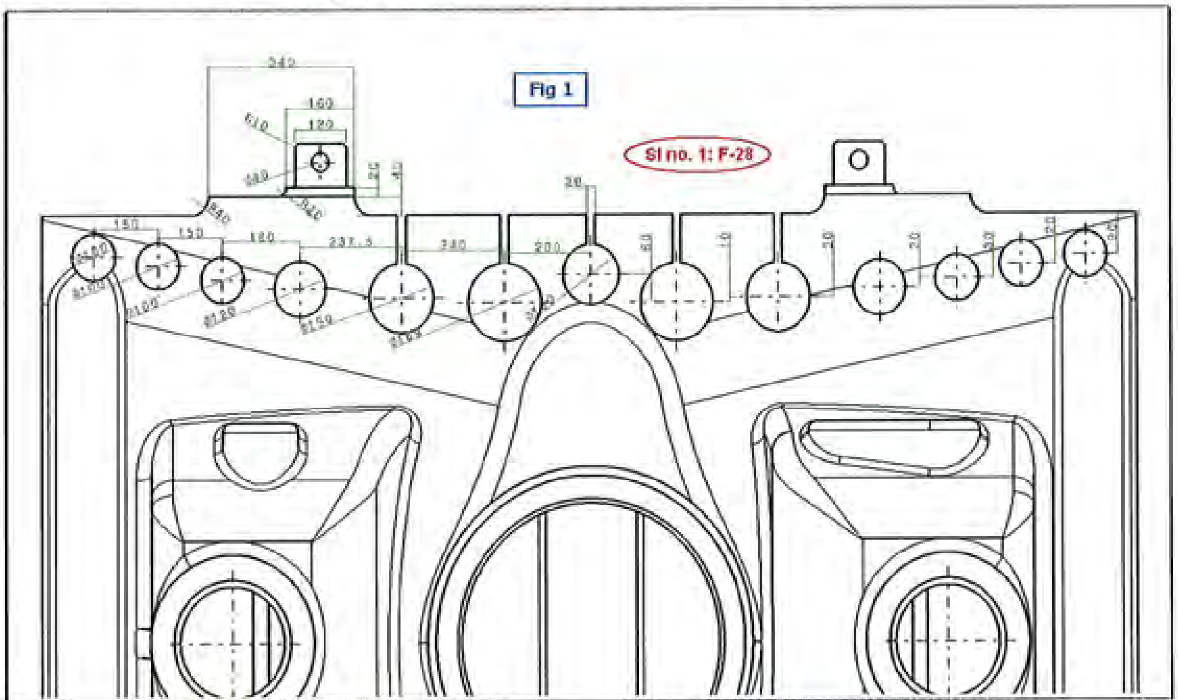

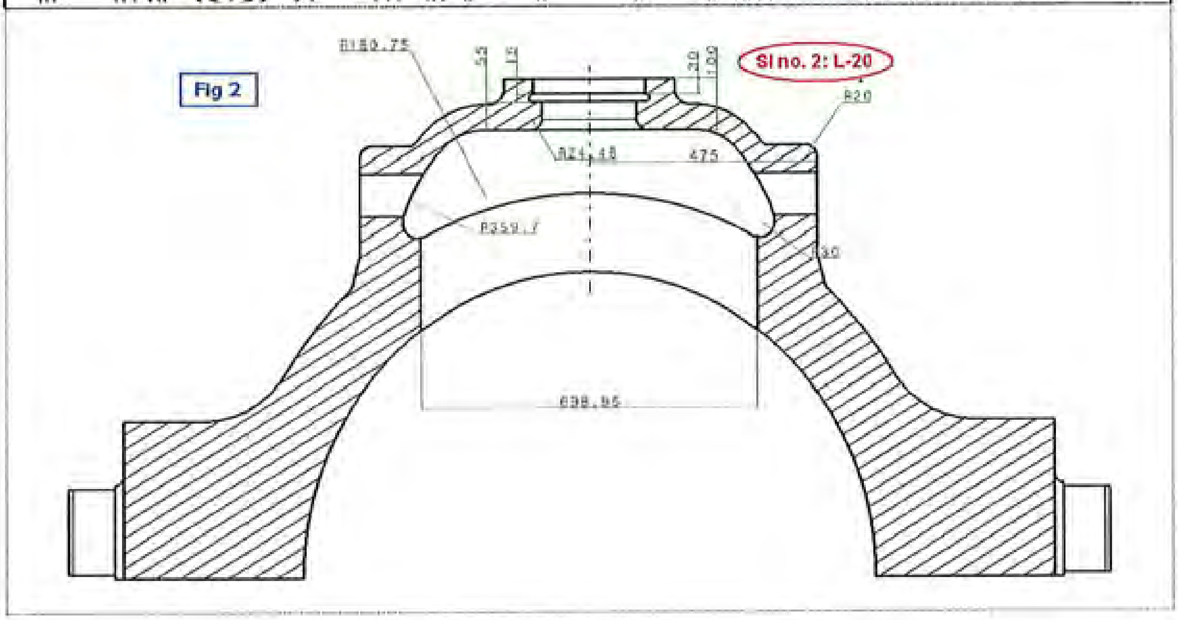

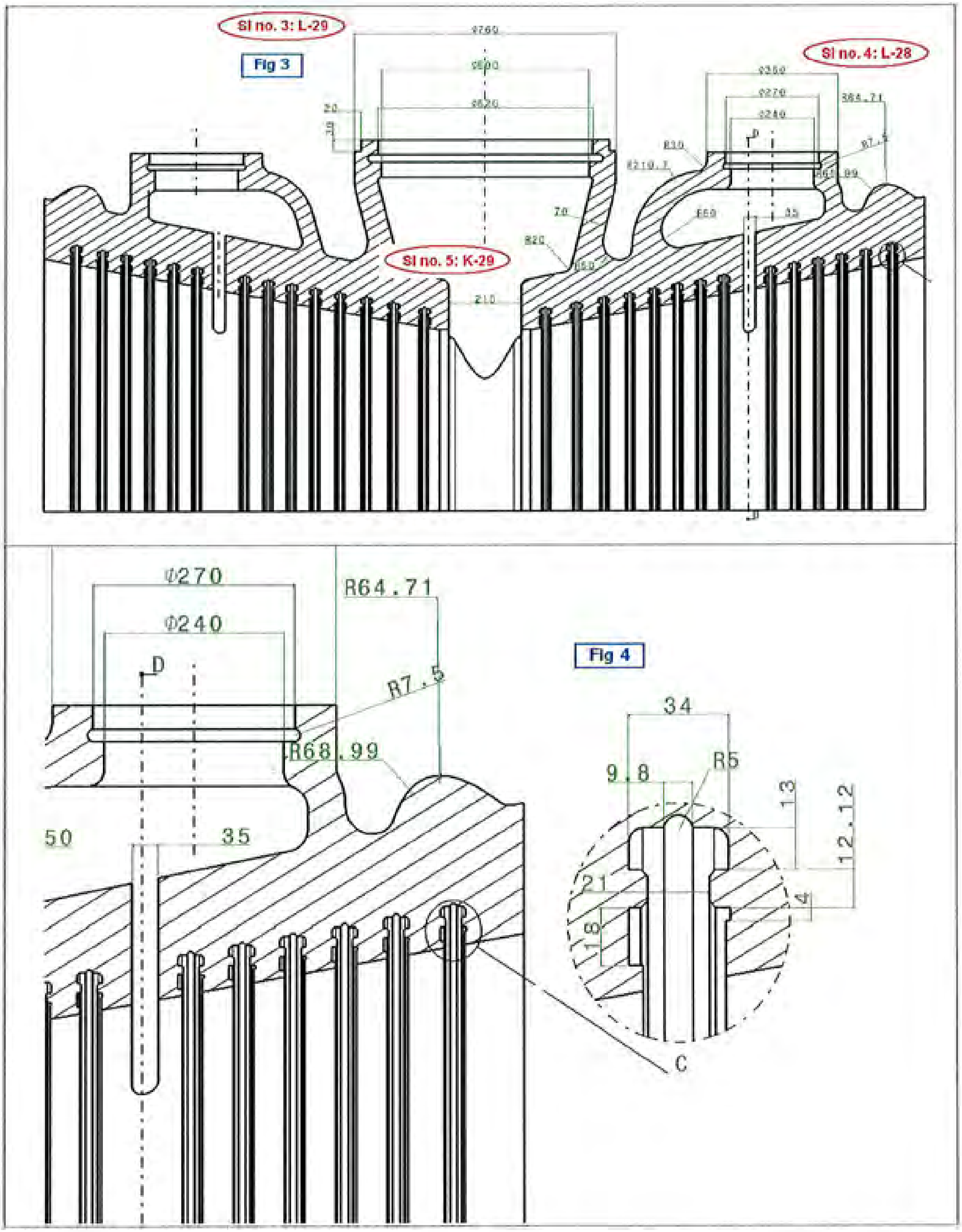

Sl no. 3: L-29
Fig 3
Sl no. 4: L-28
Sl no. 5: K-29
210
Φ270
Φ240
R64.71
R7.5
R68.99
D
50
35
Fig 4
34
9.8
R5
13
12.12
21
4
18
C

360

Fig 5

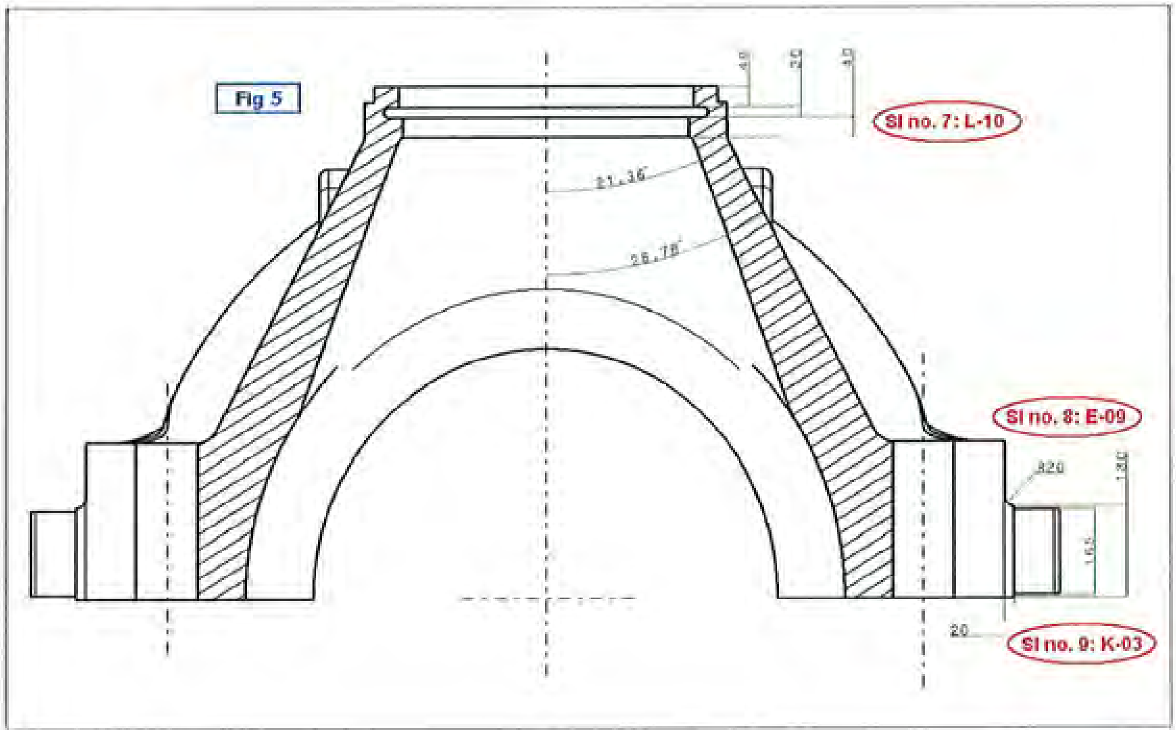

Figure 5:2: CAD model of steam turbine IP Outer Casing

5.3. IP Shaft (Dwg # 0-10201-02000C)

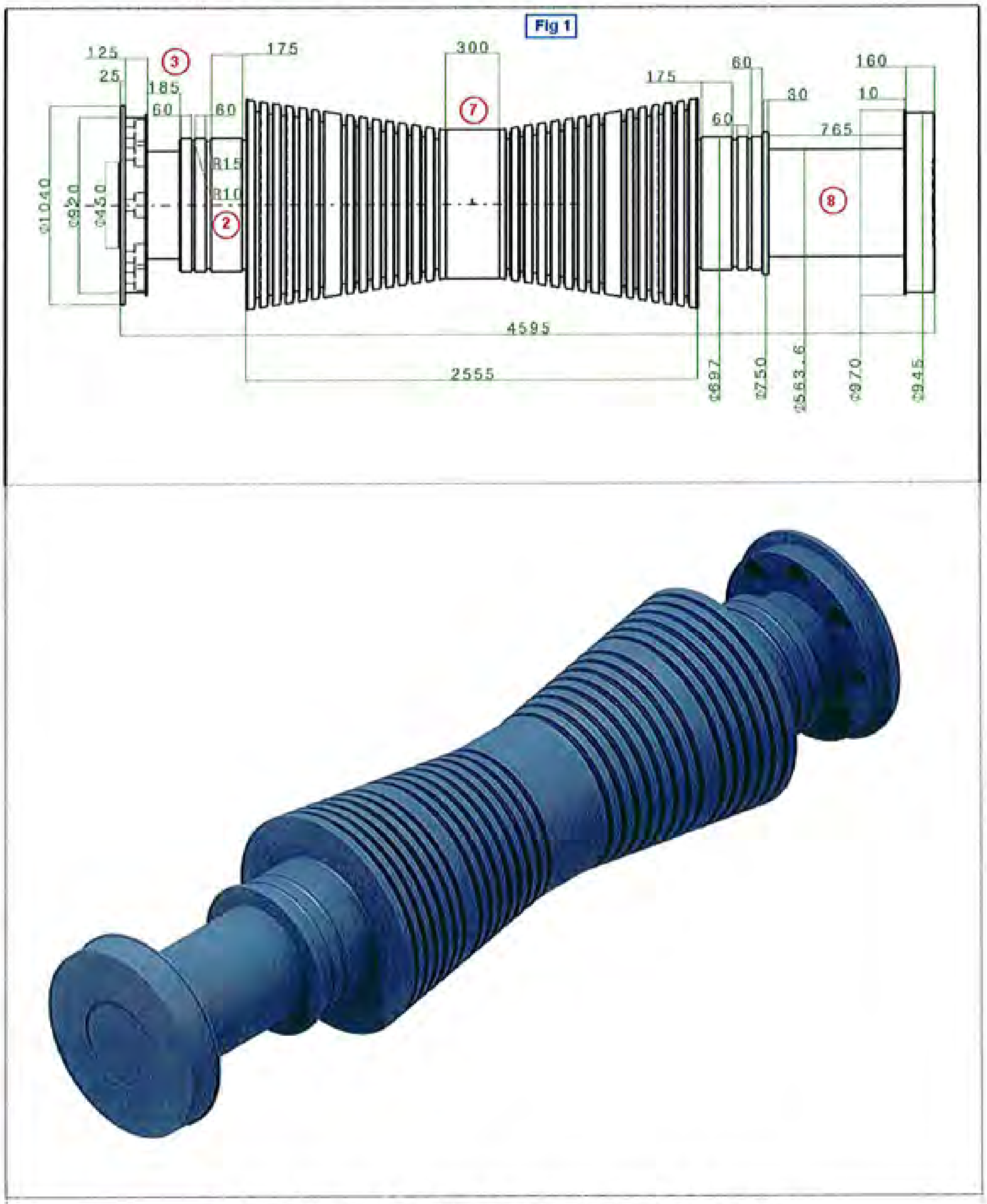

Figure 5:3: CAD model of steam turbine IP Shaft

363

5.4. LP Outer Casing

Fig 1

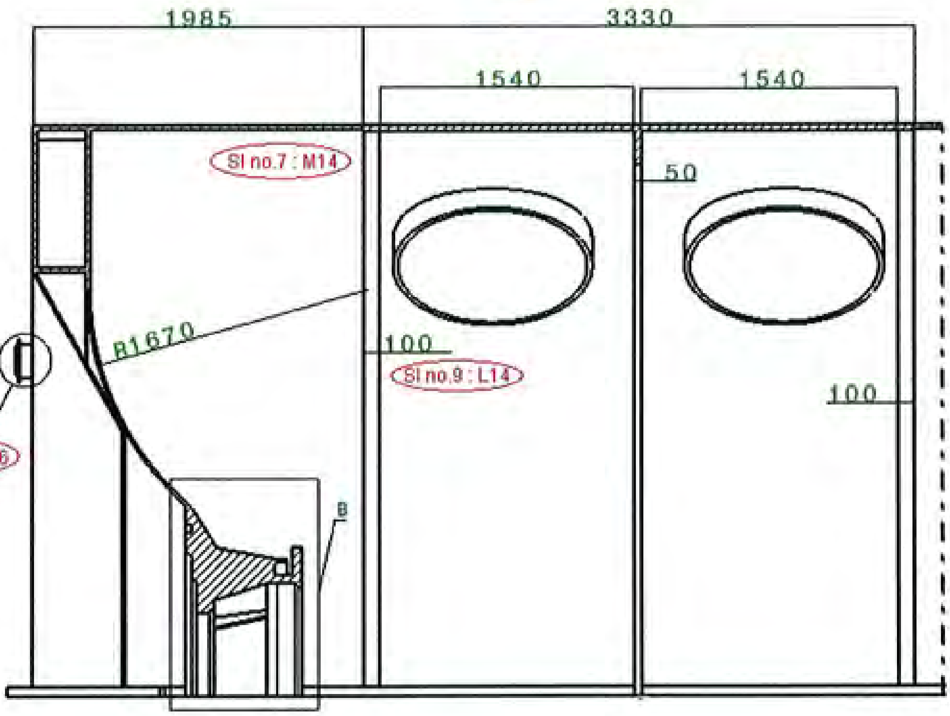

364

Fig 2

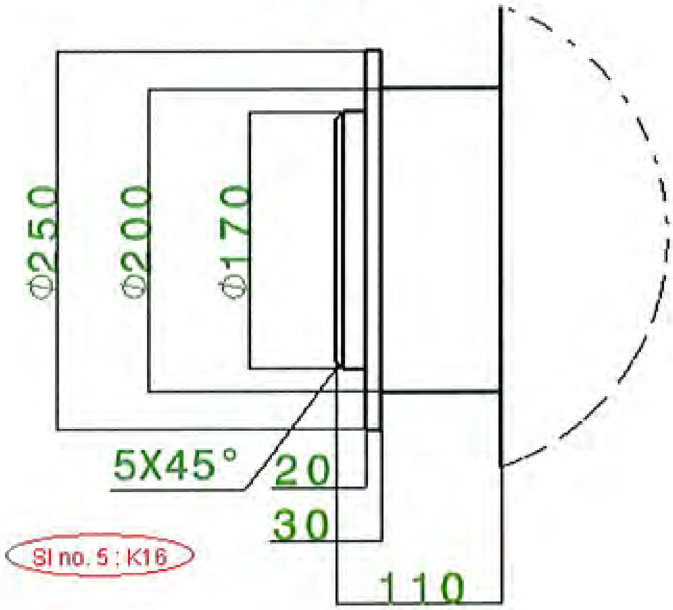

Detail A
Scale: 5:1

Fig 3

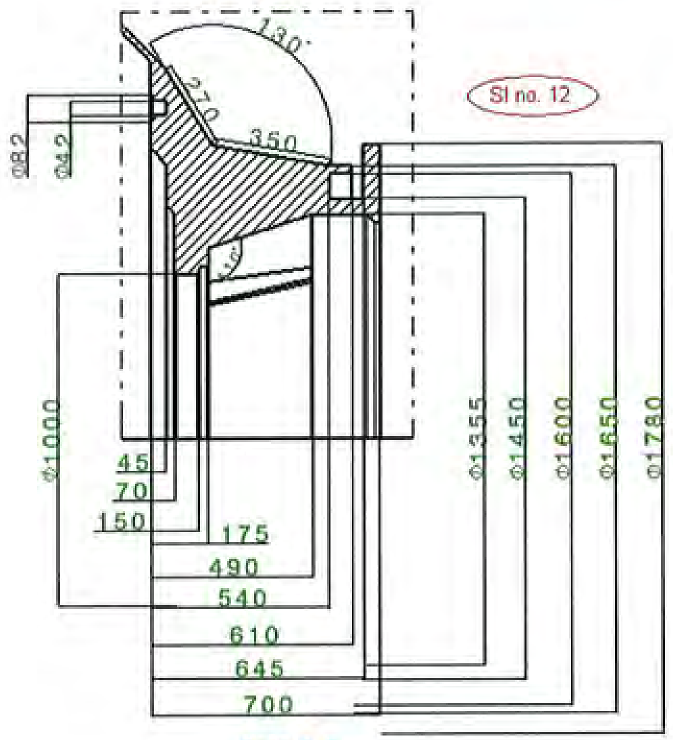

Detail B
Scale: 3:1

Fig 4

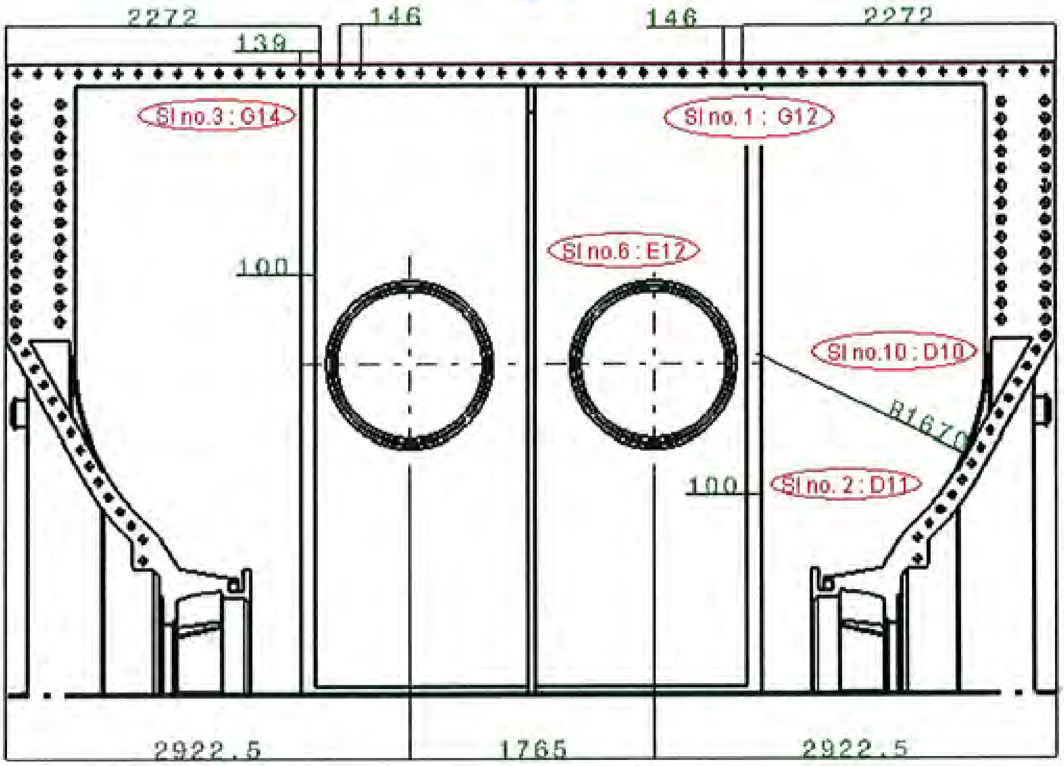

2272
146
146
2272
139
Sl no.3 : G14
Sl no. 1 : G12
Sl no.6 : E12
100
Sl no.10 : D10
R1670
100
Sl no. 2 : D11
2922.5
1765
2922.5

Fig 5

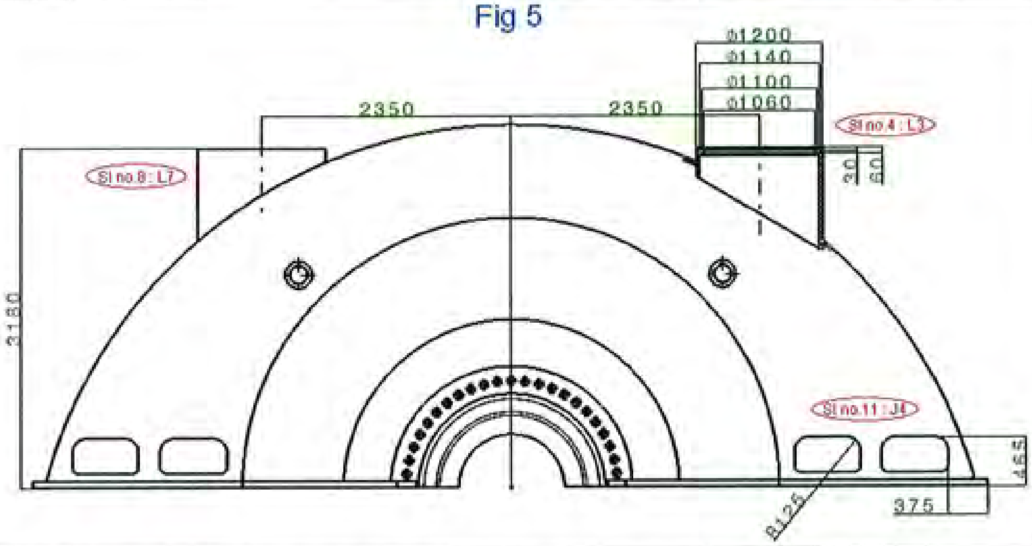

Φ1200
Φ1140
Φ1100
Φ1060
2350
2350
Sl no.4 : L3
Sl no.8 : L7
30
60
3180
Sl no.11 : J4
465
375
R125

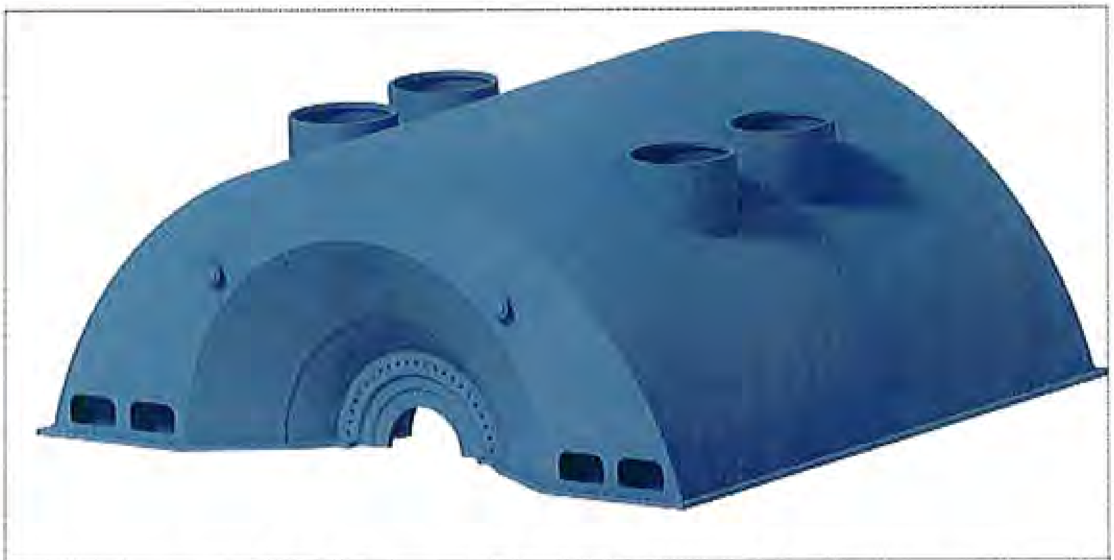

Figure 5:4: CAD model of steam turbine LP Outer Casing

5.5. LP Inner Casing (Dwg # 0-10743-02000C)

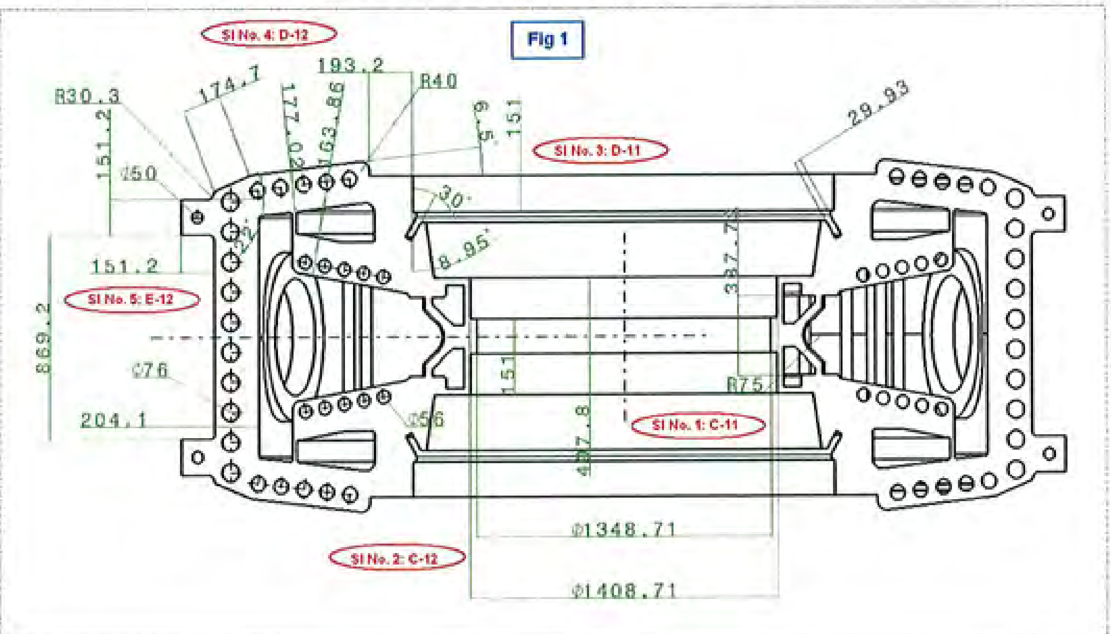

318

Fig 2

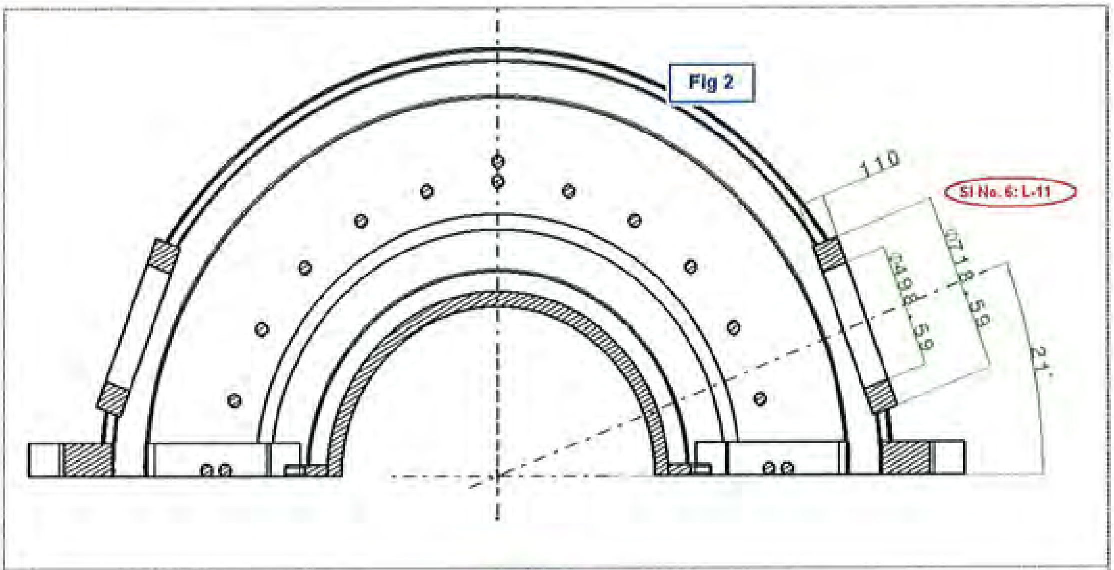

110
SI No. 6: L-11
Ø718.59
Ø498.59
21°

Fig 3

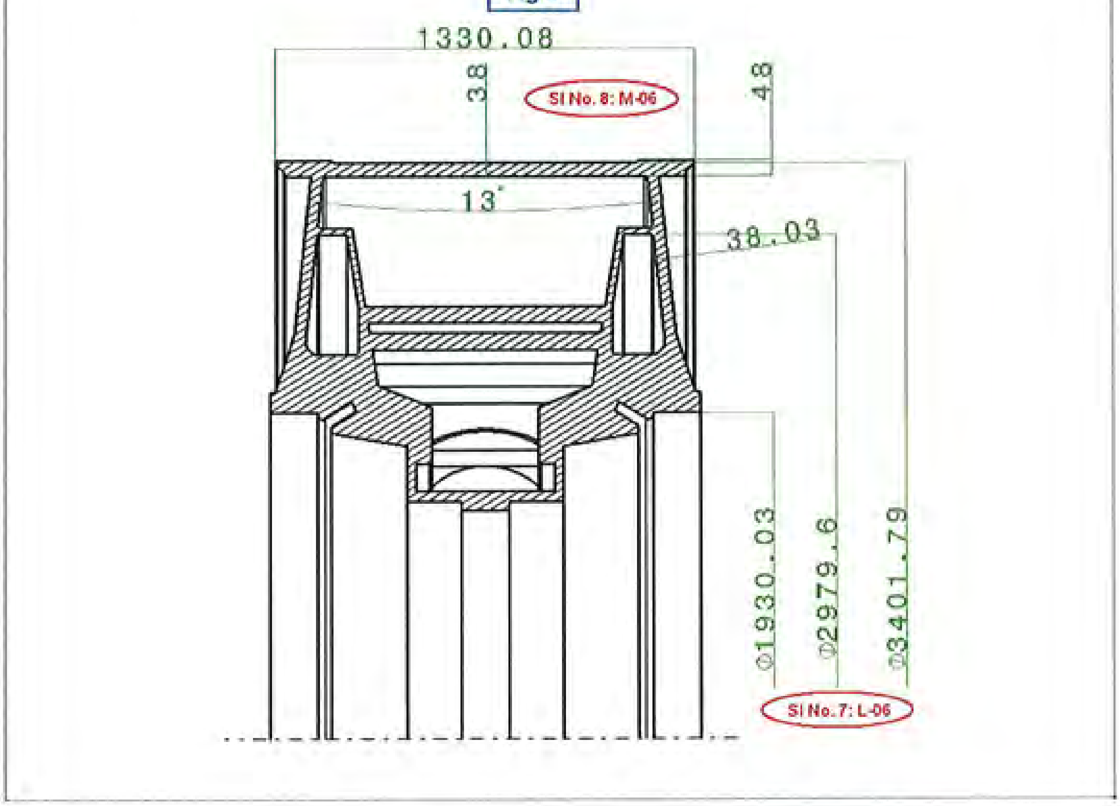

1330.08
38
SI No. 8: M-06
48
13°
38.03
Ø1930.03
Ø2979.6
Ø3401.79
SI No. 7: L-06

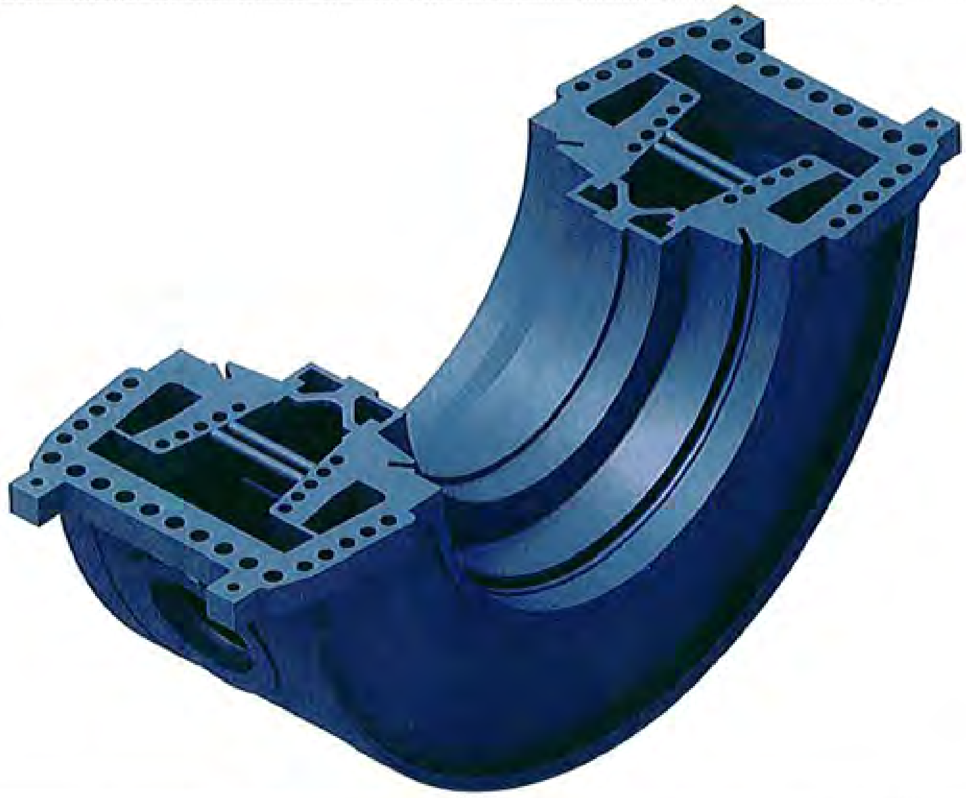

Figure 5:5: CAD model of steam turbine LP Inner Casing

5.6. LP Inner Outer Casing

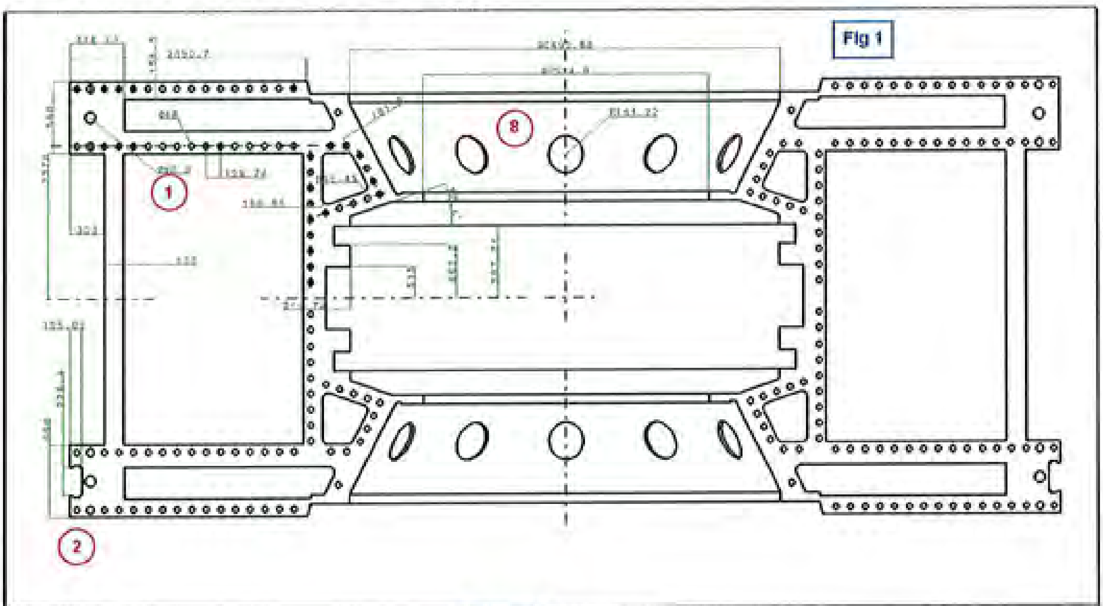

Fig 1

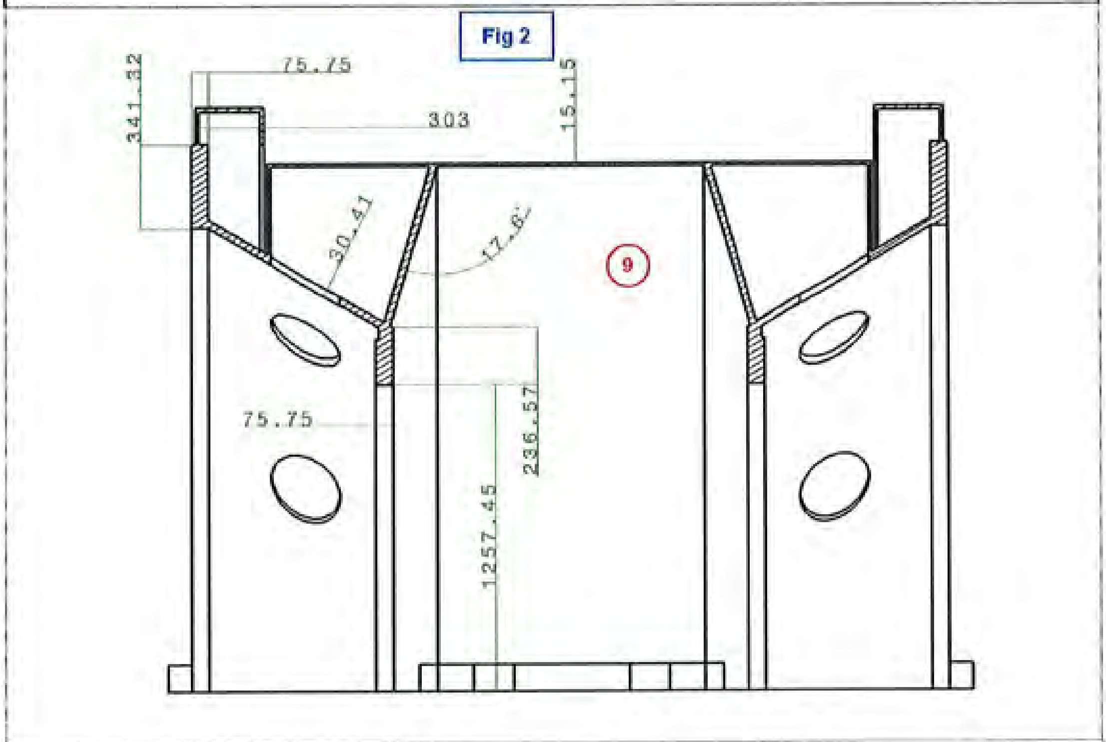

Fig 2

Figure 5:6: CAD model of steam turbine LP Inner Outer Casing

5.7. LP Shaft (Dwg # 0-10301-02000C)

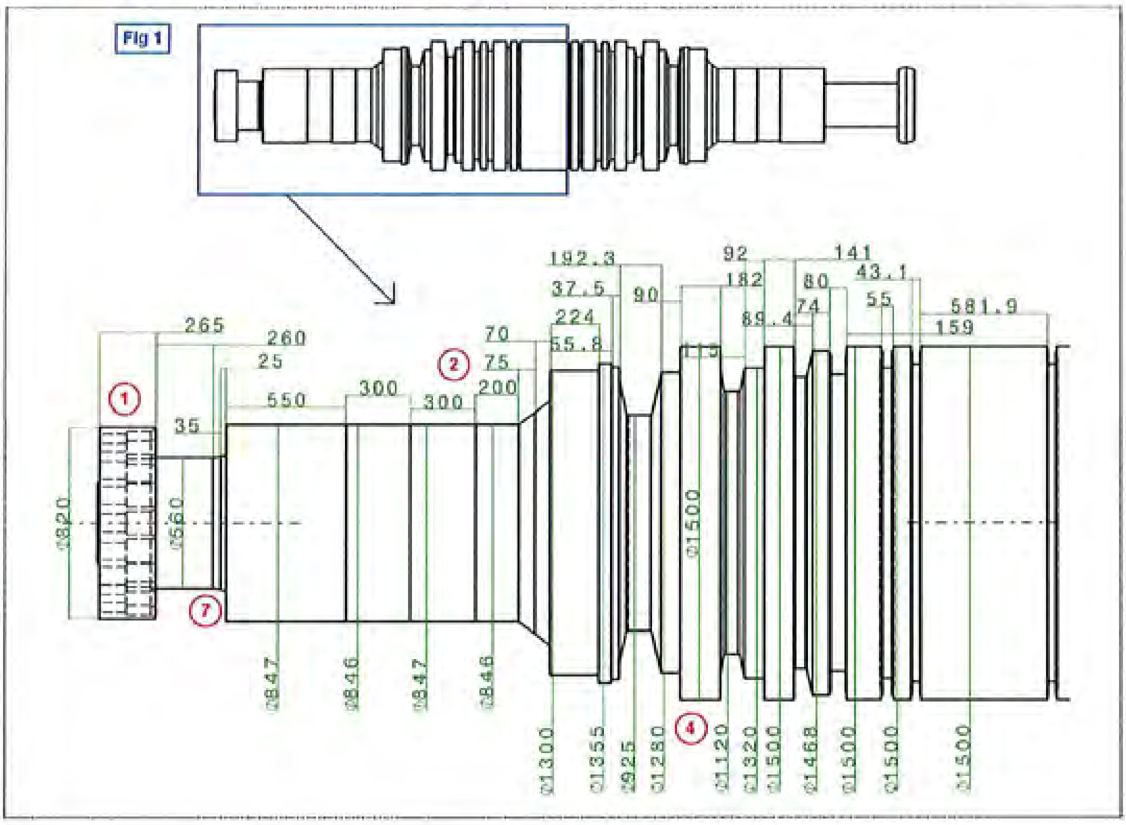

Figure 5:7: CAD model of steam turbine LP Shaft Outer Casing

374

5.8. Steam Turbine IP and LP Assembly

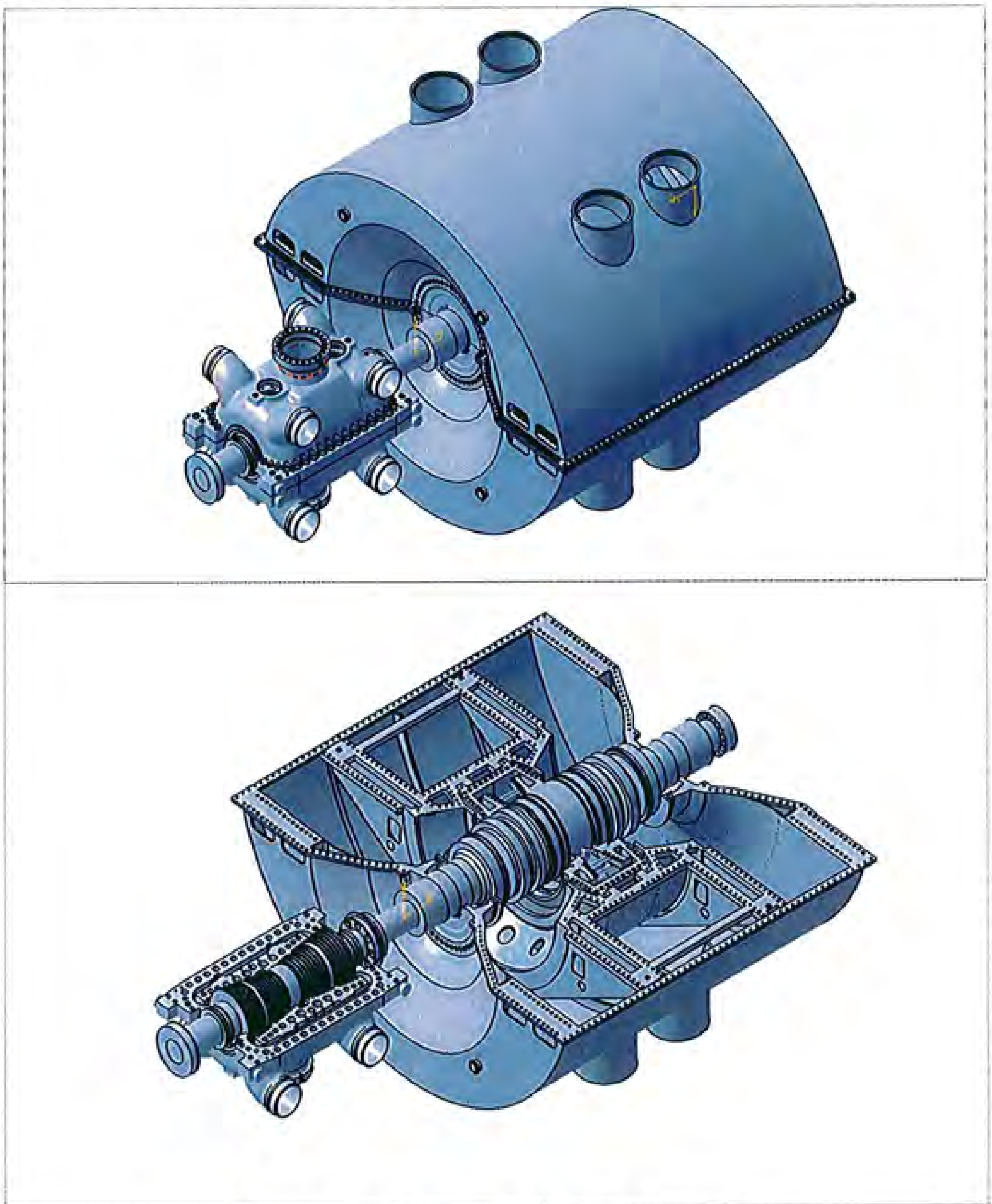

Figure 5:8: CAD Model of IP & LP Assembly

Section 6 Mesh Model Details

The meshing of IP and LP Assembly is carried out in HYPERMESH software. The snap shot of assembly & individual components are shown in Figure 6:1 to Figure 6:10. The finite element quality criteria considered in meshing is in Table 6-1. Coupled temperature-displacement elements are used in the analysis. Total number of elements in the IP Casing Assembly is complete model is 2,09,827, IP Shaft is 1,04,607, LP Casing Assembly is 2,77,189 and LP Shaft is 3,49,652.

Table 6-1: Quality criteria for meshing

Sl. No.	Component Name	Type of element	No of elements	% of elements Aspect ratio* (>5) / Tetra Collapse (<0.1)
1	IP Outer Casing	C3D4T	105220	0
2	IP Inner Casing	C3D4T	104607	2
3	IP casing assembly – Axi-symmetric	CAX4T	44893	1.24
4	IP Shaft	C3D4T	104607	0
5	IP shaft – Axi-symmetric	CAX4T	18445	0
6	LP Outer Casing	C3D4T	104607	0
7	LP Inner Casing	C3D4T	84346	0
8	LP Inner outer casing	C3D4T	88236	1
9	LP Casing assembly	CAX4T	19564	0
10	LP Shaft	C3D4T	349652	3
11	LP shaft – Axi-symmetric	CAX4T	3426	0

*Aspect ratio is the ratio of the length to width in an element of FE mesh. This ratio determines the quality of the FE results.

376

Description of the elements used-

CAX4T (Axi-sym. Quad)	4-node bilinear displacement and temperature
CAX3T(Axi-sym. Triangular)	3-node linear displacement and temperature
C3D4T(Tetra)	4-node linear displacement and temperature

The quality criteria of individual components are shown in the Table 6-1 in the right side of the individual component. The mesh quality has not been compromised at all the critical stress concentrated locations. Following figures shows the meshed components of the steam turbine.

6.1. FE Model of IP Outer Casing

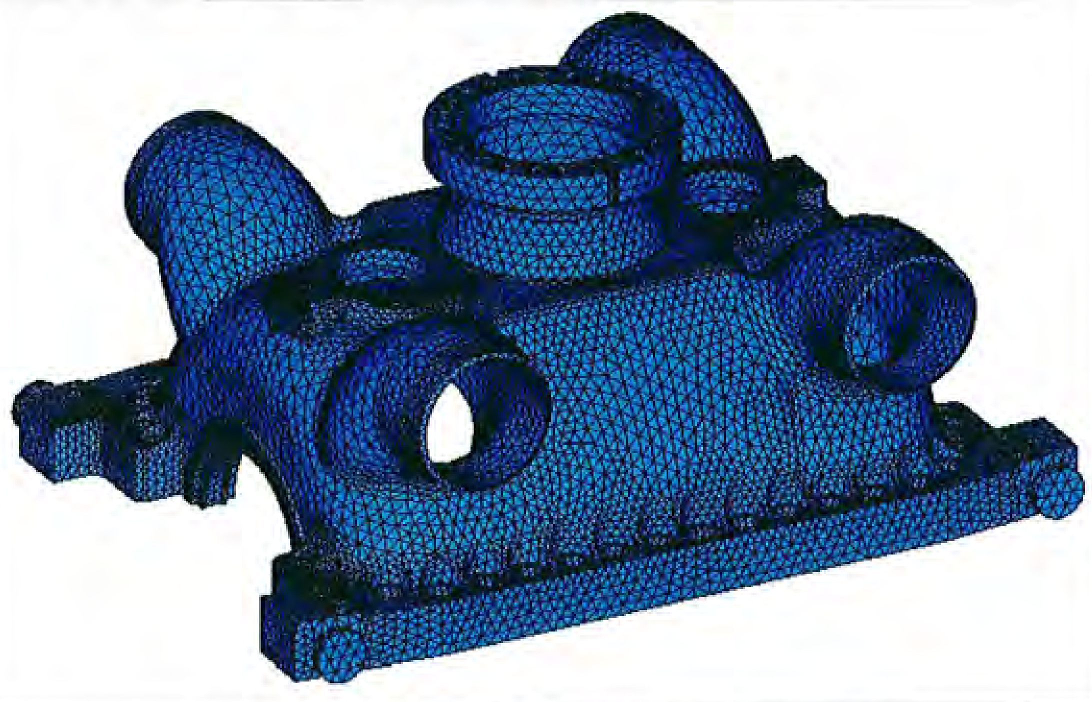

Figure 6:1: FE Model of Steam Turbine IP Outer Casing

6.2. FE Model of IP Inner Casing

Figure 6:2: FE Model of Steam Turbine IP Inner Casing

6.3. Solid FE model section – IP casing assembly

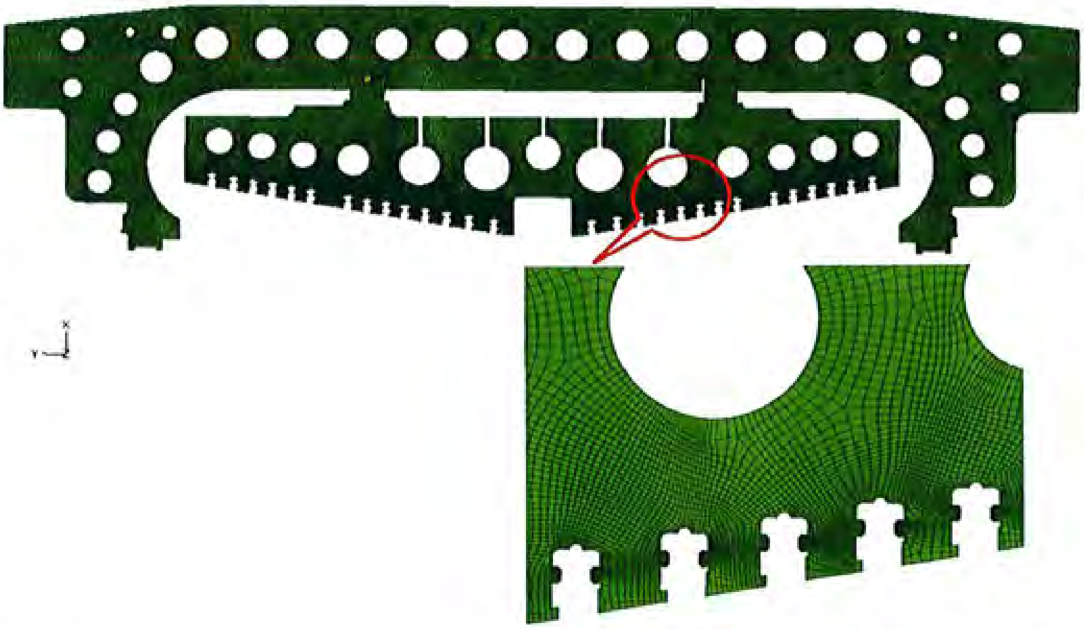

Figure 6:3: Solid FE model section of Steam Turbine IP casing assembly

6.4. FE Model of IP Shaft

Figure 6:4: FE Model of Steam Turbine IP Shaft

6.5. FE model section – IP shaft

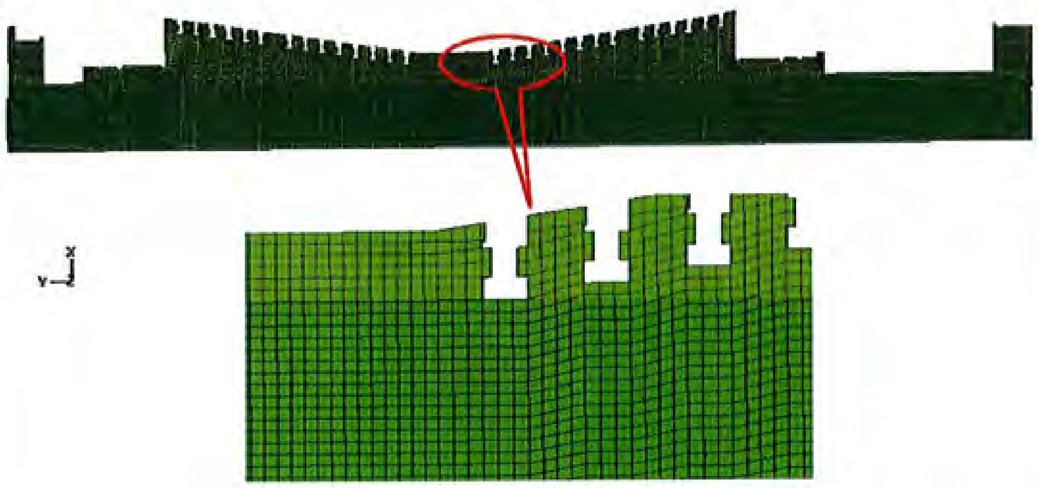

Figure 6:5 Solid FE model section of Steam Turbine IP Shaft

6.6. FE Models of LP Outer Casing

Figure 6:6: FE Model of Steam Turbine LP Outer Casing

6.7. FE Models of LP Inner Casing

Figure 6:7: FE Model of Steam Turbine LP Inner Casing Assembly

6.8. FE Model of LP Inner outer casing

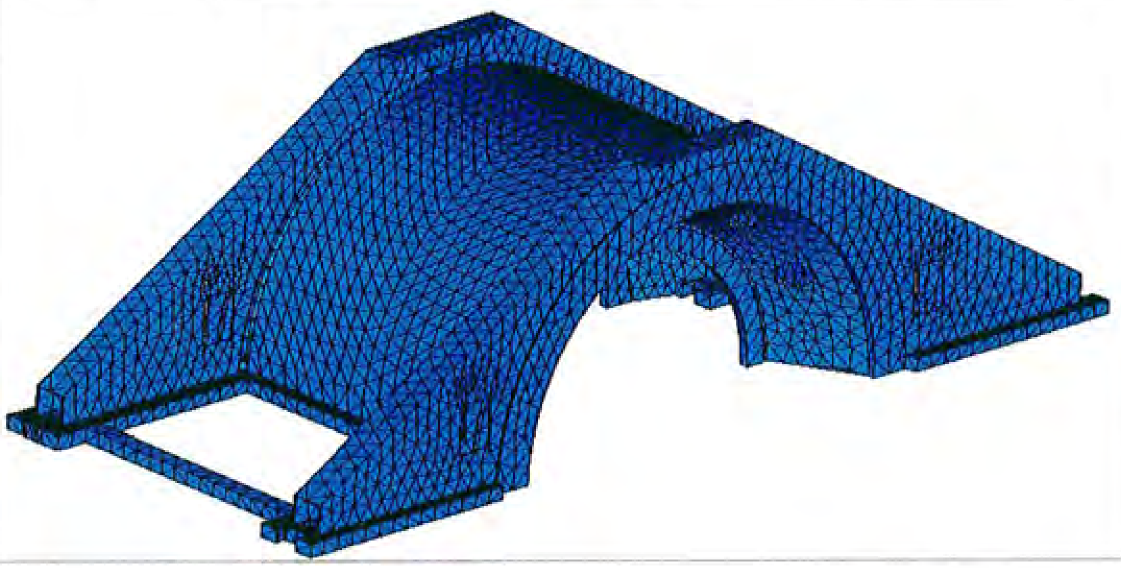

Figure 6:8: FE Model of Steam Turbine LP outer Casing

6.9. Solid FE model section – LP Casing assembly

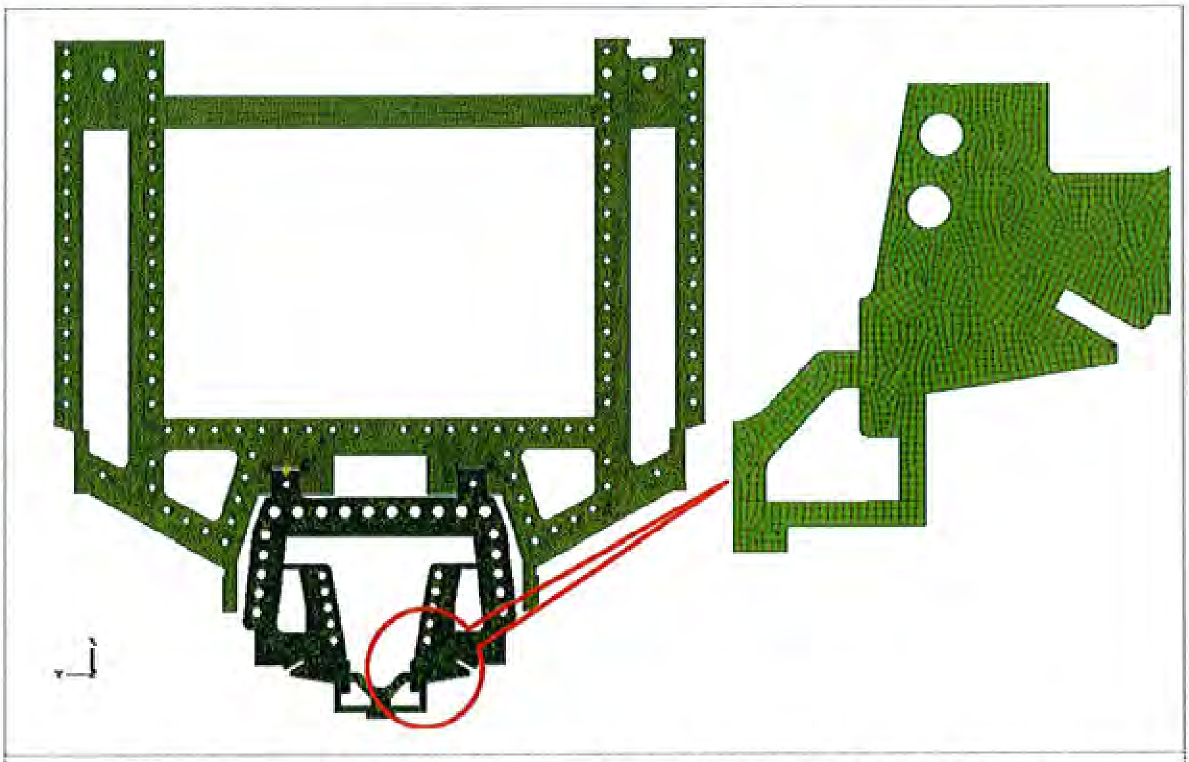

Figure 6:9: Solid FE model section of steam Turbine LP Casing Assembly

383

6.10. FE Model of LP Shaft

Figure 6:10: FE Model of Steam Turbine LP Shaft

6.11. Solid FE model section – LP shaft

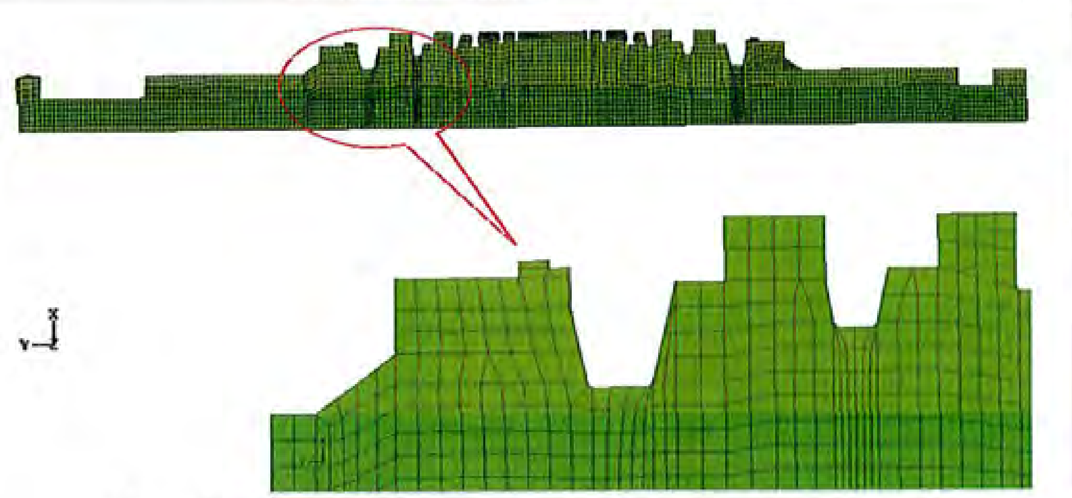

Figure 6:11: Solid FE model section of steam Turbine LP Shaft

Section 7 : FE Analysis and Results

7.1. Thermo-Mechanical Analysis of IP Casing Assembly

The IP Casing Assemply of Steam is modeled and analysis is carried out for thermal and mechanilcal loads.

7.2. IP Casing Assembly - Mechanical & Thermal Loading

The IP Casing Assembly is analysed for the Thermo-mechanical loading conditions. At one end of the IP Casing assembly, the logitudunal displacements arrested as shown in Figure 7:1 to Figure 7:3.Transient Temperature and pressure loading conditions are shown in Figure 7:4 .to Figure 7:5.

Temperature profile and stress at each startup condition are shown in Figure 7:6 to Figure 7:21 for Cold Start, Warm Start and Hot start of the turbine.

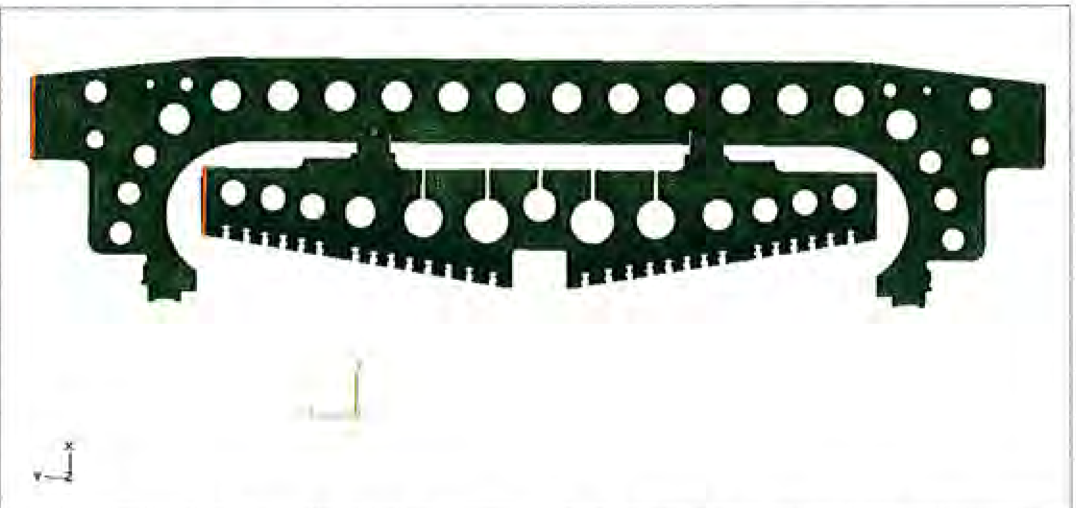

Figure 7:1: Longitudinal Displacement (Y) along Edge of the IP casing Assembly (Cut Section) is constrained

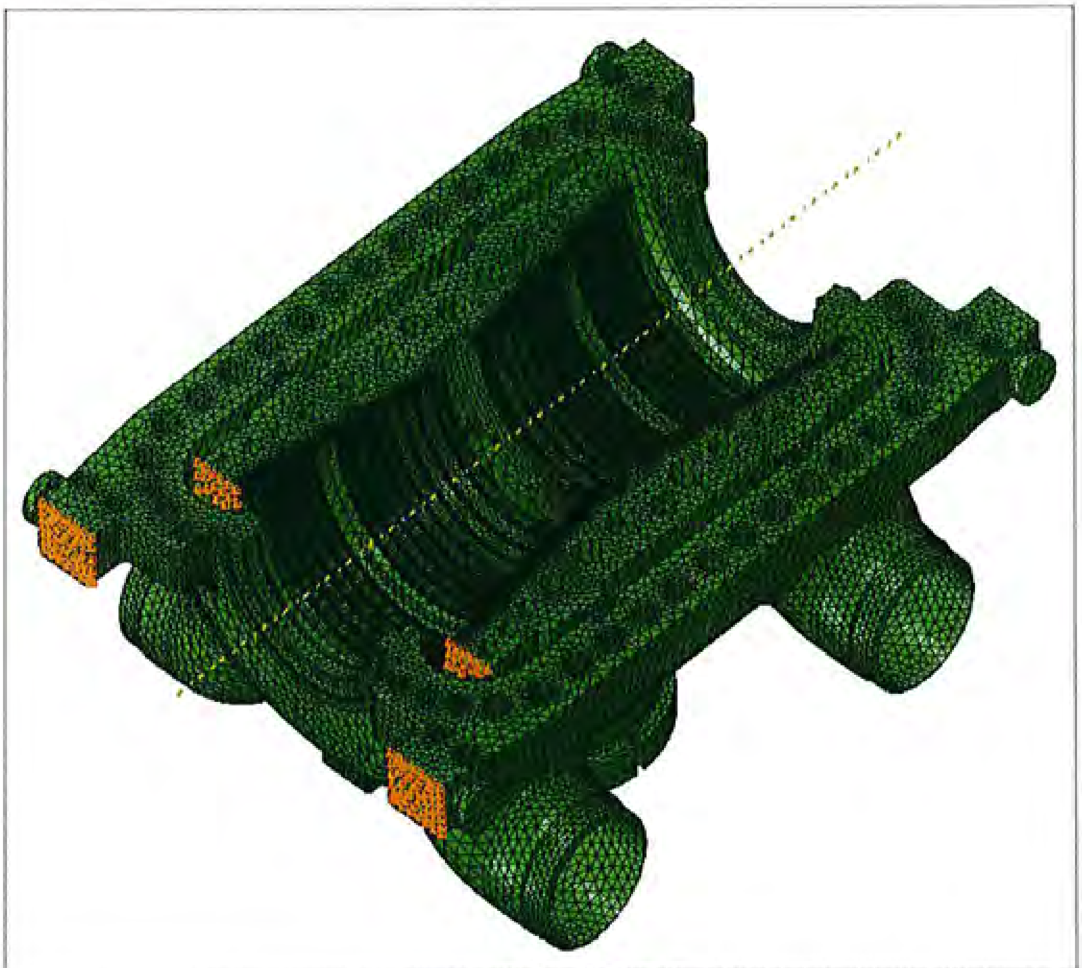

Figure 7:2: Longitudinal Displacement (Y) along Edge of the IP casing Assembly (3D View) is constrained

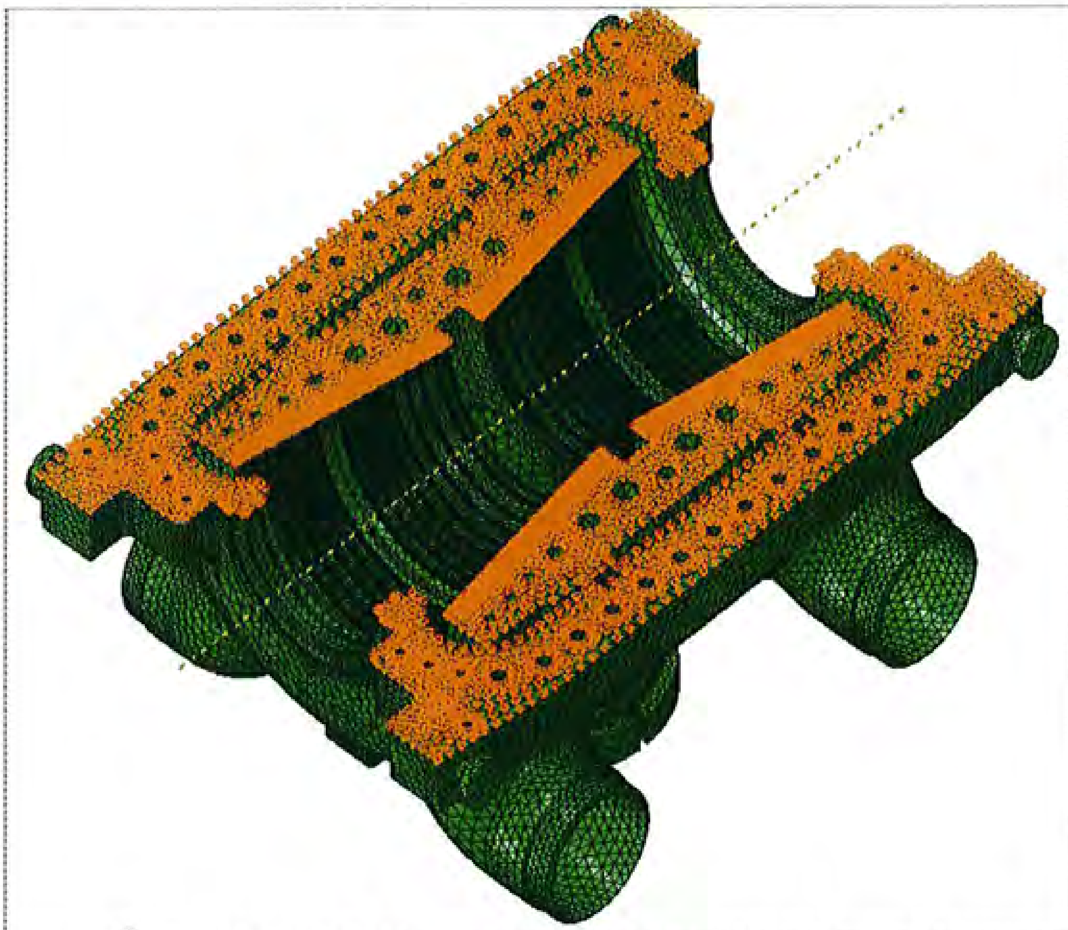

Figure 7:3:Translational displacement (z) along Edge of the IP casing Assembly (3D View) is constrained

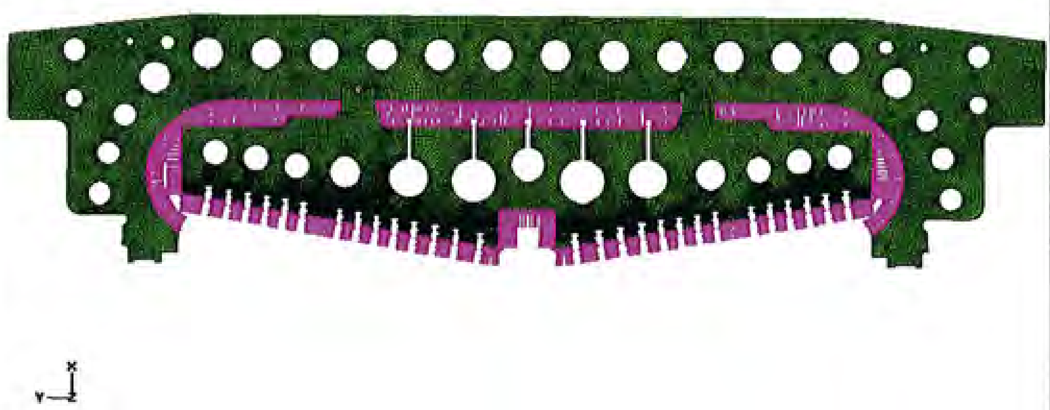

Figure 7:4: Pressure and thermal loading applied on 14 stages of IP Casing Assembly (Cut Section)

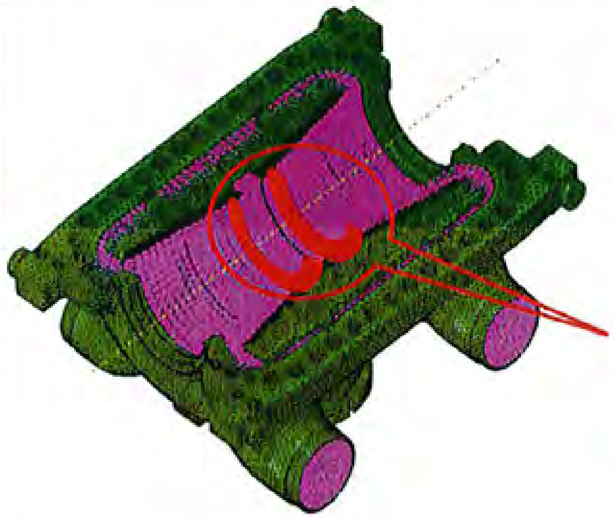

Figure 7:5: Pressure and thermal loading applied on 14 stages – IP Casing Assembly (3D View)

7.3. IP Casing Assembly - Cold Start

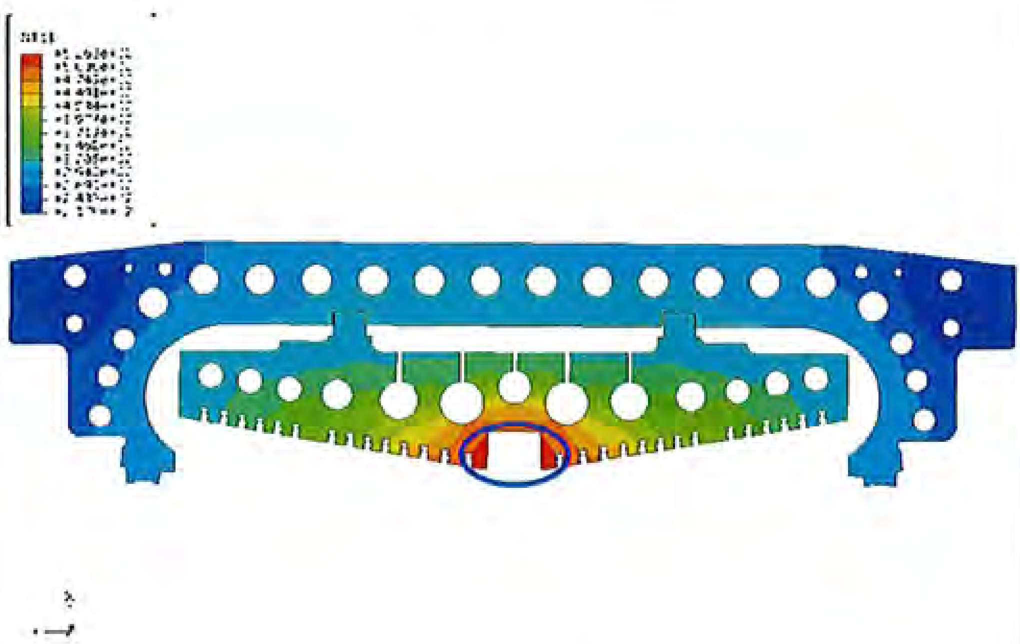

Figure 7:6: Steady State Temperature (Max. 526^{0}C) profile at the end of cold start – IP Casing Assembly (Cut Section)

306

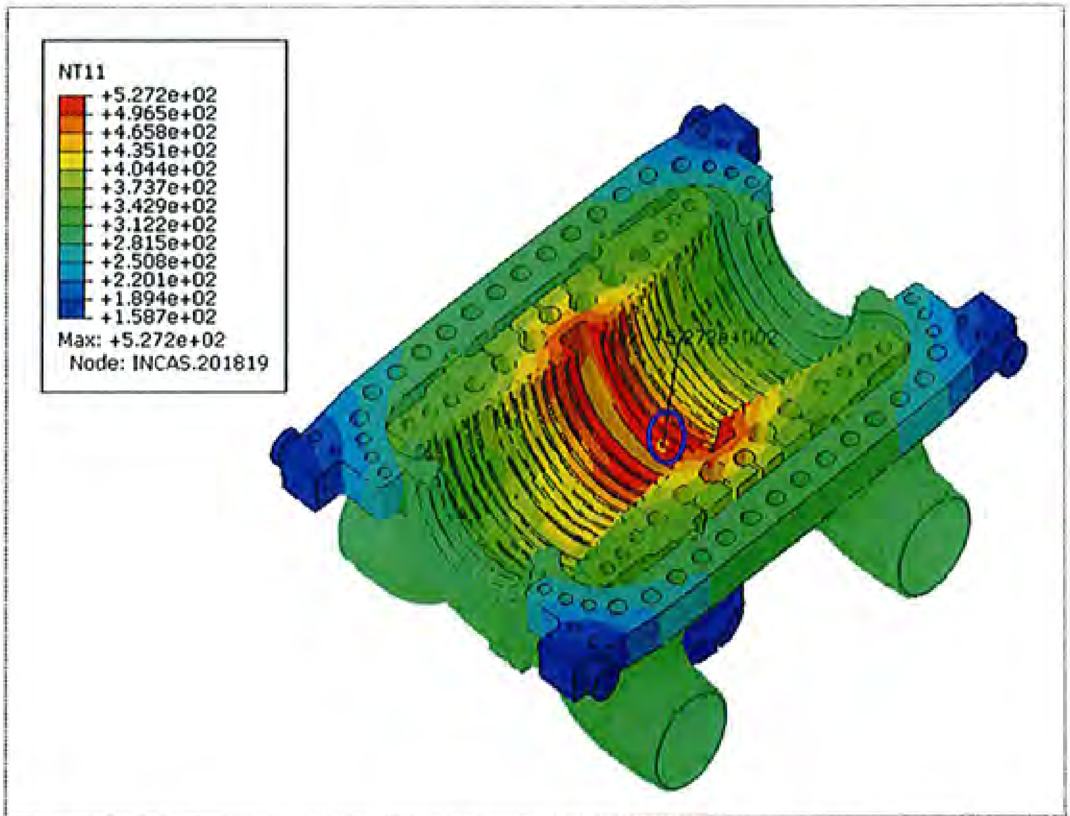

Figure 7:7: Steady State Temperature (Max. 527^{0}C) profile at the end of cold start – IP Casing Assembly (3D View)

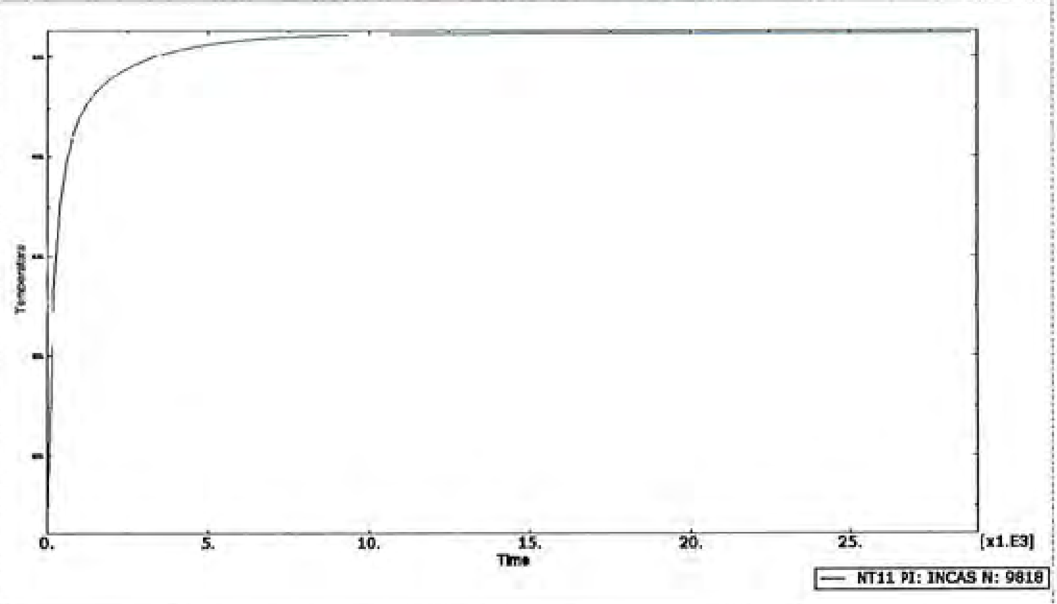

390

Figure 7:8: Transient Temperature plot at the end of cold start – IP Casing Assembly

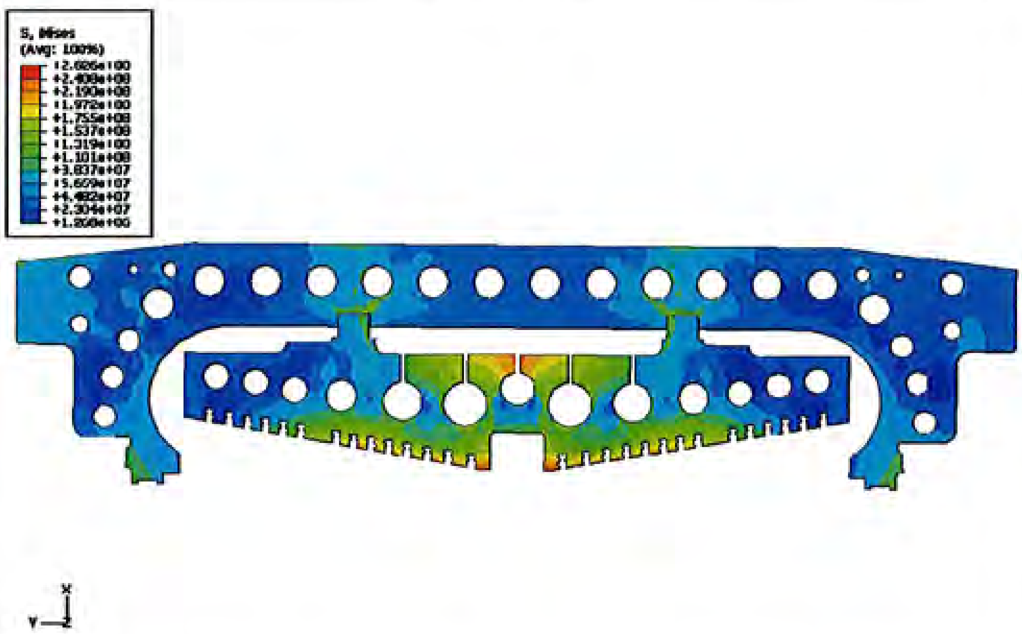

Figure 7:9: vonMises Stress Contour (Max. 262 MPa) at the end of cold start - IP Casing Assembly (Cut Section)

391

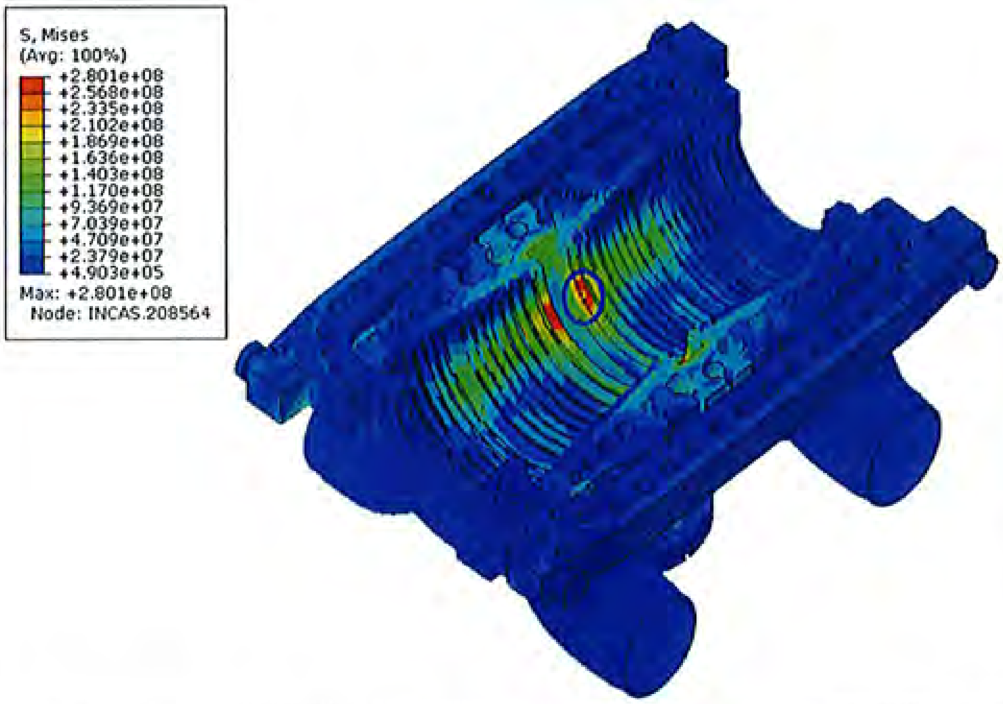

Figure 7:10: vonMises Stress Contour (Max. 280 MPa) at the end of cold start - IP Casing Assembly (3D View)

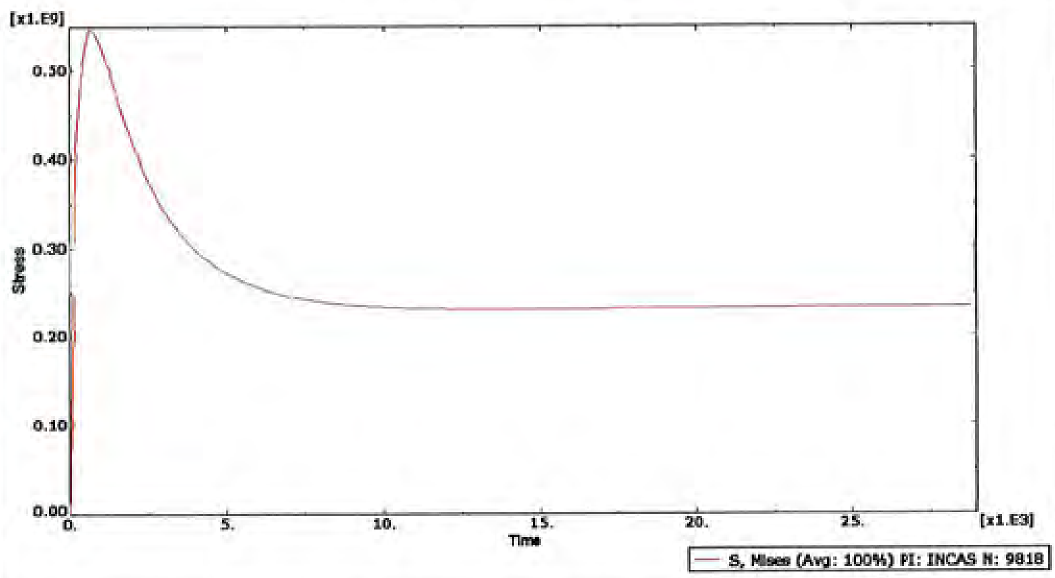

Figure 7:11: Transient Stress plot at the end of cold Start – IP Casing Assembly

7.4. IP Casing Assembly - Warm Start

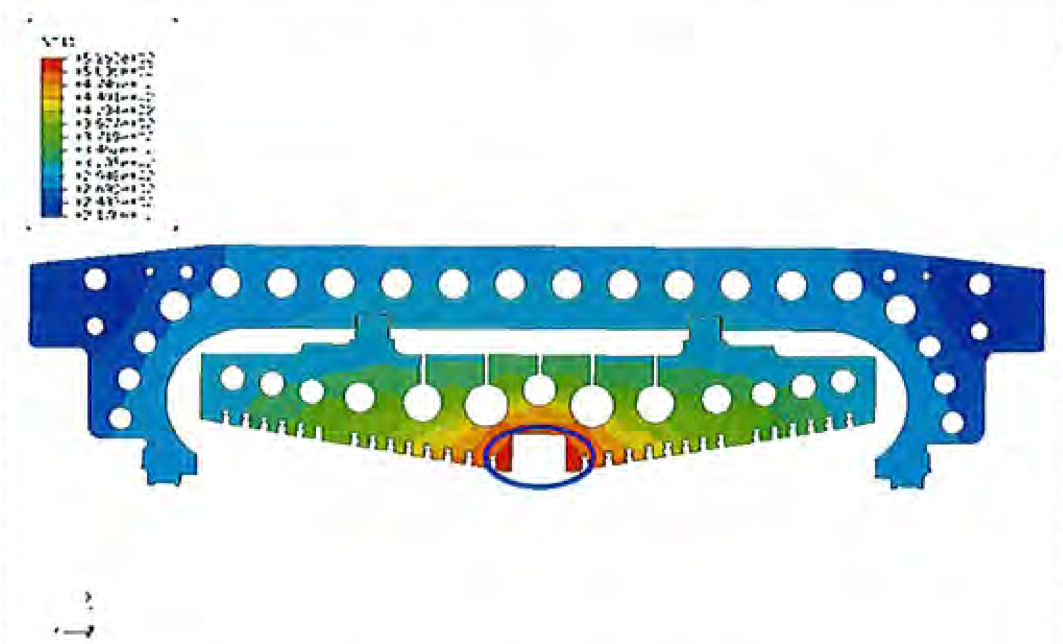

Figure 7:12: Steady State Temperature (Max. 526°C) profile at the end of warm start – IP Casing Assembly (Cut Section)

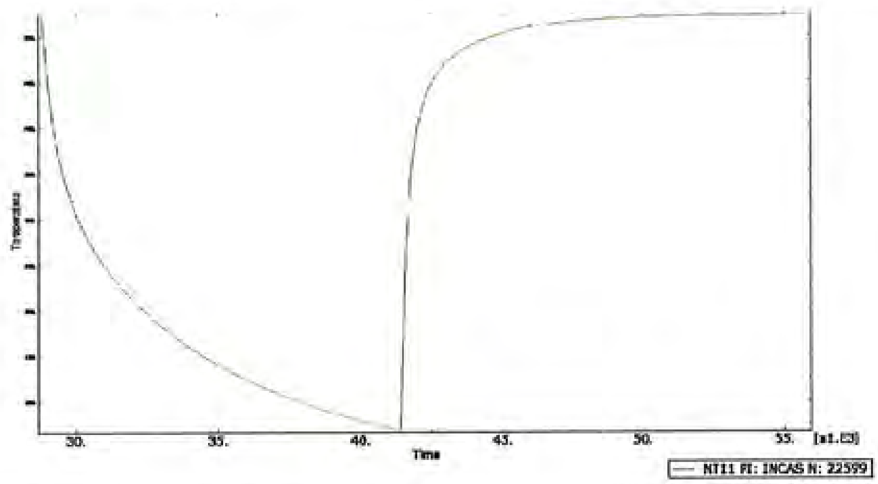

Figure 7:13: Transient Temperature plot at the end of warm start – IP Casing Assembly

393

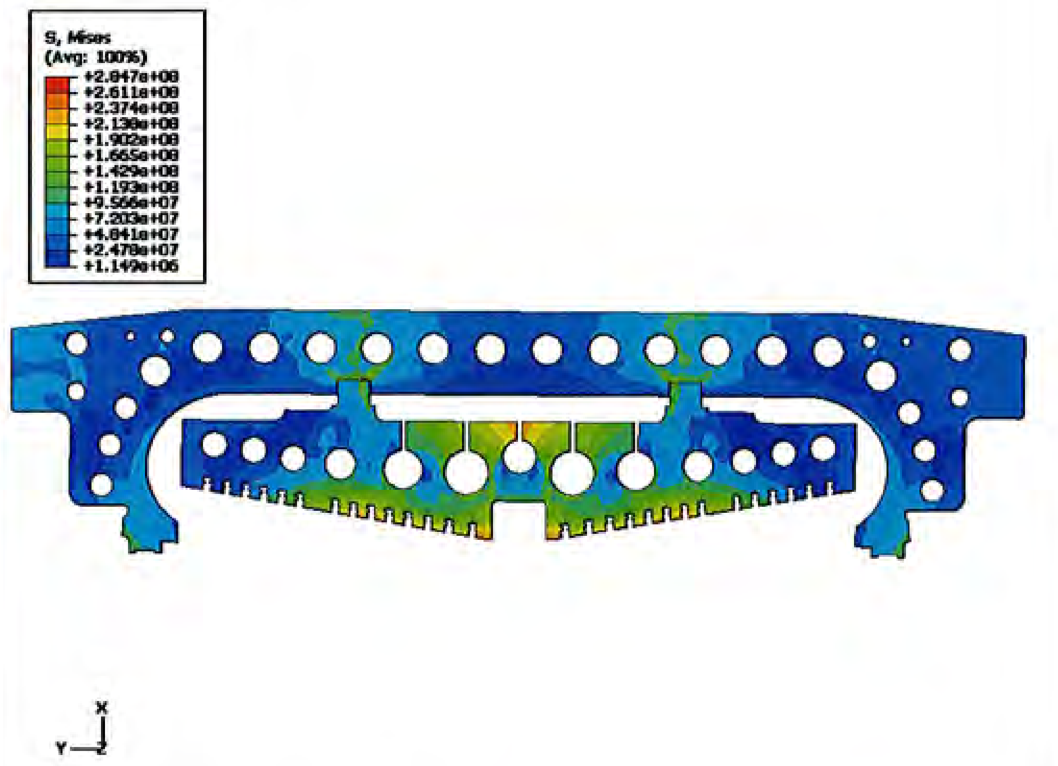

Figure 7:14: vonMises Stress Contour (Max. 284 MPa) at the end of warm start - IP Casing Assembly (Cut Section)

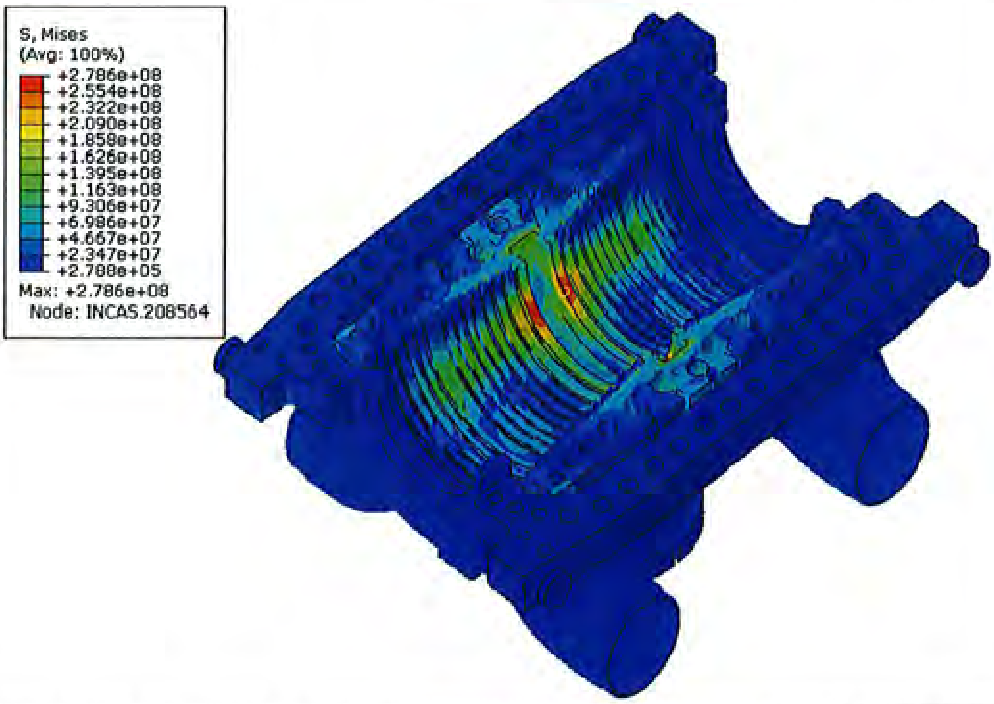

Figure 7:15: vonMises Stress Contour (Max. 278 MPa) at the end of warm start - IP Casing Assembly (3D View)

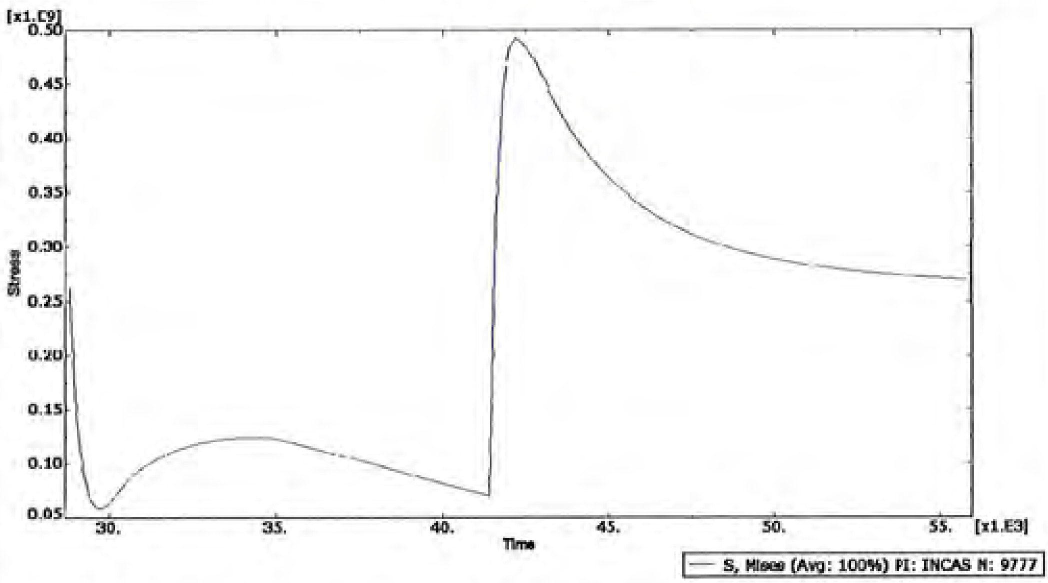

Figure 7:16: Transient Stress plot at the end of warm Start – IP Casing Assembly

395

7.5. IP Casing Assembly - Hot Start

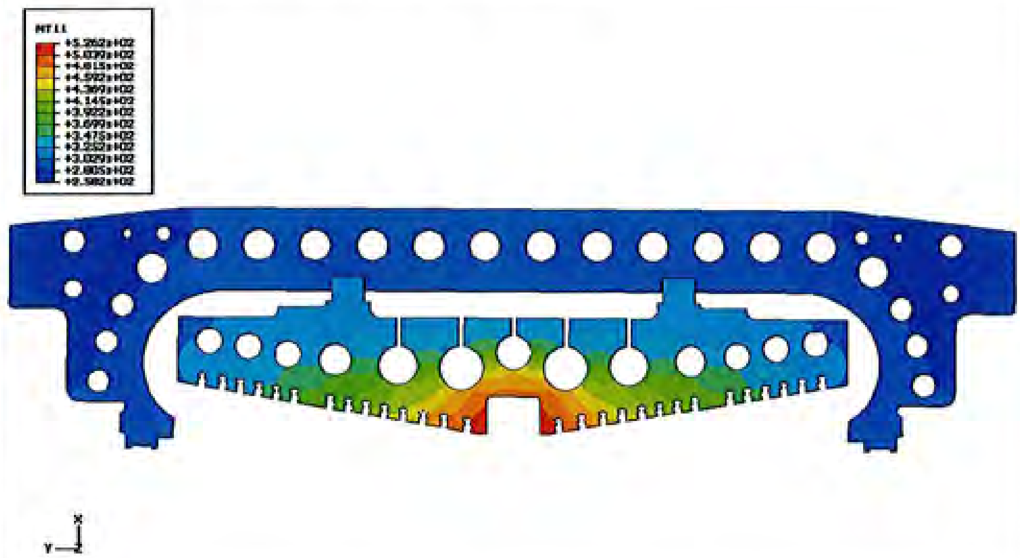

Figure 7:17: Steady State Temperature (Max. 526^{0}C) profile at the end of hot start – IP Casing Assembly (Cut Section)

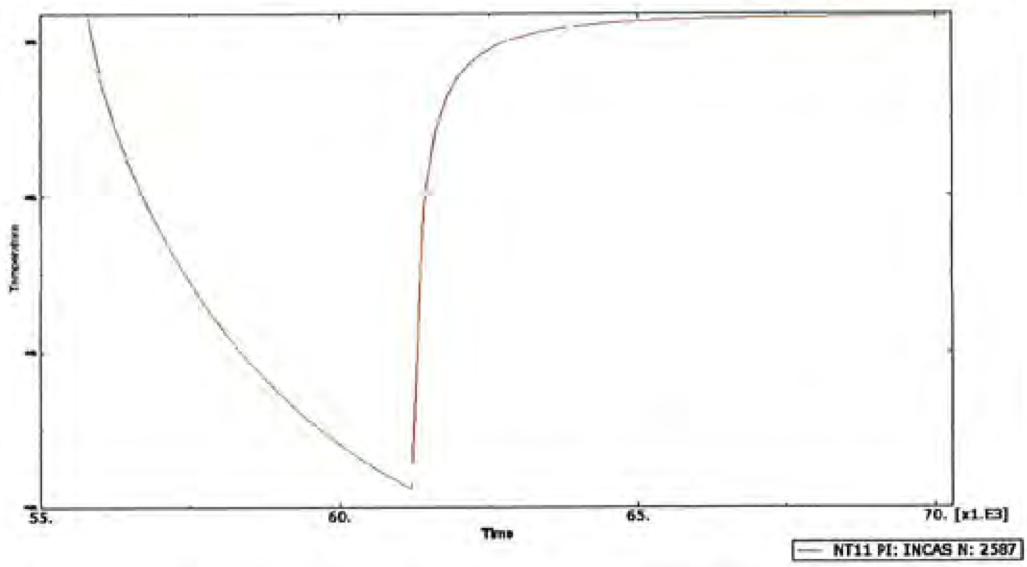

Figure 7:18: Transient Temperature plot at the end of hot start – IP Casing Assembly

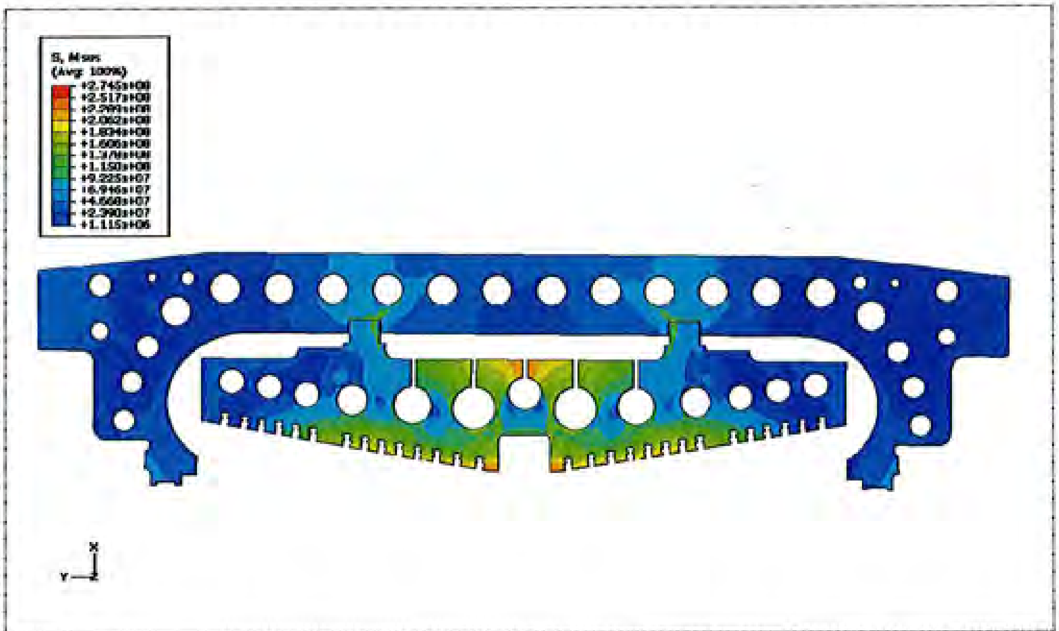

Figure 7:19: vonMises Stress Contour (Max. 274 MPa) at the end of hot start - IP Casing Assembly (Cut Section)

397

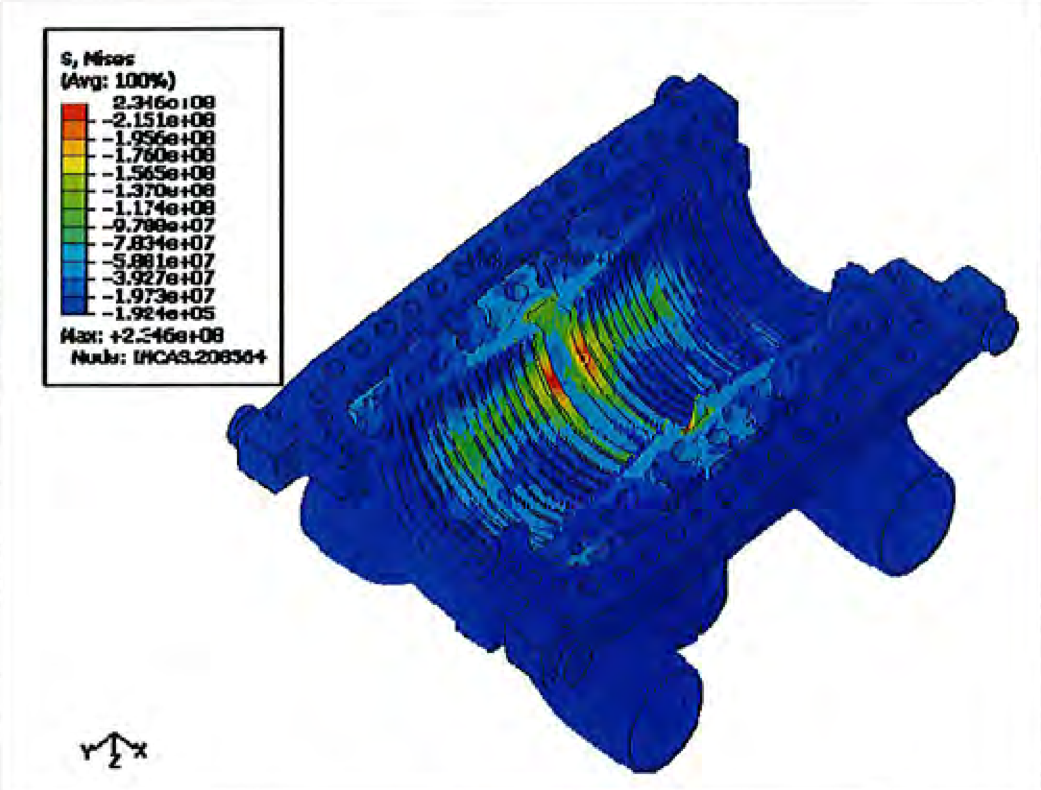

Figure 7:20: vonMises Stress Contour (Max. 234 MPa) at the end of hot start - IP Casing Assembly (3D View)

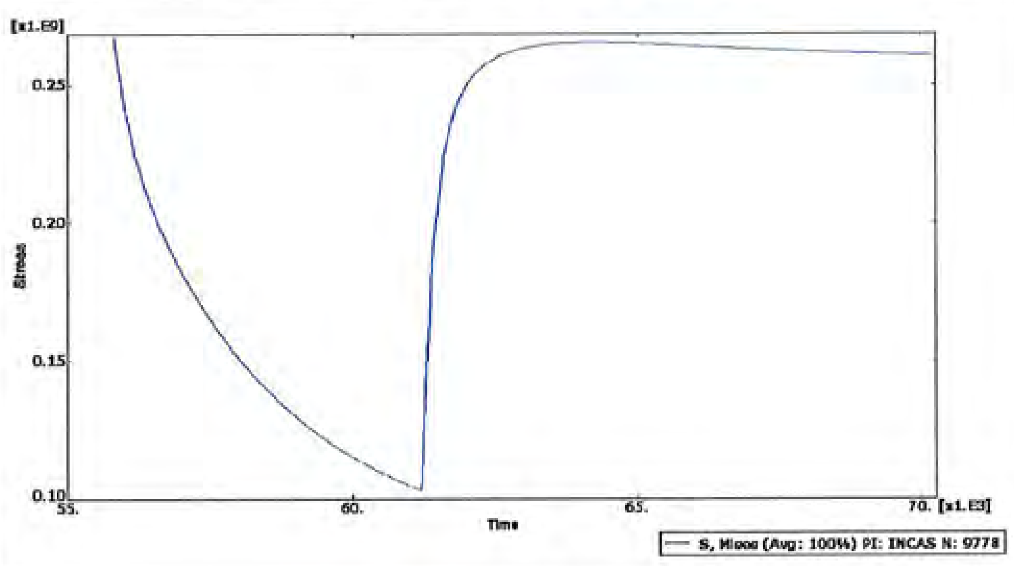

398

Figure 7:21: Transient Stress plot at the end of hot start – IP Casing Assembly

7.6. IP Shaft - Mechanical & Thermal Loading

The IP Shaft is analysed for the Thermo-mechanical loading conditions. At one end of the IP Shaft, the logitudunal displacements arrested as shown in Figure 7:22.Transient Temperature and pressure loading conditions are shown in Figure 7:23. Rotating speed of shaft is taken as 3000 rpm. The blade are not modeled but the effective mass is lumped on the shaft.

Temperature profile and stress at each startup condition are shown in Figure 7:24 to Figure 7:35 for Cold Start, Warm Start and Hot start of the turbine.

Figure 7:22: Longitudinal Displacement (Y) along Edges of the LP Shaft (Cut Section) is constrained

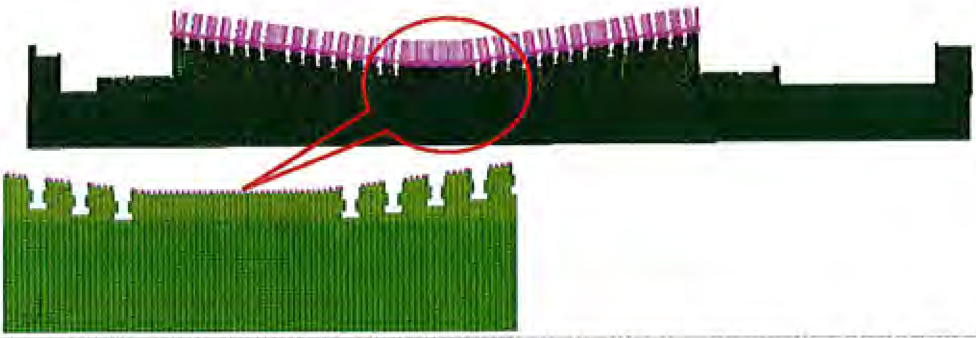

Figure 7:23: Pressure and thermal loading applied on 14 stages of IP Shaft (Cut Section)

379

7.7. IP Shaft – Cold Start

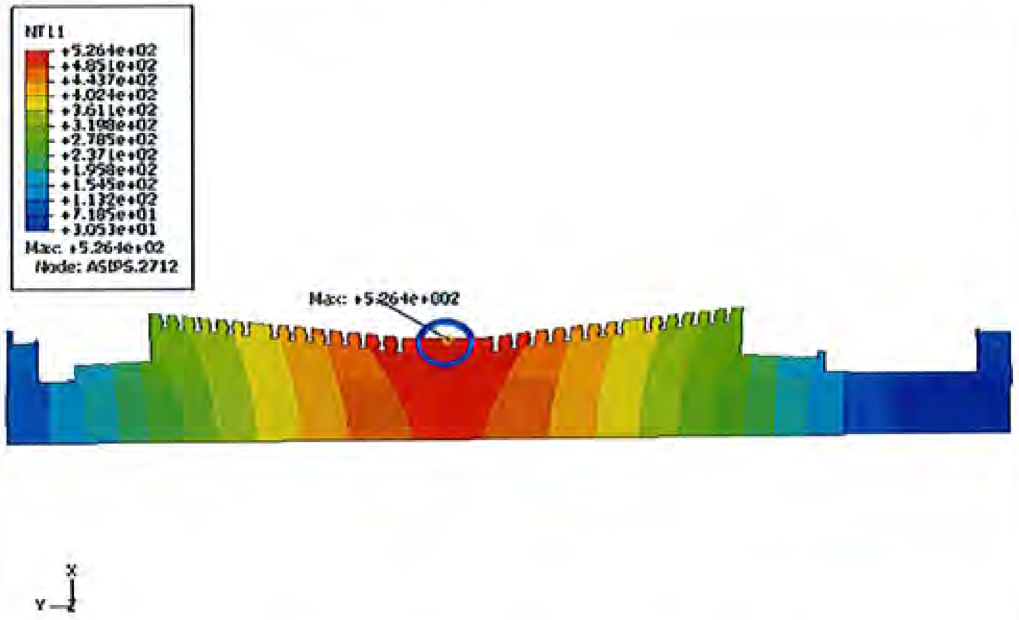

Figure 7:24: Steady State Temperature (Max. 526^{0}C) profile at the end of cold start – IP Shaft (Cut Section)

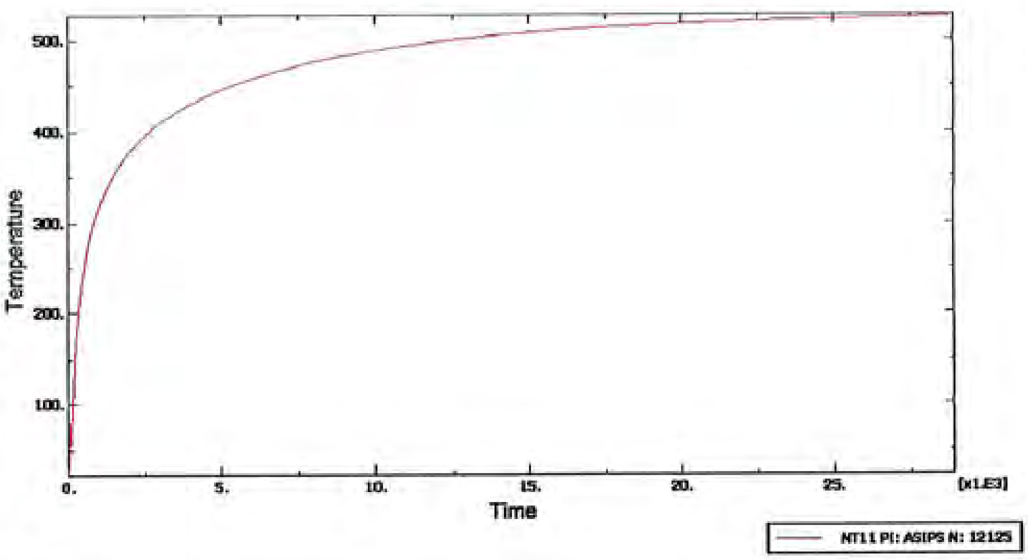

Figure 7:25: Transient Temperature plot at the end of cold start – IP Shaft

400

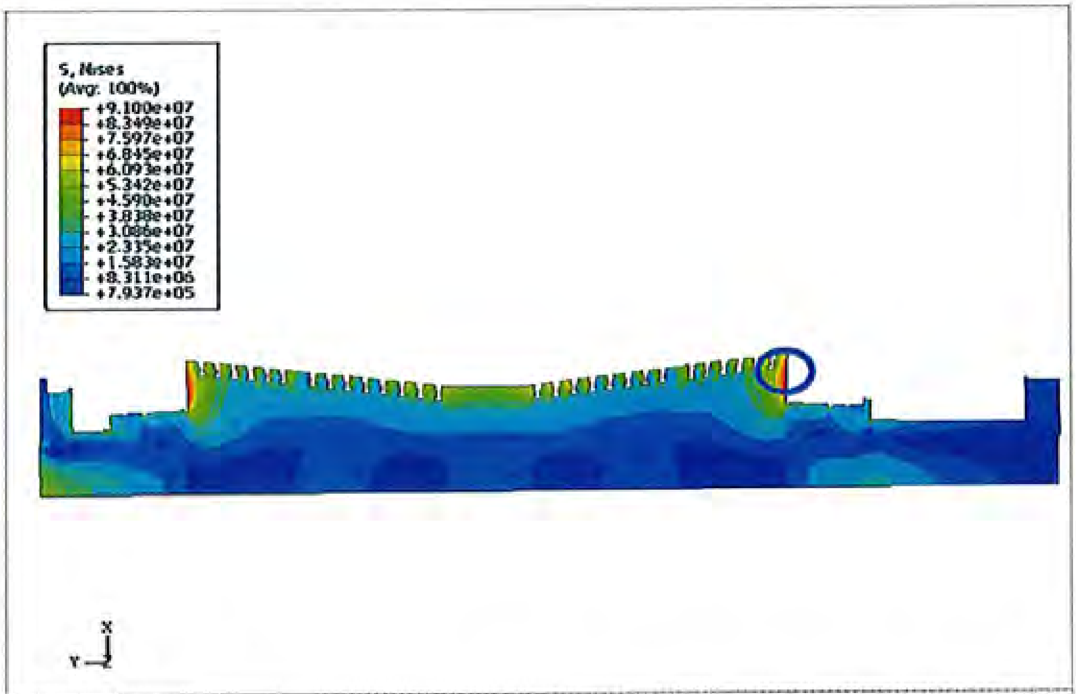

Figure 7:26: vonMises Stress Contour (Max. 91 MPa) at the end of cold start - IP Shaft (Cut Section)

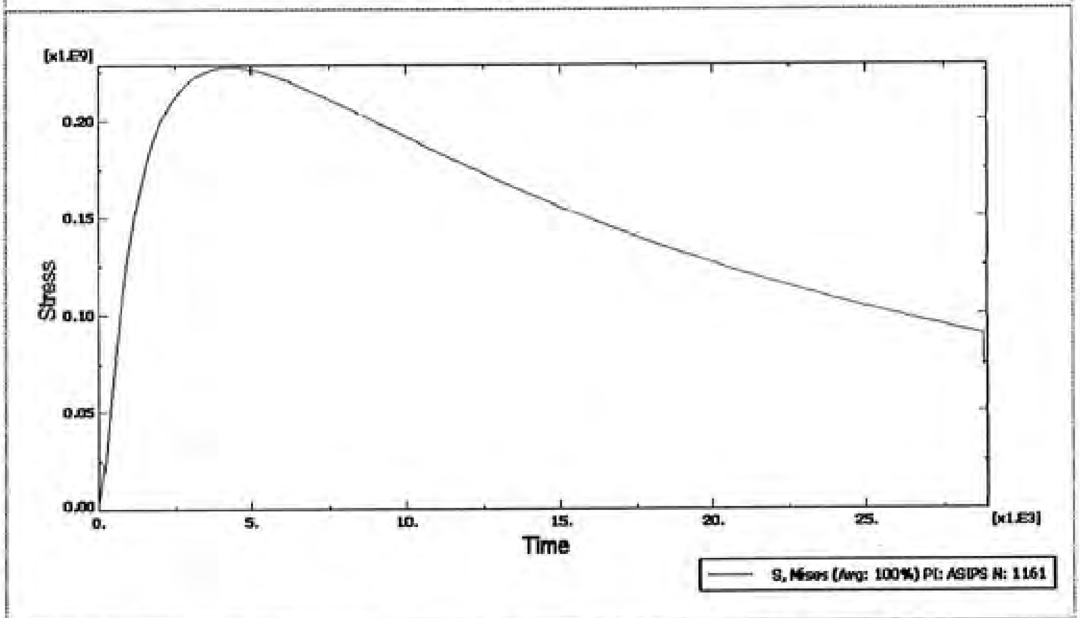

Figure 7:27: Transient Stress plot at end of cold Start – IP Shaft

7.8. IP Shaft – Warm Start

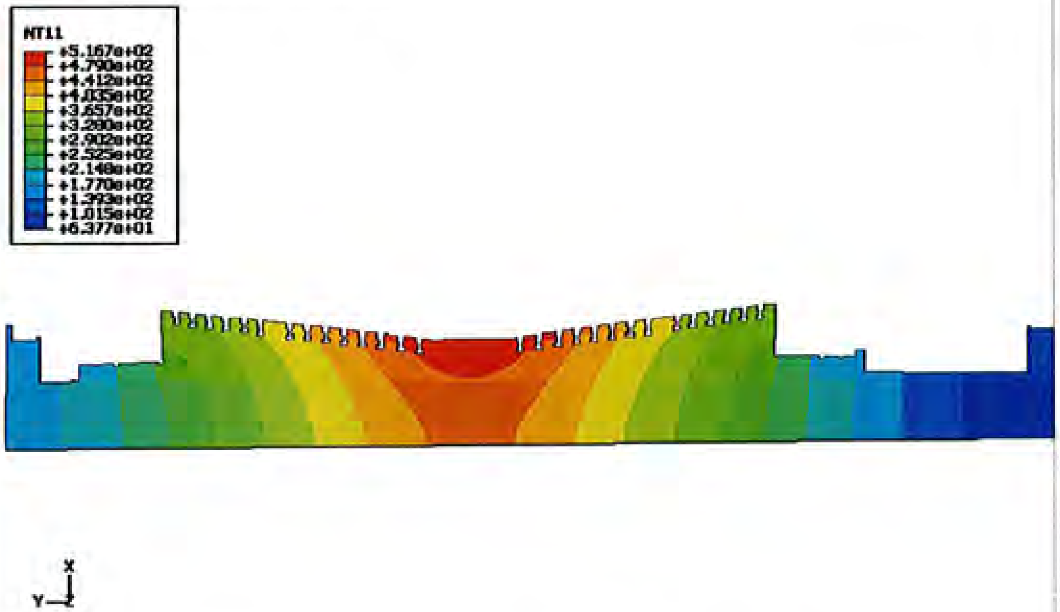

Figure 7:28: Steady State Temperature (Max. 516^{0}C) profile at the end of warm start – IP Shaft (Cut Section)

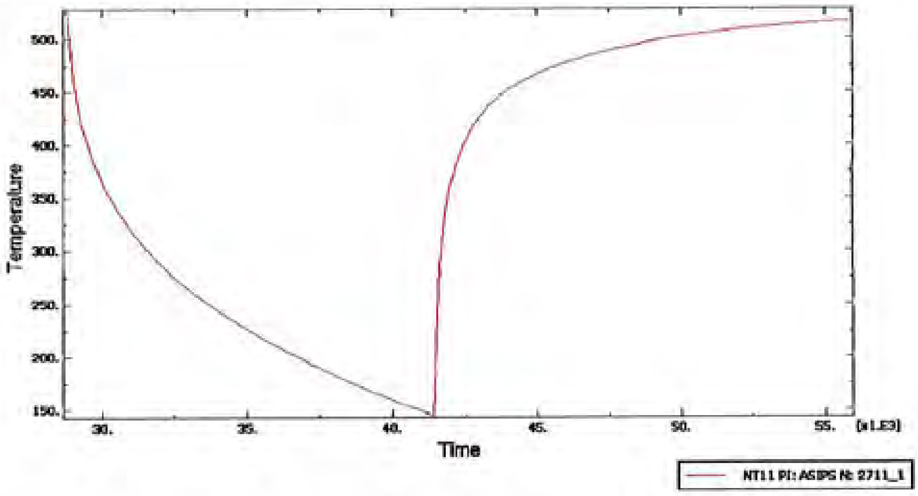

Figure 7:29: Transient Temperature plot at the end of warm start – IP Shaft

402

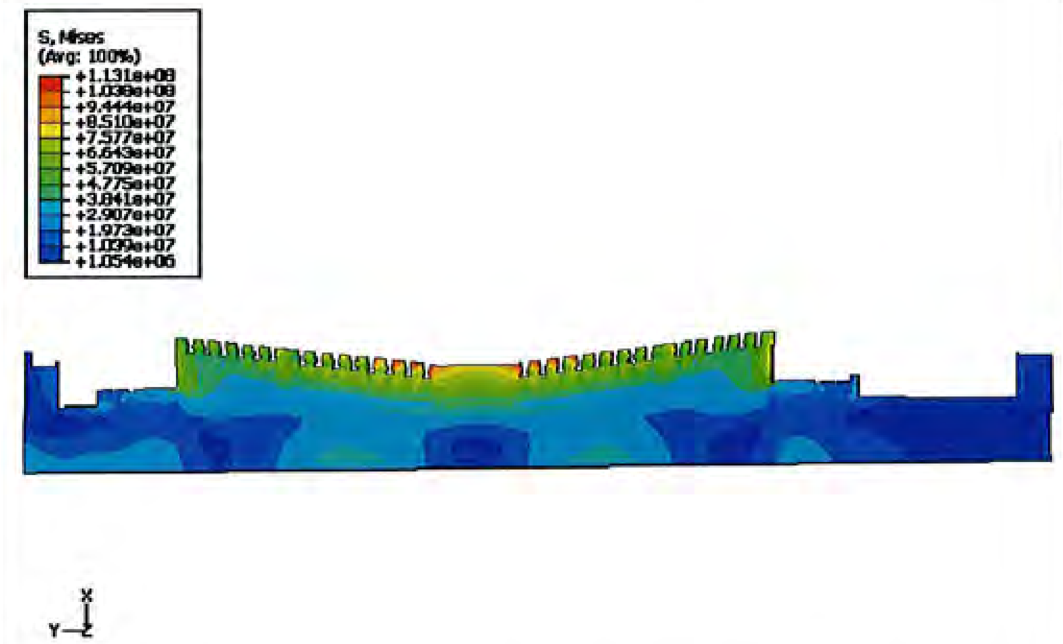

Figure 7:30: vonMises Stress Contour (Max. 113 MPa) at the end of warm start - IP Shaft (Cut Section)

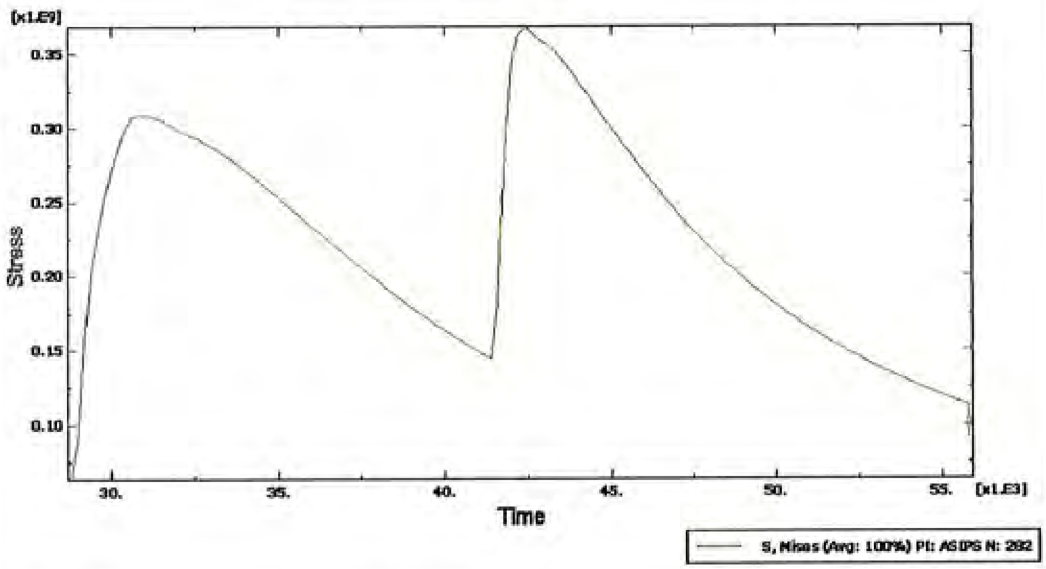

Figure 7:31: Transient Stress plot at end of warm Start – IP Shaft

7.9. IP Shaft – Hot Start

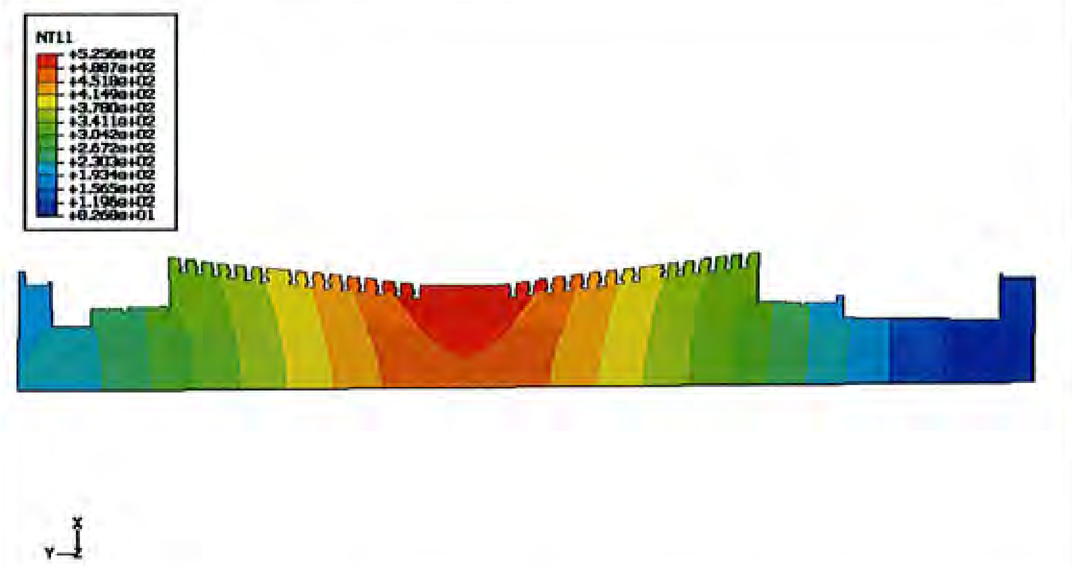

Figure 7:32: Steady State Temperature (Max. 525^{0}C) profile at the end of hot start – IP Shaft (Cut Section)

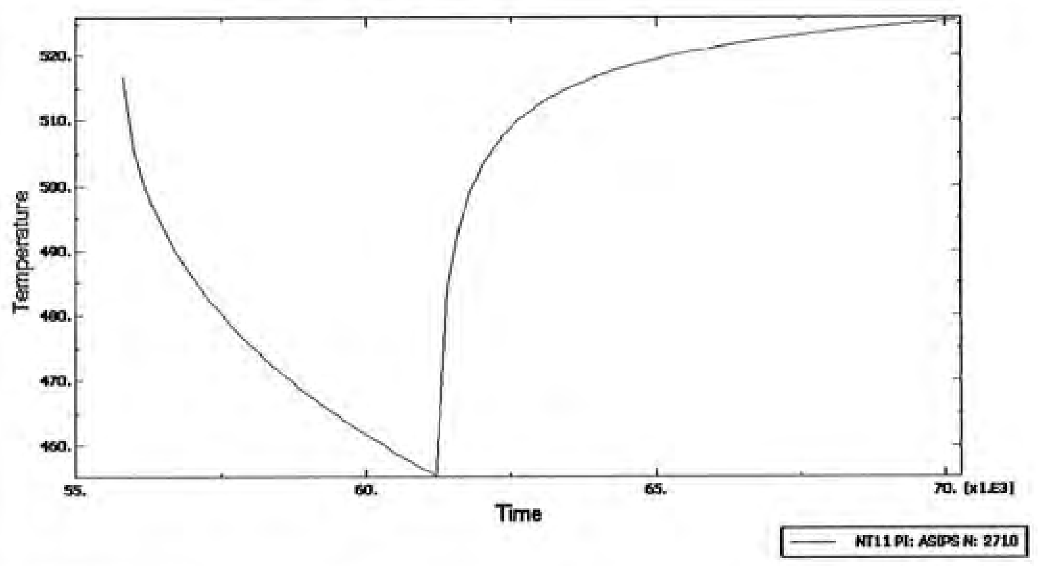

Figure 7:33: Transient Temperature plot at the end of hot start – IP Shaft

404

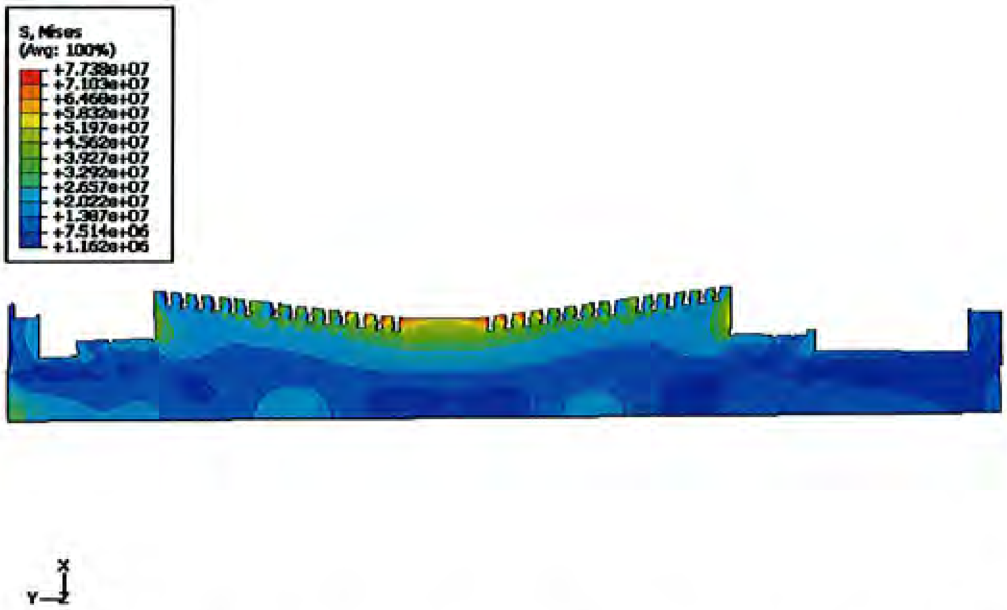

Figure 7:34: vonMises Stress Contour (Max. 77 MPa) at the end of hot start - IP Shaft (Cut Section)

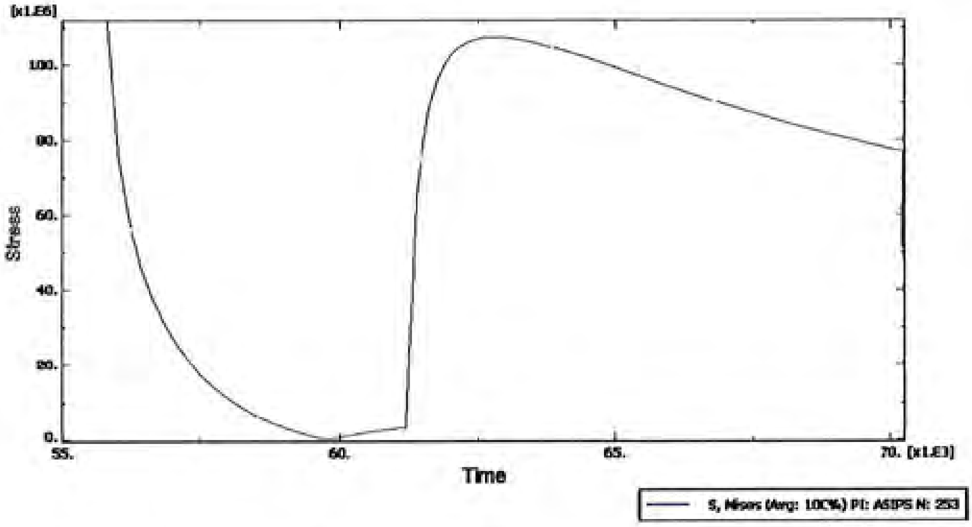

Figure 7:35: Transient Stress plot at end of hot Start – IP Shaft

7.10.IP Shaft – Cold start (Radial and Axial stress)

Radial and axial stress contours for the IP shaft is as shown below

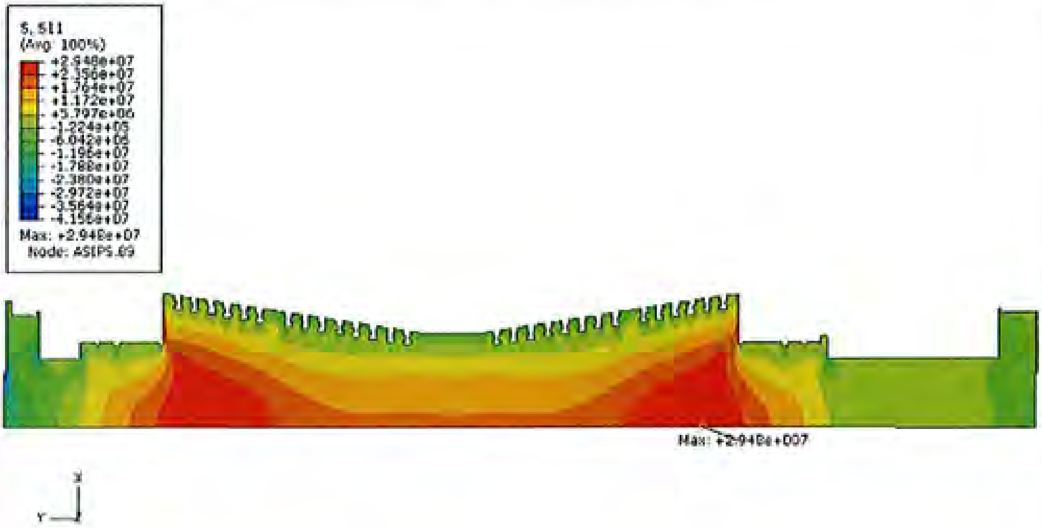

Figure 7:36: Radial stress at the end of cold start is 29MPa – IP Shaft (Cut Section)

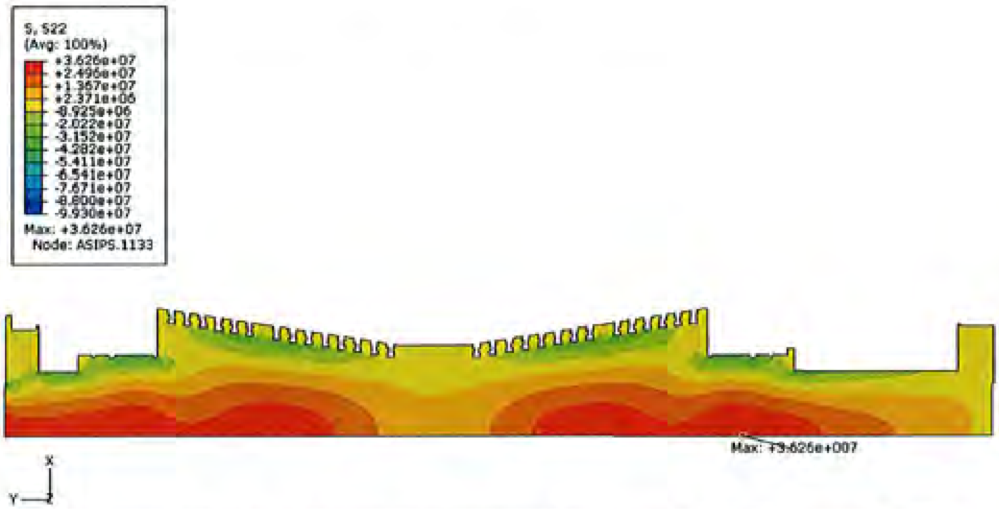

Figure 7:37: Axial stress at the end of cold start is 36MPa – IP Shaft

406

7.11.IP Shaft – Warm start (Radial and Axial stress)

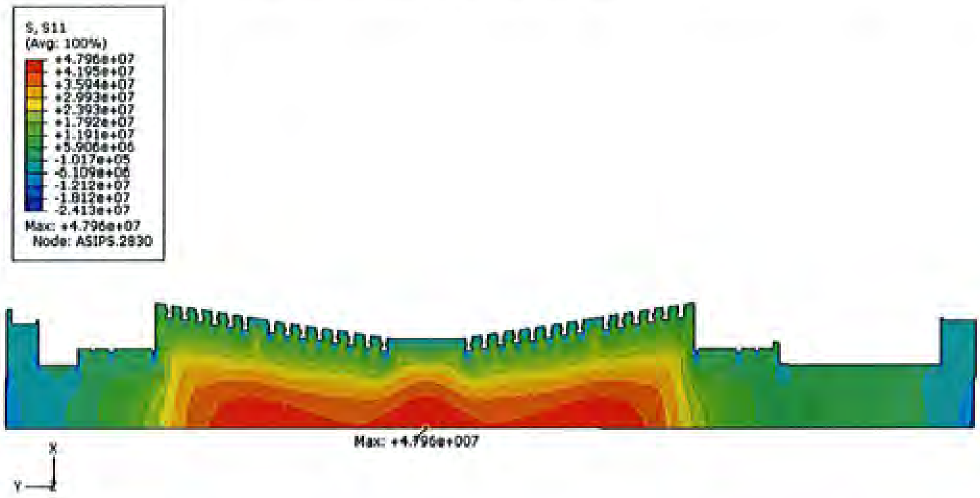

Figure 7:38: Radial stress at the end of warm start is 47MPa – IP Shaft (Cut Section)

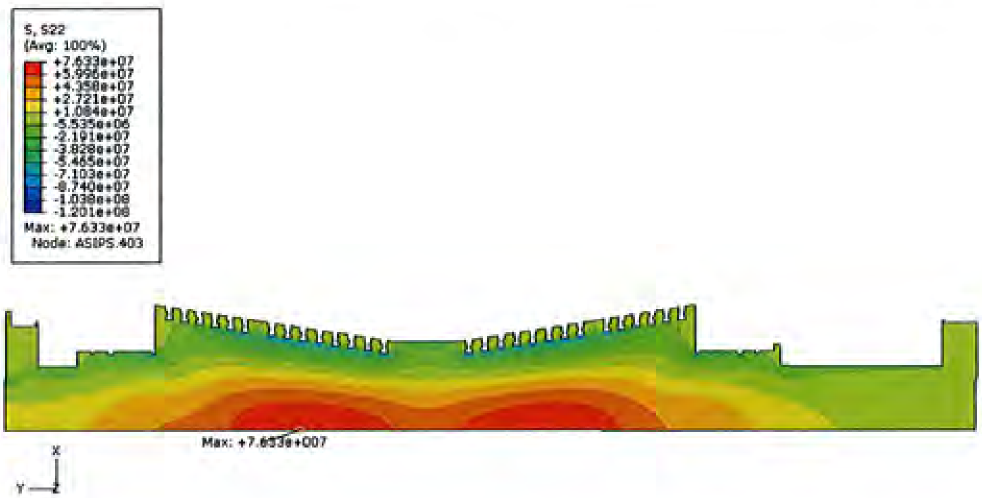

Figure 7:39: Axial stress at the end of warm start is 76MPa – IP Shaft

407

7.12. IP Shaft – Hot start (Radial and Axial stress)

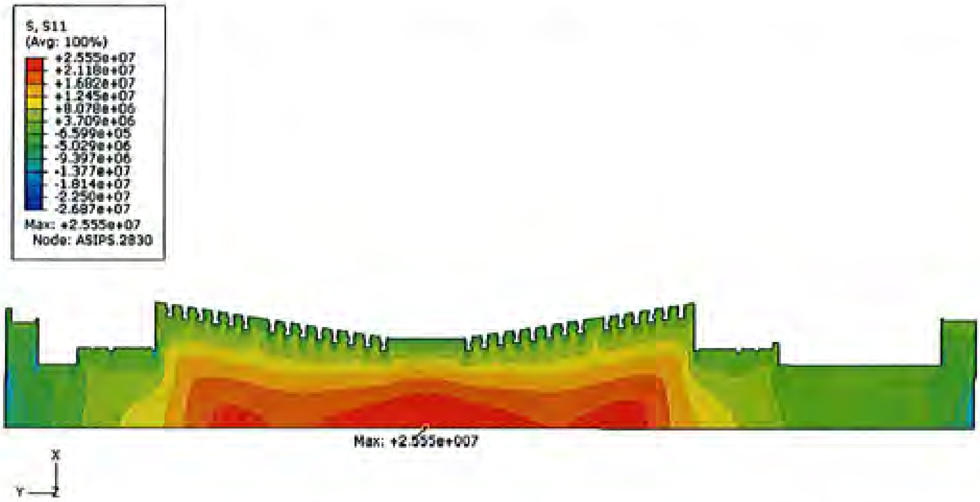

Figure 7:40: Radial stress at the end of Hot start is 25MPa – IP Shaft (Cut Section)

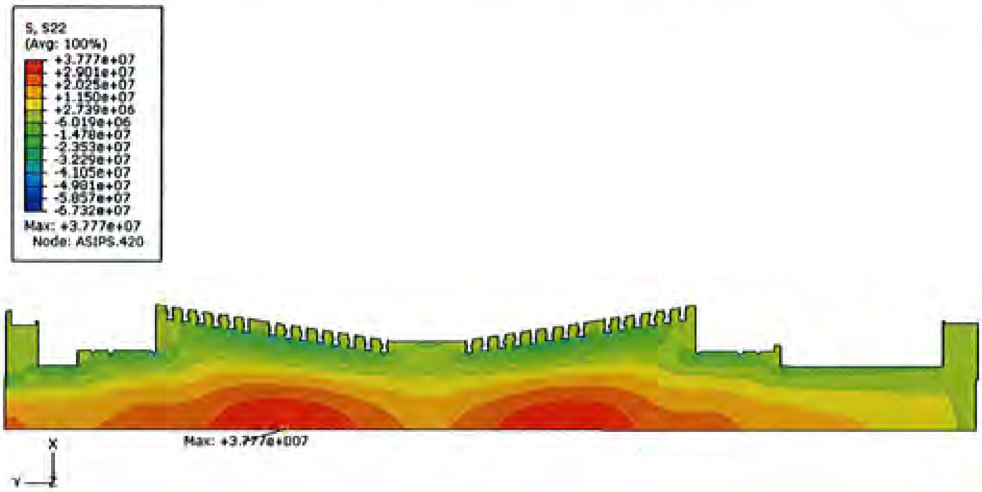

Figure 7:41: Axial stress at the end of Hot start is 37MPa – IP Shaft

408

7.13.LP Casing Assembly - Mechanical & Thermal Loading

The LP Casing (Outer casing and innter Casing Assembly) is analysed for the Thermo-mechanical loading conditions. At one end of the LP Shaft, the logitudunal displacements arrested as shown in Figure 7:42. Transient Temperature and pressure loading conditions are shown in Figure 7:43.

Temperature profile and stress at each startup condition are shown in Figure 7:44 to Figure 7:61 for Cold Start, Warm Start and Hot start of the turbine. Temperature in the LP casing is below 300degree so creep is not significant here. For analysis creep is not considered here.

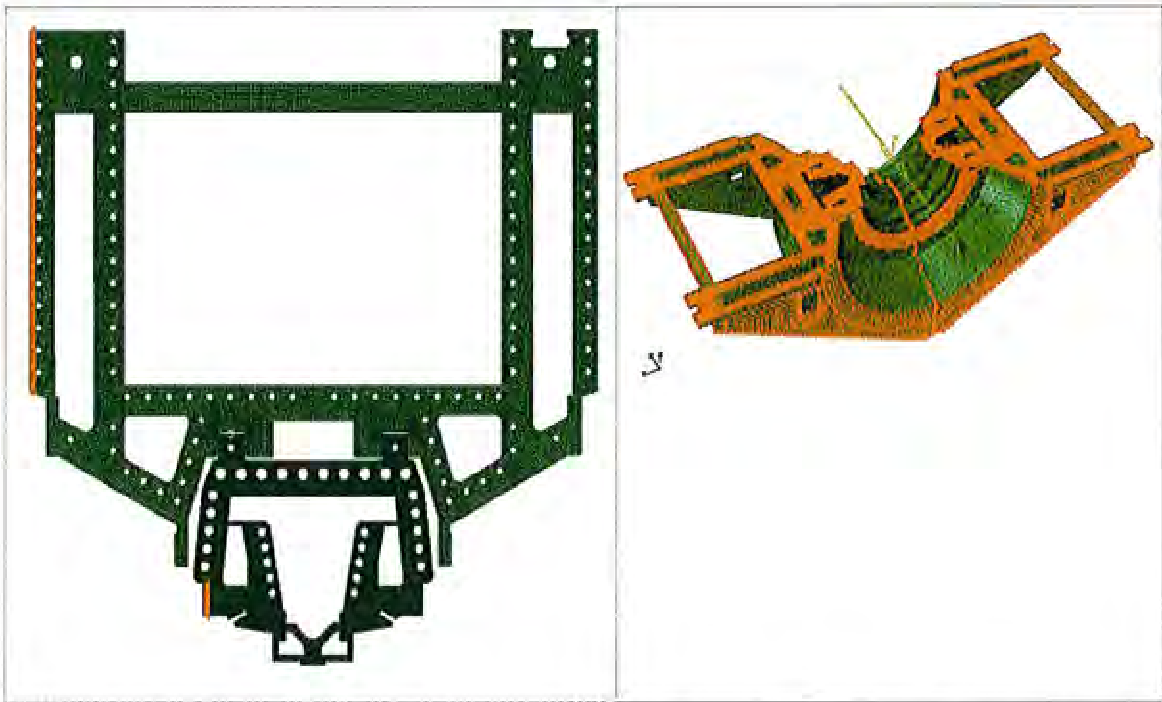

Figure 7:42: Longitudinal Displacement (Y) along Edges of the casing is constrained – LP Casing Assembly (Cut Section and 3D View)

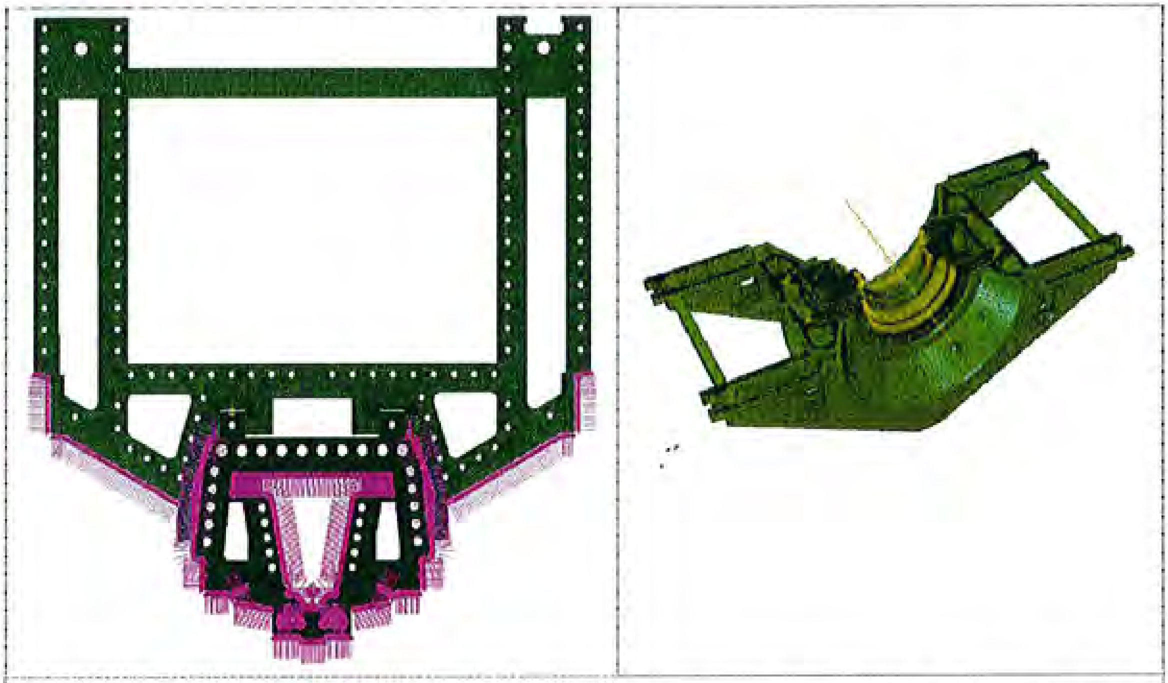

Figure 7:43: Pressure and thermal boundary conditions applied for 6 stages – LP Casing Assembly (Cut Section and 3D View)

410

7.14.LP Casing Assembly – Cold start

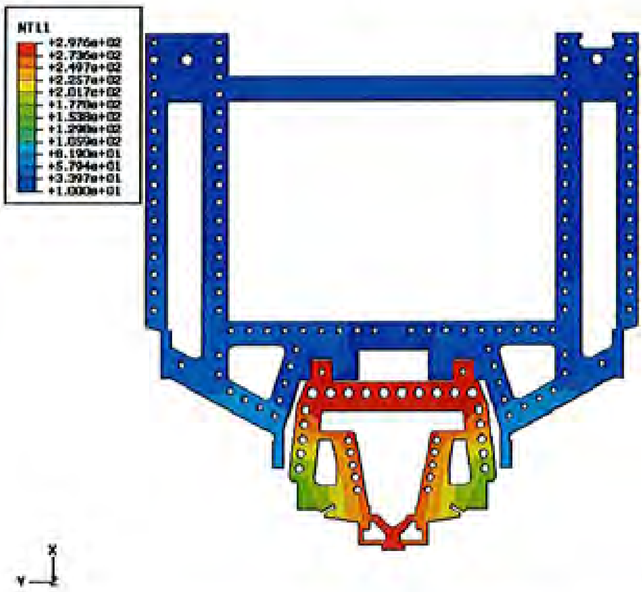

Figure 7:44: Steady State Temperature (Max. 297^{0}C) profile at the end of cold start – LP Casing Assembly (Cut Section)

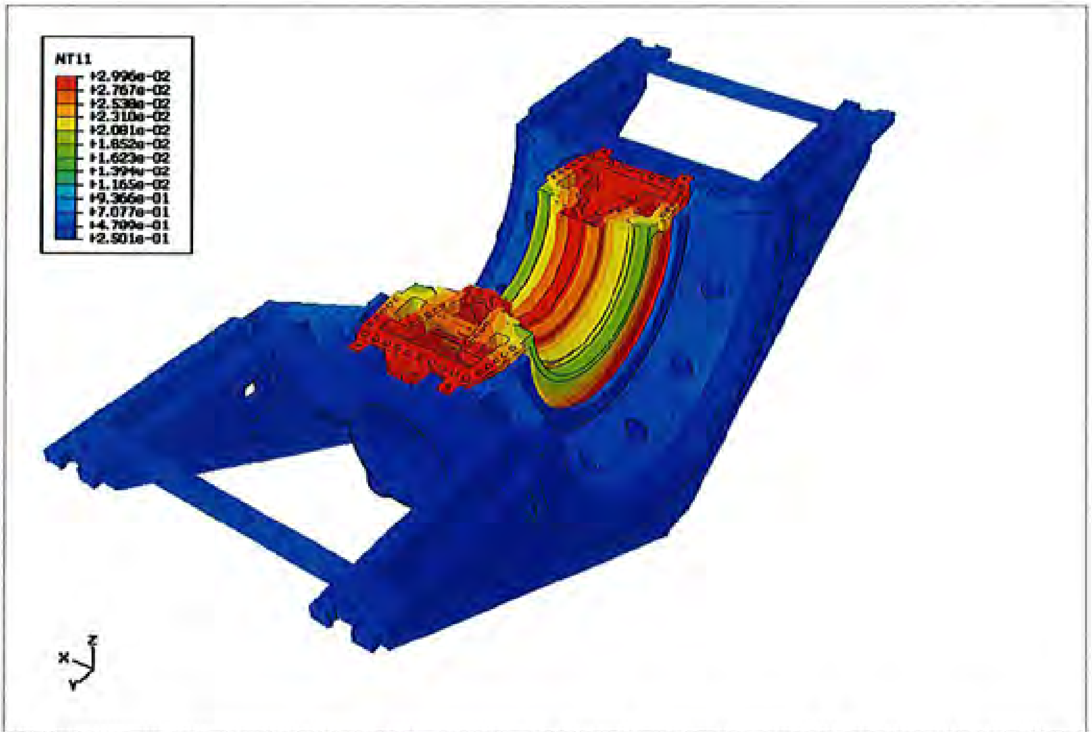

Figure 7:45: Steady State Temperature (Max. 299^{0}C) profile at the end of cold start – LP Casing Assembly (3D view)

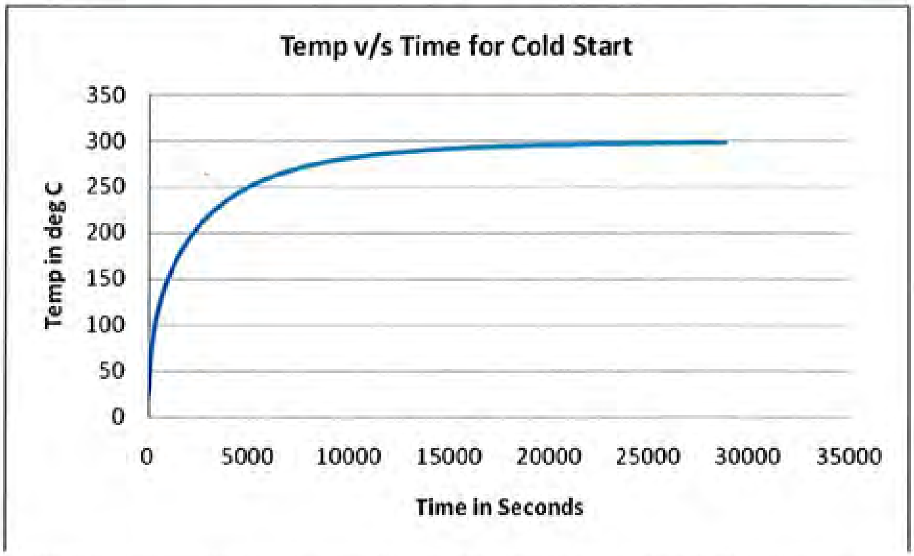

Figure 7:46: Transient Temperature plot at the end of cold start – LP Casing Assembly

412

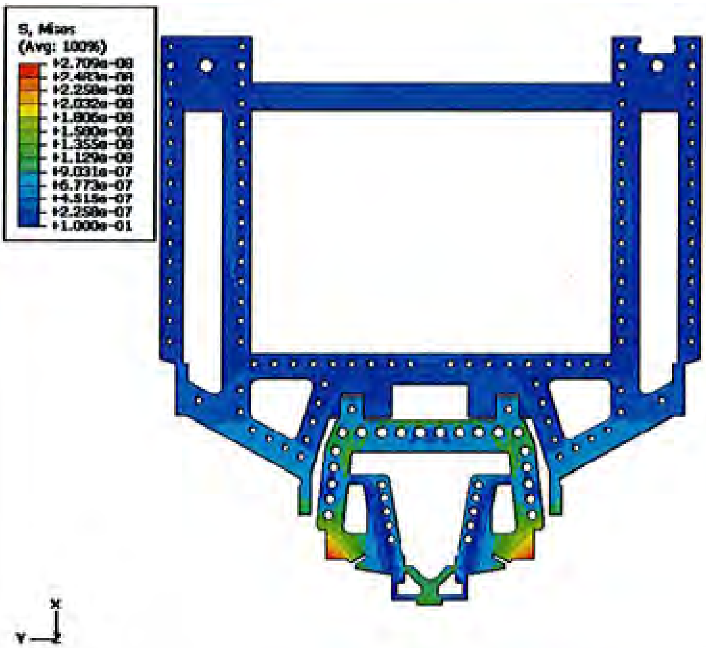

Figure 7:47: vonMises Stress Contour (Max. 270 MPa) at the end of cold start LP Casing Assembly (Cut Section)

413

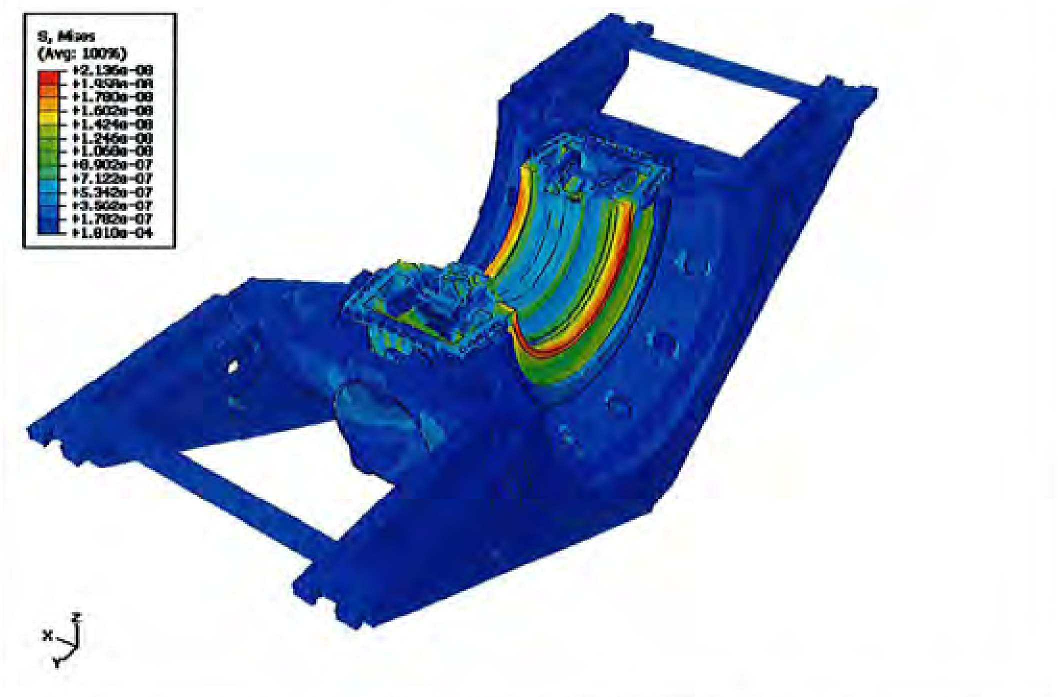

Figure 7:48: vonMises Stress Contour (Max. 213 MPa) at the end of cold start LP Casing Assembly (3D view)

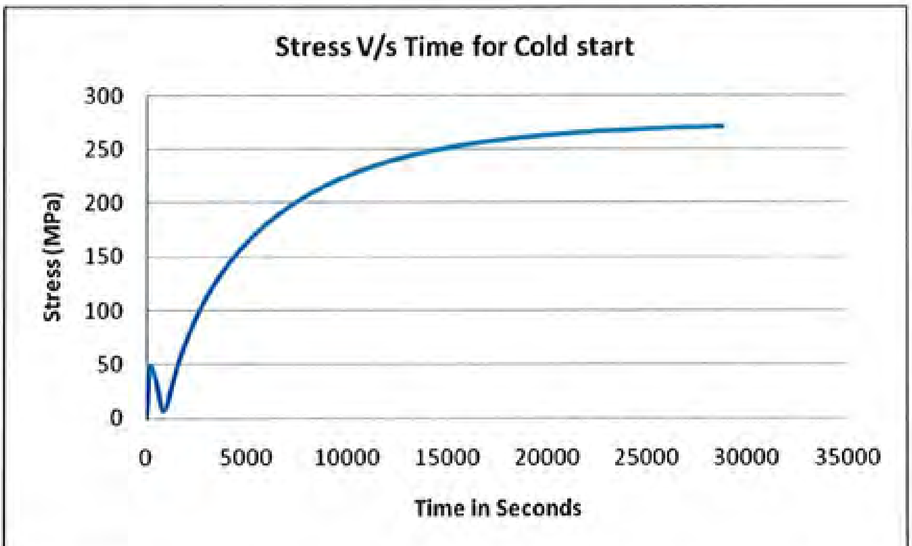

Figure 7:49: Transient Stress plot at end of cold Start – LP Casing Assembly

414

7.15. LP Casing Assembly – Warm Start

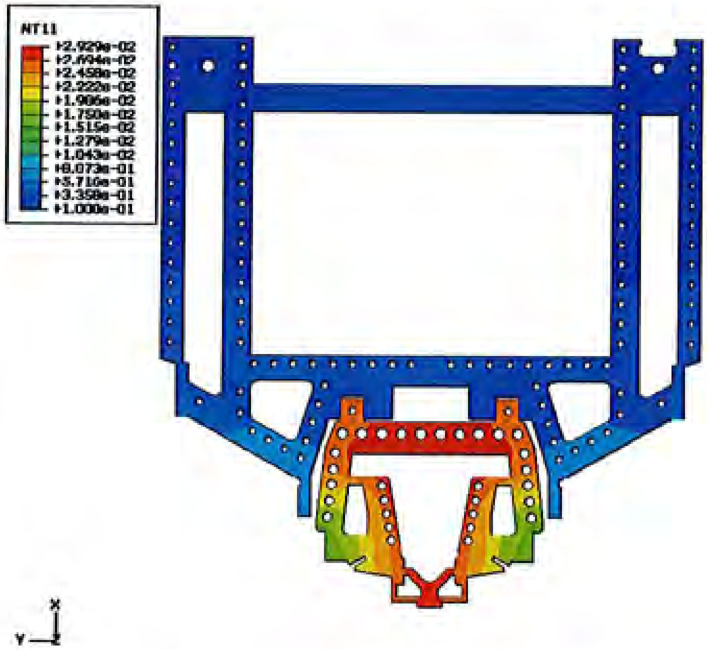

Figure 7:50: Steady State Temperature (Max. 292°C) profile at the end of warm start – LP Casing Assembly (Cut Section)

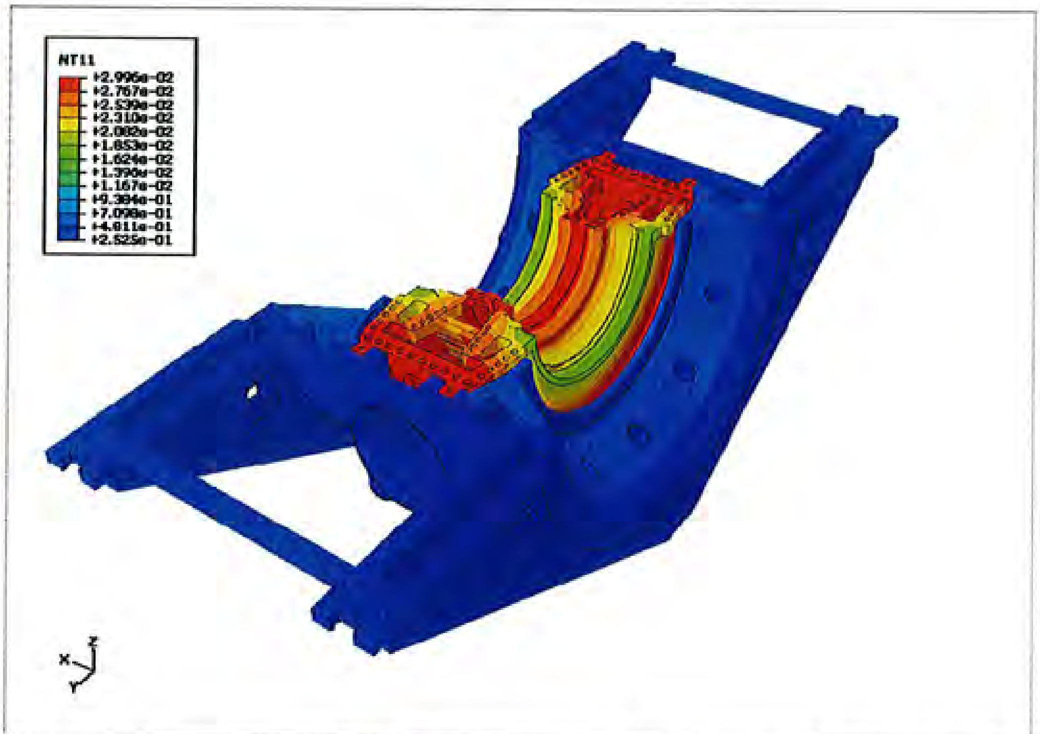

Figure 7:51: Steady State Temperature (Max. 299^{0}C) profile at the end of warm start – LP Casing Assembly (3D view)

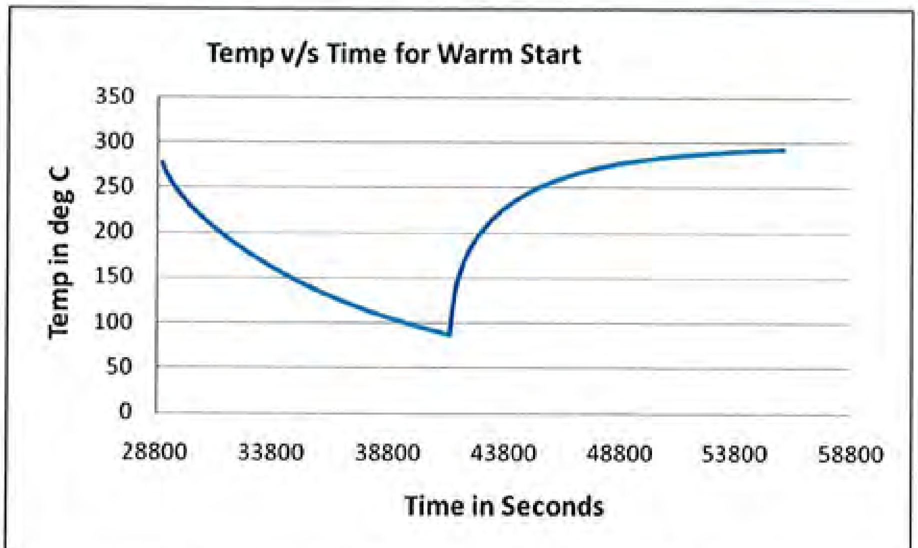

Figure 7:52: Transient Temperature plot at the end of warm start – LP Casing Assembly

46

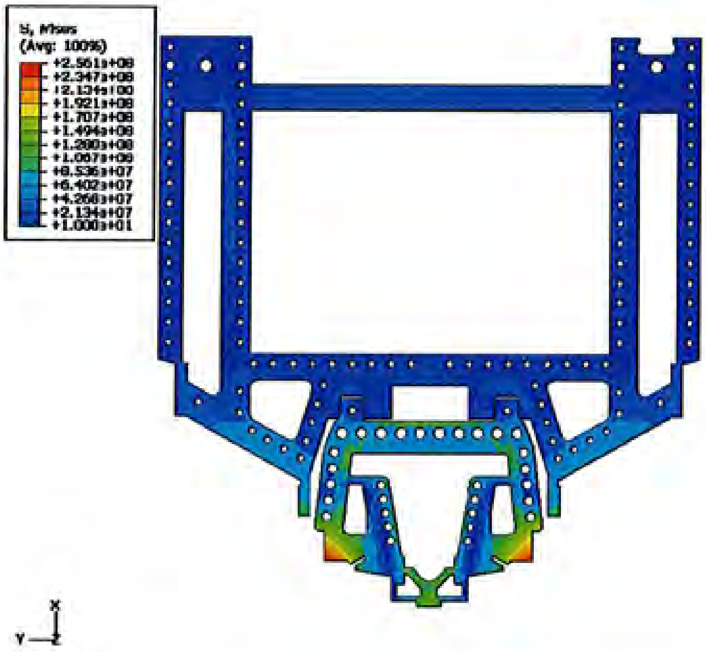

Figure 7:53: vonMises Stress Contour (Max. 256 MPa) at the end of warm start LP Casing Assembly (Cut Section)

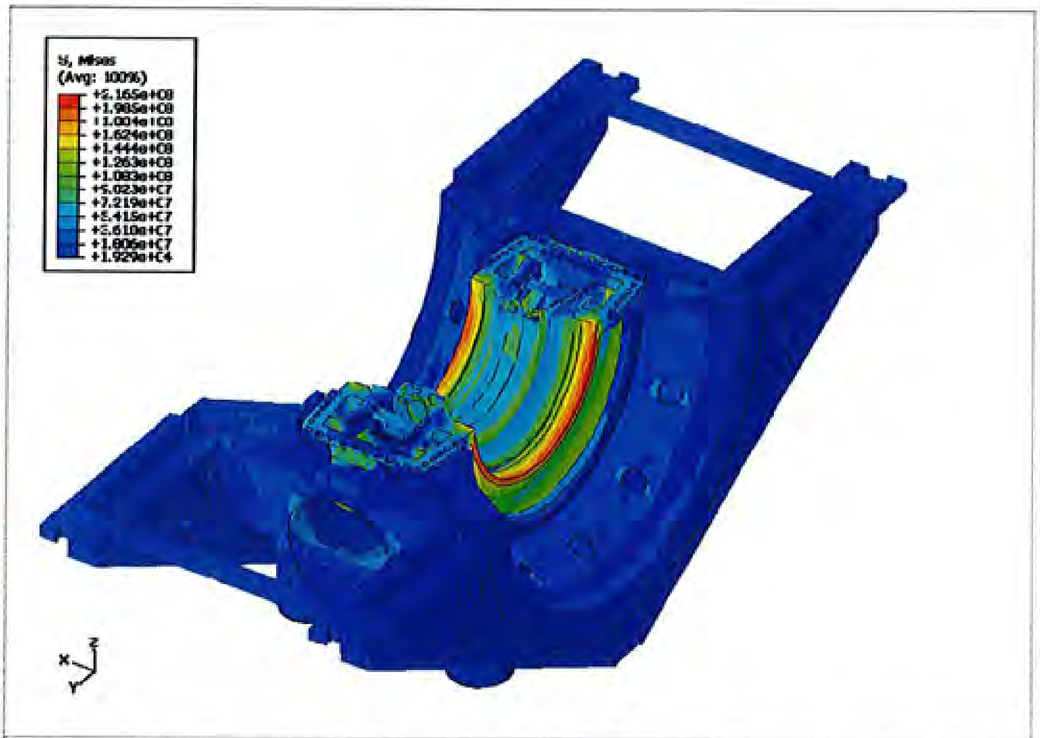

Figure 7:54: vonMises Stress Contour (Max. 216 MPa) at the end of warm start LP Casing Assembly (3D View)

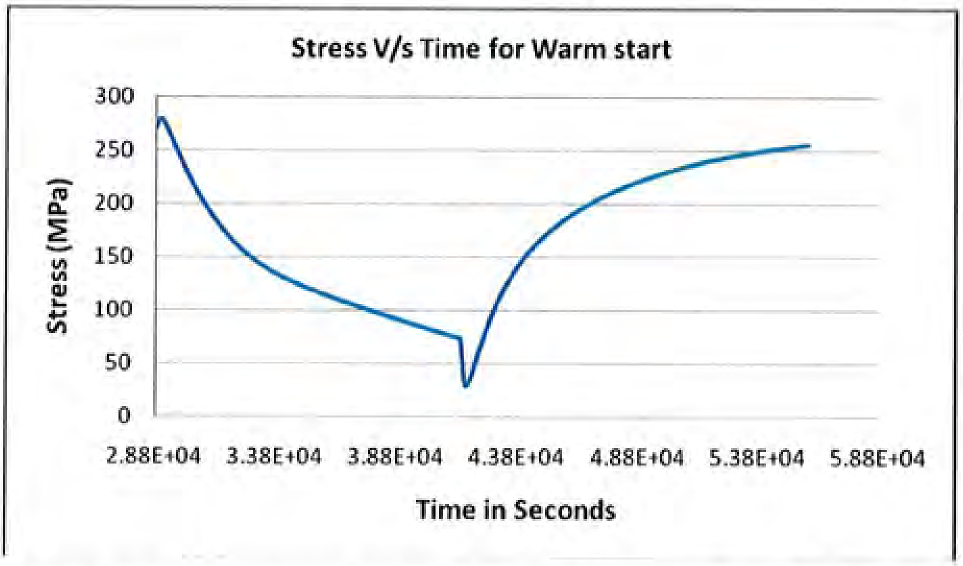

Figure 7:55: Transient Stress plot at end of warm Start – LP Casing Assembly

7.16.LP Casing Assembly – Hot Start

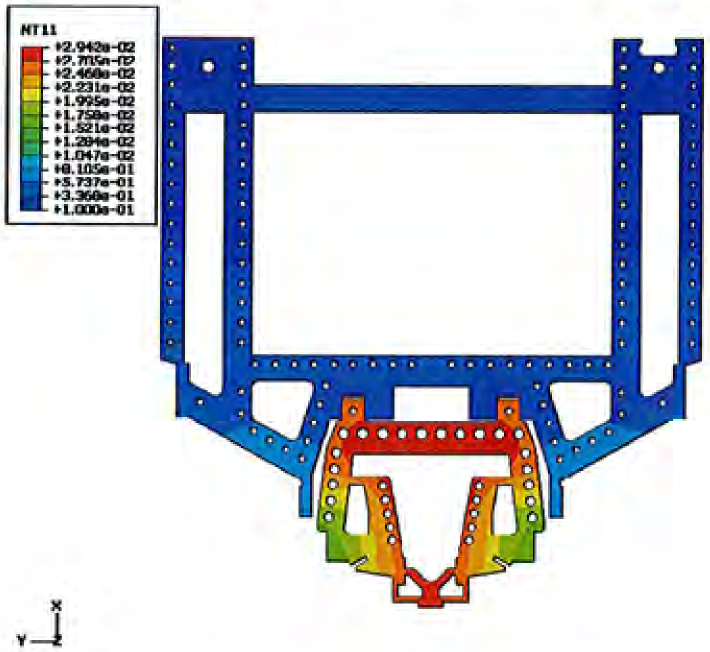

Figure 7:56: Steady State Temperature (Max. 294^{0}C) profile at the end of hot start – LP Casing Assembly (Cut Section)

419

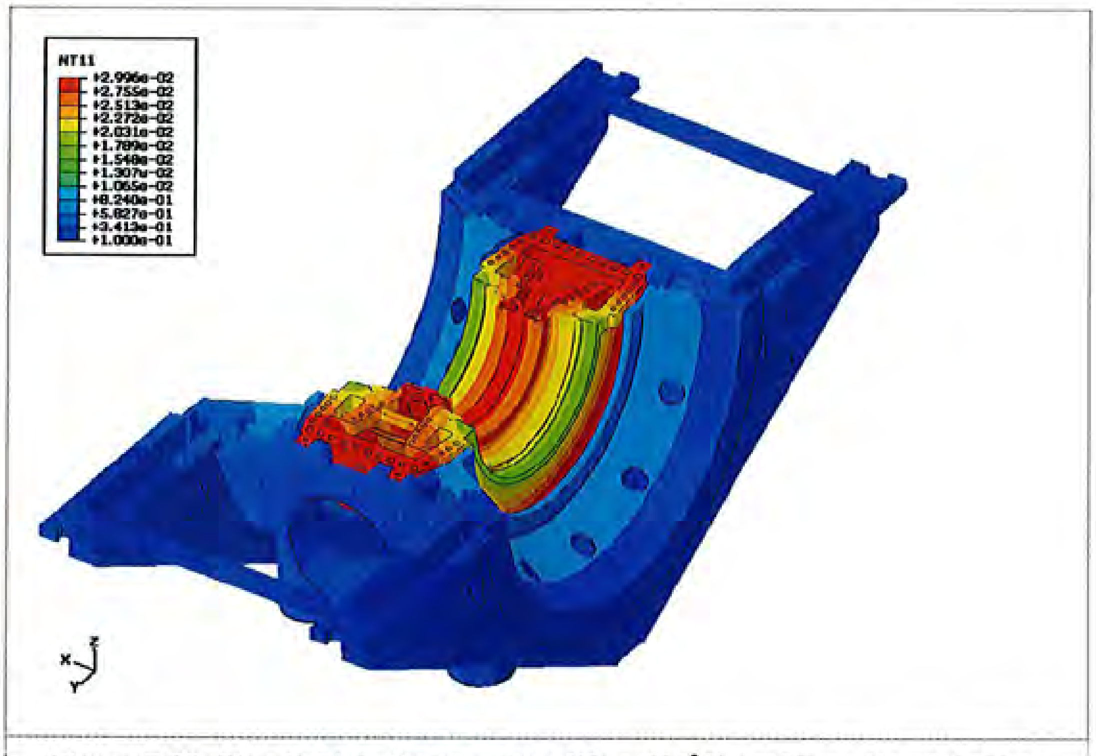

Figure 7:57: Steady State Temperature (Max. 299^{0}C) profile at the end of hot start – LP Casing Assembly (3D View)

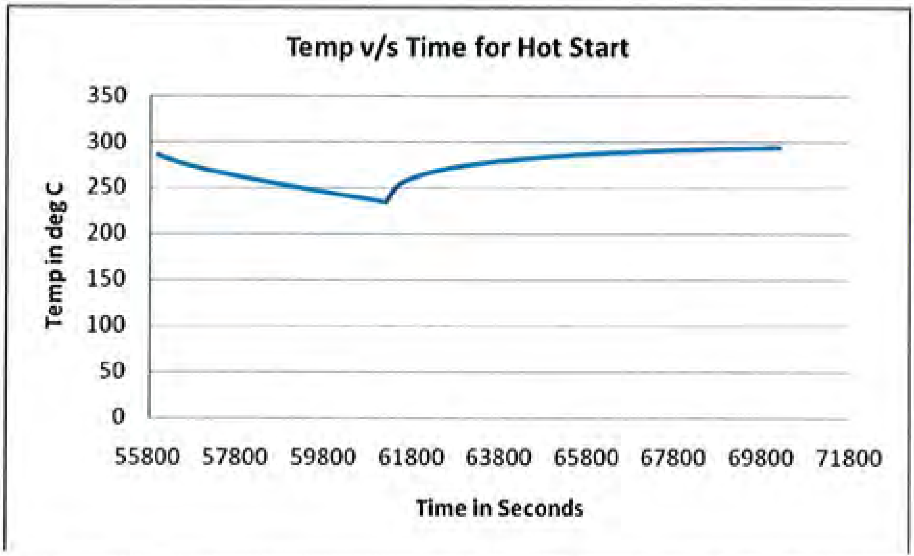

Figure 7:58: Transient Temperature plot at the end of hot start – LP Casing Assembly

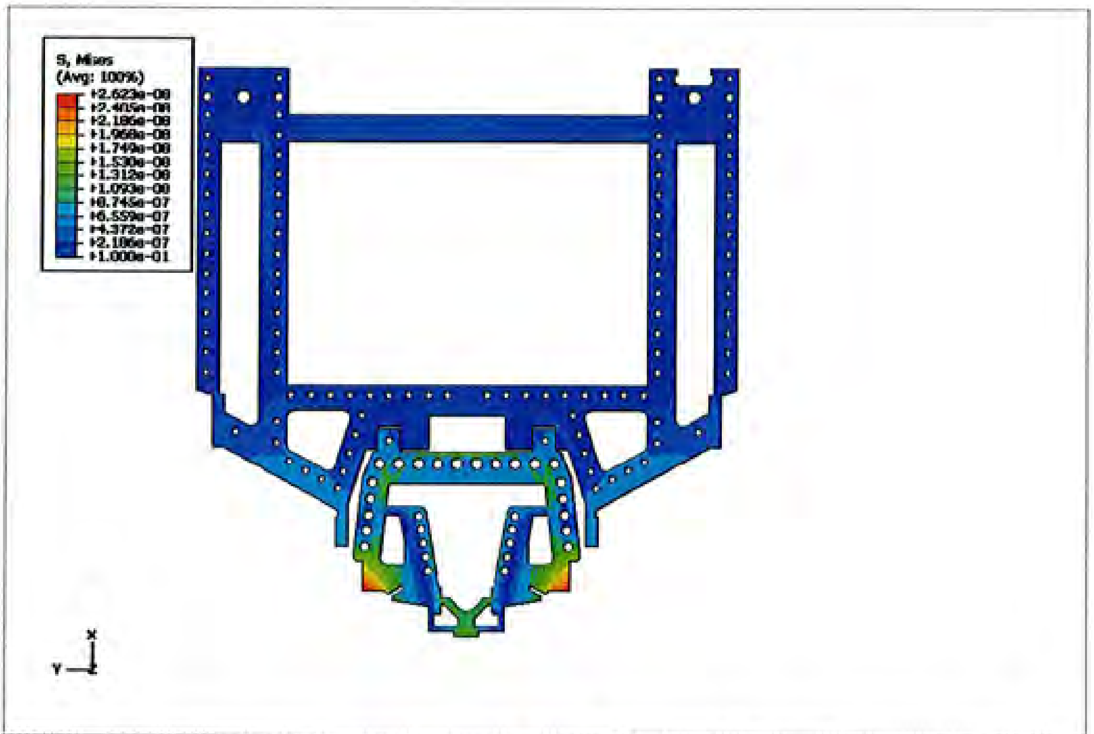

Figure 7:59: vonMises Stress Contour (Max. 262 MPa) at the end of hot start - LP Casing Assembly (Cut Section)

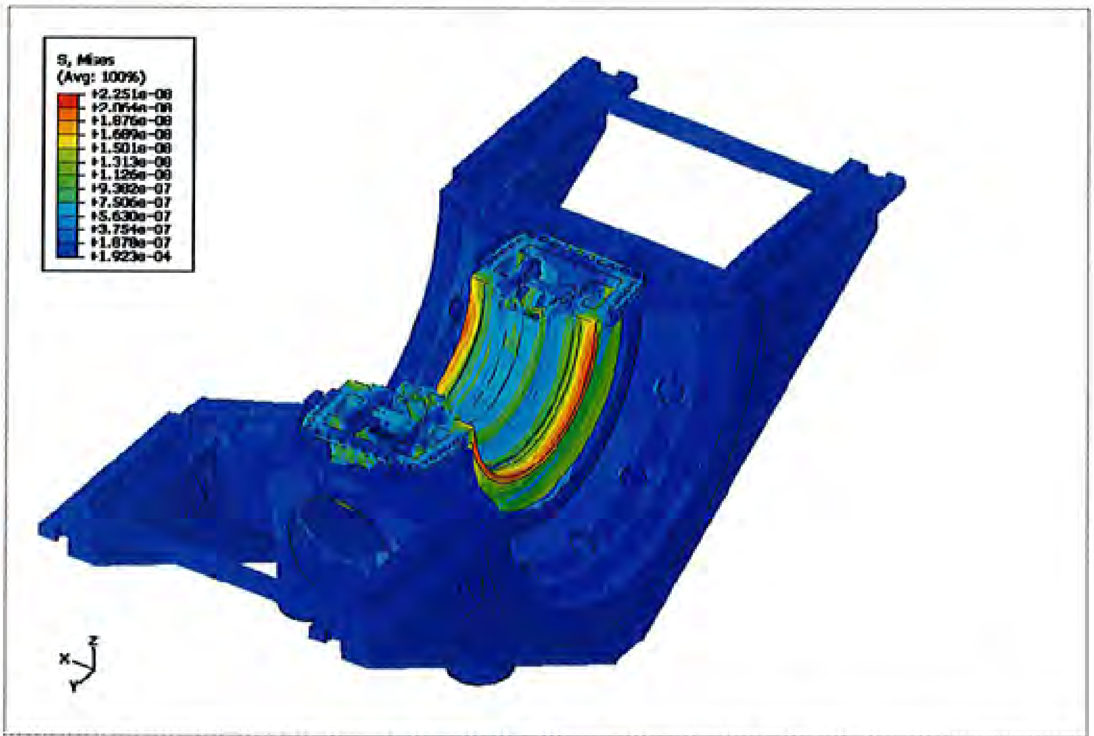

Figure 7:60: vonMises Stress Contour (Max. 225 MPa) at the end of hot start - LP Casing Assembly (3D view)

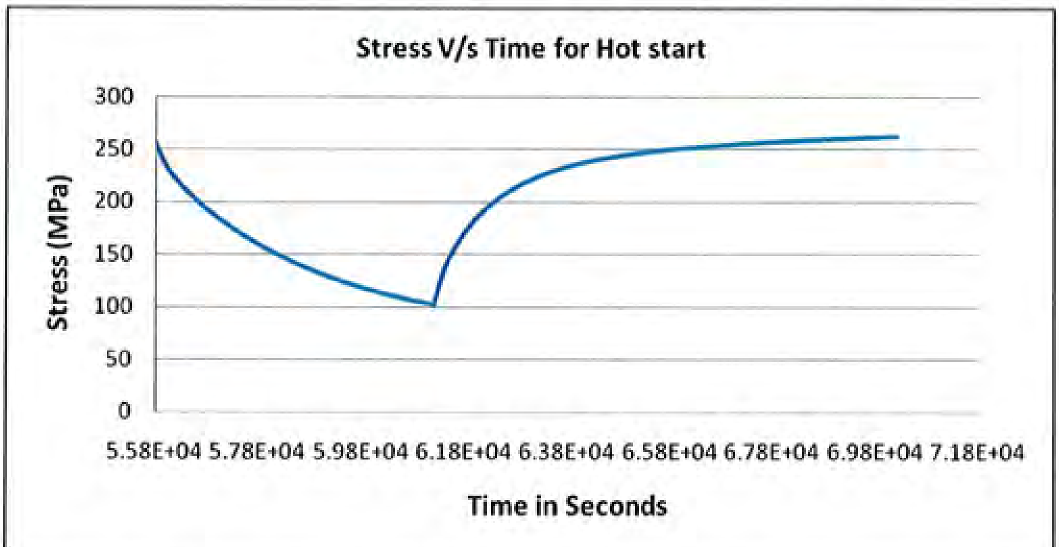

Figure 7:61: Transient Stress plot at end of hot Start – LP Casing Assembly

432

7.17. LP Shaft – Mechanical & Thermal Loading

The LP Shaft is analysed for the Thermo-mechanical loading conditions. At one end of the LP Shaft, the logitudunal displacements arrested as shown in Figure 7:62.Transient Temperature and pressure loading conditions are shown in Figure 7:63. Rotating speed of shaft is taken as 3000 rpm. The blade are not modeled but the effective mass is lumped on the shaft.

Temperature profile and stress at each startup condition are shown in Figure 7:64 to Figure 7:75 for Cold Start, Warm Start and Hot start of the turbine.

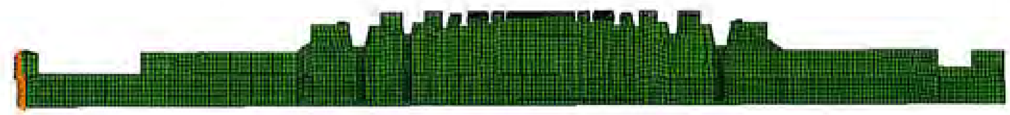

Figure 7:62: Longitudinal Displacement (Y) along Edges of the LP shaft is constrained

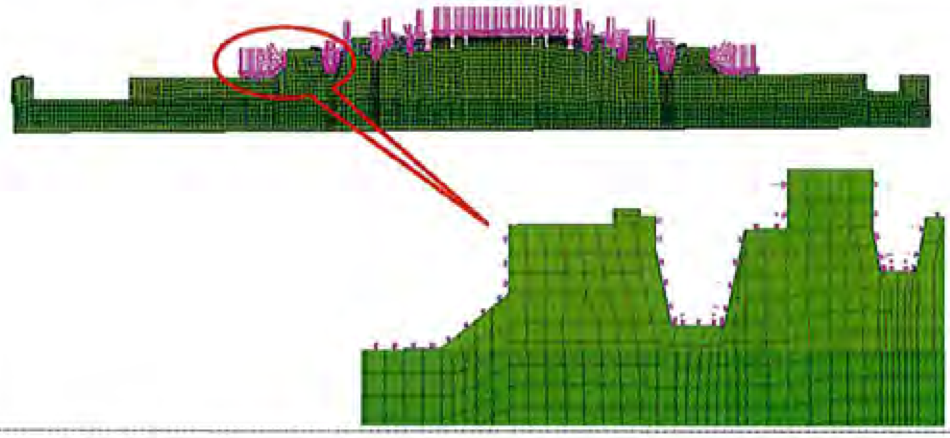

Figure 7:63: Pressure and thermal boundary conditions applied for 6 stages – LP Shaft

7.18. LP Shaft – Cold Start

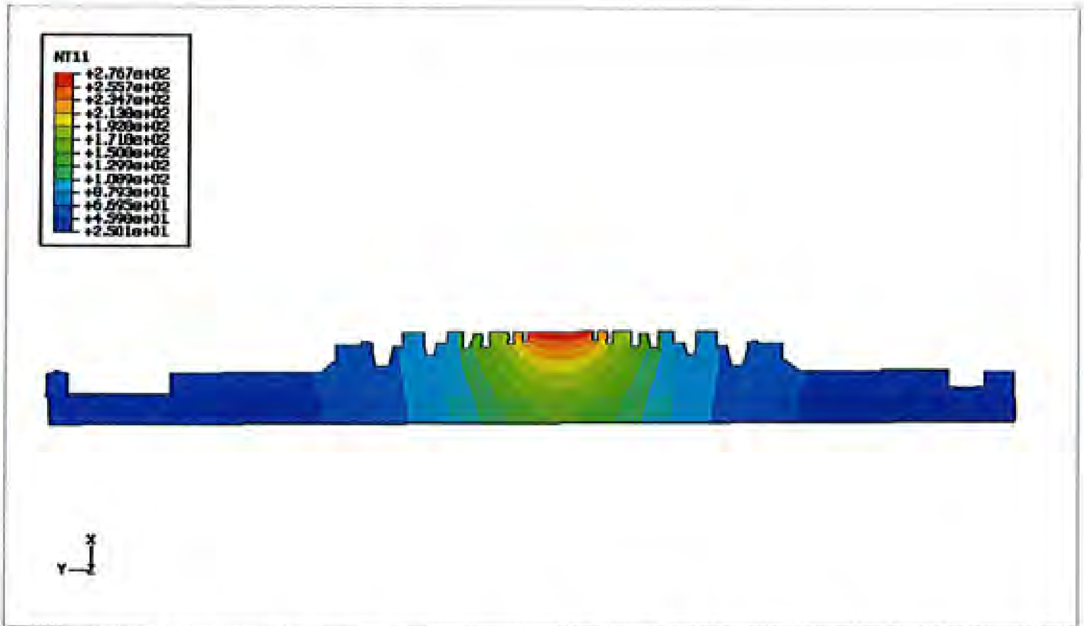

Figure 7:64: Steady State Temperature (Max. 276°C) profile at the end of cold start – LP Shaft (Cut Section)

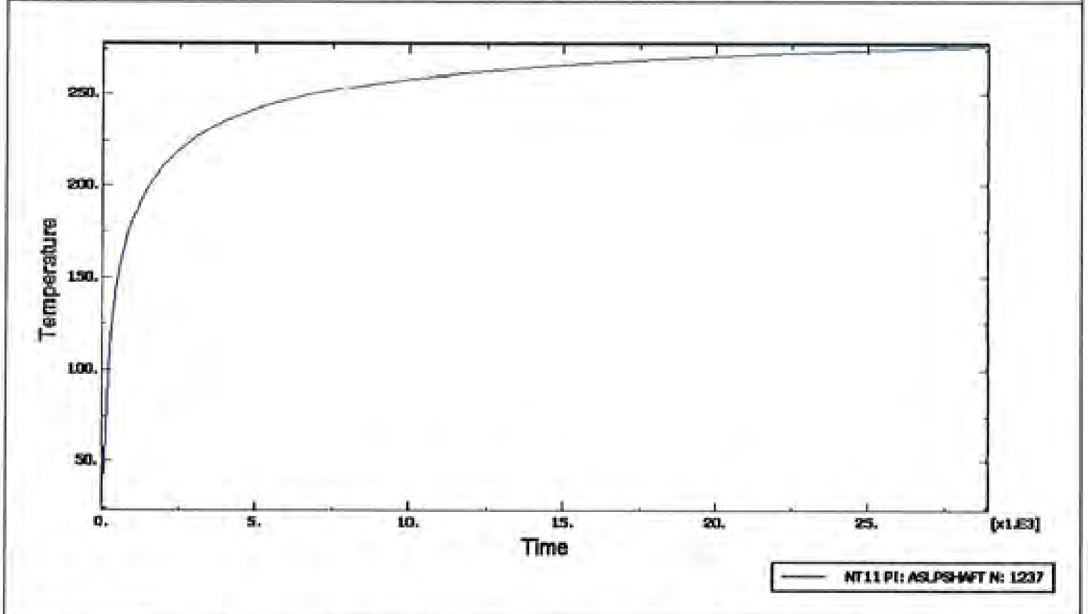

Figure 7:65: Transient Temperature plot at the end of cold start - LP Shaft

424

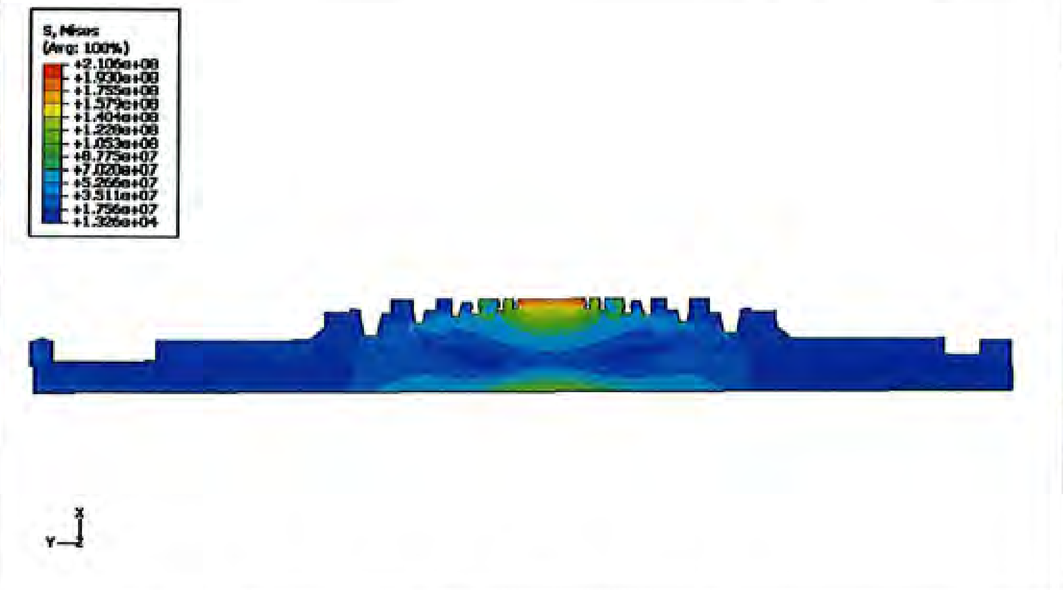

Figure 7:66: vonMises Stress Contour (Max. 210 MPa) at the end of cold start - LP Shaft (Cut Section)

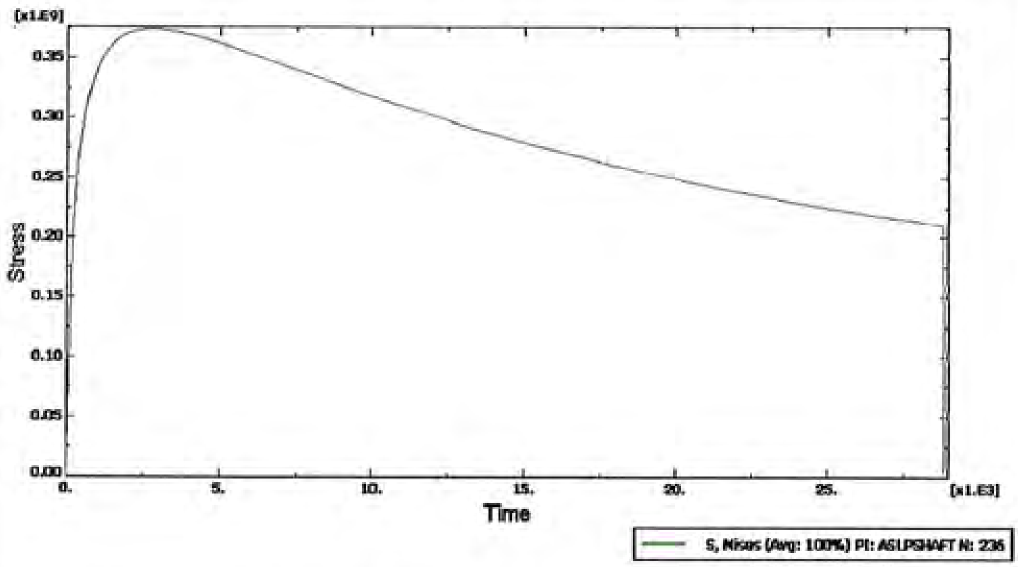

Figure 7:67: Transient Stress plot at end of cold Start – LP Shaft

7.19. LP Shaft – Warm Start

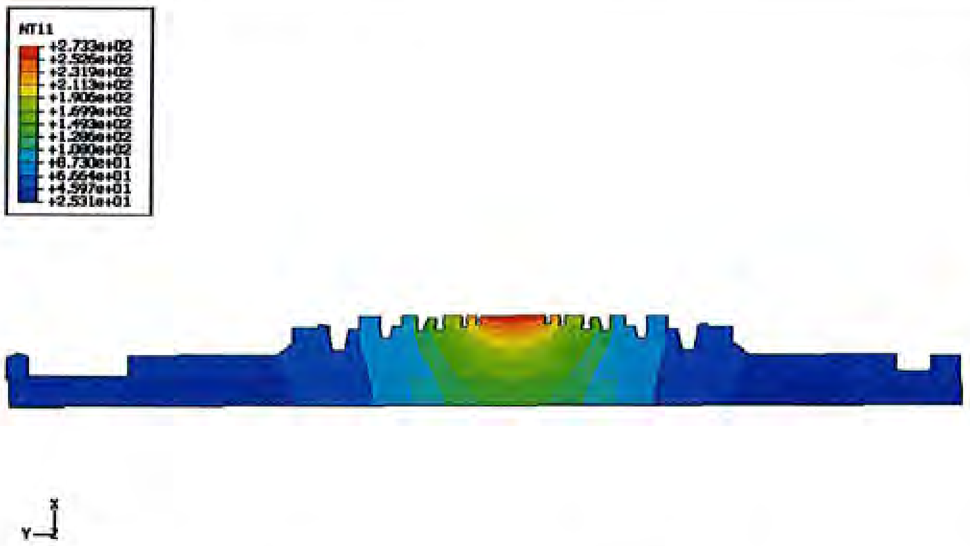

Figure 7:68: Steady State Temperature (Max. 273°C) profile at the end of warm start – LP Shaft (Cut Section)

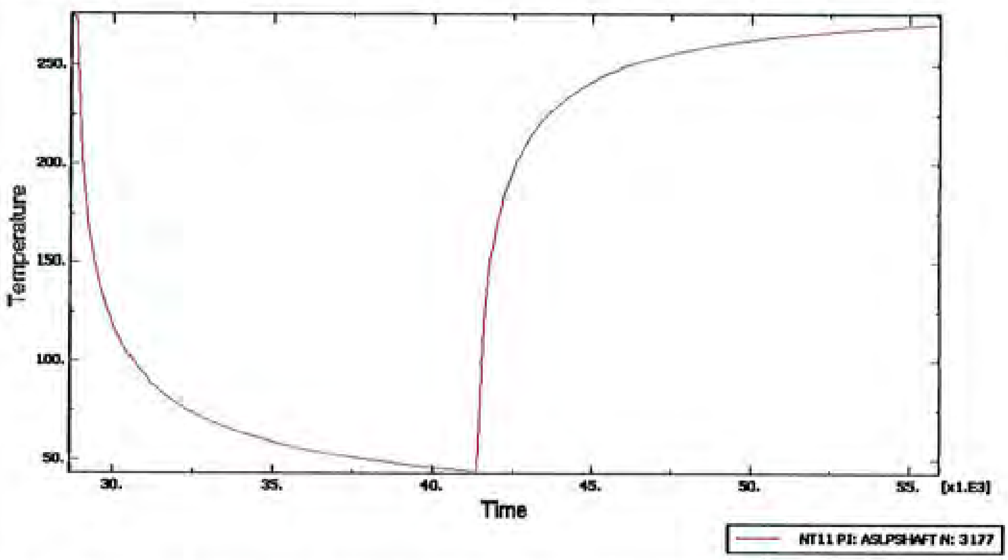

Figure 7:69: Transient Temperature plot at the end of warm start - LP Shaft

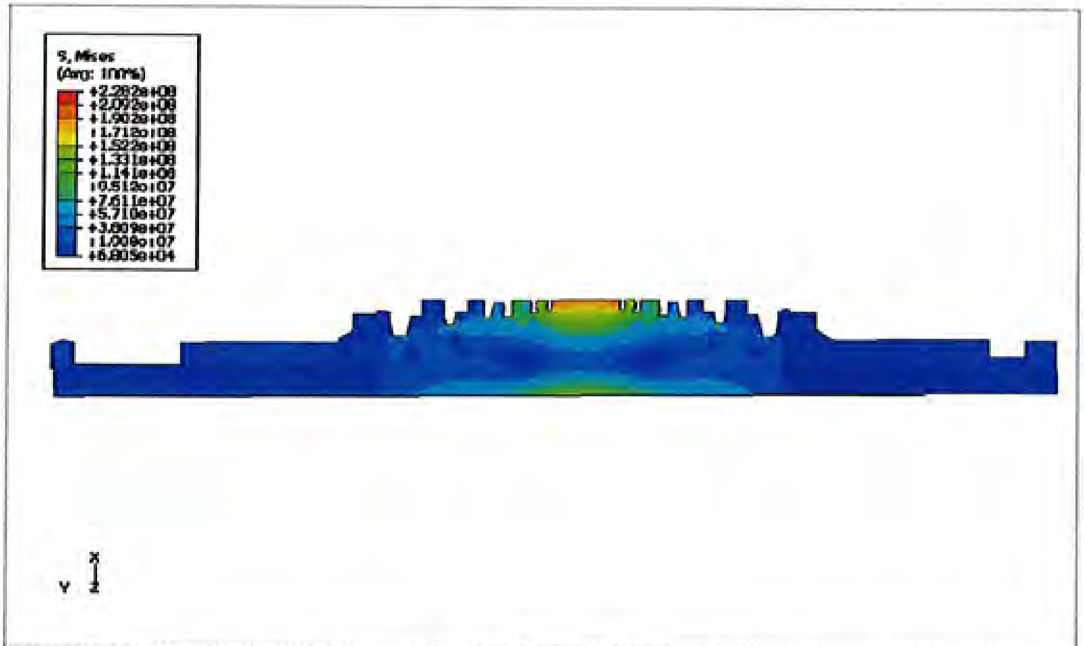

Figure 7:70: vonMises Stress Contour (Max. 228MPa) at the end of warm start– LP Shaft (Cut Section)

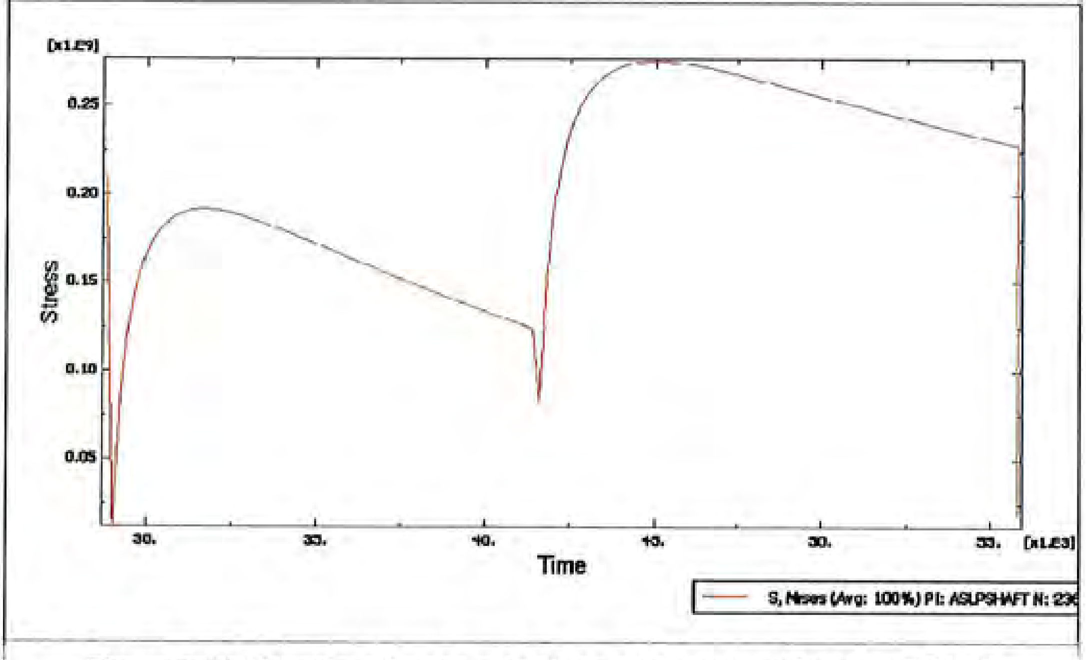

Figure 7:71: Transient Stress plot at the end of Warm Start – LP Shaft

7.20. LP Shaft – Hot Start

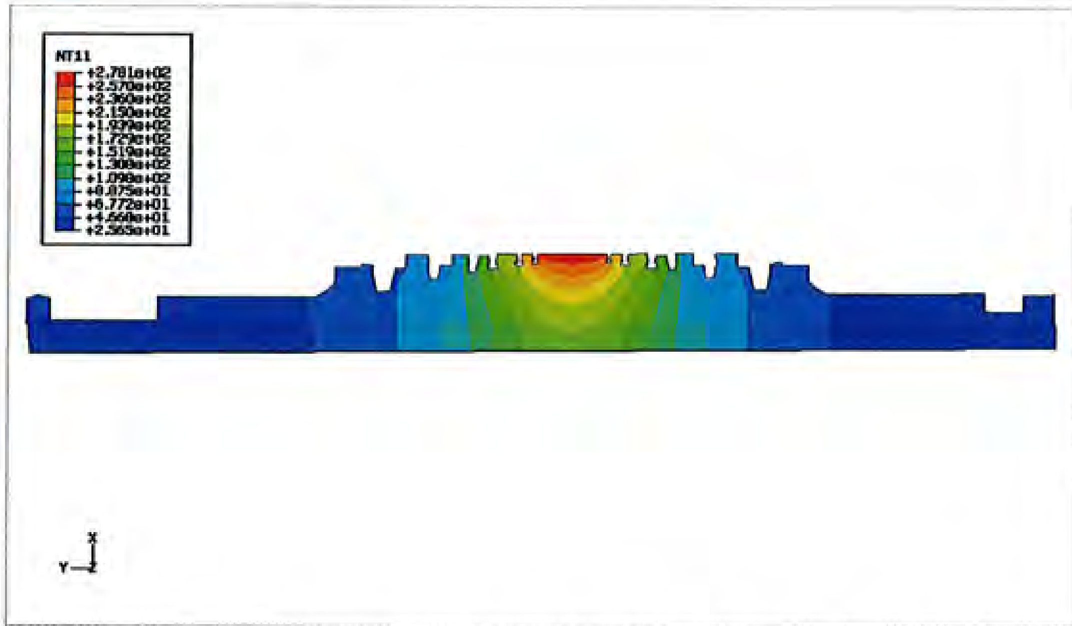

Figure 7:72: Steady State Temperature (Max. 278^{0}C) profile at the end of Hot Start – LP Shaft (Cut Section)

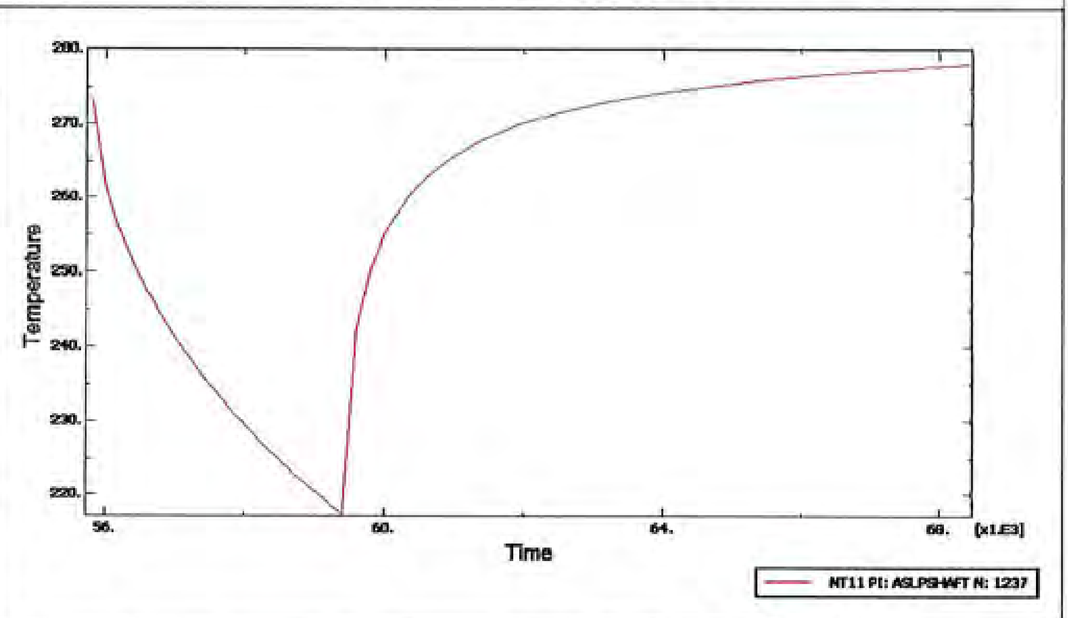

Figure 7:73: Transient Temperature plot at the end of Hot start – LP Shaft

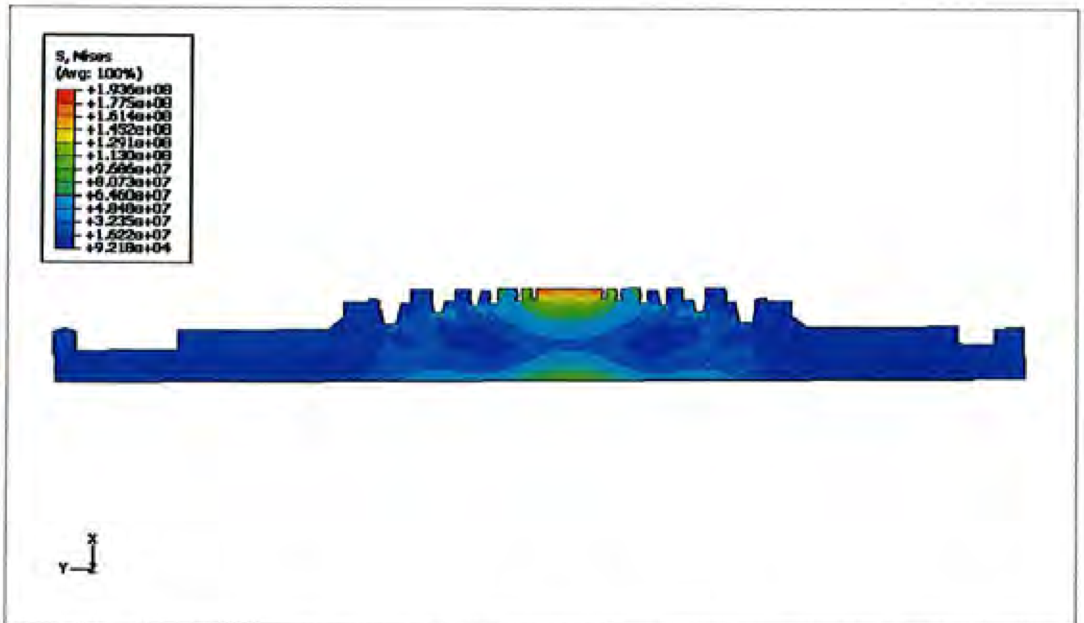

Figure 7:74: vonMises Stress Contour (Max. 193 MPa) at the end of hot start – LP Shaft (Cut Section)

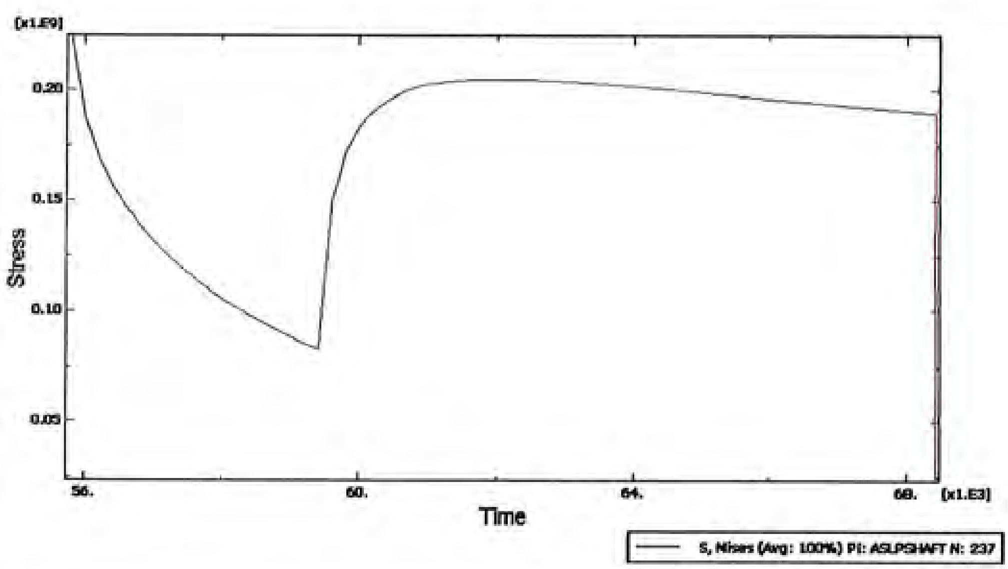

Figure 7:75: Transient Stress plot at the end of Hot Start – LP Shaft

7.21. LP Shaft – Cold start (Radial and Axial stress)

Radial and axial stress contours for the LP shaft is as shown below

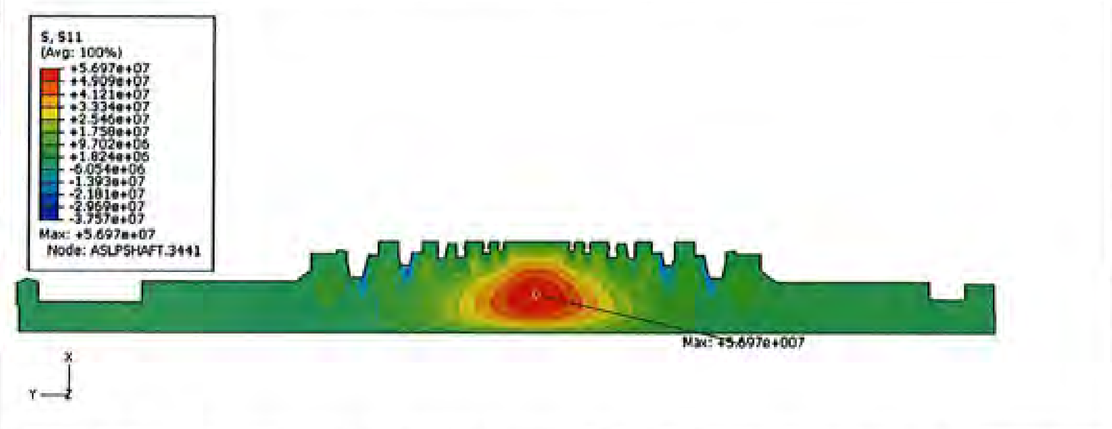

Figure 7:76: Radial stress at the end of cold start is 56MPa – LP Shaft (Cut Section)

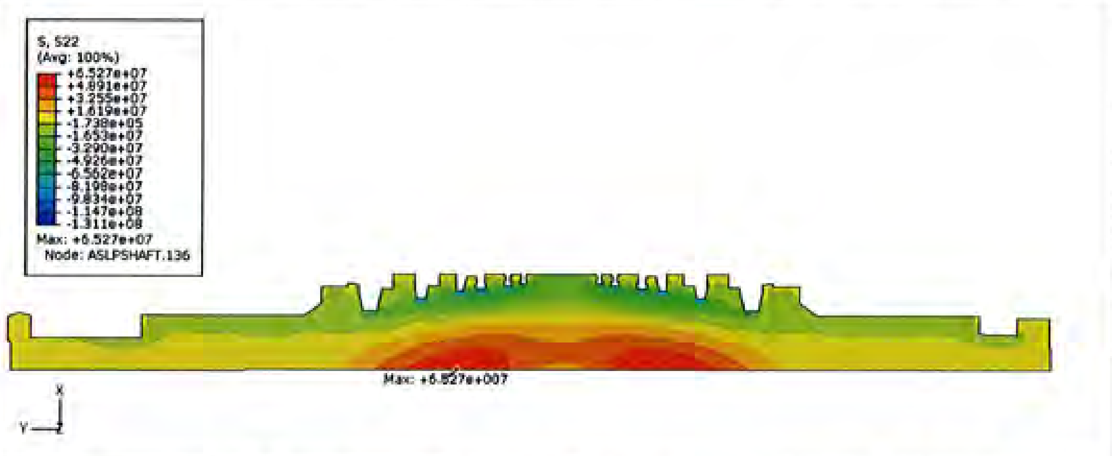

Figure 7:77: Axial stress at the end of cold start is 65MPa – LP Shaft

7.22. LP Shaft – Warm start (Radial and Axial stress)

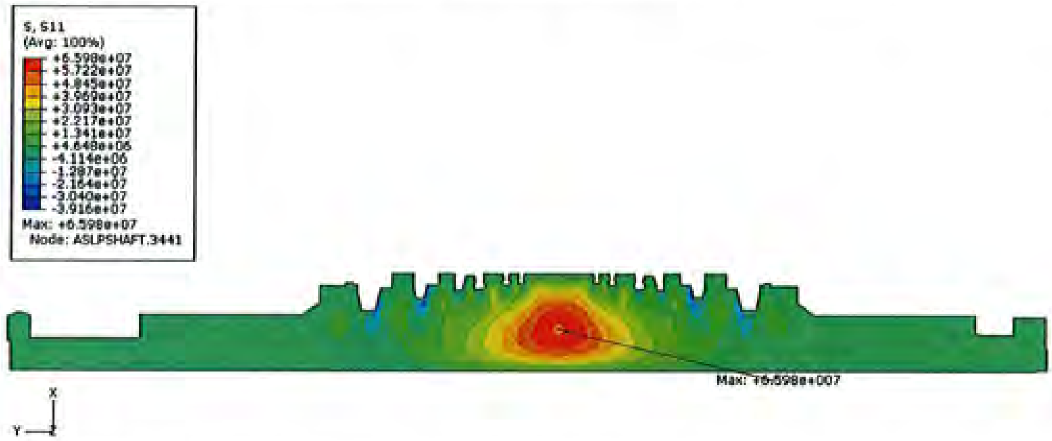

Figure 7:78: Radial stress at the end of warm start is 65MPa – LP Shaft (Cut Section)

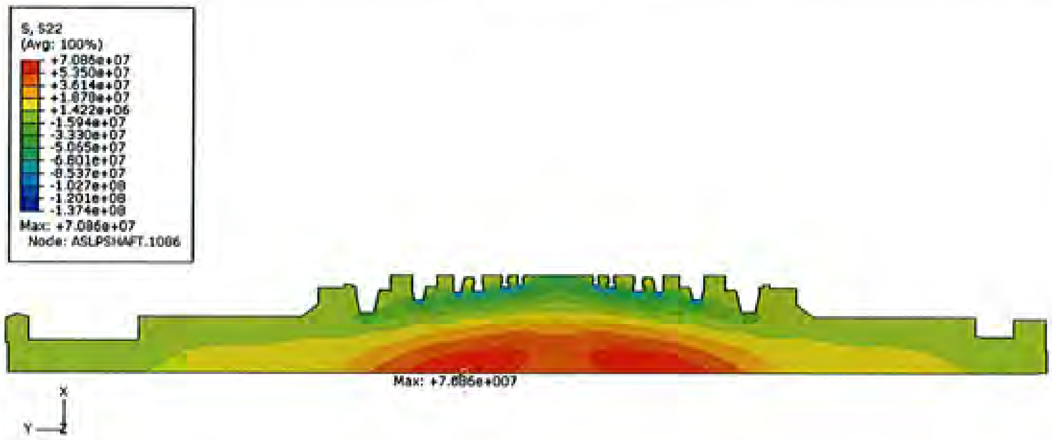

Figure 7:79: Axial stress at the end of warm start is 70MPa – LP Shaft

7.23. LP Shaft – Hot start (Radial and Axial stress)

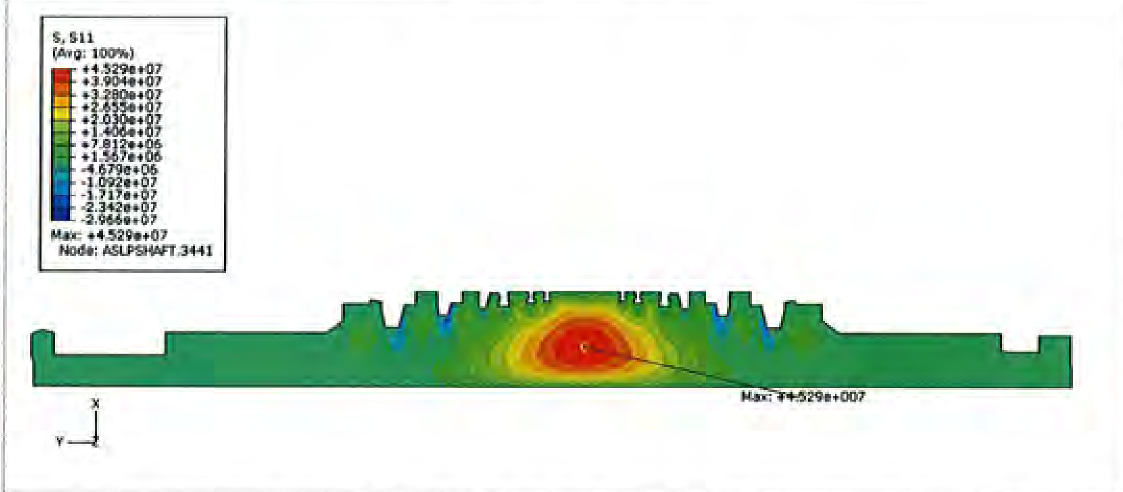

Figure 7:80: Radial stress at the end of Hot start is 45MPa – LP Shaft (Cut Section)

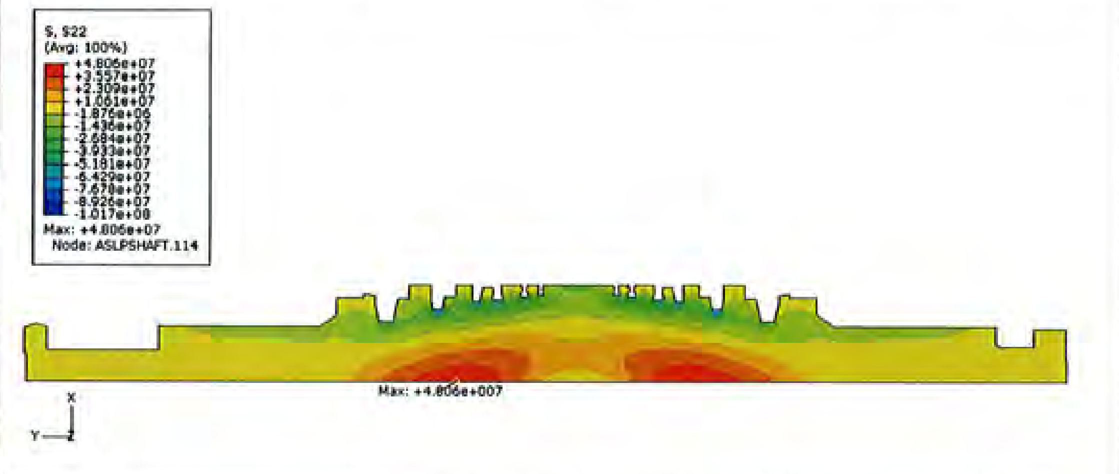

Figure 7:81: Axial stress at the end of Hot start is 37MPa – LP Shaft

7.24. Observations

The vonMises stress induced due to thermal, mechanical and Operating loading at different stages of start-up conditions are tabulated in.Table 7-1 and Table 7-2 The hoop stress is main component of vonMises Stress and other stress components are minimal.

Table 7-1: Transient Peak Stress in the IP and LP Steam Turbine

Component	Peak Transient Stress(MPa)		
	Cold Start	Warm Start	Hot Start
IP Casing Assembly	530	490	275
IP Shaft	220	360	150
LP Casing Assembly	270	256	262
LP Shaft	360	280	230

Table 7-2: Steady State Peak Stress in the IP and LP Steam Turbine

Component	Steady state Stress(MPa)		
	Cold Start	Warm Start	Hot Start
IP Casing Assembly	220	275	260
IP Shaft	90	130	80
LP Casing Assembly	270	256	262
LP Shaft	210	228	193

For LP shaft temperature is increased by 40 degree and pressure is increased by 10% for all stages, temperature and pressure is dropped by 40 degree, 10% respectivley and analysis is performed. Results were presented in **Table 7-3** below.

Table 7-3: Steady State Peak Stress in the LP shaft for temperature and pressure variation

Component	Steady state Stress(MPa)		
	Cold Start	Warm Start	Hot Start
LP shaft(40 degree temp raise, 10% pressure raise)	230	240	212
LP shaft(Actual inputs)	210	228	193
LP shaft(40 degree temp drop, 10% pressure drop)	186	182	163

433

Section 8 Life Assessment (considering Creep & fatigue)

8.1. Introduction to fatigue

- Fatigue is a process in which damage is accumulated in a material undergoing fluctuating (cyclic) loading, finally resulting in failure even if the maximum load is well below the elastic limit of the material being used. Fatigue is responsible for 90% of all mechanical engineering component failures.
- "Fatigue is the process of progressive localized permanent structural change occurring in a material subjected to conditions that produce fluctuating stresses and strains at some point or points and that may culminate in cracks or complete fracture after a sufficient number of fluctuations" – ASME definition for fatigue.

8.2. Three stages of fatigue failure

1. Crack initiation

   Cracks may initiate from the surface, occupies most of fatigue life. Almost 80% of life is consumed in crack initiation. Fe-safe software is used to predict the life for crack initiation.

2. Propagation

   Crack growth takes place in a direction normal to applied stress.

3. Fracture

   Unstable fracture occurs suddenly

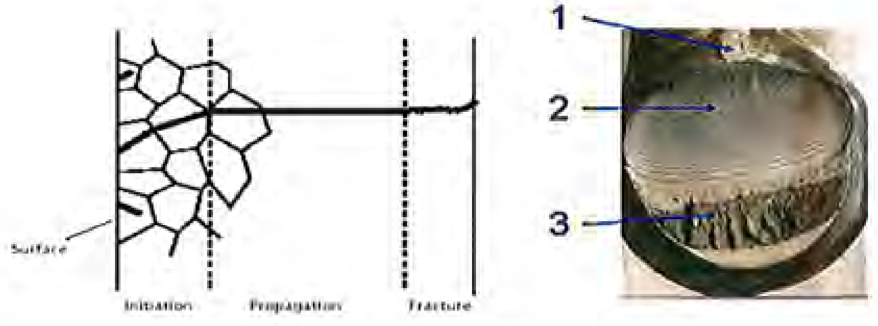

Figure 8:1: Three stages of fatigue failure

8.3. Thermo mechanical fatigue (TMF)

Thermo mechanical load involve the thermal inputs such as heat quantity, type of heat transfer will result in temperature distribution and its gradients in the system. These temperature gradient and distribution will in turn cause the mechanical stress/strain in the system.

Thermo-mechanical fatigue occurs when engineering materials are subject to simultaneous cyclical mechanical and thermal loads. Generally, both of these loads are time dependent. Mechanical loads could be the results of constraint, thermal gradients, externally applied loads, or any combination of these.

Examples of components that experience TMF: Turbine blades, disks, Heat exchangers, pipes, pressure vessels, brake discs, exhaust systems, pistons, cylinders, engine housing, Combustion chambers etc.

Thermo mechanical fatigue occurs when both stress and temperature fluctuate. The following are the parameters to be considered during TMF analysis:

1. Effect of strain rate and instantaneous temperature on fatigue damage
2. Phase relationship between stress and temperature in each cycle
3. Bulk stress relaxation
4. Effect of strain ageing(Pre-soaking) on fatigue strength
5. Superimposition of high frequency stress cycles

Calculation of strain-rate-dependent and temperature-dependent stresses:

The first step in the TMF analysis is to generate stresses that are dependent on both strain rate and temperature. This is a multi-stage process as shown below

The input to this process is an elastic principal strain sequence, derived from the original stress sequence, resolved on to the planes required for a critical plane analysis and then strain rate between each data point is calculated. Average strain rate is calculated and hold periods are identified. The hold periods can be formed by smaller cycles within the cycle or by periods of constant strain. A time step is hold if its strain rate is less than 5% of the average for the cycle. The process is repeated until no new hold periods are found and the average strain rate has attained a stable value. Consider a strain-time history as shown in figure below

435

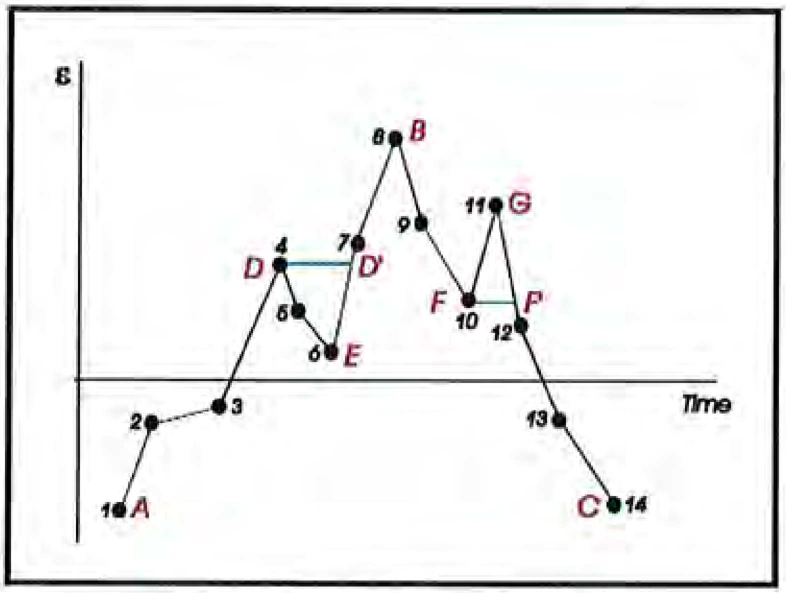

Figure 8:2: strain time history

The main cycle is A-B-C. The smaller cycle, D-E-D' is removed (to be treated separately) and leaves a 'hold' over the time D-D'. Similarly, the smaller cycle F-G-F' is remove d, leaving a 'hold' over the time F-F'. With these 'holds' removed, the strain rate between each pair of points is determined, and the average strain rate calculated. Each strain rate is then compared with the average value. This may show that the strain rate between points 2 and 3 is less than 5% of the average value. This would then be treated as a 'hold', and a new average strain rate calculated, excluding the time between points 2 and 3. Where a cycle has a temperature transition > 5°C, the damage is evaluated for each of the pair of data points in the cycle and the total damage is a time weighted average of these damage increments.

Calculation of thermal stress strain hysteresis loop

For conventional metallic materials the room temperature hysteresis loop is symmetrical in tension and compression.

$$\epsilon = \sigma/E + (\sigma/K')1/n'$$

ε - Total strain

936

σ - True stress

E - Young's Modulus

K' - Strain hardening coefficient

n'- Strain hardening component

For TMF analysis these curves are defined at a series of strain rates and temperatures. Material data is required for a number of strain rate and temperatures (Minimum 4 set of data is required. i.e. for two different temperatures and two different strain rates). For each pair of data points within each cycle, the strain rate and temperature are used to evaluate the shape of the stress-strain curve between these two points. A weighting function is used to ensure that the stress-strain response produces a closed hysteresis loop for the cycle. Below figure shows a fatigue stress strain cycle constructed considering the effect of strain rate and temperature.

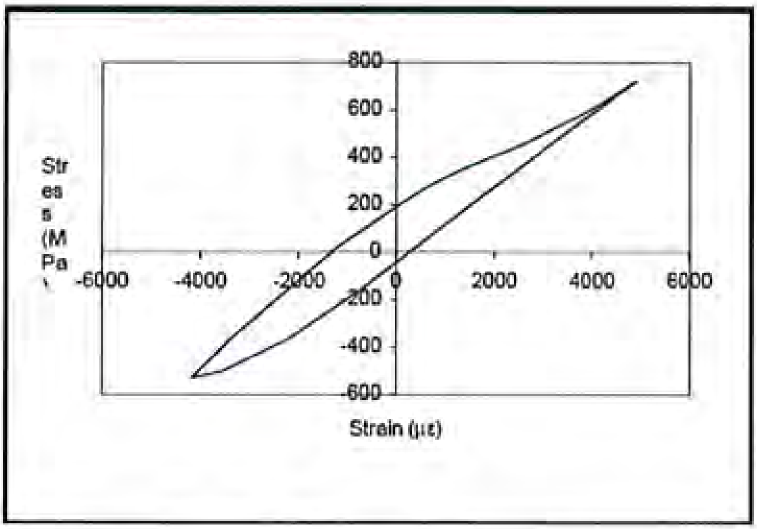

Figure 8:3: Fatigue stress- strain cycle constructed considering the effect of strain rate and temperature

For conventional materials a set of strains and associated stress for each cycle, incorporating the effects of strain rate and temperature, are derived from fatigue cycle of strain time points as shown below. The input to this process is the

437

complete fatigue cycle of strain time points with no hold periods. Input to this is the complete fatigue cycle of strain time points with no hold periods.

Starting with the first and second points in the cycle repeat this process for each point in the cycle. Since the calculation produces stresses that do not close the cycle, a weighting procedure is used progressively on each calculated stress to ensure cycle closure. The stress between each pair of data points is used, so that any changes in strain rate or temperature during the cycle are accounted for. The illustration above is for uniaxial stress state. For biaxial stresses a similar procedure is used.

Effect of strain rate and instantaneous temperature on fatigue damage

Strain life curves are defined as follows

$\Delta\varepsilon/2 = \sigma f'/E\ (2Nf)b + \varepsilon f'\ (2Nf)C$

E- Young's modulus

σf' – Fatigue strength coefficient

εf' – Fatigue ductility coefficient

b – Fatigue strength exponent

c – Fatigue ductility exponent

Δε- strain amplitude

2Nf – Number of reversals

For TMF analysis these curves are defined at a series of strain rate and temperatures (minimum two different temperatures and two different strain rates)

Effect on fatigue damage of the phase relationship between strain and temperature

During in phase (Ø = 0°) condition maximum mechanical strain coincides with maximum temperature where as during out of phase (Ø = 180°) temperature maximum coincides with minimum temperature.

Fatigue damage is dependent on phase relationship between strain and temperature. Effect is material dependent and is most pronounced in Low cycle fatigue regime where there is significant plastic strain.

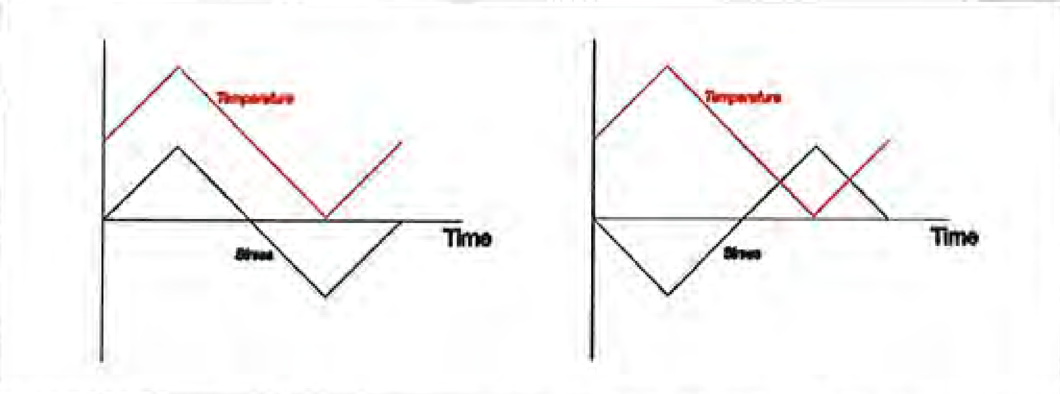

Figure 8:4: strain time history (In phase and out of phase)

In general, both in-phase and out-of-phase stress and temperature cycles are more damaging than iso thermal stress cycles. For some materials in phase stress and temperature cycles are more damaging than out of phase, but for other materials out of phase stress and temperature are more damaging.

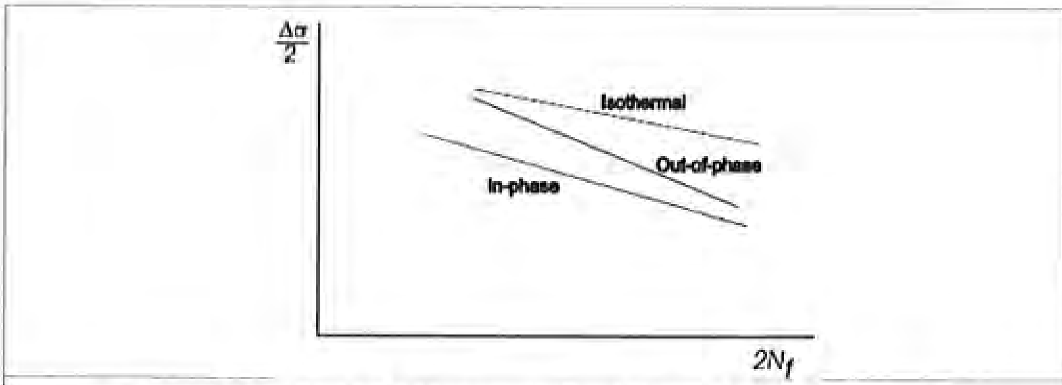

Figure 8:5: Effect of phase relationship on fatigue strength

The modification is defined in terms of two thermal factors, which are material specific. One for in-phase loading (tf1in) and the second for out of phase loading (tf2out). The parameters c and Єf' are modified as follows

c (tmf) = c/1-Ø2

Єf' (tmf) = Єf'/(1-Ø1)c

Where

Ø1 = (1-tf1in) * cos (Ø)

Ø2 = tf2out * sin (Ø)

Ø – Phase angle between strain and temperature.

If tf1- in = 1 and tf2-out = 0 then the isothermal damage curve would be used. These factors would normally be derived from the plastic strain component of the strain life curve. For each fatigue cycle, the actual phase relationship between strain and temperature is used to adjust the strain life curve.

Bulk stress relaxation

Bulk stress relaxation is a time dependent and temperature dependent phenomenon. It is the cumulative effect of transient stress relaxation and recovery over consecutive cycles, which leads to a change in the mean stress over the cycle as shown below.

440

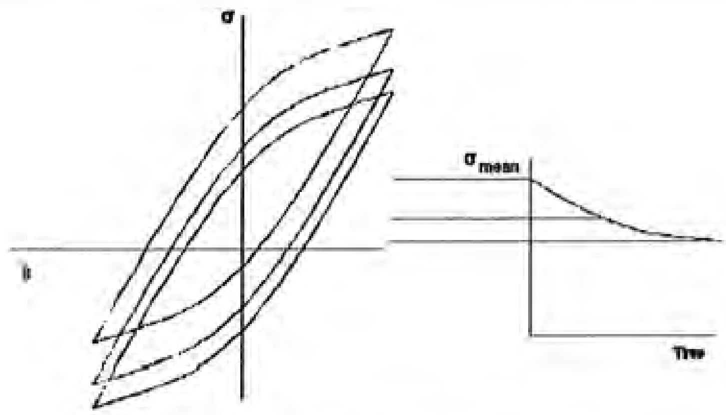

Figure 8:6: Bulk stress relaxation

Strain ageing/pre-soaking

With prolonged time at elevated temperatures, material strength properties tend to degrade due to strain-ageing, oxidation, etc. the effect is most significant early in the life of the component, and is known as strain ageing or pre-soaking. These time based properties can be combined into a "Presoak factor" describing the reduction in fatigue strength with time and temperature, where

Presoak factor, Pf = Fatigue strength at time t and temperature T/Short term fatigue strength at temperature T. Data on the change in fatigue strength is not generally available. Data on the effect of pre-soaking on ultimate strength is often used.

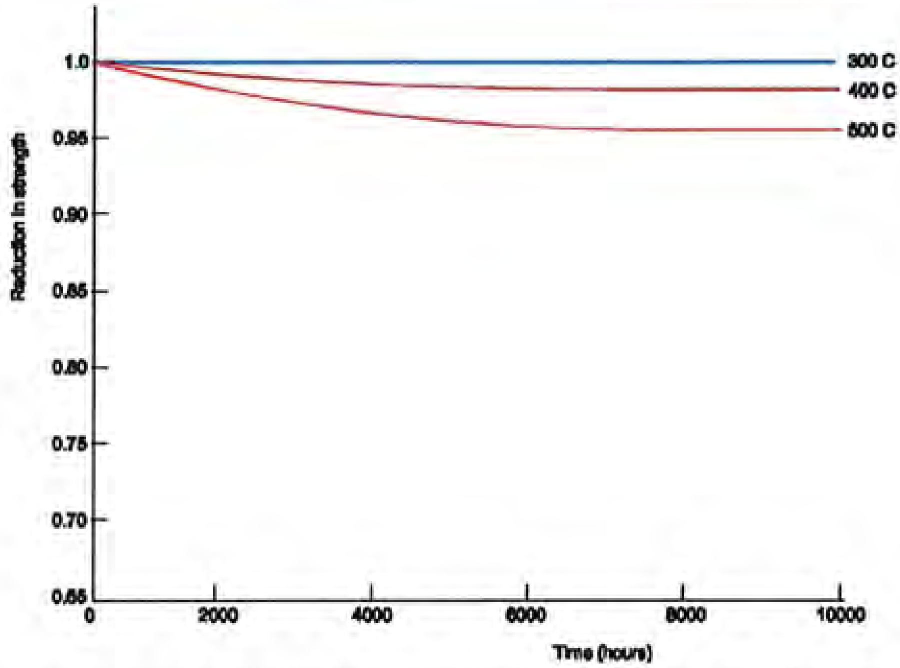

Figure 8:7: Reduction in strength as a result of pre-soak

While calculating fatigue life of TBC, one has to consider all the above mentioned factors into account for accurate fatigue life prediction under thermo mechanical loading condition.

442

8.4. Creep

Creep is the tendency of a solid material to slowly move or deform permanently under the influence of stresses. It occurs as a result of long term exposure to high levels of stress that are below the yield strength of the material. Creep is more severe in materials that are subjected to heat for long periods, and near melting point. Creep always increases with temperature.

The rate of this deformation is a function of the material properties, exposure time, exposure temperature and the applied structural load. Depending on the magnitude of the applied stress and its duration, the deformation may become so large that a component can no longer perform its function — for example creep of a turbine blade will cause the blade to contact the casing, resulting in the failure of the blade. Unlike brittle fracture, creep deformation does not occur suddenly upon the application of stress. Instead, strain accumulates as a result of long-term stress. Creep deformation is "time-dependent" deformation. The temperature range in which creep deformation may occur differs in various materials.

In the initial stage, or primary creep, the strain rate is relatively high, but slows with increasing strain. This is due to work hardening. The strain rate eventually reaches a minimum and becomes near constant. This is due to the balance between work hardening and annealing (thermal softening). This stage is known as secondary or steady-state creep. This stage is the most understood. The characterized "creep strain rate" typically refers to the rate in this secondary stage. Stress dependence of this rate depends on the creep mechanism. In tertiary creep, the strain rate exponentially increases with strain because of necking phenomena.

645

8.4.1 Creep – Fatigue interaction:

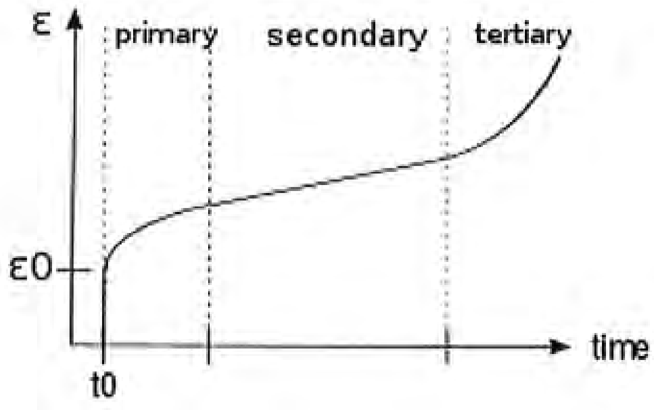

Figure 8:8: Stages of creep(Strain vs. time)

Engineering components operating hot and cyclically can experience creep and fatigue damage. Creep damage is normally due to high temperature and Fatigue damage is due to Cyclic loading Eg: Turbine blades, Turbine rotors.There are commonly occurring circumstances under which creep and fatigue can interact leading to Creep/fatigue interaction damage with very much reduced endurances.

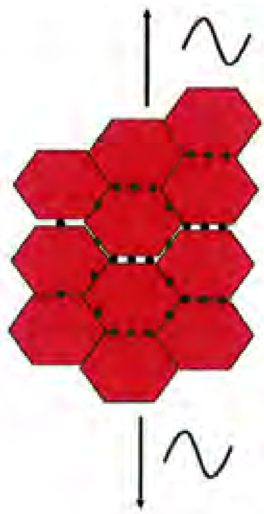

Figure 8:9: Combined creep fatigue failure

444

8.5. Introduction to FESAFE

Fatigue analysis will be performed to find out the location of crack initiation and number of cycles for crack initiation using fe-safe software.

Fe-safe is durability analysis software for finite element models. FESAFE is designed to bridge the gap between research and design. Developed by safe technology an UK based company (www.safetechnology.com). FESAFE predict the crack initiation spot and requires stress analysis results from FEA software and a loading history. Loading history can be obtained from any multibody dynamics software or from field measurements. Fe-safe calculates fatigue lives and crack sites, reliability at specified design life, factor of strength. Fe-safe interface with Abaqus, Ansys, Nastran, Pro mechanica, Hypermesh, Patran, Fem view, Cadfix, Femap.

8.6. Fe-safe analysis procedure

- FE result consists of a linear elastic solution (stress) at each node calculated for a single applied load – most conveniently unit load.
- At each node, the elastically calculated stress tensor is multiplied by the load history to give a time history of the stress tensor.
- If S_{ij} is one component of the stress tensor from the unit load linear elastic FEA and P(t) is the time history of the loading, then the time history of stress component $S_{ij}(t) = (S_{ij})^* P(t)$.
- In plane principal stresses are calculated on the surface of the model.
- Elastic strains are calculated from stresses.
- If the stress tensor represents uniaxial stress, the time history of the principal stress can be converted in to elastic-plastic stress-strains using Neuber's rule.
- Strain-time history can be used in a strain – life fatigue calculation and the associated stresses can be used to apply a mean stress correction. This procedure is repeated for each node.
- Critical plane method is used to identify the most damaging plane.
- For each of the critical planes, strains are resolved on to 3 shear planes.

- Individual fatigue cycles are identified using 'Rain flow' cycle algorithm, fatigue damage for each cycle is calculated and total damage is summed.

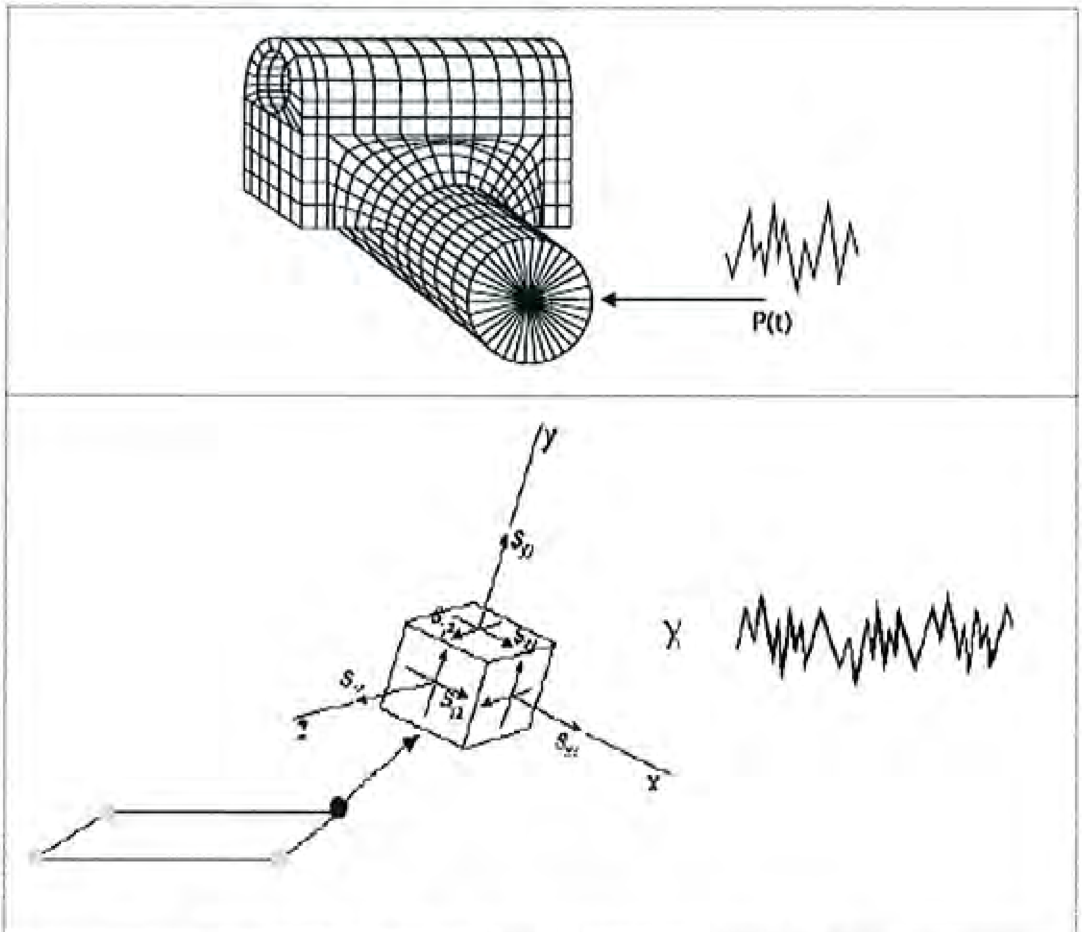

Figure 8:10: Scaling stress tensor by loading history

446

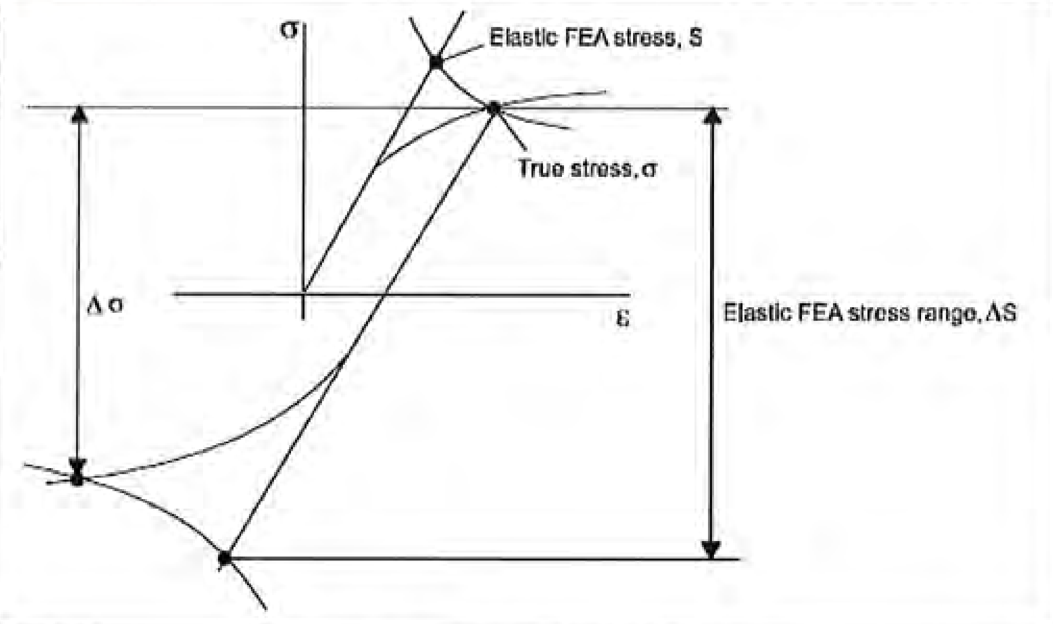

Figure 8:11: Cyclic plasticity model

8.7. Loading Cycle

FE analysis results shown in the previous section are used for fatigue analysis. Stress and temperature data for one complete cycle is considered for fatigue analysis. Stress and temperature data is imported to fe-safe and appropriate material properties for fatigue calculation have been taken from fe-safe material data base.

447

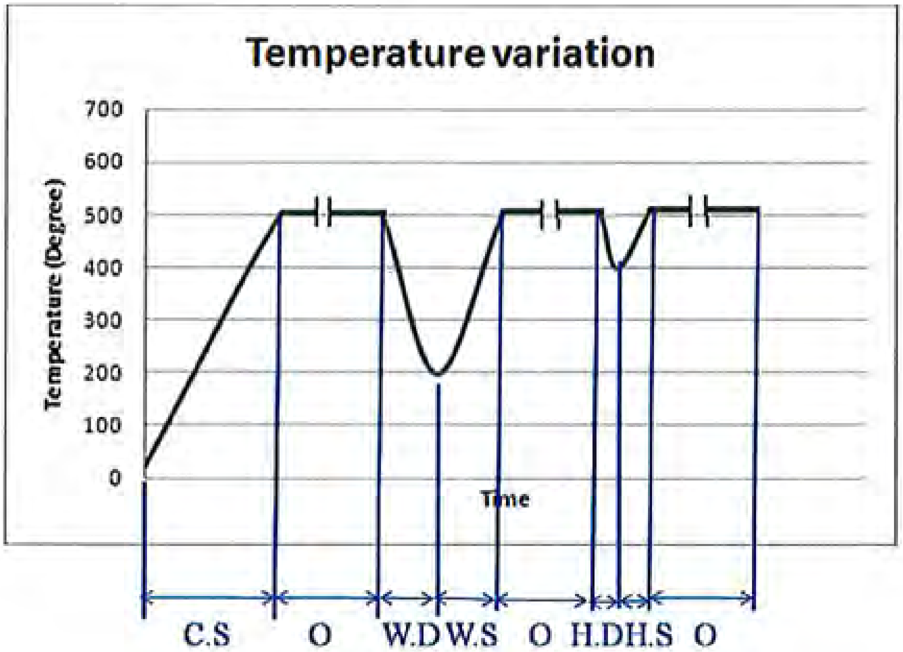

Figure 8:12: Loading Cycle

8.8. Critical Locations of failure

From the fatigue calculation life will be obtained in Log scale as shown in the contour plots. (for e.g. figures 8.13, 8.14, 8.15 etc. etc). Critical locations were marked with arrow. For e.g., in the IP casing assembly, the minimum life is 2 log (10^2) = 100 years of total life. Plant has already undergone 25 years of operation. Predicted life needs to be subtracted by 25 years to get the residual life.

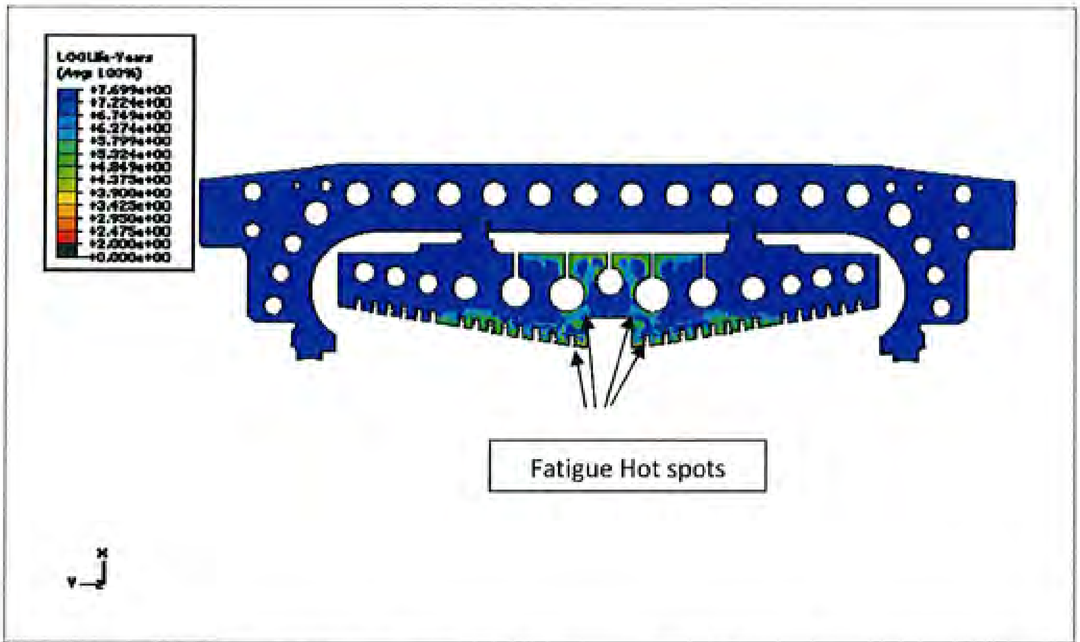

Figure 8:13: Critical Locations of failure – IP Casing Assembly

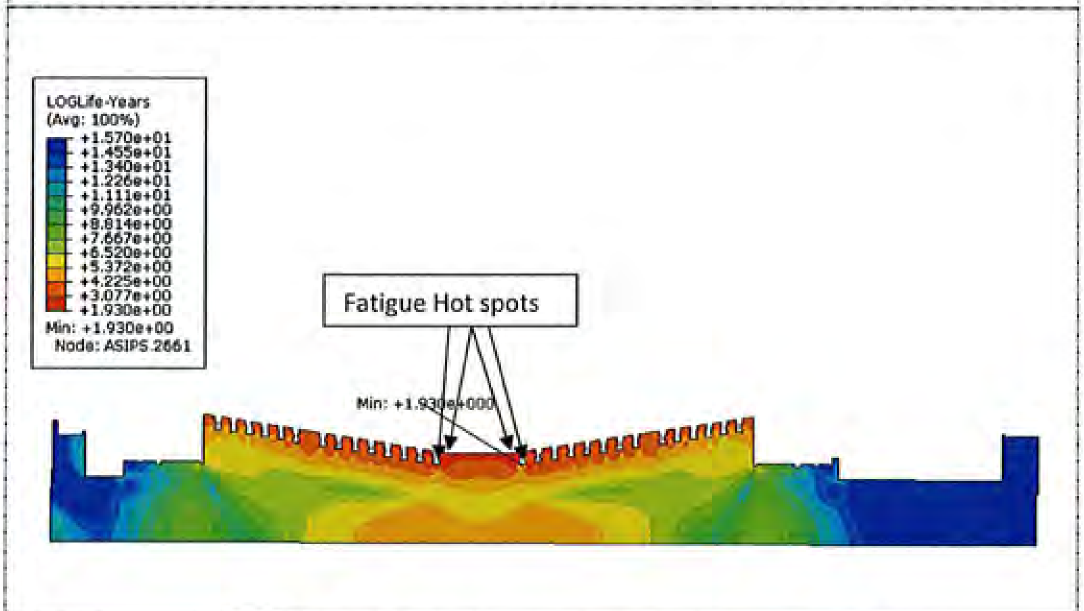

Figure 8:14: Critical Locations of failure – IP Shaft

649

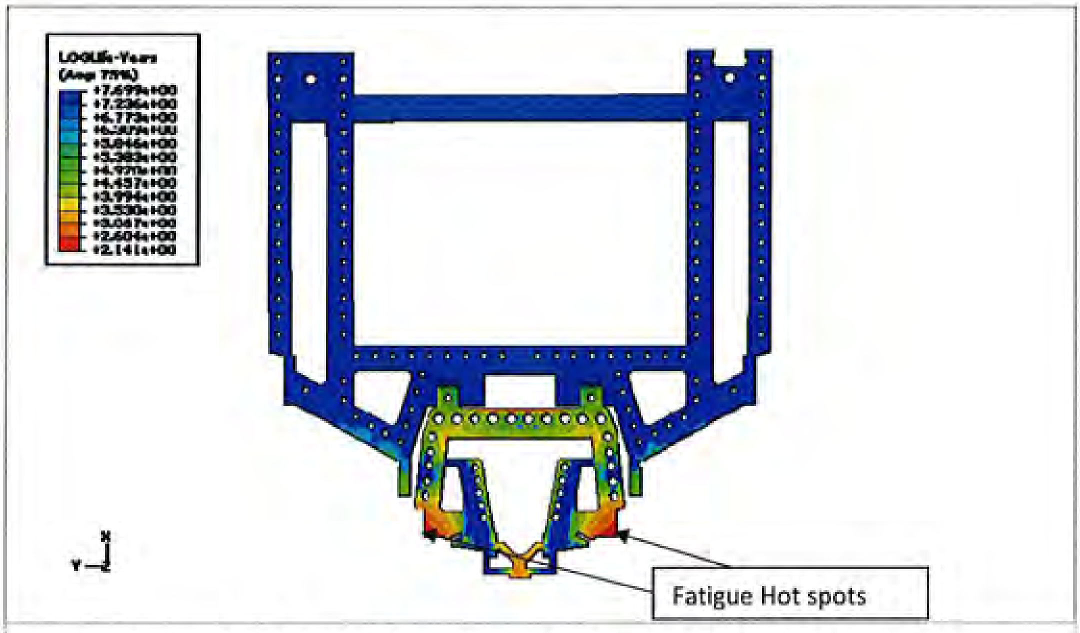

Figure 8:15: Critical Locations of failure – LP Casing Assembly

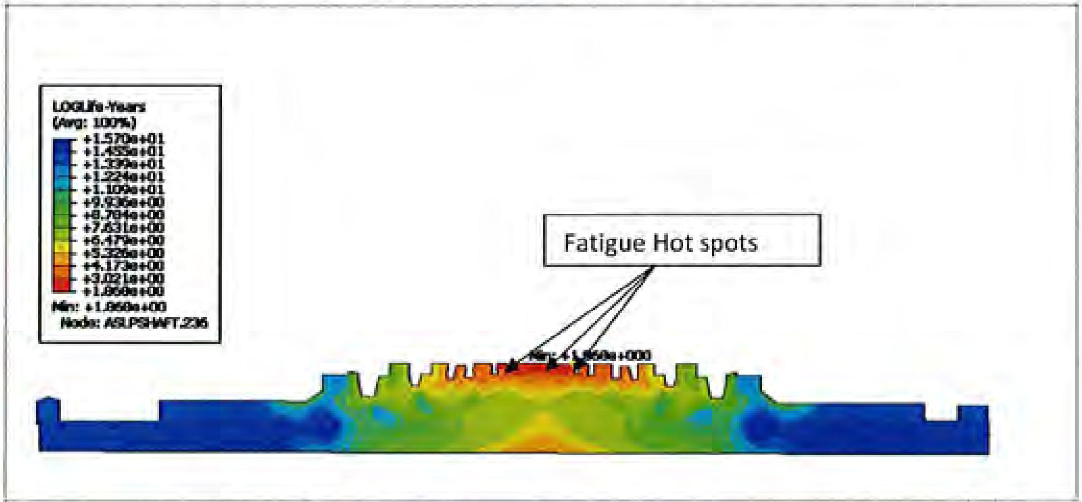

Figure 8:16: Critical Locations of failure – LP Shaft

450

8.9. Observations

From the above analysis it is observed that IP and LP components are safe for next 20 years of operation.

As per the document supplied by NASL number of thermal cycle for five years - Hot startup:5, Warm startup:23,Cold startup:6. We have multiplied this data by 5 that is Hot startup:25, Warm startup:115, Cold startup:30 to arrive at the number of cycles during the past 25 years. The remaining life in terms of cycles is tabulated below.

Table 8-1: Remaining life of the component in terms of cycles

Turbine	Log Life	Life In years	Remaining Hot Start-up Cycles	Remaining Warm Start-up cycles	Remaining Cold Start-up cycles
IP Casing Assembly	10**2	100	75	345	90
IP Shaft	10**1.93	85	60	276	72
LP Casing Assembly	10**2.14	138	113	520	136
LP Shaft	10**1.86	72	47	216	57

For IP casing assembly crack may start from the inlet and first stage and all other regions are safe.

For IP & LP shaft crack may start from the steam inlet location and first stage.

For LP casing cracks may initiate from the 3rd stage.

The critical locations prone to failure are shown in the above picture. These regions need attention during NDT. This analysis is performed under the following assumptions: steam is free from any impurities, wear and tear, corrosion is not considered, damage of any part in the assembly in turn damage other parts.

157

Section 9 Conclusion

From FE analysis following are the conclusions:

- By extrapolating the available start – stop data, we arrived at the number of cycles during the past 25 years. Hot startup:25, Warm startup:115, Cold startup:30,. The remaining life in terms of cycles / years is tabulated below.

The FE analysis is carried out for different startup (cold, warm and hot) and shutdown (warm drop and hot drop) conditions and operating loading conditions. The present study involves numerical study of the steam turbine subjected to thermo-mechanical forces and life estimation due to thermo-mechanical, creep and fatigue loads.

IP Inner casing is highly stressed (530 MPa) near the inlet and first stage.

IP rotor is stressed near the inlet and last stage. Inlet becomes critical because of higher temperature and pressure of steam.

In LP casing assembly, Inner casing shows the stress of 256MPa near the third stage of the turbine.

In LP rotor high stress (360 MPa) is observed near the inlet. This is due to higher pressure and temperature of steam at inlet.

These locations need to be frequently checked during the inspection and NDT.

FE analysis results show that stress is within safe limit of the material. Fatigue analysis predicted some hot spots.

Any deviation from the given geometry, material properties and operational data will lead to varied life prediction.

182

The remaining life in terms of cycles is tabulated below.

Table 9-1: Remaining life of the component in terms of years

Turbine components/Life	Total Creep life Years (N2)	Total Fatigue life Years(N1)	Total Creep fatigue life Years(N)	Remaining creep fatigue life Years(N-25)
LP Inner and outer casing	No significant creep in LP casing	138	138	113
LP Rotor	No significant creep in LP Rotor	72	72	47
IP Inner and outer casing	87	100	47	22
IP rotor	80	85	41	16

N1 & N2 values are taken from fe-safe calculations.

Total Creep fatigue life(N) is calculated using the following formula (Miner's Rule)

$25/N = 25/N1 + 25/N2$

- The locations as described in the observation section, needs to be frequently checked during the inspection and NDT.
- **From observations in Finite Element simulations and fatigue computations, it can be concluded that the life of the turbine (IP & LP) is expected to be beyond 20 years except IP rotor, in which life is observed to be 16 years.**

453

ALSTOM

Volume- I-B

Chapter – 09

Photographs

NTPC ALSTOM
Power Services Pvt. Ltd.

9.0 TESTING PHOTOGRAPHS

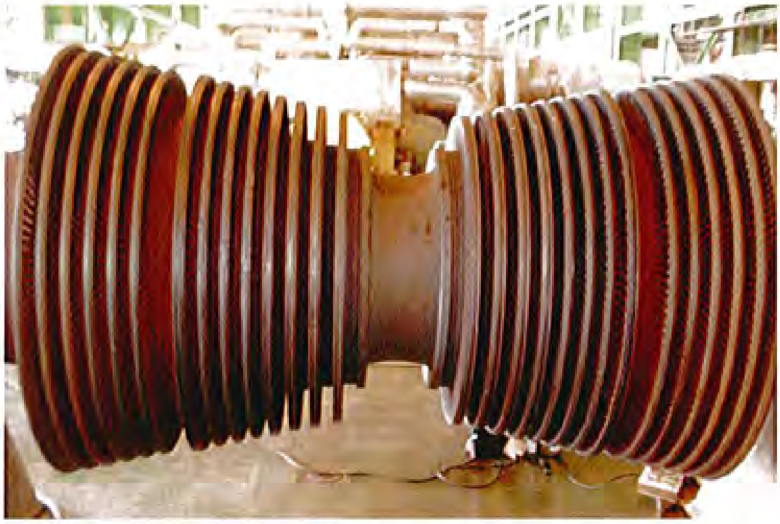

The view of Coil MPI testing on IP rotor.

The view of replica on IP rotor.

The view of Coil MPI testing on IP inner casing.

The view of Coil MPI testing on IP top inner casing.

The view of technical discussion with J- Power officer on testing location.

The view of damage sealing strip in IP top inner casing.

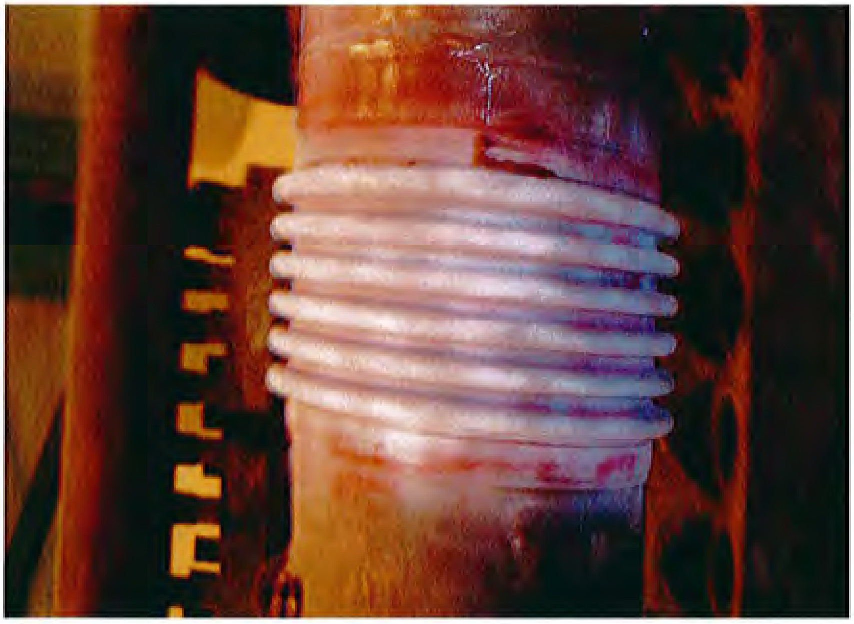

The LPT on expansion bellow of IP top outer casing

The view of LPT on bottom bearing no 4

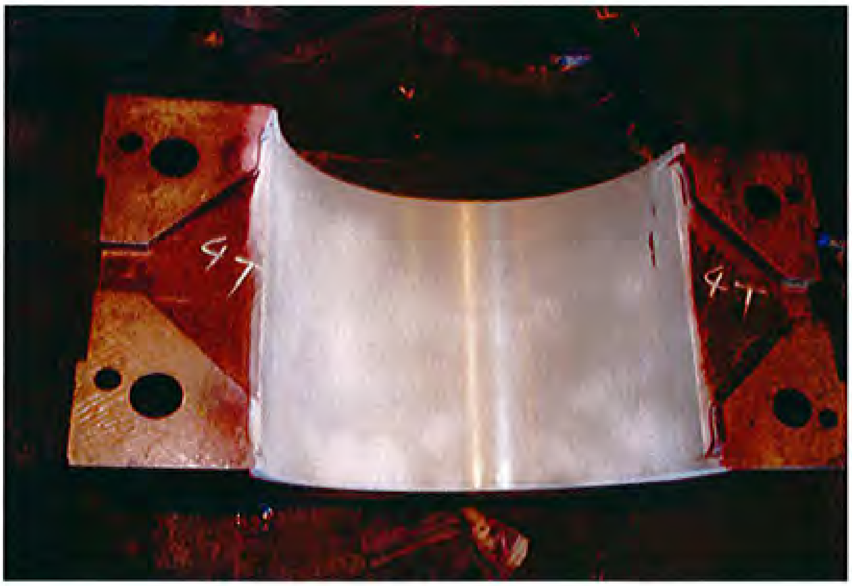

The view of LPT on top bearing no 4

The photograph of UT on bearing.

The view of MPI on bearing housing pedestal.

The full of LP rotor.

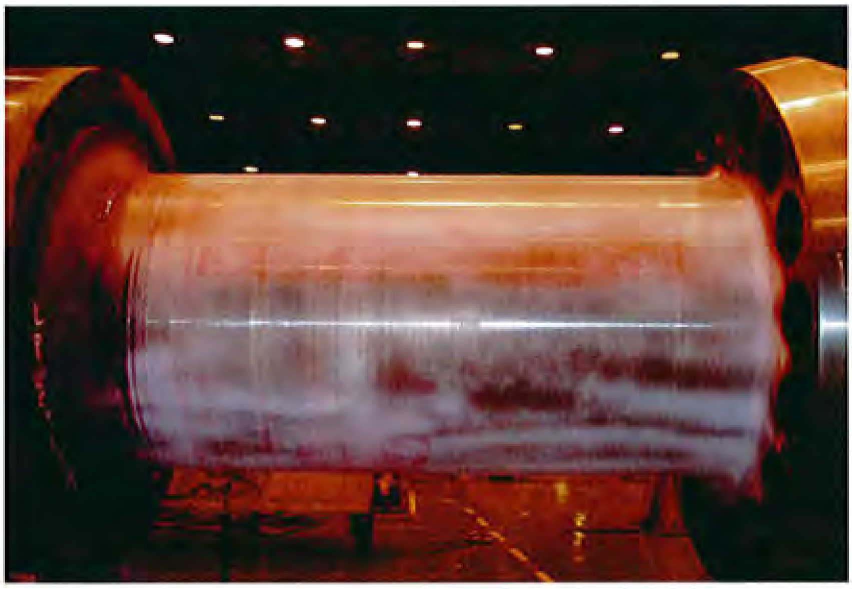

The LPT of Journal area of LP rotor.

461

The UT of general area of LP rotor.

The view of MPI on parting plane of LP bottom casing.

462

The view of erosion on LP top outer casing.

The view of erosion on LP top outer casing.

The view of deposits on LP top outer casing.

The view of deposits on LP top outer casing diapharm blades.

The view of damage of fixed blade profile of LP top outer casing

The steam erosion observed on blade of LP rotor.

The view of cleaning of LP rotor blades.

The photograph of Coil MPI testing on LP rotor.

The view of eddy current testing.

The view of MPI on LP casing studs.

The view of NFT on LP rotor.

The view of coupling bolt ready for LPT.

The view of UT testing on welding of HRH line.

The cleaning of weld joint for testing at CRH line 9th floor.

The MPI testing on weld joint of CRH line 9th floor.

The cleaning of Scrub joint of HRH Line for testing.

470

The view of replica at Y joint of HRH line.

The view of MPI on MS line weld joint near strainer Ground floor.

The view of MPI testing on Y joint of MS line 6th floor.

212

The view of weld joint cleaning at Y joint of HRH line.

The view of MPI testing on strainer.

The view of damage body of strainer MS -1.

The view of LPT test on IP SV -1

The view of LPT test on IP SV -4

The view of LPT test on L

ALSTOM

Volume-I B
END

NTPC ALSTOM
Power Services Pvt. Ltd.

965